Investigations of a Formulated Substitute for Colostrum

Syaza Yasirah Binte Abu Bakar

Bachelor of Pharmaceutical Sciences Advanced with Honours

Monash University

A thesis submitted for the degree of

Doctor of Philosophy

at

Monash University

February 2023

Drug Delivery, Disposition and Dynamics
Monash Institute of Pharmaceutical Science
381 Royal Parade
Parkville, Victoria 3052

To mama and papa

Copyright Notice

Contents

Abstract

Colostrum is the primary diet for infants providing bioactive components that are essential for the optimal development of organs and the colonisation of microbiota in the gut, while preventing infectious diseases such as necrotising enterocolitis from occurring. The benefits of bioactive factors such as lipids, proteins and oligosaccharides in colostrum for gut health have been previously demonstrated. However, there is emerging evidence to suggest that lipid digestion might play an important role in the transport and bioavailability of poorly water-soluble nutrients and potentially bioactive components to the gut and systemic circulation of infants. Despite this, there have been no reports of human colostrum being assessed in the context of lipid digestion. Thus, evaluating the lipid and free fatty acid composition of human colostrum before and during digestion and linking it to structural behaviour is important in generating a holistic picture of the behaviour of colostrum and providing a deeper understanding to enable invention of substitutes for colostrum where required. Due to the small quantities of human colostrum being secreted only for 36 hours postpartum, alternatives such as donor human milk and formulas are fed to premature infants. However, because of differences in content and composition of bioactive factors in donor human milk and formulas compared to human colostrum, these alternatives might lack the ability to promote the healthy development of infants. Hence, the primary aim of this study was to prepare a colostrum substitute formulation that possesses bioactivity and behaves similarly as human colostrum during digestion. Since a major yet less researched aspect of human colostrum is the lipid component and the effects of lipid digestion on structural behaviour is unknown, mimicking the lipid behaviour in a colostrum substitute formulation is hypothesised to be important. Once the aspect of lipid behaviour resembles that of human colostrum, the addition of other biorelevant components and assessing their impact on gut health (using an *in vitro* cell model) is a next step towards *in vivo* evaluation.

The first part of the thesis involved the use of *in vitro* digestions of colostrum and mature milk with gas chromatography coupled to a flame ionisation detector to map lipid composition before and during digestion, with structure formation measured using synchrotron-based small angle X-ray scattering. The second component of this thesis involved the reconstitution of water-soluble components from mature milk into colostrum substitute formulation and evaluation of the influence of these components on the digestion profile and self-assembly of lipids during digestion. Finally, the effects of bioactive carbohydrates and assembled milk-like systems (including the colostrum substitute formulation) on colonising bacteria and its impact on the localisation of a tight junction protein and expression levels of an anti-inflammatory cytokine were examined using an *in vitro* necrotising enterocolitis model. The findings of this thesis provide an insight into issues surrounding the assembly of a colostrum substitute formulation that can resemble human milk/colostrum more closely than current fortifiers and formulas

in terms of composition and structural behaviour during digestion, and potentially reducing some of the characteristics associated with necrotising enterocolitis.

Declaration of authorship

I hereby declare that this thesis contains no material which has been accepted for the award of any other degree or diploma at any university or equivalent institution and that, to the best of my knowledge and belief, this thesis contains no material previously published or written by another person, except where due reference is made in the text of the thesis.

This thesis includes two first-author papers published in peer reviewed journals. The core theme of the thesis is correlating the link between the composition and structural behaviour during digestion and decreasing the effects of necrotising enterocolitis *in vitro*. The ideas, development and writing up of all the papers in the thesis were the principal responsibility of myself, the student, working within the Drug Delivery, Disposition and Dynamics at the Monash institute of Pharmaceutical Sciences, under the supervision of Professor Ben J. Boyd.

The inclusion of co-authors reflects the fact that the work came from active collaboration between researchers and acknowledges input into team-based research.

In the case of Chapter 1 and 3, my contribution to these works involved the following:

Thesis chapter	Publication title	Status *(published, in press, accepted or returned for revision)*	Nature and % of student contribution	Co-author name(s), nature and % of co-author's contribution*	Co-author(s), Monash student Y/N*
1	Human milk composition and the effects of pasteurisation on the activity of its components	Published (Trends in Food Science & Technology)	75% Conceptualisation, investigation, writing – original draft, visualisation	1) Salim, Malinda: writing – review & editing, supervision 5% 2) Clulow, Andrew J: writing – review & editing, supervision 5% 3) Nicholas, Kevin R: writing – review & editing, supervision 5%	No No No

				4) Boyd, Ben J: input writing – review & editing, visualisation, supervision 10%	No
3	Impact of pasteurization on the self-assembly of human milk lipids during digestion	Published (Journal of Lipid Research)	65% Conceptualisation, methodology, software, formal analysis, investigation, writing – original draft, visualisation	1) Salim, Malinda: validation, formal analysis, investigation, writing – review & editing, supervision 5% 2) Clulow, Andrew J: validation, formal analysis, investigation, writing – review & editing, supervision 5% 3) Hawley, Adrian: software, resources 5% 4) Pelle, Joseph: data software, resources 3% 5) Geddes, Donna T: resources 2% 6) Nicholas, Kevin R: writing – review & editing, supervision 5% 7) Boyd, Ben J: input conceptualisation, resources, writing – review & editing, supervision 10%	No No No No No No No

I have not renumbered sections of published papers in order to generate a consistent presentation within the thesis.

Student name: Syaza Yasirah Binte Abu Bakar

Student signature: [redacted] **Date:** 24th February 2023

I hereby certify that the above declaration correctly reflects the nature and extent of the student's and co-authors' contributions to this work. In instances where I am not the responsible author I have consulted with the responsible author to agree on the respective contributions of the authors.

Main Supervisor name: Prof. Ben Boyd

Main Supervisor signature: [redacted] **Date:** 24th February 2023

Publications during enrolment

S.Y. Binte Abu Bakar, M. Salim, A.J. Clulow, K.R. Nicholas, B.J. Boyd. Human milk composition and the effects of pasteurisation on the activity of its components. Trends in Food Science & Technology. 2021. 111:166-174.

S.Y. Binte Abu Bakar, M. Salim, A.J. Clulow, A. Hawley, J. Pelle, D. Geddes, K.R. Nicholas, B.J. Boyd. Impact of pasteurization on the self-assembly of human milk lipids during digestion. Journal of Lipid Research. 2022. 63(5):100-183

N.F. Khan, M. Salim, **S.Y. Binte Abu Bakar**, K. Ristroph, R.K. Prud'homme, A. Hawley, B.J. Boyd, A.J. Clulow. Small-volume in vitro lipid digestion measurements for assessing drug dissolution in lipid-based formulations using SAXS. International Journal of Pharmaceutics. 2022. 4:100-113.

A.J. Clulow, **S.Y. Binte Abu Bakar**, M. Salim, C.J. Nowell, A. Hawley, B.J. Boyd. Emulsions containing optimum cow milk fat and canola oil mixtures replicate the lipid self-assembly of human breast milk during digestion. Journal of Colloid Interface Science. 2021. 588:680-691.

Manuscripts in preparation

S.Y. Binte Abu Bakar, M. Salim, A.J. Clulow, A. Hawley, J. Pelle, D. Geddes, K.R. Nicholas, B.J. Boyd. Replicating the structural behaviour of lipids in a colostrum substitute formulation to human colostrum.

S.Y. Binte Abu Bakar, M. Salim, A.J. Clulow, D. Geddes, K.R. Nicholas, B.J. Boyd. A synthetic colostrum substitute protects intestinal cells against inflammation in an *in vitro* NEC model.

Acknowledgements

This research was supported by an Australian Government Research Training Program (RTP) Scholarship, Monash International Tuition Scholarship (MITS) and Enhanced Research Experience (ERE) funding.

Firstly, I would like to thank my supervisor, Prof. Ben Boyd. I am thankful for all the times you have encouraged and believed in me at times where I thought that the tasks were impossible. Thank you for letting me rant and cry my eyes out in your office. Thank you for getting me Daniel's Donuts whenever we have to pull 24-48 h shifts at the Synchrotron and dropping me home as I was a walking zombie after those shifts.

I would like to thank my co-supervisors: Dr. Malinda Salim – for guiding me in my experiments and ensuring that my calculations were correct. I loved it whenever you shared adorable cat photos with me as they lifted my mood! Dr. Andrew Clulow – for ensuring that we were always taken care of at the Synchrotron particularly in accompanying me to the pharmacy late one night when I was unwell. I'll be sure to remember all of the stories about your kids that you shared with us! Prof. Kevin Nicholas – for being so patient and having countless meetings with me during my last set of experiments. Thank you for your expertise, advice and guidance on the immunology field – definitely something that I can add to my resume in the future!

Thank you to the beamline scientists at the Australian Synchrotron for your support and expertise regardless of the time of the night. A special thank you to Joseph Pelle from the HMST lab who willingly helped me with my analytical work. I enjoyed hearing your stories about your new pet, hopefully we can have more coffee catch ups in the near future! I am truly appreciative for all the advice that my panel, Prof. Natalie Trevaskis, Dr. John Quinn and Dr. Gillian Opie, have provided me throughout the course of my candidature and Prof. Donna Geddes for providing the highly valuable human colostrum samples for this research.

I am so grateful to the whole Boyd group: Anna Pham, Jamie Lam, Ellie Ponsonby-Thomas, Mubtasim Murshed, Tom Eason, Bryce Barber, Cindy Xiao, XiaoHan Sun, Gisela Ramirez, Kellie May, Linda Hong and Nafia Khan for constantly encouraging me, going on walks between our experiment time points and making me laugh. All of you have helped me in and out of the lab and I could not thank all of you enough. I would also like to thank Jae Pyun and Rekha Shandre for their invaluable assistance despite their own hectic schedule during my final set of experiments.

Finally, to mama and papa thank you for being my pillars of strength. Being away especially during Covid was tough but mama and papa's constant messages and video calls kept me going. There were several times where I felt overwhelmed and cried but mama and papa just knew the right words to comfort and encourage me.

List of abbreviations

ε	Extinction coefficient
λ	Wavelength
1D	1-dimensional
2D	2-dimensional
2θ	Scattering angle
2'-FL	2'-Fucosyllactose
3'-FL	3'-Fucosyllactose
3'-SL	3′-Sialyllactose
4-BPBA	4-bromophenylboronic acid
6'-SL	6′-Sialyllactose
A_1 or A_2	Absorbance
ACN	Acetonitrile
A.U.	Arbitrary units
B. infantis	*Bifidiobacterium longum* subspecies (subsp.) infantis
BSSL	Bile salt-stimulated lipase
BSA	Bovine serum albumin
$CaCl_2$	Calcium chloride
cDNA	Complementary DNA
CFU	Colony-forming unit
CPP	Critical packing parameter
CSM	Colostrum substitute mixture
Ct	Threshold cycle
d	Light path
DAG	Diglyceride
DHM	Donor human milk
DMEM/F-12	Dulbecco's modified Eagle's medium/Nutrient Mixture F-12
DMSO	Dimethyl sulfoxide
DOPC	1,2-dioleoyl-sn-glycero-3-phosphocholine
DPBS	Dulbecco's phosphate buffer saline
EDTA	Trypsin-ethylenediamintetraacetic acid

FA	Fatty acid
FAME	Fatty acid methyl ester
FBS	Fetal bovine serum
FFA	Free fatty acid
GC-FID	Gas chromatography coupled to a flame ionisation detector
GIT	Gastrointestinal tract
h	Hours
H_2	Hexagonal
HBM	Human breast milk
HCl	Hydrochloric acid
HMO	Human milk oligosaccharide
HTST	High-temperature short-time
I_2	Inverse micellar cubic
ICP-OES	Inductively coupled plasma - optical emission spectrometry
IF	Infant formula
IL-10	Interleukin-10
IS	Internal standard
L_α	Lamellar
Lac	Lactose
LC	Liquid crystalline
LCMS	Liquid chromatography-mass spectrometry
LC-PUFA	Long-chain polyunsaturated fatty acid
LNT	Lacto-N-Tetraose
LNnT	Lacto-N-neotetraose
LPS	Lipopolysaccharide
MAG	Monoglyceride
min	Minutes
mmol	Millimole
MRM	Multiple reaction monitoring
mRNA	Messenger RNA
MRS	de Man-Rogosa-Sharpe

MUFA	Monounsaturated fatty acid
MUP	Lithium mupirocin
MW	Molecular weight
NAD	Nicotinamide adenine dinucleotide
NaOH	Sodium hydroxide
NEC	Necrotising enterocolitis
NICU	Neonatal intensive care unit
PBS	Phosphate-buffered saline
PCA	Principal component analysis
PTV	Programmed temperature vapourisation
PUFA	Polyunsaturated fatty acid
q	Scattering vector
q_{peak}	q value of corresponding peak
RF	Response factor
rRNA	Ribosomal RNA
RT-qPCR	Quantitative real-time polymerase chain reaction
SAXS	Small angle X-ray scattering
SFA	Saturated fatty acid
sIgA	Secretory immunoglobulin A
SPE	Solid phase extraction
TAG	Triacylglycerol
TBU	Tributyrin unit
TEER	Transepithelial electrical resistance
TOS	Galactooligosaccharide
UHT	Ultra-high temperature
v/v	volume per volume
w/w	weight per weight
w/v	weight per volume
x	Characteristic peak multiplier

Chapter 1: Introduction

This chapter is based on a manuscript that has been published in 'Trends in Food Science & Technology'. For the purposes of the publication, only mature non-pasteurised and pasteurised human breast milk were analysed. However, this chapter of the thesis will also include a literature review of human colostrum for premature infants as well as the overall Hypotheses and Aims for the thesis.

Human milk composition and the effects of pasteurisation on the activity of its components

Syaza Y. Binte Abu Bakar[a], Malinda Salim[a], Andrew J. Clulow[a], Kevin R. Nicholas[a] and Ben J. Boyd[a,b*]

[a]Drug Delivery, Disposition and Dynamics, Monash Institute of Pharmaceutical Sciences, Monash University, 381 Royal Parade, Parkville, Victoria 3052, Australia

[b]ARC Centre of Excellence in Convergent Bio-Nano Science and Technology, Monash Institute of Pharmaceutical Sciences, Monash University, 381 Royal Parade, Parkville, Victoria 3052, Australia

*Corresponding author details: Postal Address: Monash Institute of Pharmaceutical Sciences, Monash University (Parkville Campus), 381 Royal Parade, Parkville, VIC 3052, Australia. Telephone: +61 3 99039112; Fax: +61 3 99039583.

Email: ben.boyd@monash.edu

Published online on February 25th, 2021

Citation: Trends Food Sci. Technol. (2021) 111:166-174

DOI: https://doi.org/10.1016/j.tifs.2021.02.055

Keywords: human milk, lipids, proteins, composition, bioactivity, pasteurisation

1.1 Introduction

Breastfeeding for the first six months of life is universally recognised as the normative standard of infant feeding [1]. Milk provides nutrients such as proteins, lipids and human milk oligosaccharides (HMOs) that are optimal for growth, development and general health of infants [2, 3]. While most people are familiar with human breast milk, human colostrum is often overlooked for its importance. Otherwise known as 'liquid gold', this thick yellowish liquid is secreted before human milk and is important for nourishing and protecting infants from diseases. Although some bioactive components are present in both colostrum and mature breast milk, the amounts of these components differ greatly throughout lactation [4]. For example, the former is rich in proteins, vitamins and HMOs that serve as immune protective factors and developmental factors [4, 5]. In contrast, a greater amount of lactose, amino acids, fat and short- and medium-chain free fatty acids are found in mature human milk than colostrum [6, 7]. In addition, the content of trace minerals is similar between colostrum and mature milk, with the exception of calcium being less abundant in colostrum than milk whereas copper and zinc decrease over the course of lactation [8, 9]. Despite varying amounts of nutritional factors in human colostrum and mature milk, lipids found in these sources of nourishment are crucial for providing energy to infants. In infants, the consumption of lipids from human colostrum and mature milk provides approximately 45–55% of the total energy intake [10]. Regardless of the differences in total lipid content and fatty acid (FA) composition in human colostrum and mature milk due to disparities in the diet, age and parity of mothers, triacylglycerols (TAGs) comprise around 98 *wt%* of the total lipid fraction [11]. Through the digestion of long-chain TAGs, long-chain polyunsaturated FAs (LC-PUFAs) are produced and subsequently absorbed, thereby aiding in the development of the brain and central nervous system in infants [12, 13]. Furthermore, the digested lipids are able to self-assemble into highly ordered colloidal structures called lipid liquid crystalline (LC) structures [14]. These lipid LC structures could potentially fulfil a nutritional function in the gut either as a trigger for the release of bioactives or as chaperones for membrane-bound bioactives in the intestinal milieu of infants [15-17].

1.2 Issues faced by premature infants: diminished gut microbiome and necrotising enterocolitis (NEC)

Preterm birth is defined as birth before 37 weeks of gestation and is the leading cause of perinatal and neonatal death among children under the age of 5 with approximately 15 million infants born prematurely every year [1]. While 1 million die as result of complications, those who survive are vulnerable to mature onset of diseases such as a diminished immune system, poor body temperature regulation and impaired respiration [18, 19]. Premature death occurs in developing countries as a result of a lack of feasible and hygienic interventions. Although preterm death in developed countries is less prevalent than developing countries, premature infants in the former are still not receiving optimum nourishment. The absence of bioactive factors in current alternatives fed to premature infants could

potentially cause growth rates to accelerate too rapidly and compromise the development of organs thereby resulting in increased chances of mature onset of diseases [20]. Instead, a crucial component to ensure successful treatment for premature infants is the consumption of human colostrum. However, as colostrum is produced in small quantities (5-20 mL) and only during postpartum, mothers are limited to other alternatives such as pasteurised donor human milk (DHM) or bovine milk-based fortifiers for human milk [21, 22]. Nonetheless, vital nourishment might not be readily available from these alternatives to improve health outcomes [21-25]. As a result, the absence of colostrum in the early days of life could potentially lead to chronic side effects such as limited development of the gastrointestinal tract (GIT) [23, 24, 26] .

The human GIT is the largest immune organ in the body and acts as an interface to the external environment. This immune organ is critical in preventing the entry of harmful pathogens while housing beneficial bacteria that are advantageous in maintaining intestinal homeostasis, regulating digestion and immune function [27]. During the first 3 months of life, aberrations in gut microbial composition are influential in impacting the immunological development of infants. One of the key factors responsible for promoting intestinal microbiota and ensuring maturation of GIT in infants is the onset of colostrum ingestion. It has been demonstrated that term infants who receive colostrum display a favourable composition of gut microbiota dominated by bifidobacteria as compared to preterm infants and/or term infants who are formula fed [25]. The difference in the composition of infant gut microbiome is a result of the presence of one of the bioactive factors in human colostrum/milk that is, HMOs, which is absent in bovine-derived infant formulas [28]. While HMOs do not directly nourish infants, these growth factors enrich commensals that are proficient at utilising these carbohydrates [29]. One such subspecies is *Bifidiobacterium* longum subspecies (subsp.) infantis (*B. infantis),* which metabolises HMOs leading to the colonisation and remodelling of intestinal microbiome of colostrum/breast-fed infants [30, 31]. Heiss *et al.,* reported the importance of the supplementation of HMOs to the colonisation of *B. infantis* in mice, which led to a cascading effect of host benefits including a reduction of the fecal calprotectin (a marker of pathogen-induced inflammation) and expression of pro-inflammatory cytokines while preserving intestinal barrier function [32-36]. There are thus several interventions that have sought to exploit HMOs to promote the desirable health outcomes linked to *B. infantis* [37, 38].

Other studies such as Widdowson *et al.*, instead focused on the cumulative effect of the bioactive components in colostrum/milk on the physiological changes of newborn pigs. It was found that the GIT in newborn pigs increased substantially in weight, size and DNA content during the first 24 postnatal hours but no changes were observed when the animals were prevented from suckling and were fed solely with water [39]. Similarly, Yamashiro *et al.*, illustrated that breast-fed mongrel puppies displayed accelerated enteric mucosal growth over the first four days of life [40]. The morphological appearance of jejunal microvilli in the mother-reared animals was well developed, with thickened and lengthened microvilli as compared to those in the newborn and artificially-reared animals. In both studies, it was

claimed that the bioactive components in colostrum were likely to promote the development of GIT. Yamashiro *et al.*, discussed the functionality of the epidermal growth factor in exerting a trophic effect on the epithelia thereby accelerating the maturation and stimulation of cell proliferation. Together with other bioactives, it is highly probable that these components played a central role in the enhanced enteric mucosal growth [26].

Furthermore, the bioactive components in colostrum are able to reduce the likelihood of infants generating diseases such as necrotising enterocolitis (NEC). NEC is a disease pertaining to the damage and death of cells in the intestine that causes profound inflammation and intestinal injury. Approximately 7% of low-birth-weight (≤ 1,500 g at birth) preterm infants are highly susceptible to NEC, which is a major cause of long-term sequelae and mortality [41]. While NEC may be lethal for some premature infants, others will be at risk with acute and chronic complications such as impaired neurodevelopment and bowel syndrome [42]. It is suggested that early phases of NEC include a combination of insufficient digestion and nutrient fermentation, inadequate immune responses stimulated by resident bacteria, decreased mucosal protection and weak bile pool for lipid absorption [43, 44]. Although the GIT is fully developed by 20 weeks of gestation, the function of the GIT remains immature until the third trimester. With mucus levels remaining low and placental nutrient transport being impaired, preterm infants are particularly vulnerable to NEC predisposition including diminished intestinal barrier function, intestinal immune defences and intrauterine growth restrictions [45-47]. To reduce the onset of NEC in preterm infants, the feeding of human colostrum would enable the bioactive factors present to provide protection against NEC while exerting immunomodulatory, antioxidant and growth-promoting effects [48, 49].

1.3 Comparison between human colostrum and donor human milk (DHM)

In contrast to term infants who are able to receive human colostrum, premature infants are often fed with alternatives such as DHM provided by human milk banks, or infant formulas [50]. While infant formulas have been reported to be able to provide nutrients for growth and weight gain in premature infants, these results were in part attributed to increased electrolyte intake and subsequent water retention [51]. Since formulas are mainly derived from bovine milk, proteins from bovine milk have not only shown to lead to inappropriate growth in preterm infants but also upregulate inflammatory processes that could compromise the integrity of the gut epithelial border and thus aid in the translocation of pathogens and toxins into the gut [52]. In addition, bovine milk is highly abundant in medium-chain saturated FAs. Although medium-chain FAs are added with an aim to be easily digested in an infant's gut, infants and neonates hold a smaller concentration of bile salts (1-5 mM) in their duodenum as compared to adults (5–25 mM) [53]. The low concentration of bile salts would not only potentially hamper the hydrolysis of lipids and lead to fat malabsorption but osmotic shock could also

occur in infants, especially preterm infants. Consequently, preterm infants would be reliant on alternate feeding procedures such as continuous nasogastric drip, nasojejunal feeding and intravenous alimentation to counter the loss in fluids [54].

Instead, a preferred option to infant formula is DHM, which provides additional protective and developmental factors that are not found in formulas [55]. Although DHM are fortified and offers benefits for infants beyond calorific content, the main concerns include nutrition and microbiology safety. Firstly, majority of DHM is supplied by mothers who have delivered at term and initiated lactation. However, considerable differences in macronutrient composition (protein, carbohydrate, fat) exist between term and preterm milk. For example, despite the short gestation period, mothers who deliver preterm secrete milk that contains a higher level of protein than mothers who give birth at term during the first month of lactation [56, 57]. Similarly, carbohydrate and fat content in preterm milk is significantly greater than in term milk, while gradually increasing throughout the course of lactation [58, 59]. These observations indicate a pronounced effect of gestational period and lactation on nutrient content in human milk. Furthermore, discrepancies in nutrient composition also arise due to differences in hormonal balance and metabolic regulation [60, 61]. These factors in addition to genetic and dietary factors could lead to inter-individual changes found in human milk components and thus affect the nutrients received by infants from DHM [62, 63]. In addition to diversity in macronutrient content in DHM, another challenge of providing DHM to infants is to minimise the potential risk of transmitting infectious diseases, which is particularly important for premature infants who are more susceptible to bacterial infections. Holder pasteurisation, in which the milk is heated at 62.5 °C for 30 min, is recommended by the Human Milk Banking Association of North America (HMBANA), the United Kingdom Association for Milk Banking (UKAMB) and is included in current Australian guidelines [64, 65]. While the recommended Holder pasteurisation technique was adopted in the dairy industry historically to prevent the transfer of pathogens to consumers and increase the shelf life of milk without specific concern for bioactivity of the components of bovine milk, these conditions may not necessarily be ideal for DHM. The content and composition of HMOs and lipids, and the bioactivity of native proteins and enzymes might be compromised during the heat treatment process [66]. There is thus a need for an enhanced nutrient strategy through the formulation of a colostrum substitute mixture, which is able to replicate the content and composition of the nutritional components required to promote a healthy development of infants.

1.3.1 Overall macronutrient composition in human colostrum, mature milk and DHM

The macronutrient composition of human colostrum, mature (non-pasteurised) milk and pasteurised DHM varies among mothers depending on diet, ethnicity and other factors, with a summary of the content of proteins, carbohydrates and lipids from recent studies illustrated in **Table 1.1**. These

components are responsible for providing both nutritional and non-nutritional functions resulting in the growth and healthy development of infants. Based on this table, it can be seen that there are variations in the concentrations of these components. For instance, colostrum contains a greater amount of proteins than mature and pasteurised DHM. Thus, despite feeding infants with pasteurised DHM, infants are still not receiving the optimal amount of nutrition that is otherwise obtained when fed with colostrum that may depend on the volume consumed. Despite the growing efforts to produce formulas with a composition that more closely resembles human milk, it is difficult to compensate for the lack of immunological and protective factors that are present in human colostrum and mature milk, thereby contributing to divergence in the development of infants who are breast-fed and those who are formula-fed [21]. One of the bioactive components that is responsible for this difference is the proteins in human colostrum and mature milk. These proteins not only generate amino acids for growth but also comprise peptides that have non-nutritional functions [48].

Table 1.1. Macronutrient composition of human colostrum, mature (non-pasteurised) milk and pasteurised donor human milk (DHM). Results are expressed as mean ± SD based on previous studies: [a] [59, 67-70], [b] [68-74], [c] [75-78], [d] [4, 79-81], [e] [80-83], [f] [59, 84-90], [g] [77, 78, 91, 92].

Macronutrient (g/100 mL)	Human colostrum	Mature (non-pasteurised) milk	Pasteurised DHM
Protein	1.78 ± 0.28^{a}	1.16 ± 0.16^{b}	1.17 ± 0.31^{c}
Lactose	5.17 ± 0.20^{d}	6.64 ± 0.90^{b}	6.81 ± 0.31^{c}
Oligosaccharide	2.00 ± 0.21^{d}	1.29 ± 0.33^{e}	1.20 ± 0.28^{e}
Lipid	3.08 ± 0.85^{f}	3.87 ± 0.95^{b}	2.92 ± 1.06^{g}

1.3.2 Proteins in colostrum, mature milk and DHM: differences in content and bioactivity

The proteins in human colostrum and mature milk are mainly classified into whey and casein fractions, with the whey proteins being more abundant in human colostrum and mature milk. These whey proteins serve a wide range of functions such as acting as a defence mechanism against pathogens, nutrient sequestration, modification of intestinal microflora, neutralising microbial toxins and production of CHO [67, 93]. Among the whey proteins found in human colostrum and mature milk, the predominant ones include lactoferrin, secretory immunoglobulin A (sIgA), α-lactalbumin, and lysozyme comprising approximately 30% of the total protein content (**Table 1.2**) [94]. Some of these proteins such as lactoferrin have multiple roles, which include antibacterial activities, stimulating immune functions and working synergistically with lysozyme to enable the hydrolysis of the outer cell wall of Gram-positive bacteria [95]. Moreover, following the digestion of casein and whey proteins, peptides and glycans are released thereby amplifying the functional roles of these proteins [68]. Despite the large concentration of whey proteins in human colostrum and mature milk, the ratio of whey/casein proteins sharply decreases as lactation progresses from 90:10 whey/casein in colostrum to 60:40

whey/casein in mature milk [25]. Hence, the higher abundance of these proteins in colostrum is able to provide a greater nutritional impact on the healthy postnatal development of an infant as compared to feeding an infant with mature breast milk [96].

Table 1.2. Concentrations of major proteins in human colostrum and mature milk and their biological effects. Results are expressed as mean ± SD. Table adapted from Haschke *et al.*, and Lönnerdal *et al* [67, 68].

	Concentration (mg/mL)			
Protein	**Human colostrum**	**Mature milk**	**Characteristics**	**Biological effects**
Lactoferrin	5.60 ± 0.55	1.48 ± 0.19	-Non-heme iron binding glycoprotein -Positively charged at pH 7.0; hydrophilic	- Antimicrobial, antioxidant, and immunomodulatory effects [97] -Stimulates intestinal cell proliferation and differentiation [98]
Secretory immunoglobulin A (sIgA)	5.45 ± 1.79	1.15 ± 0.62	-Antibody -Neutral (amphiphilic)	-Affects the composition of the gut microbiota, anti-infective and anti-inflammatory [99]
α-lactalbumin	4.43 ± 0.87	1.73 ± 0.25	- Negatively charged at pH 7.0; hydrophilic	- Antimicrobial activity against *Escherichia coli, Klebsiella pneumoniae*, staphylococcus, streptococcus, and C. *albicans* [100]
Lysozyme	0.32 ± 0.02	0.0729 ± 0.0547	-Glycoside hydrolase -Positively charged at pH 7.0; hydrophilic	- Acts synergistically with lactoferrin to degrade the internal membrane of Gram-negative bacteria [101] -Antiviral activity [102]

Another important aspect to consider apart from the concentration of proteins in human colostrum and mature milk is their bioactivity. A decrease in the bioactivity might render these proteins ineffective or display a lack of immunoprotective functions. While pasteurised DHM is a preferred option to formulas for premature infants, the processing steps involved in producing DHM may alter the biological function or bioavailability of the components. During the heating step in pasteurisation, a considerable loss of bioactivity of proteins occurs at the expense of minimising bacterial load [103]. For example, the immunoprotective functions of lactoferrin, sIgA and lysozyme are reduced by as much as 80% by pasteurisation, which potentially results in immunocompromised neonates [104]. A clinical study conducted by Cossey *et al.,* illustrate that NEC and the incidence of late-onset sepsis were more severe in premature infants fed with DHM when compared to those who were breastfed with human colostrum and non-pasteurised (mature) human milk [105]. Furthermore, although there are other heat

treatment processes such as high-temperature short-time (HTST) and ultra-high temperature (UHT) sterilisation, a small change in temperature could result in adverse effects in terms of the bioactivity of the immune components. Therefore, regardless of the heat treatment process adopted, the bioactivity of proteins and their overall capability to exert their nutritional and non-nutritional functions would be diminished to a certain extent.

1.3.3 Carbohydrates in DHM compared with human colostrum/milk: minimal changes in bioactivity

Aside from proteins, carbohydrates are another important component of human colostrum and mature milk. The two main classes of carbohydrates in human colostrum and mature milk include the disaccharide lactose and HMOs. While the former is the most abundant sugar in human colostrum and mature milk, the latter is an elongation of lactose with galactose, N-acetylglucosamine, fucose and sialic acid units. Due to the structures of HMOs, which mimic the carbohydrate portion of glycoproteins and glycolipids of epithelial cell membranes, this bioactive component is able to inhibit the binding of pathogenic microorganisms to the epithelial cell surface of infants, whilst lactose is a source of energy for infants [106]. Additionally, as a result of their prebiotic and immunomodulatory properties, HMOs play a protective role against infections such as NEC.

Unlike the content of proteins which are reduced in DHM, the content of lactose and the composition of HMOs are unaffected by pasteurisation [83, 107]. While this may seem that the functionality of the HMOs in DHM is similar to that of in non-pasteurised human milk/colostrum with regards to preventing the onset of NEC in infants, these carbohydrates in DHM are still able to engage in Maillard reactions [83, 108]. The Maillard reaction is a chemical reaction between amino acids and reducing sugars, importantly between the lysine residues in milk proteins and lactose, respectively [108]. During this reaction, the carbohydrates react with the amino acid side chains of the milk proteins resulting in early Maillard products. This ‘early Maillard reaction’, which typically occurs at 120–130 °C, involves the condensation of lactose with lysine, resulting in the formation of an Amadori product (1-deoxy-1-amino-lactulosyllysine). While there might not be any major changes in the activity of oligosaccharides, this early Maillard reaction could potentially reduce the nutritional value of proteins due to modification of lysine residues, which are no longer available for digestion. Although most pasteurisation techniques are carried out below 120 °C resulting in the unchanged composition of oligosaccharides in DHM, other processing steps could alter the composition and reduce the content of HMOs in DHM. However, as pasteurisation is an extensive process that includes several freeze-thaw cycles and container changes, these steps might reduce the bioactivity and content of these HMOs [109]. Hence, given these potential risks and the higher abundance of HMOs in colostrum (20 mg/mL) than DHM (13 mg/mL), colostrum would still be the preferred option in preventing the likelihood of NEC from occurring in preterm infants [110, 111].

1.3.4 Lipid content and fatty acid (FA) composition in human colostrum, mature milk and DHM

Lipids in human colostrum and mature milk are a major source of metabolic and total energy intake in infants and provide important nutrients such as saturated and unsaturated FAs and transport lipid-soluble vitamins [112]. Since human colostrum and mature milk lipids offer many biological benefits such as improved GIT function, lipid metabolism, growth and neurodevelopment, it is imperative that the overall quality, total content and composition of lipids are monitored across lactation and following pasteurisation [112]. Several techniques have been implemented to determine the total content of lipids in human milk. A commonly used technique is the modified gravimetric method, which has been used as the bench mark to measure lipids in human colostrum and mature milk [113]. This technique is based on measuring the mass of a dried lipid extract following extraction into chloroform/methanol mixtures [113]. However, the gravimetric method could overestimate the lipid content due to a partitioning step that is selective towards hydrophobic compounds in milk and not solely lipid compounds. Cerbulis and Custer have demonstrated that the extraction solvent (chloroform/methanol) was able to extract approximately 2 *wt*% of total casein in milk, proving that other components could have contributed to the total lipid content [114].

Despite several techniques used to quantify the amount of lipids in human milk and colostrum, the total lipid content could differ among techniques. For instance, as mentioned above the gravimetric method could overestimate the lipid content, while the creamatocrit and esterified FA assay methods might lead to the underestimation of lipids due to either the degradation of the TAGs in milk fat globules into more water soluble FAs or the disruption of ester linkages of the TAGs [86, 115]. Some studies indicate that the lipid content in colostrum is lower than in mature milk whereas other studies reported that the former has a higher lipid content than the latter [4, 59, 84, 116]. These variations could instead be attributed to maternal and environmental factors such as time elapsed between nursing, adiposity, parity and stage of lactation of mothers supplying these human colostrum and milk samples [85]. Despite variations in reported lipid content across lactation, it was found in a study conducted by A. Cavazos-Garduño *et al.*, that the content of lipids remains the same following pasteurisation of human milk [117]. A slight loss of lipids might still occur during pasteurisation but this is normally attributed to the adherence of lipids to the surface of containers, pipelines and feeding systems rather than the heating temperatures [92].

Apart from the total content of lipids, which remain unchanged after pasteurisation, the composition of lipids comprising saturated FAs (SFAs) (C10:0, C12:0, C14:0, C16:0, C17:0, C18:0, C20:0, C22:0, C24:0), MUFAs (C14:1, C15:1, C16:1, C17:1, C18:1, C20:1, C22:1, C24:1) and PUFAs (C18:2, C18:3, C20:2, C20:3, C20:4, C20:5, C22:4, C22:5, C22:6) were found to be maintained after pasteurisation [118]. However, similar to variations in the lipid content across lactation, the FA

composition of human colostrum and mature milk also differ from each other [84, 87]. The difference in the positional distribution of FAs along the glycerol backbone at the *sn*-1, *sn*-2 and *sn*-3 positions of a TAG molecule should thus be considered [119]. The composition of these FAs in their respective esterification sites not only defines the nutritional and physicochemical properties of the TAG molecules but would ultimately dictate the 2-monoglyceride (MAG) and free FA (FFA) products formed during digestion [120]. Upon hydrolysis of TAGs by lipases, the hydrophilic head groups of the 2-MAGs and FFAs released are hydrated while the hydrophobic chains associate with one another to prevent interaction with water. This causes the digested products to self-assemble into mixed colloidal structures. Therefore, the structure of a TAG molecule in human colostrum and mature milk would influence the types of lipid LC phases formed and may in turn affect the ability of these colloidal phases to deliver lipophilic nutrients to be absorbed into the systemic circulation of infants.

The difference in the relative amounts of these FAs found in human colostrum and mature milk are presented in **Fig. 1.1**. It can be seen that the predominant essential FAs in both colostrum and mature milk are monounsaturated oleic acid (C18:1), saturated palmitic acid (C16:0) and polyunsaturated linoleic acid (C18:2) (**Fig. 1.1**) [121].

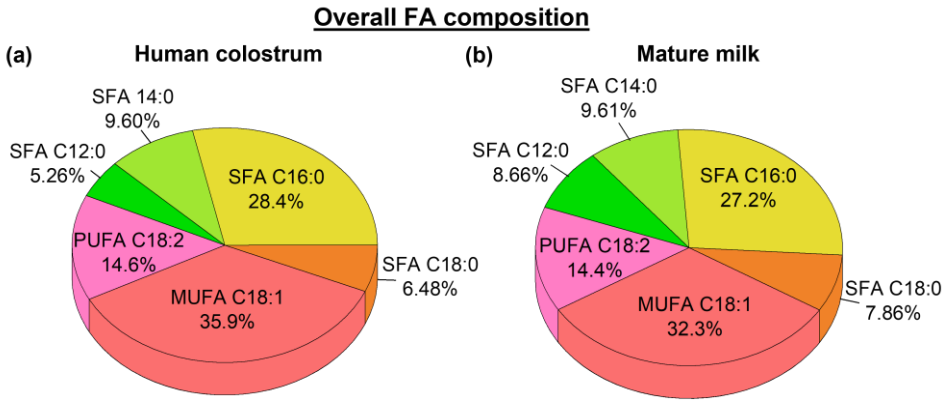

Figure 1.1. Abundance of the major fatty acids (FAs) constituting the triglycerides (TAGs) in (a) human colostrum and (b) mature milk. Abbreviations: saturated fatty acid (SFA), polyunsaturated fatty acid (PUFA), monounsaturated fatty acid (MUFA).

However, there are variations in the percentages of these major FAs in the *sn*-1, *sn*-2 and *sn*-3 positions between the two systems. For example, colostrum consists of 52% and 41% of C18:1 being the predominant FA at *sn*-1 and *sn*-3, respectively, whereas mature milk contains a lower percentage of C18:1 at those positions with 49% at *sn*-1 and 35% at *sn*-3 (**Fig. 1.2**). Similarly, colostrum has a greater amount of C16:0 FA (58%) at *sn*-2 as compared to mature milk with 52% of C16:0 (**Fig. 1.2**).

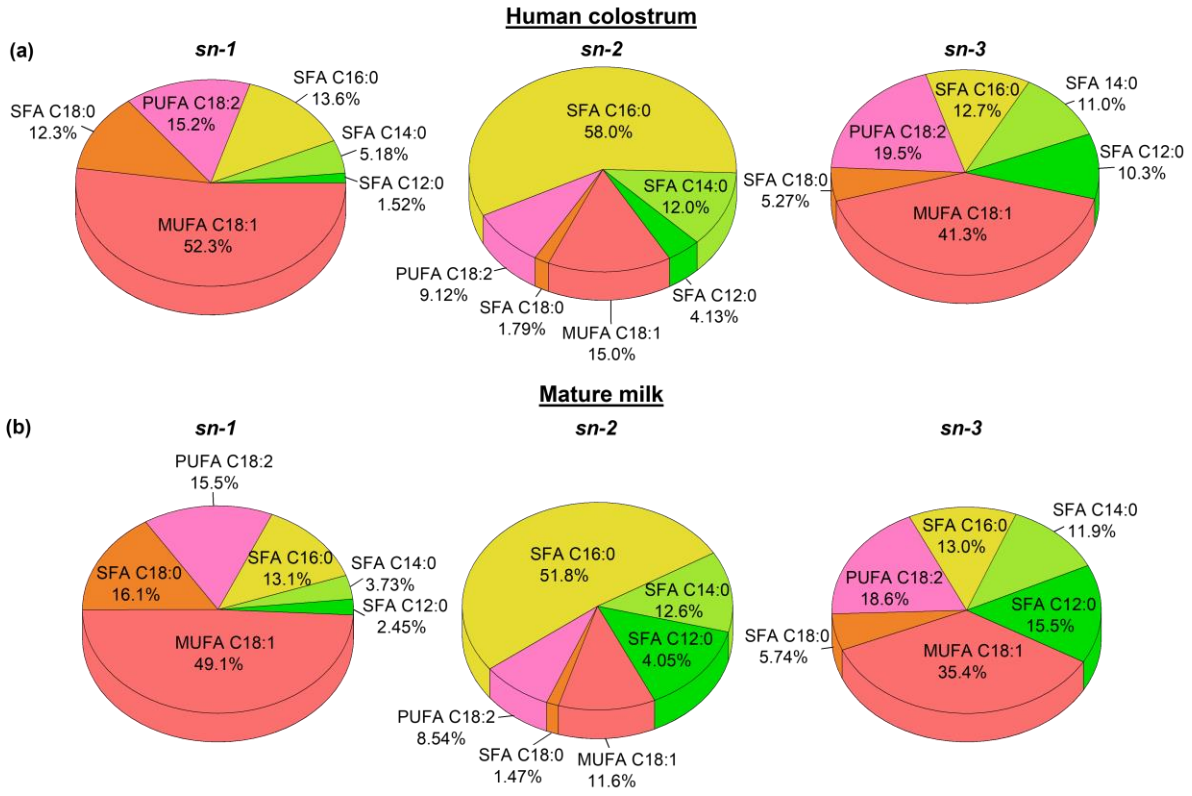

Figure 1.2. The positional distribution (*sn*-1, *sn*-2 and *sn*-3 positions) of the abundant FAs in TAGs in (a) human colostrum and (b) mature milk. Abbreviations: saturated fatty acid (SFA), polyunsaturated fatty acid (PUFA), monounsaturated fatty acid (MUFA). Figure adapted from Martin *et al.*, [121].

The difference in the relative distribution of these FAs between the outer (*sn*-1 and *sn*-3) and *sn*-2 positions in the TAG molecule of human colostrum and mature milk might lead to variations in the FFA composition and 2-MAG formed during the digestion of colostrum and milk lipids. For instance, during the digestion of C18:1/C16:0/C18:1 (oleic/palmitic/oleic) TAGs, the two outer oleic acids in the *sn*-1 and *sn*-3 positions are first cleaved by lipases thus liberating two free oleic acid molecules and one molecule of 2-monopalmitin [122]. The stereo-specific positioning of palmitic acid at the *sn*-2 position reduces the loss of calcium that would otherwise occur due to the formation of highly insoluble calcium palmitate if free palmitic acid was liberated from the *sn*-1 or *sn*-3 positions during digestion [123-125]. The complexation of calcium ions by palmitic acid in the digesting milk reportedly improves the absorption of FFAs [126]. The relative amount and specificity of the placement of FAs in the three positions of milk TAGs by the mammary gland thus not only affects the FFAs absorbed but also the nature of 2-MAG and unesterified FAs delivered to tissues. The high absorption of fat, efficient processing with positive energy balance and net tissue growth underlines the biological significance of the TAG structure.

1.4 Digestion of human colostrum and mature milk lipids

The digestion and absorption of dietary lipids is a complex process, which is reliant on factors such as enzymatic hydrolysis and solubilisation of lipolytic products in bile salt/phospholipid mixed micelles [127]. In a healthy human adult, the digestion and absorption of dietary fat is almost complete with at least 95% of the consumed fat being absorbed [128]. In comparison, the extent of digestion and absorption in infants has been reported to be approximately 80–90% due to factors such as a small bile pool, low intraduodenal concentrations of pancreatic lipase and bile salt-stimulated lipase (BSSL) [129]. Nonetheless, the lipids in human colostrum and milk are not only essential in the growth and development of an infant but have also been shown to be of interest in recent years as a lipid-based formulation [130-132]. The initial digestion process begins in the mouth with lingual lipase, followed by gastric lipase in the stomach, which accounts for about 10–30% of the total lipid digestion [128]. Lipases cleave the FAs from the TAG, leading to the production of 1,2-/2,3-diglycerides (DAGs) and FFAs. The DAGs and remaining TAGs are then hydrolysed in the upper small intestine by pancreatic lipase, which is responsible for the majority of the lipid digestion (approximately 70–90%). This enzyme acts at the oil-water interface, generating 2-MAG and FFAs [122] (**Fig. 1.3**). Concurrently, gall bladder contractions lead to the secretion of bile, containing phospholipids, cholesterol and bile salts [133, 134]. These bile components subsequently integrate the lipophilic digestion products to form vesicles and mixed micelles, thereby providing fresh surface of the substrate oil droplets for further hydrolysis activity [122]. Through the process of digestion, these amphiphilic products self-assemble to form lyotropic lipid LC structures [135, 136].

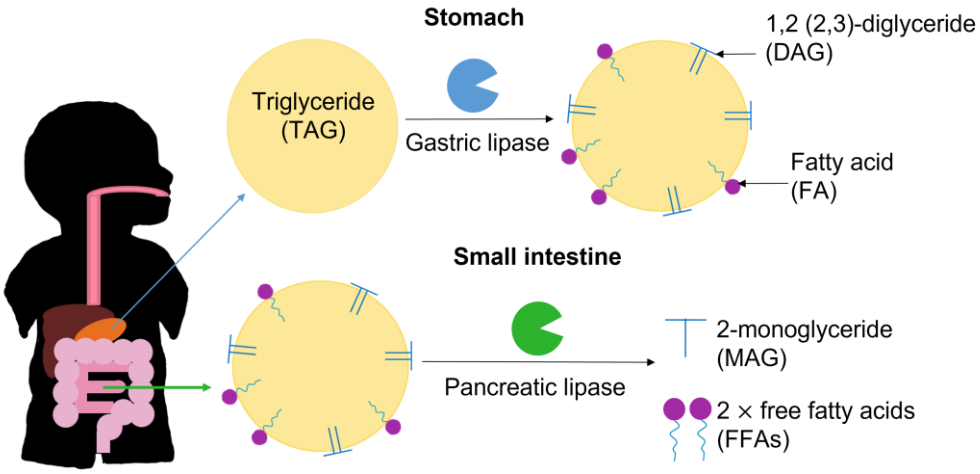

Figure 1.3. Schematic of the digestion of TAGs and subsequent products formed in the stomach and small intestine.

1.4.1 Formation of lipid liquid crystalline (LC) structures during digestion

While the TAGs that dominate the lipid content before digestion are amorphous and do not self-assemble to form complex lipid LC structures in water, the more polar lipid digestion products (MAGs and FFAs) are generally amphiphilic and self-assemble in aqueous media [135, 137] (**Fig 1.4**). These

lipid LC structures formed can range from simple lamellar bilayers to more complex phases with internalised water channels such as inverse cubic and inverse hexagonal phases. The inverse cubic phase can be further categorised as the cubic micellar I_2 phase (*Fd*3*m* spacegroup) and the bicontinuous cubic phases, which includes the *Im*3*m* and *Pn*3*m* phases [137]. Upon changes in the physiological conditions such as pH, ionic strength and calcium levels, the lipid LC mesophases are able to transition to other structures [138]. These mesophases, shape and curvature of the lipid liquid crystalline structure can be characterised using the critical packing parameter (CPP). The CPP is dependent on the area of the polar head group (a_0), volume (v) and length of hydrophobic tail (l_c) and expressed as follows [137]:

$$CPP = \frac{v}{a_0 l_c} \quad (1)$$

For CPP values <1/3, the shape of the critical packing will adopt that of a cone, forming a spherical micelle structure due to a larger area of the hydrophilic head group than hydrophobic tail. As the CPP of the lipid increases, the hydrophobic component becomes increasingly bulky and conforms to more negatively curved structures (bending towards aqueous phase i.e. water-in-oil) such as lamellar bilayers (CPP = 1) and inverse type architecture; cubic micellar *Fd*3*m* phase (CPP > 1) (**Fig. 1.4**). With the various types of lipid LC structures proving to be of interest within the pharmaceutical research field as vehicles for delivering poorly water-soluble drugs, these lipid LC structures could also function as carriers for poorly water-soluble nutrients [131, 139, 140].

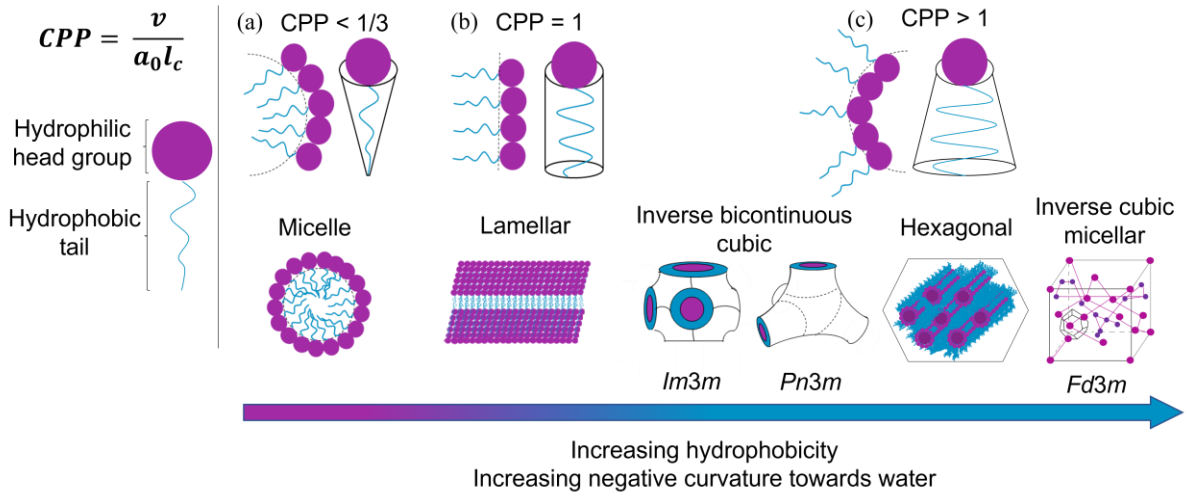

Figure 1.4. The critical packing parameter (CPP) of amphiphiles (example lipids) and the resulting morphology with different interfacial curvature for (a) micelles, (b) lamellar phase and (c) inverse cubic and hexagonal phases. Figure adapted from van 't Hag *et al.*, [141].

1.4.2 Bile salt-stimulated lipase (BSSL): role in human colostrum and mature milk and activity following pasteurisation

In contrast to adults who hold a greater concentration of bile salts than infants, the capacity for bile salts to solubilise MAGs and FFAs in a micellar form in an infant's GIT might be considerably

reduced [142]. However, human colostrum and mature milk contains an additional enzyme, BSSL, which is not found in bovine milk. In the presence of bile salts, BSSL has high lipase and esterase activity and complements the low levels of pancreatic enzymes in infants and serves to drive lipolysis towards completion [13]. Despite the presence of activating bile salt in the gastric environment, BSSL has shown negligible activity against TAGs in the stomach. However, in the higher pH and increased bile salt concentration of the duodenal fluids, this lipase becomes activated and functions synergistically with pancreatic lipase to further hydrolyse the partially digested TAGs [143]. The promoting effect of BSSL on intraluminal lipolysis was evident where a rapid release of glycerol was observed during the lipolysis of trioleoylglycerol by a mixture of BSSL and pancreatic lipase when compared to when only pancreatic lipase was present [12]. This highlights the lack of positional selectivity in BSSL activity, unlike pancreatic lipase that selectively hydrolyses TAGs at the *sn*-1 and *sn*-3 positions. BSSL further hydrolyses 2-MAGs to form glycerol and three FFAs as the lipolysis products of TAGs [143]. This demonstrates the ability of BSSL to drive the lipid digestion process to completion, potentially hydrolysing most of the colostrum and mature milk TAGs under conditions similar to those predominant in the intestine of an infant [144].

Although BSSL in human colostrum and mature milk has been shown to have a crucial role in the digestion of lipids in infants, the activity of this lipase is lost during the pasteurisation of human milk. It has been reported that BSSL and pancreatic lipase are heat labile with a loss of lipolytic activity related to the degree of heat applied [143]. Pasteurisation of human milk resulted in the complete inactivation of BSSL with a reduction in the activity of the enzyme from 36.6 U/mL (where U/mL refers to enzyme activity in 1 mL of milk) to 0 U/mL [145]. The denaturation of BSSL, which subsequently decreases its activity, was attributed to the heat-labile property of the lipase [146]. Although Holder pasteurisation is the recommended process to obtain pasteurised DHM, this process together with other types of heat treatment techniques including HTST, have been shown to suppress the activity of BSSL [92, 147, 148]. Consequently, the reduced activity or complete inactivation of BSSL would lead to unfavourable consequences for the digestion and absorption of lipids by newborns. Therefore, despite optimising the parameters used for any pasteurisation method, formulating a colostrum substitute mixture, which minimises the need for any heating or processing steps would be a more suitable alternative in preserving the bioactivity of not only enzymes but also proteins, HMOs and lipids.

1.5 Summary

Previous studies have been directed at understanding the ability of human colostrum as an optimum enteral of diet for infants. Bioactive components such as proteins, carbohydrates and lipids are essential in stimulating a healthy development of infants while preventing the onset of infectious diseases from occurring. The higher abundance and bioactivity of these components in colostrum as compared to current alternatives fed to premature infants, highlights the importance of this ‘liquid gold’

to be consumed by infants, particularly preterm infants to stimulate a healthy development of the gut while reducing the onset of NEC.

1.6 Project hypotheses

Although the benefits of these bioactive factors towards organ development and preventing diseases from occurring in infants have been previously demonstrated, there have been no reports of human colostrum being assessed in the context of lipid digestion. As lipids are shown to form lipid LC structures during digestion, it is hypothesised that these colloidal structures are critical in the bioavailability of lipophilic nutrients for premature infants with a weak bile pool for lipid absorption. Moreover, although preterm infants have been shown to have fewer episodes of NEC due to the HMOs remaining activated in DHM, the bioactivity and content of other factors such as proteins, enzymes and FFAs released during digestion are reduced. Hence, there is a pressing need to prepare a colostrum substitute formulation, which would be able to exert beneficial effects similar to that of human colostrum while performing more efficiently than current infant formulas and DHM *in vitro*. Therefore, the general hypotheses of this thesis are as follows:

1. Different stages of lactation and pasteurisation of human milk will influence the FFA composition and structural behaviour of lipids during digestion.
2. Colostrum substitute mixtures designed to have a simplified TAG composition similar to human colostrum lipids will exhibit the same lipid self-assembly when emulsified and digested.
3. Addition of reconstituted HMOs to a colostrum substitute will provide equivalent performance with respect to biomarkers of NEC compared to human milk and better than infant formula.

1.7 Project aims

To address the hypotheses above, the general aims of this project are:

1. To evaluate the FFA composition and structural behaviour of mature non-pasteurised human milk, pasteurised DHM and human colostrum during digestion – hypothesis 1.
2. To correlate the lipid and FA composition before digestion and FFA composition released during the digestion of the colostrum substitute formulation and human colostrum to the formation of lipid LC structures during *in vitro* digestion– hypothesis 2.
3. To determine whether the negative impact of NEC inducing factors on gut cells can be prevented using HMO-supplemented colostrum substitute formulation compared to infant formula – hypothesis 3.

Chapter 2: General materials and methods

The central focus of the early parts of the thesis is the behaviour of lipid in colostrum and human breast milk under digestion. *In vitro* lipolysis experiments were therefore fundamental in addressing the first two aims of this project. This digestion model was coupled to small-angle X-ray scattering (SAXS) to obtain real-time monitoring of the formation of lipid liquid crystalline (LC) structures over the course of digestion of mature human milk, pasteurised donor human milk (DHM), human colostrum and the colostrum substitute formulations. In this thesis, a correlation between the composition of free fatty acids (FFAs) released during the digestion of human colostrum, mature non-pasteurised milk and pasteurised DHM on the structural behaviour of lipids was evaluated (Chapter 3). The impact of the composition of FFA released during the digestion of human colostrum and the colostrum substitute formulation on the self-assembly of lipids was also determined (Chapter 4). Chapter 4 also entails the influence of reconstituted water-soluble components on the digestibility and structural behaviour of the colostrum substitute lipids. Lastly, an *in vitro* NEC model was implemented to analyse whether bifidobacteria cultured on carbohydrates alone and milk-like systems as a whole (infant formula, mature non-pasteurised milk and colostrum substitute formulation) would modulate the integrity of monolayer and increase the expression of an anti-inflammatory cytokine in intestinal epithelial cells (Chapter 5).

2.1 General materials

2.1.1 Human milk, colostrum and colostrum substitute formulations

Human breast milk collected between day 10-15 was donated by the Mercy Health Breastmilk Bank (Heidelberg, VIC, Australia) with ethics approval from the Mercy Health Human Ethics Research Committee (Application 2017-035). Colostrum samples collected between day 2-4 were donated by the University of Western Australia with ethics approval from the Monash University Human Research Ethics Committee (Project ID 21047). The human milk and colostrum samples were stored at -20 °C and prior to analyses, they were thawed and agitated using a vortex mixer for 5 min.

The colostrum substitute formulations were prepared using lipids (0.7 g lipid in 20 g formulation; 3.5 *wt%* total fat) that were mostly abundant in human colostrum [121]. Tricaprin (C10:0, > 98% purity), trilaurin, (C12:0, > 98% purity), trimyristin (C14:0, > 95% purity), tristearin (C18:0, > 80% purity) and triolein (C18:1, > 80% purity with the major impurity being trilinolein; C18:2) were purchased from Tokyo Chemical Industry Co. (Tokyo, Japan) and tripalmitin (C16:0, > 85% purity) was obtained from Sigma Aldrich (St Louis, MO, USA). Casein from bovine milk (technical grade) from Sigma Aldrich (St Louis, MO, USA) and lactose monohydrate (AERO FLO 65 inhalation lactose) were added to 19.3 g of tris buffer (50 mM trizma-maleate buffer at pH 6.5, which also contained 5 mM $CaCl_2.2H_2O$ and 150 mM sodium chloride and 6 mM sodium azide) in a 20 g formulation to emulsify the lipids. Casein is a poorly water-soluble protein, which exists as a micellar complex with calcium phosphate and constitutes approximately 10% and 40% of the total protein content in human colostrum and mature human milk, respectively [67, 68]. Casein (49.8 mg/ 20 g formulation)/tris buffer mix was

ultrasonicated using a microtip ultrasonicator (Misonix, Newton, CT) with an amplitude of 30, 5 s on/off for 2 min 30 s. The ultrasonication process was repeated 3-4 times, agitating the mixtures between ultrasonication cycles until all casein particles were dispersed. Following sonication, lactose monohydrate (1.09 g/ 20 g formulation), the most abundant sugar in human colostrum and milk, was then included in the buffer. Lastly, any water lost to evaporation during ultrasonication was replaced with ultrapure water.

2.1.2 Materials for *in vitro* digestion experiments

A 50 mM solution of trizma-maleate (tris) buffer was prepared consisting of trizma®-maleate, which was purchased from Sigma-Aldrich (St Louis, MO, USA), 5 mM calcium chloride dihydrate (> 99% purity) from Ajax Fine Chemicals (Seven Hills, NSW, Australia), 150 mM sodium chloride (> 99.7% purity) from Chem Supply (Gillman, SA, Australia) and 6 mM sodium azide (> 99% purity) from Merck (Darmstadt, Germany). The tris buffer solution (~900 mL) was then adjusted to pH 6.5 using HCl or NaOH (0.1M or 1.0 M) before making up the volume to 1 L. This buffer solution was used in all of the *in vitro* digestion experiments and the specific volumes of the tris buffer are described in each experimental chapter (Chapters 3 and 4).

Porcine pancreatin extract (USP grade) was obtained from Southern Biologicals (VIC, Australia). Pancreatin lipase was extracted by adding 25 mL of water to 20 g of pancreatin extract in a 50 mL polypropylene tube and vortexing until thoroughly dispersed. The hydrated pancreatin was subsequently centrifuged (parameters: 4 °C, 2205 *g* for 15 min) and the supernatant containing the pancreatic lipase was aliquoted to a fresh Falcon tube before being centrifuged again. After the second spin, the supernatant was aliquoted (5 mL) into 20 mL scintillation vials and freeze-dried for 72 h. Following freeze-drying, the lyophilised lipase extract was pooled into 50 mL polypropylene tubes and stored at -20 °C until use. Prior to each *in vitro* digestion, the freeze-dried lipase was dispersed in tris buffer. The mass of lipase required for each digestion experiment depended on the enzyme activity (approximately 700-1000 tributyrin units; TBU/mL of digest). Steps taken to determine the enzyme activity of pancreatic lipase are described in section 2.2.4.

2.1.3 Materials for gas chromatography coupled to a flame ionisation detector (GC-FID)

The following triglyceride (TAG) standards used in the gas chromatography coupled to a flame ionisation detector (GC-FID) experiments were purchased from Tokyo Chemical Industry Co. (Tokyo, Japan): tricaprin (C10:0, > 98% purity), trilaurin, (C12:0, > 98% purity), trimyristin (C14:0, > 95% purity), tripalmitin (C16:0, > 99% purity), tristearin (C18:0, > 80% purity), triolein (C18:1, > 80% purity with the major impurity being trilinolein; C18:2). Triundecanoin (used as internal standard; C11:0, > 99% purity) was purchased from Nu-Chek Prep (Elysian, MN, USA). These TAGs were diluted in chloroform (ACS, ISO, reagent) and methanol (HPLC basic) obtained from Merck

(Darmstadt, Germany). Details on the concentration of standards used and the GC-FID parameters are described in Chapters 3 and 4.

To characterise the release of FFAs during the digestion of human colostrum, mature non-pasteurised human milk, pasteurised DHM and the colostrum substitute formulations, fatty acid methyl ester (FAME) standard mixtures (nominal purity of all standards was > 99%) containing the following methyl esters from Nu-Chek Prep (Elysian, MN, USA) were used: methyl butyrate (C4:0), methyl pentanoate (C5:0), methyl hexanoate (C6:0), methyl heptanoate (C7:0), methyl octanoate (C8:0), methyl nonanoate (C9:0), methyl decanoate (C10:0), methyl undecanoate (C11:0), methyl laurate (C12:0), methyl tridecanoate (C13:0), methyl myristate (C14:0), methyl pentadecanoate (C15:0), methyl palmitate (C16:0), methyl heptadecanoate (C17:0), methyl stearate (C18:0), methyl oleate (C18:1), methyl linoleate (C18:2), methyl α-linolenate (C18:3) and methyl undecenate (used as internal standard; C11:1, > 99% purity). The FFAs from the colostrum/milk/formulation systems were obtained at the end of the digestion of these samples followed by a solid phase extraction step. These methods are further described in Chapters 3 and 4. The FFAs were subsequently derivatised into FAMEs using methanolic HCl (3 M), which was purchased from Sigma Aldrich (St Louis, MO, USA), as the derivatising agent.

2.1.4 Materials for *in vitro* necrotising enterocolitis (NEC) experiments

Enterocyte-like human colon adenocarcinoma Caco-2 cells, passages 38-43, were obtained from ATCC (Manassas, Virginia, USA) HTB-37 while HT29-MTX cell lines, passages 54-59, were purchased from Sigma Aldrich (St Louis, MO, USA) HTB-52. Through the implementation of a NEC-inducing factor, this *in vitro* NEC model was used in the present study to determine whether the supplementation of a bifidobacterial subspecies, *Bifidiobacterium longum* subspecies (subsp.) infantis (*B. infantis)* cultured on carbohydrates alone and milk-like systems as a whole, would influence the integrity of the intestinal epithelial monolayer and the expression of an anti-inflammatory cytokine. Unlike Caco-2 cells, which have the capacity to spontaneously differentiate into a monolayer of cells possessing the morphology and functionality typical of absorptive enterocytes as those found in the small intestine, HT29 cells differentiate into goblet mucus secreting cells [149-151]. Despite these differences in characteristics, both cell lines have been used extensively as *in vitro* intestinal models to assess NEC in experimental conditions [151-154].

To maintain the Caco-2 cells, Dulbecco's modified Eagle's medium/Nutrient Mixture F-12 (DMEM/F-12; Thermo Fisher Scientific, VIC, Australia) was supplemented with heat-inactivated fetal bovine serum (FBS; Sigma Aldrich, St Louis, MO, USA), non-essential amino acids (Thermo Fisher Scientific, VIC, Australia), penicillin and streptomycin (Sigma Aldrich, St Louis, MO, USA) while the HT29-MTX cells were maintained in RPMI-1640 medium (Thermo Fisher Scientific, VIC, Australia). As the dissociation reagent, trypsin-ethylenediamintetraacetic acid (EDTA; Thermo Fisher Scientific,

Rockford, IL) was used to detach the cell monolayers from the flasks. To stimulate a leakage in the intestinal epithelial layer by destroying tight junction proteins, the cell monolayers were treated with lipopolysaccharide (LPS; Sigma Aldrich, St Louis, MO, USA) [155]. Subsequently, the NEC-induced cells were incubated with *B. infantis* S12 (Creative Enzymes, Shirley, NY, USA*)*, which is a common type of bifidobacteria found in the gut of infants [156]. Through the metabolism of soluble carbohydrate oligomers, this bifidobacterial subspecies is able to adhere to intestinal epithelial cells thus leading to increased expression levels of tight junction proteins and anti-inflammatory capacity [157-159]. As the sole carbon source for the bacteria, *B. infantis* was grown in the presence of lactose (Foremost, Middleton, USA), human milk oligosaccharides (HMOs) extracted from mature non-pasteurised human milk or pure 2'-fucosyllactose (2'-FL) and lacto-N-neotetraose (LNnT) [both oligosaccharides obtained from Biosynth Carbosynth Ltd (Compton, UK)]. Following this, the bacteria subspecies was then cultured in the presence of milk-like systems: preterm infant formula, which was kindly provided by Mercy Health Breastmilk Bank (Heidelberg, VIC, Australia), mature non-pasteurised human milk and the colostrum substitute mixture. Additional materials and the nutritional contents of the preterm infant formula, mature non-pasteurised human milk and colostrum substitute formulation are further listed in Chapter 5.

2.2 General methods

2.2.1 Preparation of colostrum substitute formulations

The colostrum substitute mixtures were formulated by characterising the most abundant lipids found in human colostrum using GC-FID (section 2.2.2 and further elaborated in Chapters 3 and 4). Additionally, by incorporating the fatty acid (FA) compositions that could correspond to each TAG based on the GC-FID results of human colostrum, the mass of each TAG was calculated. **Table 2.1** shows the amount of each FAs determined in human colostrum. The amounts of homo-triglycerides were then determined to prepare a total of 0.7 g lipid in 20 g emulsions (3.5 *wt%* total fat). With regards to the non-homo-triglycerides, whose molecular weights do not correspond directly to that of a homo-triglyceride such as C46 (18:0/16:0/12:0) and C52, the amount of these TAGs was rounded to the nearest TAG; C48 (16:0/16:0/16:0) and C54 (18:0/18:0/18:0), respectively.

Table 2.1. Amount of each fatty acid (FA) found in human colostrum using GC-FID and the amount of each FAs added to the colostrum substitute using homo-triglycerides.

Fatty acid	FA composition before digestion (*sn*-1, *sn*-2 and *sn*-3 positions) (*wt%*)	
	Human colostrum	Colostrum substitute formulation
C10:0	3.4	3.4
C12:0	4.3	4.3
C14:0	1.9	1.9
C16:0	13.2	13.2
C18:0	2.5	2.5
C18:1 C18:2	74.7	74.7

The lipids were subsequently emulsified in tris buffer containing either casein proteins and lactose (explained in section 2.1.1; buffer was termed as 'without water-soluble nutrients') or reconstituted HMOs, proteins and salts from mature non-pasteurised human milk (buffer was termed as 'with water-soluble nutrients') (**Fig. 2.1**). These reconstituted water-soluble nutrients were obtained by centrifuging human milk samples at at 5000 *g* for 60 min at 4 °C. The supernatant containing the water-soluble nutrients was then aliquoted (5 mL) into 20 mL scintillation vials and freeze dried for 48 h. Following this, the lyophilised water-soluble nutrients were reconstituted in tris buffer. Further details on the preparation of these buffers are explained in Chapter 4. After adding the buffers to the molten lipids, the colostrum substitute mixtures were then melted in an oven at 70-75 °C. The mixtures were then emulsified using tip ultrasonication before subsequent *in vitro* experiments.

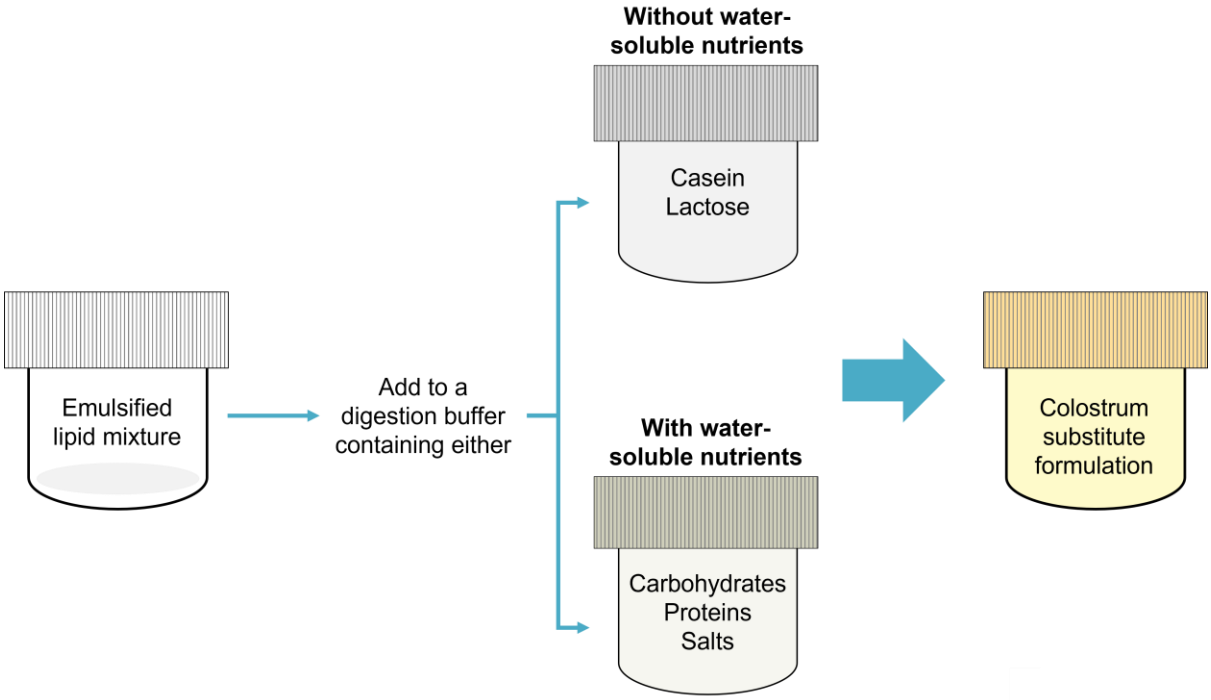

Figure 2.1. Schematic representation of the preparation of a 20 g colostrum substitute formulation. This amount was required to prepare a 3.5 *wt%* emulsion, which consisted of 0.7 g lipids in a total of 20 g aqueous solution made up of either a digestion buffer containing only casein proteins (0.5 g/20 g colostrum substitute mixture) and lactose (1.1 g /20 g colostrum substitute mixture) or a digestion buffer containing reconstituted water-soluble nutrients (HMOs, proteins and salts) from mature non-pasteurised human milk. These reconstituted water-soluble nutrients were obtained from the supernatant of centrifuged human milk samples. A total amount of 1.58 g of reconstituted water-soluble nutrients is needed for a 20 g colostrum substitute mixture.

2.2.2 Characterisation of lipids and fatty acids (FAs) using gas chromatography coupled to a flame ionisation detector (GC-FID)

Gas chromatography coupled to a flame ionisation detector (GC-FID) was used to analyse a mixture of TAGs, FA and FFA composition of undigested and digested milk, colostrum and colostrum substitute mixtures. A schematic diagram of the GC-FID set-up is shown in **Fig. 2.2** below and further

details regarding the sample preparation and the GC-FID parameters used to characterise the lipid, FA and FFA compositions are outlined in Chapters 3 and 4. This robust technique is highly sensitive in the detection of organic compounds, which are thermally stable and resistant to thermal re-arrangement [160]. As TAGs in milk (and colostrum) are considered as a group of high-boiling range compounds, GC-FID is a suitable method as the final temperatures of the column can reach to a value of 350 °C or higher [161]. In the GC-FID experiments used in this study, the compounds were eluted depending on their chain lengths; short-chain FAs would elute out of the column before the medium- and long-chain FAs. Prior to the injection of the samples into the capillary column, the glass liner that sits in the injector port should also be taken into consideration. Depending on the type of injection, whether it is programmable temperature vapourisation (PTV), on-column injection or split/splitless injection, different types of glass liners should be used. Additionally, the quartz wool in the liner should be removed so as to prevent adsorption of peaks of interest, tailing and loss of sensitivity. After the samples were injected into a capillary column using a PTV split injector, the analytes were then passed through a column using helium as the carrier gas at a constant flow rate. At this step, the temperature programme chosen would influence the flow of the analytes through the column and consequently the sensitivity of the peaks obtained. Once the analytes reached the FID, hydrogen gas was mixed with the analytes and an oxygen inlet was used to assist in the combustion process. As the analytes were combusted, hydrocarbons (CH) from the analytes generated ions in which the carbon atoms would produce CH radicals and in turn produce CHO+ ions. The ions were detected on a collector plate and the signal was converted to a peak. The quantification of each lipid/FA/FFA was then calculated based on the area under each peak and the concentration was subsequently corrected using response factors.

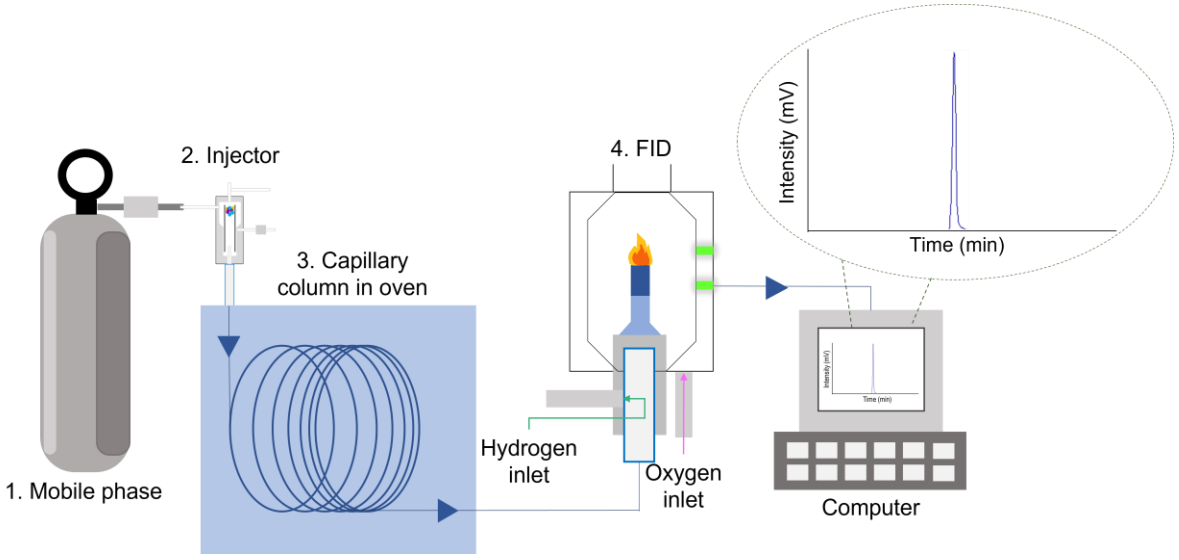

Figure 2.2. Schematic diagram of gas chromatography coupled to a flame ionisation detector (GC-FID) set up. Samples were injected into the capillary column, which sits in an oven and carried through the column using a mobile phase. The samples were then combusted using the FID and detected on collector plates before being converted to a plot of intensity against time. The area under the peak corresponded to the concentration of the sample.

2.2.3 *In vitro* digestion experiments

In vitro digestion experiments were performed on human colostrum, mature non-pasteurised milk, pasteurised DHM and the colostrum substitute formulations according to methods described previously [120, 162]. The storage conditions and preparation of each sample used for the digestion experiments are described in each chapter. A schematic diagram of the *in vitro* lipolysis set-up is shown in **Fig. 2.3** below. The samples were added into a thermostatted glass vessel (maintained at a constant temperature of 37 °C) connected to a pH stat auto titrator (Metrohm® AG) under constant magnetic stirring. The apparatus was connected to a computer and operated using Tiamo 2.0 software (Metrohm®). To simulate the gastric environment, the pH of the samples was adjusted to 3.000 ± 0.003 using 5.0 M HCl. Pepsin [13.9 mg; from porcine gastric mucosa (lyophilised powder) purchased from Sigma Aldrich (St Louis, MO, USA)] and fungal gastric lipase [27.8 mg; obtained from Connell Bros Australasia Pty Ltd (Croydon South, VIC, Australia)] were then added to the samples. After an hour of gastric digestion, the pH of the samples was then adjusted using HCl or NaOH (0.2-5.0 M) to a value of 6.500 ± 0.003 to mimic intestinal conditions. Pancreatic lipase suspension (2.25 mL of reconstituted freeze-dried lipase with tris buffer with an activity of ~700-1000 TBU/mL of digest) was added to the samples to initiate intestinal digestion leading to the release of monoglycerides (MAGs) and FFAs.

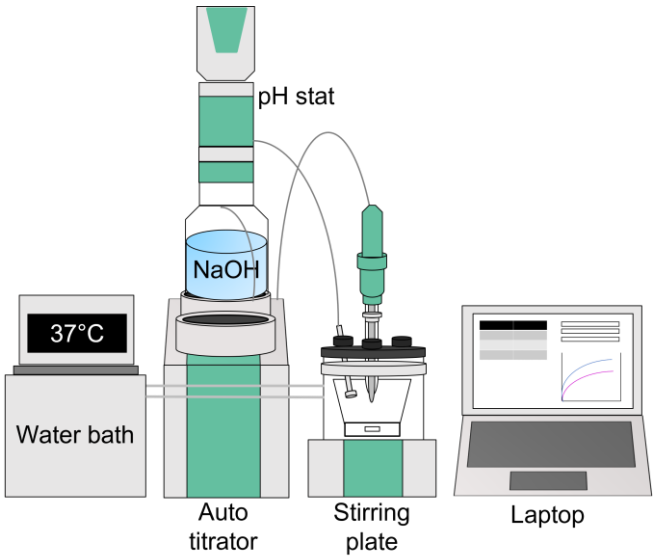

Figure 2.3. Schematic diagram of the *in vitro* digestion set-up. Samples were loaded into the vessel and maintained at 37 °C and pH 6.5 to mimic the intestinal environment. Pancreatic lipase was then manually injected into the vessel to initiate the digestion process and NaOH was titrated to ensure that the pH remained at 6.5.

Throughout the digestion of lipids, 0.2 M NaOH was added to maintain the pH at 6.5 to counter the decrease in pH as a result of the liberation of FFAs. Assuming that the consumption of NaOH was only through the evolution of ionised FFAs by lipolysis, the amount of titrated (ionised) FFAs was determined following the subtraction of volume of NaOH (required to maintain the pH at 6.5) from the blank digestion (colostrum, milk and formulations with no lipids). After 120 min of intestinal digestion,

the pH of the digested samples was increased to pH 9.0 using NaOH ('back titration'), for which the molar amount of NaOH required corresponds to the amount of unionised FFAs present at the end of digestion. Together with the amount of ionised FFAs determined earlier, the total amount of FFAs released during digestion was calculated with the following equation:

$$Extent\ of\ digestion\ (\%) = \frac{Ionised\ FFAs\ (mmol) + Unionised\ FFAs\ (mmol)}{Theoretical\ FFAs\ (mmol)} \times 100\% \quad (1)$$

2.2.4 Test for lipolytic activity of pancreatin

The enzymatic activity of lipase was determined using the tributyrin units (TBU) test typically yielding an activity between 700-1000 TBU/mL of digest. One TBU refers to the amount of enzyme required to release 1 μmol of butyric acid per min. A known mass of freeze-dried pancreatic lipase was reconstituted in a known volume of tris buffer to prepare at least 2.1 mL of reconstituted lipase. Tris buffer (18 mL) was added into a thermostatted digestion vessel, which was maintained at 37 °C and under constant magnetic stirring. Following this, tributyrin (5.8 mL/6 g) was added into the vessel before adjusting the pH to a value of 7.500 ± 0.003 using 1-2 M of HCl or NaOH. After 15 min of stirring, 2 mL of reconstituted lipase was added to the vessel to initiate digestion for 10 min. The FFAs released during digestion was titrated using NaOH (0.6 M) via an autoburette (Metrohm®, Switzerland). A graph of FFAs liberated (μM) against time (min) was plotted and the slope obtained directly correlates to the enzyme activity (TBU).

2.2.5 Determination of colloidal structures using small angle X-ray scattering (SAXS)

Small angle X-ray scattering (SAXS) experiments were carried out on the SAXS/WAXS beamline at the Australian Synchrotron (Australian Nuclear Science and Technology Organisation, Clayton, VIC, Australia) [163] to determine the formation of lipid LC structures. This technique involves the use of a monochromatic beam of X-rays with a particular wavelength (λ) passing through a sample. The X-ray beam interacts with the electron density within the sample causing the photons to be scattered. The scattering of the photons is a result of the segregation of the lipidic and aqueous regions in the LC phases causing variations in electron densities. This process results in constructive (bright spots) or destructive (dark spots) interference at the detector leading to the formation of a 2D scattering pattern. The intensity from these interference patterns was then measured as a function of scattering angle (2θ). The 2D diffraction patterns recorded were subsequently radially integrated into 1D scattering plots of scattered X-ray intensity against scattering vector (q) using the in-house developed software *Scatterbrain*. The scattering vector, q, is expressed as shown in Equation 2:

$$q = \left(\frac{4\pi}{\lambda}\right) \sin\left(\frac{2\theta}{2}\right) \quad (2)$$

where λ is the wavelength and 2θ is the scattering angle. In the 1D scattering profiles, the presence of lamellar, hexagonal and cubic LC phases was determined based on their characteristic diffraction peaks (**Fig. 2.4**) [137].

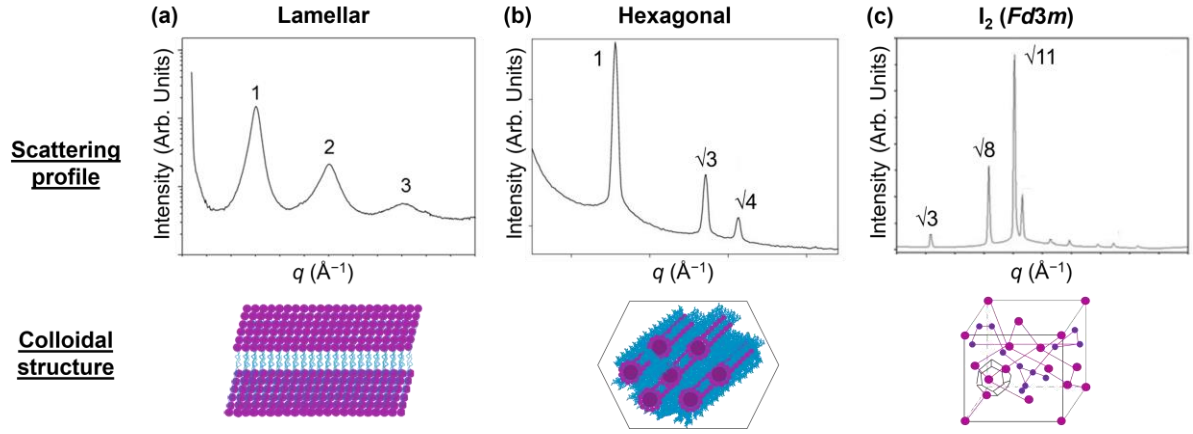

Figure 2.4. Scattering profiles with reciprocal ratios of the Bragg peaks indicated and the corresponding colloidal structures of (a) lamellar phase with peak q ratios of 1: 2: 3, (b) hexagonal phase with peak q ratios of 1: √3: √4, and (c) I_2 (*Fd*3*m*) phase, with peak q ratios of √3: √8: √11. Images were adapted from Hyde and Fong *et al.*, [137, 164].

Following this, the lattice parameters or physical dimension of unit cells in the crystal lattice, a, were calculated using the equations below (Equation 3A, 3B and 3C) based on the characteristic peak multiplier (x) and q value of the corresponding peak (q_{peak}):

Lamellar phase: $a = \frac{2\pi x}{q_{peak}}$ where x = 1, 2 or 3 (3A)

Hexagonal phase: $a = \frac{4\pi\sqrt{x}}{q_{peak}\sqrt{3}}$ where x = 1, 3 or 4 (3B)

Micellar cubic $Fd3m$ phase: $a = \frac{2\pi\sqrt{x}}{q_{peak}}$ where x = 3, 8 or 11 (3C)

2.2.6 *In vitro* lipolysis coupled to small angle X-ray scattering (SAXS): flow through measurements

The *in vitro* digestion model coupled with SAXS was used to determine real-time lipid LC structure formation during the digestion of lipids [165]. The *in vitro* digestion apparatus described in section 2.2.3 was coupled to the SAXS/WAXS beamline at the Australian Synchrotron (Australian Nuclear Science and Technology Organisation, Clayton, VIC, Australia) [163]. A peristaltic pump was used to aspirate a fraction of the digest at a flow rate of approximately 10 mL/min via silicone tubing through a 1.5 mm diameter quartz capillary mounted in the X-ray beam. Pancreatic lipase was then added remotely using a syringe driver and the 2D SAXS patterns were recorded with a 5 s acquisition time and 15 s delay between each measurement. An X-ray beam with a photon energy of 13.0 keV (wavelength, λ =0.954 Å) was utilised in this investigation. A sample-to-detector distance of around 1.7 m (approximate q range of 0.01 < q < 1.09 $Å^{-1}$) was used to monitor the lipid LC liquid structures

formed during digestion. A schematic diagram of the *in vitro* digestion model coupled to SAXS is shown in **Fig. 2.5** below:

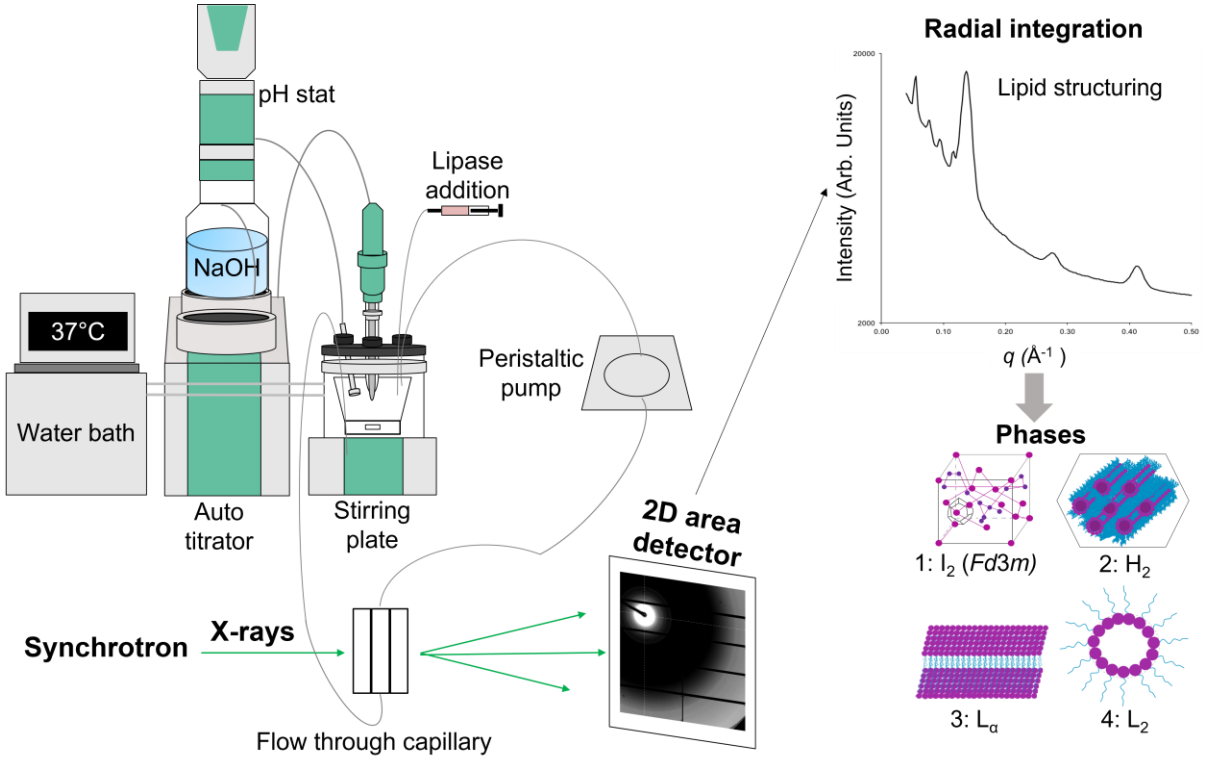

Figure 2.5. Schematic diagram of *in vitro* digestion apparatus coupled to small angle X-ray scattering (SAXS). The sample in the digestion vessel was pumped through the flow through capillary, which was aligned with the X-ray source. The digestion was initiated by injecting the pancreatic lipase remotely using the syringe driver. A scattering image was detected on the 2D area detector every 20 s (5 s acquisition, 15 s delay) before the measurements were radially integrated to determine a 1D scattering plot. The reciprocal ratios of the Bragg peaks from the plot corresponded to the colloidal structures formed.

2.2.7 Modelling necrotising enterocolitis (NEC) in intestinal epithelial cells

An *in vitro* NEC model was required to determine the effects of bioactive carbohydrates and assembled milk-like systems on colonising bacteria and its impact on the localisation of a tight junction protein and expression levels of an anti-inflammatory cytokine. While some studies have adopted the use of *in vivo* NEC models, others implemented intestinal epithelial cell models to study the effects of NEC-associated factors [166-172]. Due to logistical reasons, an *in vitro* NEC model was desirable in the present study. As Caco-2 and HT29-MTX cells constitute the most widely used intestinal cell lines for NEC and show common features of the small intestine, these two cell lines were selected. To best characterise an *in vitro* experimental NEC model, these intestinal epithelial cells were treated with LPS, mimicking the damage to the gut epithelium as seen *in vivo* [173]. The details are as follows:

Caco-2 and HT29-MTX cells were grown for 14 days postconfluence to achieve fully differentiated monolayers and treated with LPS, which induced a lesion in the cell monolayers. This resulted in changes in permeability and mucosal injury thereby mimicking the damage to the gut epithelium, which is also observed in *in vivo* NEC models [173, 174]. As a way to counter the effects

of LPS in the intestinal cell lines, both cell lines were simultaneously treated with carbohydrates only-grown *B. infantis* or milk-like systems-grown *B. infantis.* In the presence of carbohydrates such as human milk oligosaccharides (HMOs), this bifidobacteria metabolises HMOs leading to the colonisation and remodelling of the intestinal microbiome [175-177]. The role of *B. infantis* is further extended to modulating the localisation of a tight junction protein, occludin, and promoting the gene expression levels of occludin and anti-inflammatory interleukin (IL-)10 cytokine [157, 159, 178, 179]. The experimental conditions and methods are explained in Chapter 5.

2.2.7.1 Measurement of gene expression levels of interleukin- (IL) 10 and occludin using quantitative real-time polymerase chain reaction (RT-qPCR)

To identify changes in IL-10 and occludin gene expression in response to LPS-induced cells, which were subsequently treated with *B. infantis* cultured on carbohydrates and milk-like systems, quantitative reverse-transcriptase real-time polymerase chain reaction (RT-qPCR) was performed on RNA isolated from treated Caco-2 and HT29-MTX cells. This sensitive molecular biology technique is widely used to detect and quantify relative RNA abundance with small amounts of complementary DNA (cDNA) required. As the starting material in this method, RNAs are first transcribed into cDNA by reverse transcriptase from total or messenger RNA (mRNA) using primers (**Fig. 2.6**). While the type of primers used will dictate the specific location of the RNA to cDNA template transcription, oligo(dT)s was used in this current study. This type of primer amplifies a template from the 3' end poly(A) tail resulting in truncated cDNA at the 5'end and reduces the risk of bias in cDNA synthesis [180]. Once the RNA has been converted to cDNA, PCR primers of the gene of interest (in this case IL-10 and occludin) are added together with the RT-PCR mix before amplifying the cDNA sample to obtain PCR products. Another factor to consider during RT-qPCR experiments is the reference or housekeeping genes. The purpose of housekeeping genes is to minimise variance due to instability of RNA, differences in quality or quantity of mRNA across samples that may arise during extractions of RNA [181]. These genes are selected based on their lack of response to the changes in the external environment of the cells and thus expressed at a constant level. As a normaliser and widely used housekeeping gene, β-actin was utilised in the present RT-qPCR experiments [182]. The relative fold-change of the gene of interest in the treated cells was then determined based on the fluorescence detected from the IL-10 and occludin genes at the threshold cycles and normalised to that of the housekeeping gene. The experimental conditions are outlined in detail in Chapter 5.

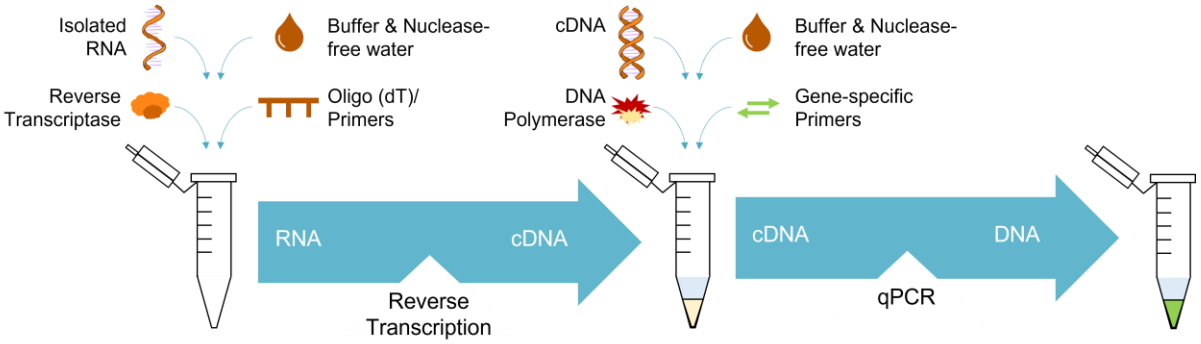

Figure 2.6. Schematic diagram of quantitative reverse transcriptase-polymerase chain reaction (RT-qPCR) involving the conversion of RNA to cDNA using a reverse transcriptase followed by amplifying the converted DNA (cDNA) to DNA using gene-specific primers.

Chapter 3: Impact of free fatty acid composition released during the digestion of human colostrum and milk on the structural behaviour of lipids

This chapter is based on a manuscript that has been published in the 'Journal of Lipid Research'. For the purposes of the publication, only mature non-pasteurised and pasteurised human breast milk were analysed. However, this chapter will include the following changes due to the specific aims of this thesis:

- Comparison of human colostrum against mature non-pasteurised human milk and pasteurised donor human milk
- Only 'low fat' human colostrum will be included due to the limited supply of human colostrum

Impact of pasteurization on the self-assembly of human milk lipids during digestion

Syaza Y. Binte Abu Bakar[1], Malinda Salim[1], Andrew J. Clulow[1,2], Adrian Hawley[2], Donna T. Geddes[3], Kevin R. Nicholas[1] and Ben J. Boyd[1,4*]

[1]Drug Delivery, Disposition and Dynamics, Monash Institute of Pharmaceutical Sciences, Monash University, 381 Royal Parade, Parkville, Victoria 3052, Australia

[2]Australian Synchrotron, ANSTO, 800 Blackburn Road, Clayton, Victoria 31698, Australia

[3]School of Molecular Science, The University of Western Australia, M310, 25 Stirling Highway, Crawley Western Australia 6009, Australia

[4]Department of Pharmacy, University of Copenhagen, Universitetsparken 2, 2100 Copenhagen, Denmark

*Corresponding author details: Postal Address: Department of Pharmacy, University of Copenhagen, Universitetsparken 2 2100 København Ø, Denmark. Telephone: +45 35 33 60 00.

Email: ben.boyd@sund.ku.dk

Published online on 1st May 2022

Citation: J. Lipid Res. 2022. 63(5):100-183

DOI: https://doi.org/10.1016/j.jlr.2022.100183

Keywords: human breast milk, lipids, digestion, fatty acid, development, nutrition, gas chromatography, calcium levels, colloidal structures, bile salts

3.1 Abstract

Human colostrum and mother's own milk is critical for the survival and development of infants. These sources of nutrition contain components that protect against infections while stimulating immune maturation. In cases where the mother's own milk is unavailable, pasteurised donor human milk (DHM) is the preferred option. Although the lipid and fatty acid (FA) composition of undigested milk throughout the course of lactation and the minimal impact of pasteurisation on the FA composition have been shown, no correlation has been made between comparing the different stages of lactation and the impact of pasteurisation on the free fatty acid (FFA) composition. Subsequently, the FFA composition of these colostrum and milk systems could dictate the structural behaviour of lipids during digestion, which could act as delivery mechanisms for poorly water-soluble nutrients and potentially bioactive components. Pooled human colostrum, mature non-pasteurised human milk and pasteurised DHM from a single donor was used in this study. The evolving FFA composition during digestion was determined using gas chromatography coupled to a flame ionisation detector (GC-FID). *In vitro* digestion coupled to small angle X-ray scattering (SAXS) was utilised to investigate the influence of different calcium levels, fat content and the presence of bile salts on the extent of digestion and structural behavior of human milk lipids. Almost complete digestion was achieved when either bile salts were added to the systems containing high calcium to milk fat ratio or when the human milk samples were sonicated, with similar structural behaviour of lipids during digestion of both types of human milk being apparent. In contrast, colostrum did not exhibit the same phases as human milk, with only a lamellar phase remaining persistent throughout digestion due to differences in the FFA composition released. Despite these differences in the colostrum and milk systems, the formation of lipid liquid crystalline (LC) structures acts as a roadmap for the design of colostrum substitute mixtures, which are rich in nutritional factors and more effective than pasteurised DHM in promoting the healthy development of infants.

3.2 Introduction

Breastfeeding in the first six months of life is associated with the healthy growth and development of infants [1]. Human milk is universally accepted as the normative standard for infant feeding due to its unique nutritional composition and the presence of bioactive components that lower the risk of illnesses while stimulating immune function, establishing the gut microbiome, signaling physiological development and providing antimicrobial activity to reduce infection [183]. While most people are familiar with human breast milk, human colostrum is often overlooked for its importance. This thick yellowish liquid, which is secreted before human milk, contains bioactive components that are in greater abundance or have a higher bioactivity than mature human milk. Although variations in the amounts and bioactivity of these nutritional factors differ between colostrum and mature milk, the lipids found in these sources of nourishment are crucial for providing energy to infants. In infants, the consumption of lipids from human colostrum and mature human milk provides approximately 45–55% of the total energy intake [10]. Unfortunately, as colostrum is produced in small quantities and only during

postpartum or in cases where the mother's own milk is unavailable, pasteurised donor human milk (DHM) is the preferred option [55]. This is often the case for hospitalised preterm or ill infants receiving care in neonatal intensive care units. To ensure that DHM is free from viral and bacterial pathogens that might be either transmitted from the donor or acquired during collection and storage of milk, DHM is subjected to a Holder pasteurisation process (62.5 °C for 30 min) [64]. Although pasteurisation ensures the microbiological safety of the milk, this heat treatment process might inactivate enzymes such as bile salt-stimulated lipase (BSSL), which is important in the lipid digestion process [67]. Hence, intestinal lipid absorption could be significantly altered when an infant is fed with pasteurised instead of human colostrum or mature non-pasteurised human milk [184].

Digestion of lipids is a crucial process in enabling absorption of the polar digestion products to occur. The generation of more polar lipids induces the formation of lyotropic lipid liquid crystalline (LC) structures [14], which are believed to play a critical role in promoting the transport and bioavailability of poorly water-soluble elements to the systemic circulation. The total lipid content of human colostrum and mature human milk comprises around 98 *wt*% triacylglycerols (TAGs) but the total lipid content and fatty acid (FA) composition in human colostrum and mature human milk varies with diet, age and parity [11]. TAGs are molecules with a glycerol backbone esterified with FAs at the *sn*-1, *sn*-2 and *sn*-3 positions [119]. Human colostrum and mature human milk fat are characterised by high contents of palmitic (C16:0) and oleic acids (C18:1) with the former primarily esterified at the *sn*-2 position and the latter concentrated in the *sn*-1 and *sn*-3 positions. While LC-PUFAs have been shown to improve neurodevelopmental outcomes in infants, saturated FAs such as palmitic acid are also ubiquitous in tissues and play a key role in neuronal signaling, calcium ion channel activity and anti-inflammatory effects [185, 186]. The selective distribution of these FAs in the TAG molecules contributes to the overall enhancement of digestion and absorption of lipids in the gastrointestinal tract (GIT) [126, 187]. Through the process of lipolysis, TAGs are hydrolysed into diacylglycerols (DAGs), monoacylglycerols (MAGs) and free fatty acids (FFAs).

In a healthy human adult, the digestion and absorption of dietary fat is almost complete with at least 95% of the consumed fat being absorbed [128]. In comparison, the extent of digestion and absorption in infants has been reported to be approximately 80–90% due to factors such as a small bile pool, low intraduodenal concentrations of pancreatic lipase and BSSL [129]. Nonetheless, the lipids in human colostrum and milk are not only essential in the growth and development of an infant but have also been shown to be of interest in recent years as a lipid-based formulation [130-132]. Pancreatic lipase in the upper small intestine accounts for more than 70% of the lipid digestion by hydrolysing the two outer ester bonds leading to the liberation of one *sn-2* MAG and two FFAs [122]. While this occurs, gall bladder contractions lead to the secretion of bile, containing phospholipids, cholesterol and bile salts [134]. These bile salts further help to emulsify the colostrum and milk lipid droplets and subsequently integrate the insoluble products from the hydrolysis of TAGs to form vesicles, mixed

micelles and more complex lipid LC systems, thus increasing the oil-water surface area for hydrolytic activity.

BSSL, an enzyme constituent of human colostrum and mature non-pasteurised human milk, in part enables the self-assembly process through the release of FFAs [12]. BSSL has a higher intestinal activity than pancreatic lipase in hydrolysing ester bonds and is more effective at liberating the long chain-polyunsaturated FAs that are essential to the development of an infant's organs such as the brain and central nervous system [13]. Thus, although infants have low intraluminal bile salt concentrations (1-5 mM), the presence of BSSL can drive the digestion of lipids in the case where pancreatic lipase is insufficient to do so. In addition to bile salts, endogenous calcium, which is naturally found in milk and milk-like systems and typically included in the digestion buffers used in *in vitro* digestion experiments, also increases the extent of digestion through the removal of the FAs from the oil-water interface of the lipid droplet by calcium ions [188]. As this occurs, not only is the accessibility of the substrate for the lipase increased but the interaction between the calcium ions and FAs also results in the formation of calcium soaps. Hence, both bile salts and calcium act as enhancement tools in the digestion process, which could affect the fate of lipophilic nutrients in the systemic circulation.

Currently, the majority of the published studies either focus on the lipid composition of human colostrum and mature human milk before digestion or evaluate the self-assembly of lipids during digestion using *in vitro* models [126, 135, 189]. However, there have been limited reports that investigate the correlation between these two aspects. This study compares the different stages of lactation and the impact of pasteurisation on the FFA composition and the subsequent effect on the types of lipid LC phases formed during *in vitro* digestions (**Fig. 3.1**). Gas chromatography coupled to a flame ionisation detector (GC-FID) was used to characterise the relative percentages of each FFA released during digestion. Based on these results, the influence on the FFAs liberated during digestion on the formation of colloidal structures was determined using small-angle X-ray scattering (SAXS).

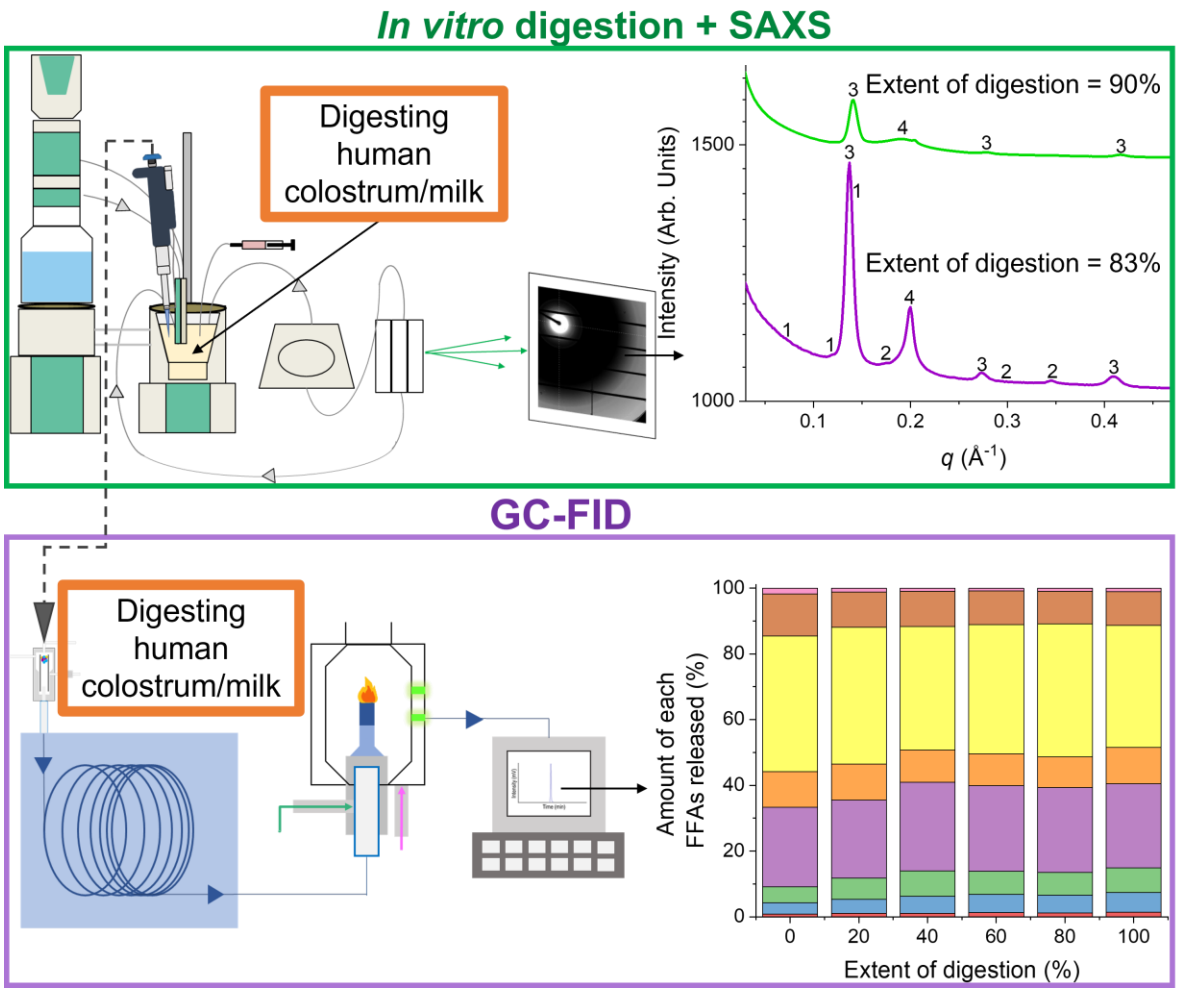

Figure 3.1. Schematic diagram illustrating the two primary experimental approaches to link the free fatty acid (FFA) composition of human colostrum, mature non-pasteurised human milk and pasteurised donor human milk [determined using gas chromatography coupled to a flame ionisation detector (GC-FID)] and self-assembly of lipids [monitored using an *in vitro* lipolysis model coupled to *in situ* small-angle X-ray scattering (SAXS)] during the digestion of these colostrum and milk samples.

3.3 Materials & methods

3.3.1 Standards and materials

Human colostrum samples were donated by the University of Western Australia with ethics approval from the Monash University Human Research Ethics Committee (Project ID 21047). Human breast milk was donated by the Mercy Health Breastmilk Bank (Heidelberg, VIC, Australia) with ethics approval from the Mercy Health Human Ethics Research Committee (Application 2017-035) and following the principles of the Declaration of Helsinki. The human colostrum, mature non-pasteurised human milk and pasteurised DHM samples were stored at -20 °C and prior to analyses, they were thawed and agitated using a vortex mixer for 5 min. Tricaprylin (C8:0, > 99% purity), methyl undecenate (C11:1, > 99% purity), glyceryl tridecanoate (C13:0, > 99% purity), glyceryl triundecanoate (C11:0, > 99% purity), monopalmitin (C16:0, >99% purity) and oleic acid (C18:1, >99% purity) were

obtained from Nu-Chek Prep. (Elysian, MN, USA). Fatty acid methyl esters (FAME) standard mixtures containing the following methyl esters were also purchased from Nu-Chek Prep. (Elysian, MN, USA): methyl butyrate (C4:0), methyl pentanoate (C5:0), methyl hexanoate (C6:0), methyl heptanoate (C7:0), methyl octanoate (C8:0), methyl nonanoate (C9:0), methyl decanoate (C10:0), methyl undecanoate (C11:0), methyl laurate (C12:0), methyl tridecanoate (C13:0), methyl myristate (C14:0), methyl pentadecanoate (C15:0), methyl palmitate (C16:0), methyl heptadecanoate (C17:0), methyl stearate (C18:0), methyl oleate (C18:1), methyl linoleate (C18:2), methyl α-linolenate (C18:3). Tricaprin (C10:0, > 98% purity), trilaurin, (C12:0, > 98% purity), trimyristin (C14:0, > 95% purity), tristearin (C18:0, > 80% purity) and triolein (C18:1, > 80% purity with the major impurity being trilinolein) were purchased from Tokyo Chemical Industry Co. (Tokyo, Japan). Calcium chloride dihydrate (> 99% purity) and sodium hydroxide pellets (> 97% purity) were purchased from Ajax Fine Chemicals (Seven Hills, NSW, Australia). Absolute ethanol was purchased from Merck (Darmstadt, Germany). 1,2-dioleoyl-sn-glycero-3-phosphocholine (DOPC) was purchased from Cayman Chemical Company (Michigan, USA). Hydrochloric acid (36% aqueous solution) was obtained from LabServ (Longford, Ireland). Sodium chloride (> 99.7% purity) was purchased from Chem Supply (Gillman, SA, Australia). Tripalmitin (C16:0, ≥ 85% purity), sodium azide (> 99% purity), chloroform (ACS, ISO, reagent), and methanol (HPLC basic) were obtained from Merck (Darmstadt, Germany). Methanolic HCl (3 M), *n*-hexane (≥ 98% purity, gas chromatography), *tert*-butyl methyl ether (99.8% purity, anhydrous), acetic acid (99.8% purity, anhydrous), 4-bromophenylboronic acid (4-BPBA), sodium taurodeoxycholate hydrate (95% purity), trizma®-maleate (reagent grade) and pepsin from porcine gastric mucosa (lyophilised powder) were purchased from Sigma Aldrich (St Louis, MO, USA). Pancreatin extract (USP grade) was obtained from MP Biomedicals (Solon, OH, USA). Fungal lipase 8000 was purchased from Connell Bros Australasia Pty Ltd (Croydon South, VIC, Australia). The lipid standards were stored at -20 °C until further use and unless otherwise stated, all chemicals were used without further purification and water was acquired from a Merck Q-POD Ultrapure Water Remote Dispenser (Darmstadt, Germany).

3.3.2 Determination of micronutrient composition using inductively coupled plasma - optical emission spectrometry (ICP-OES)

Inductively coupled plasma - optical emission spectrometry (ICP-OES) was used to determine the concentration of multiple elements within the human colostrum and milk samples. The ICP-OES experiments were carried out at the University of Melbourne in collaboration with the Melbourne TrACEES Platform. The human colostrum and milk samples were thawed to room temperature, mixed by manually shaking and agitated using a vortex mixer. Briefly, 0.5 g of each sample was weighed into polytetrafluoroethylene vessels and 5 mL of nitric acid (70% *w/w*, AR grade) from Ajax Fine Chemicals (Seven Hills, NSW, Australia) was added to each sample. The samples were subsequently digested using a Milestone Ethos microwave digestion system with the following temperature parameters: heated

to 240 °C over 25 min and maintained at 240 °C for another 30 min. The digested samples were then diluted to 50 mL with deionised water and the concentration of trace micronutrients were analysed using an inductively coupled plasma optical emission spectrometer (PerkinElmer Optima 4300DV). The sample introduction system consisted of a concentric nebuliser, a baffled cyclonic spray chamber, and a 2.0 mm alumina injector. The instrument settings are shown in **Table 3.1** below.

Table 3.1. Inductively coupled plasma-optical emission spectrometry (ICP-OES) parameters for the determination of mineral contents in human colostrum and milk.

ICP-OES operating parameters		**Analytical wavelengths and plasma view**		
RF power	1300 W	**Element**	**Wavelength (nm)**	**Plasma view**
Plasma flow	15 L/min	Potassium	766.49	Axial
Auxiliary flow	0.2 L/min	Sodium	589.59	Axial
Nebuliser flow	0.80 L/min	Calcium	393.37	Radial
Read delay	30 s	Phosphorous	213.62	Axial
Auto Integration (min-max)	1 - 5 s	Magnesium	285.21	Axial

The micronutrient composition of the human colostrum and milk samples is detailed below in **Table 3.2**.

Table 3.2. Micronutrient composition of human colostrum, mature non-pasteurised human milk and pasteurised donor human milk (DHM) (quantities are mg/100 mL).

Mineral content (mg/100 mL)	**Human colostrum**	**Mature non-pasteurised human milk**	**Pasteurised DHM**
Potassium	60.3	36.9	46.0
Sodium	46.2	111.1	18.5
Calcium	16.2	28.7	30.1
Phosphorous	13.2	16.2	18.4
Magnesium	3.8	4.3	3.5
Iron	0.1	0.24	0.15

3.3.3 Analysis of triglyceride (TAG) composition using gas chromatography coupled to a flame ionisation detector (GC-FID)

3.3.3.1 Extraction of lipids

Total lipids were extracted from pooled human colostrum, mature non-pasteurised human milk and pasteurised DHM samples by a single donor (n = 3 each) following the method previously described by Folch *et al.*, [113]. Briefly, human colostrum and milk samples (1.61 mL each) were spiked with 2 mg/mL triundecanoin in chloroform as an internal standard. The samples were subsequently mixed with

1.08 mL chloroform and 0.54 mL methanol (2:1, *v/v*), agitated using vortex mixing and centrifuged at 1503 *g* for 10 min. The clear homogenate was then transferred to a separating funnel. Water (2:10, *v/v* ratio of water:homogenate) was mixed with the homogenate and allowed to stand for 10 min for full phase separation to occur. The organic layer (bottom phase) was collected in a round bottom flask. Residual lipids in the aqueous layer were subsequently extracted with 2:1 *v/v* chloroform/methanol (1:1 *v/v* aqueous to organic solvents) and allowed to stand for 10 min until phase separation occurred. The organic layer from the second extraction was combined with the previous collection in the same round bottom flask. The solvent of the combined organic layers was then evaporated to dryness in a rotary evaporator (initially 400 mbar, 100 rpm, 45 °C and pressure was continuously decreased to 0 mbar to remove any traces of solvent remaining). The lipid content was determined by weighing the difference between the empty round bottom flask at the start of the experiment and the same flask that contained the extracted lipids.

3.3.3.2 Chromatographic conditions for TAG analysis

The extracted lipids were then dissolved in chloroform to a final concentration of 2 mg/mL and analysed using GC-FID. The analyses were performed on a PerkinElmer Clarus® 680 gas chromatograph (Beaconsfield, United Kingdom), equipped with a capillary ZB-1HT (100% dimethylpolysiloxane) column with a length of 12.5 m, an internal diameter of 0.32 mm and a siloxane film thickness of 0.10 μm (Phenomenex Inc., California, USA). The lipid samples (1 μL) were injected into a programmed temperature vapourisation (PTV) split injector (split ratio 1:50). The following PTV temperature program for the injector port was adopted: 60 °C, held for 0.2 min, increased to 370 °C at the maximum heating rate (~125 °C/min) and this temperature was held for 5.0 min. Oven conditions were: 250 °C, held for 2.0 min, heated up to 360 °C at a rate of 3.8 °C/min and temperature held for 4.0 min. The carrier gas was helium (1.54 mL/min, constant flow) and the FID was kept at 370 °C. The average concentration of each TAG was automatically determined by the instrument software and statistical analyses were conducted using a one-way analysis of variance (ANOVA) to determine the significance (p-value < 0.05) of any differences in the TAG content between human colostrum, mature non-pasteurised human milk and pasteurised DHM.

3.3.4 Particle size measurement

Particle size distributions of the fat globules from the re-dispersed human colostrum, mature non-pasteurised human milk and pasteurised DHM samples were measured by laser light scattering using a Mastersizer 2000 (Malvern Panalytical, United Kingdom), equipped with a He-Ne red laser of wavelength 633 nm and an LED blue laser of wavelength 466 nm. Light scattering from both lasers was combined to detect volume size distributions ranging from 10^{-2} to 10^{4} μm. Background measurements were taken with water flowing through the cell and the colostrum/milk samples were then added dropwise until the obscuration of the red laser was 5-10% (equivalent to the obscuration of the blue laser being 7-14%). The refractive indexes of the colostrum/human milk fat globules and water

were taken to be 1.46 and 1.30, respectively. The absorbance of the colostrum/human milk fat globules was taken as 0.001 for analysis. The volume-weighted mean diameter of the particles was then recorded as $D_{4,3}$ generated by the in-built instrument software based on calculated size distributions by volume.

3.3.5 *In vitro* lipolysis

In vitro lipolysis was performed on human colostrum, mature non-pasteurised human milk and pasteurised DHM samples using methods described previously [162, 165]. The colostrum and human milk samples were stored at -20 °C and thawed immediately prior to digestion. The colostrum and human milk samples were re-dispersed and added into a thermostatted glass vessel (maintained at a constant temperature of 37 °C) connected to a pH stat auto titrator (Metrohm® AG) under constant magnetic stirring. The apparatus was connected to a computer and operated using Tiamo 2.0 software (Metrohm®). To simulate the gastric environment, the pH of the sample was adjusted to 3.000 ± 0.003 using 5.0 M HCl. Pepsin (13.9 mg) and fungal gastric lipase (27.8 mg) were then added to the sample. After an hour of gastric digestion at 37 °C, the pH of the sample was then adjusted using HCl or NaOH (0.2-5.0 M) to a value of 6.500 ± 0.003 to mimic intestinal conditions before 2.25 mL of reconstituted pancreatic lipase suspension was injected into the sample. The lipase suspension was prepared by dispersing pancreatin in water followed by centrifugation before freeze-drying the supernatant to provide a powder form. This freeze-dried pancreatic lipase was dispersed in the digestion buffer (50 mM trizma-maleate buffer at pH 6.5, which also contained 5 mM $CaCl_2.2H_2O$ and 150 mM sodium chloride and 6 mM sodium azide). The activity of pancreatic lipase was approximately 700 tributyrin units/mL of digest (measured independently by adding 2 mL of reconstituted lipase solution to 6 g of tributyrin stirred vigorously with 18 mL of digestion buffer).

Throughout the digestion of the colostrum and human milk lipids, 0.2 M NaOH was added to maintain the pH at 6.5 to counter the decrease in pH as a result of the liberation of FFAs. Assuming that the consumption of NaOH was only through the evolution of ionised FFAs by lipolysis, the amount of titrated (ionised) FFAs was determined following the subtraction of the volume of NaOH (required to maintain the pH at 6.5) from the blank digestion (colostrum/milk with the lipids removed). To prepare this blank digestion, 30 mL of colostrum/milk was centrifuged at 4500 *g* at 4 °C for 15 min before removing the lipid layer and collecting the supernatant (which was measured to contain around 0.2% lipid using gravimetric analysis as described in section 3.3.3.1). After 120 min of intestinal digestion of either colostrum/human milk or the blank, the pH of the digested milk was increased to pH 9.0 using NaOH ('back titration'), for which the molar amount of NaOH required corresponds to the amount of unionised FFAs once the background and back-titration are subtracted. Together with the amount of ionised FFAs determined earlier, the total amount of FFAs released during digestion was calculated. Based on the GC-FID results and previous literature reports, the theoretical amounts of FFAs released by the colostrum, mature non-pasteurised and pasteurised human milk samples were approximately

1.58, 2.85 and 2.66 mmol, respectively [87]. Subsequently, the extent of digestion was calculated using Equation 1 assuming that 1 mol of TAG generates 2 mol of FFAs:

$$Extent\ of\ digestion\ (\%) = \frac{Ionised\ FFAs\ (mmol) + Unionised\ FFAs\ (mmol)}{Theoretical\ FFAs\ in\ colostrum\ or\ human\ milk} \times 100\% \quad (1)$$

3.3.5.1 Effects of different concentrations of calcium and human milk fat content on digestion

The initial concentration of calcium in the digestion buffer was set at either 5 or 100 mM. For the digestion experiments using 'high fat milk', 20 mL of human milk and freeze-dried digestion buffers were added to the vessel. These freeze-dried digestion buffers were prepared by aliquoting 5 mL of either 5 or 100 mM calcium digestion buffer into 20 mL glass scintillation vials and freeze-dried for approximately 48 h using a VirTis Wizard 2.0 freeze dryer. The freeze-dried digestion buffers (285 mg) were weighed in 20 mL glass scintillation vials using an analytical balance before adding to the 'high fat milk' samples. For the experiments involving 'low fat milk', the colostrum and milk samples were diluted 4-fold i.e. 5 mL of colostrum/milk was added to 15 mL of digestion buffer with added calcium such that the final calcium concentrations were 5 or 100 mM. Based on the gravimetric and GC-FID analyses (section 3.3.3), the fat content of human colostrum, mature non-pasteurised human milk and pasteurised DHM are shown in **Table 3.3** below. The digestion experiments were then conducted following the protocol above in section 3.3.5.

Table 3.3. Fat content of human colostrum, mature non-pasteurised milk and pasteurised donor human milk (DHM).

Sample	Fat content (*w/v%*)	
	High fat	**Low fat**
Human colostrum	3.3	0.8
Mature non-pasteurised human milk	4.3	1.1
Pasteurised DHM	3.7	0.9

3.3.5.2 Preparation of bile salt micelles

DOPC (102 mg) was weighed in a round bottom flask using an analytical balance before dissolving it in chloroform. The chloroform was then removed using a rotary evaporator (initially 400 mbar, 50 rpm, 40 °C and the pressure was continuously decreased to 0 mbar). Following this, 327 mg of sodium taurodeoxycholate hydrate was added to the dried extract. Approximately 90 mL of 50 mM trizma-maleate buffer at pH 6.5 was then added to the same round bottom flask. The mixture was then bath sonicated and made up to a total volume of 100 mL. The final concentration of bile salt and phospholipid was 4.7 mM and 1.0 mM respectively.

3.3.6 Small angle X-ray scattering (SAXS): flow through measurements

Small angle X-ray scattering (SAXS) experiments were conducted according to the methods described in 'Chapter 2.2.6 *In vitro* lipolysis coupled to small angle X-ray scattering (SAXS): flow through measurements'. An X-ray beam with a photon energy of 13.0 keV (wavelength, λ = 0.954 Å)

was utilised in this investigation. A sample-to-detector distance of around 1.7 m (q range of approximately $0.01 < q < 1.09$ Å^{-1}) was used to monitor the LC structures formed during digestion. The equations for calculating the lattice parameter of each LC phase are defined in Chapter 2 in section '2.2.5 Determination of colloidal structures using small angle X-ray scattering (SAXS)'.

3.3.7 Small angle X-ray scattering (SAXS): precipitated calcium soaps

Calcium soaps of oleic acid and oleic acid mixed with monopalmitin (FFA:MAG ratio = 2:1) were prepared using a previously reported procedure [136]. Briefly, the lipids were dissolved in absolute ethanol saturated with calcium chloride ([lipids] ~ 20 mg/mL). Calcium soaps were then precipitated by adding ethanolic sodium hydroxide solution (0.117 M) such that the moles of sodium hydroxide matched the number of moles of lipid in the mixtures. The dispersions were loaded into special glass capillaries (Charles Supper, Natick, MA) and placed directly in the path of the X-ray beam (wavelength = 0.954 Å, photon energy = 13.0 keV) for measurement of their scattering patterns. 2D SAXS patterns were recorded with a Pilatus 1M detector and an acquisition time of 1 s. The sample-detector distance was ~1.6 m, which gave an accessible q-range of 0.013–0.652 Å^{-1}. An example of an X-ray scattering profile of calcium soaps is presented in **Fig. 3.6** and the C-H stretching vibrations from calcium-free fatty acid complexes shown in **Fig. A1** in the 'General Appendix' section.

3.3.8 Free fatty acid (FFA) composition analysis using GC-FID

3.3.8.1 Preparation of free fatty acid methyl esters (FAME) from human colostrum and milk

A solid phase extraction method as previously described by Agren *et al.*, was adopted to separate FFAs from the other components of human colostrum, mature non-pasteurised human milk and pasteurised DHM using a single aminopropyl column [190]. Briefly, 500 mg/6 mL ISOLUTE® aminopropyl columns (Biotage, Uppsala, Sweden) were washed with acetone/water (7:1, *v/v*) and hexane. The digested human colostrum and milk aliquots (1 mL each collected during digestion described in section 3.3.5 with no back-titration step and lipolysis inhibited with 1 *v/v*% 0.5 M 4-BPBA in methanol) were dissolved in 4.84 mL hexane/0.145 mL *tert*-butyl methyl ether/0.0145 mL acetic acid (100:3:0.3, *v/v*) mixture and applied to the column after centrifugation. The FFAs were eluted with chloroform/methanol/acetic acid (100:2:2, *v/v*) and collected in round bottom flasks. The collected FFAs were then evaporated to dryness in a rotary evaporator (initially 400 mbar, 50 rpm, 40 °C and the pressure was continuously decreased to 0 mbar to remove any traces of volatile solvent remaining). Following this, 200 µL of hexane was added to the dried extract.

To derivatise the FFAs into free FAMEs, methanolic HCl (3 M) was used as the derivatising agent. In an amber glass vial equipped with rubber-lined screw caps, the FFAs dissolved in hexane were added to 240 µL of internal standard FAME C11:0, prepared in the same solvent, 240 µL internal

standard TAG C13:0, 1.6 mL of methanol, 1.6 mL of methanolic HCl and 667 µL of hexane. The vials were firmly capped, shaken vigorously and heated at 100 °C for 1 h. After cooling down to room temperature, 1.56 mL of water was added and shaken vigorously before centrifugation at 1200 *g* for 5 min. The upper organic layer was then transferred into GC vials for analysis.

3.3.8.2 Chromatographic conditions for FAME analysis

A polar column (70% cyanopropyl polysilphenylene-siloxane) with a length of 30 m, an internal diameter of 0.25 mm and a film thickness of 0.25 µm was used for the analyses of free FAMEs (Trajan Scientific Pty Ltd, Australia). The samples (1 µL) were injected into a PTV split injector (split ratio 1:50). The temperature of the injector port was maintained at 250 °C throughout the run. Oven conditions were: 60 °C, held for 2.0 min, increased to 200 °C at 10 °C/min and increased to 240 °C at 5 °C/min and temperature held for 1.0 min. The carrier gas was helium (1.00 mL/min, constant flow) and the FID was kept at 250 °C. The average concentration of each FAME was automatically determined by the instrument software. Following this, the average concentration of each FFA was calculated using the response factor as described in the following section 3.3.8.3. The variation in the amount of each FFA released during the digestion of colostrum, mature non-pasteurised human milk and pasteurised DHM was subsequently determined using principal component analysis (PCA) in Orange software (version 3.22.0) developed by the University of Ljubljana [191].

3.3.8.3 Calculation to determine the concentration of each free fatty acid (FFA)

The response factor (RF) for each FAME present in the calibration standard solution is calculated relative to the internal standard (IS) as follows [192]:

$$RF = \frac{\%\ mass\ of\ FAME\ standard\ in\ mix\ \times area\ of\ IS}{\%\ mass\ of\ IS\ \times area\ of\ FAME\ standard\ in\ mix}$$

Based on the RF values and area under each peak of FAME using GC-FID, the concentration of each FAME was determined:

$$Concentration\ of\ FAME = \left(\frac{Adjusted\ area\ of\ FAME}{Area\ of\ IS} \div RF\ of\ FAME\right) \times concentration\ of\ IS$$

The concentration of each FFA was then calculated using the stoichiometric factor (Si) to convert FAME to FFA (**Table 3.4**):

Table 3.4. Conversion of free fatty acid methyl ether (FAME) to free fatty acid (FFA) based on the molecular weight of FAME, their respective homogenous triglyceride (TAG) and stoichiometric factor (Si) [192].

Fatty acid	Molecular weight of FAME (g/mol)	Molecular weight of TAG (g/mol)	Si of FAME
C4:0	102.1	302.4	0.98727
C6:0	130.2	386.5	0.98950
C8:0	158.3	470.7	0.99116

C10:0	186.3	554.9	0.99284
C11:0	200.3	596.9	0.99334
C12:0	214.4	639.0	0.99347
C13:0	228.4	681.1	0.99402
C14:0	242.4	723.2	0.99450
C15:0	256.4	765.3	0.99493
C16:0	270.5	807.3	0.99482
C17:0	284.5	849.4	0.99520
C18:0	298.5	891.5	0.99553
C18:1	296.5	885.5	0.99550
C18:2	294.5	879.4	0.99536
C18:3	292.5	873.4	0.99533

$$Si\ (TAG) = \frac{Molecular\ weight\ of\ TAG}{3 \times molecular\ weight\ of\ FAME}$$

3.4 Results

The results and discussion in this chapter primarily revolves around understanding the digestion behaviour of mature non-pasteurised human milk, pasteurised DHM and human colostrum and correlating how the lipid composition prior to digestion and FFA composition released during the digestion of these milk/colostrum systems influence the self-assembly of lipids.

3.4.1 Digestion of mature non-pasteurised human milk and pasteurised DHM

3.4.1.1 Effect of gastric step on the overall (gastric + intestinal) digestibility of human milk

The formation of self-assembled structures during digestion is dependent on the extent of conversion of the non-polar TAGs to polar MAGs and FFAs. Thus, it is important that digestion is as close to complete as possible for the findings to represent the potential *in vivo* situation. Initially, (as-supplied) mature non-pasteurised human milk (5.9% fat) and pasteurised DHM (5.5% fat) were digested in the simulated small intestinal condition at pH 6.5 and without digestion buffer, that is, no added calcium and salts. The extents of digestion were low; only 45.4 ± 7.6% and 27.5 ± 4.6% of the lipids in non-pasteurised milk and pasteurised DHM were digested, respectively (**Fig. 3.2a**). Additionally, although a gastric digestion step (pH 3.0) was introduced prior to the intestinal digestion (pH 6.5), the extents of digestion of non-pasteurised milk (50.5 ± 8.4% digested) and pasteurised DHM (39.8 ± 6.7% digested) did not result in a significant increase to the intestinal phase of digestion (**Fig. 3.2b**). Particle size distributions of the non-pasteurised milk and pasteurised DHM are shown in **Fig. 3.2c**, with an averaged $D_{4,3}$ of 53.2 μm and 118 μm, respectively. Due to the smaller particle size distribution of the non-pasteurised lipid droplets than pasteurised DHM, this resulted in a faster rate and greater extent of digestion of non-pasteurised than pasteurised milk (**Fig. 3.2**).

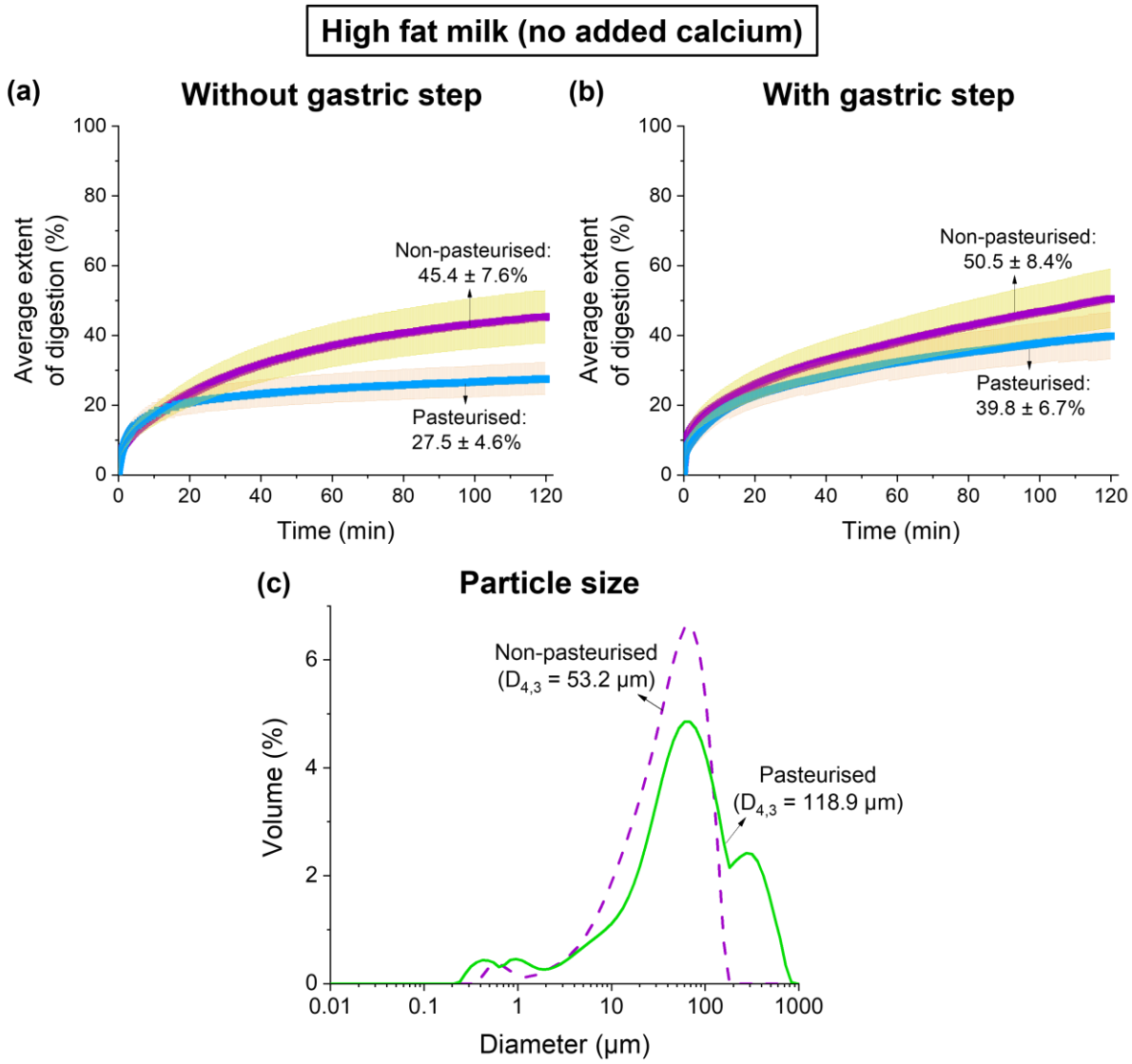

Figure 3.2. Extent of digestion of (as-supplied) high fat non-pasteurised human milk (purple with yellow error bars; 5.9% fat) and high fat pasteurised donor human milk (blue with orange error bars; 5.5% fat) by pancreatic lipase at pH 6.5 (a) without a gastric pre-digestion step and (b) with a gastric digestion step. (c) Particle size distributions of non-pasteurised (purple dashed line) and pasteurised donor human milk (green solid line).

3.4.1.2 Effect of varying levels of calcium and fat content on the digestibility of human milk

To drive the extent of digestion further towards completion (to be more representative of the situation *in vivo*), calcium was added during the digestion of human milk at a final concentration of 5 mM and 100 mM. The results in **Fig. 3.3a and b** show that the digestibility of both types of human milk were affected by increasing the concentration of calcium. With an added calcium concentration of 5 mM, 62.5 ± 6.2% and 42.1 ± 8.1% of the non-pasteurised milk and pasteurised DHM were digested, respectively (**Fig. 3.3a**) with **Fig. A1** ('General Appendix' section) illustrating the localisation of the digested milk components. When the added concentration of calcium was increased from 5 to 100 mM, the final extent of digestion of non-pasteurised milk increased to 77.3 ± 7.4% and that of pasteurised

DHM to 54.6 ± 9.1% (**Fig. 3.3b**). However, as incomplete digestion was still observed, the samples were diluted 4-fold to reduce the fat content of mature non-pasteurised human milk and pasteurised DHM relative to calcium. Comparing the same calcium levels, the decrease in fat content led to an increase in extent of digestion for both types of human milk. For instance, at 5 mM calcium, the extents of digestion of low-fat mature non-pasteurised human milk (1.5% fat) and pasteurised DHM (1.4% fat) increased to 77.4 ± 3.9 % and 61.3 ± 5.5%, respectively (**Fig. 3.3c**) as compared to when high-fat human milk samples were used (**Fig. 3.3a**).

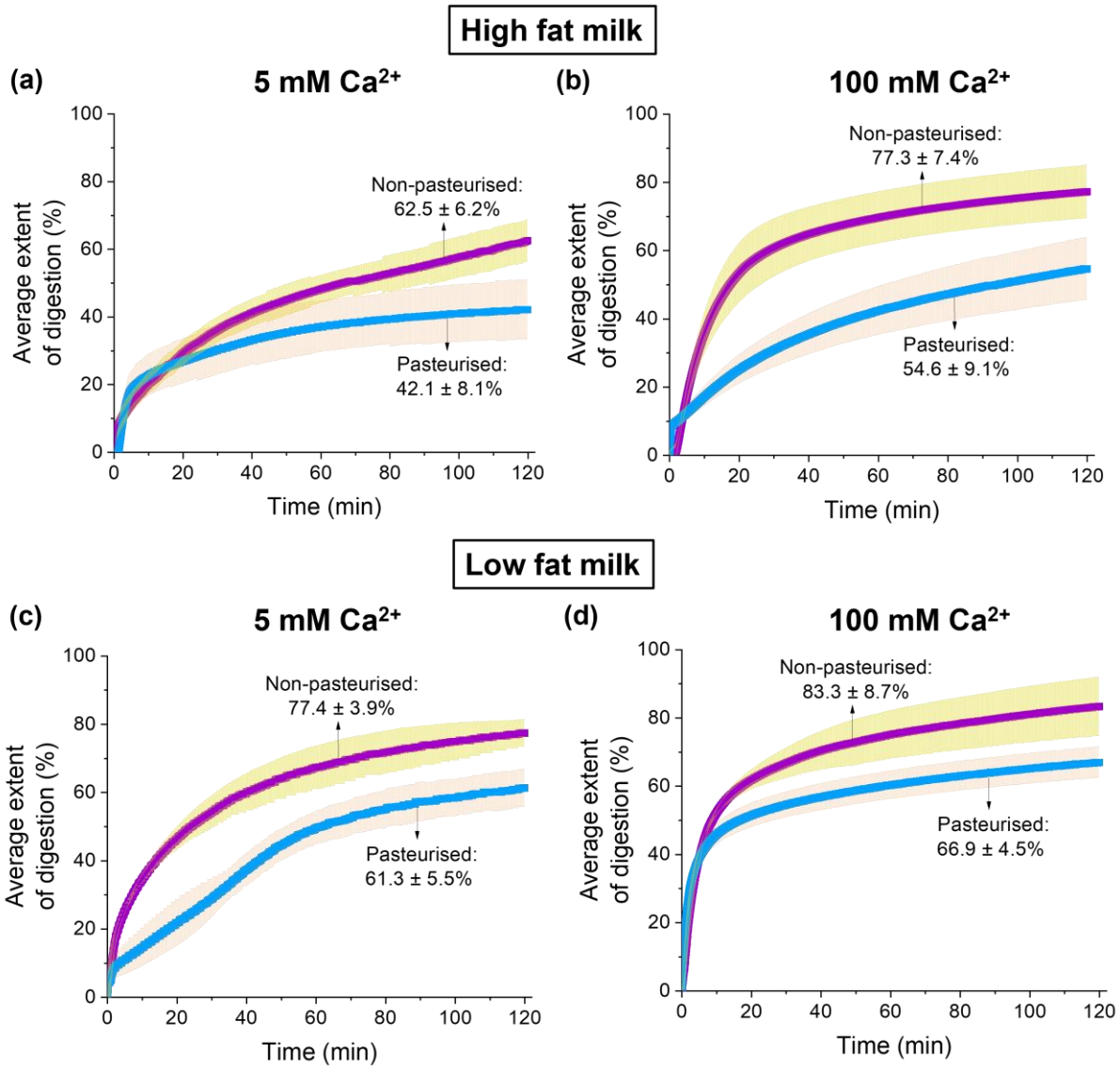

Figure 3.3. Extent of digestion of high fat non-pasteurised human milk (purple with yellow error bars; 5.9% fat) and high fat pasteurised donor human milk (blue with orange error bars; 5.5% fat) when (a) 5 mM and (b) 100 mM calcium were included in the digestion buffers. The effect of fat content was also investigated by using low fat non-pasteurised human milk (purple with yellow error bars; 1.5% fat) and low fat pasteurised donor human milk (blue with orange error bars; 1.4% fat) with (c) 5 mM and (d) 100 mM calcium.

3.4.1.3 Effect of bile salt micelles on the digestibility of human milk

While increasing the ratio of calcium:fat increased the extent of digestion of the human milk samples, the addition of bile salt micelles to the low-fat milk systems with high calcium level (100 mM calcium) led to a decrease in the particle size distribution (**Fig. 3.4a and b**) while causing a significant increase in the extent of digestion of both types of human milk (90.1 ± 6.8% digestion for mature non-pasteurised human milk and 70.4 ± 7.1% digestion for pasteurised DHM) (**Fig. 3.4c**). Moreover, when the gastric step was included in the digestion, mature non-pasteurised human milk attained essentially complete digestion of 96.9 ± 3.1% within 20 min of digestion while that of pasteurised DHM was 80.7 ± 9.3% after 120 min of digestion (**Fig. 3.4d**).

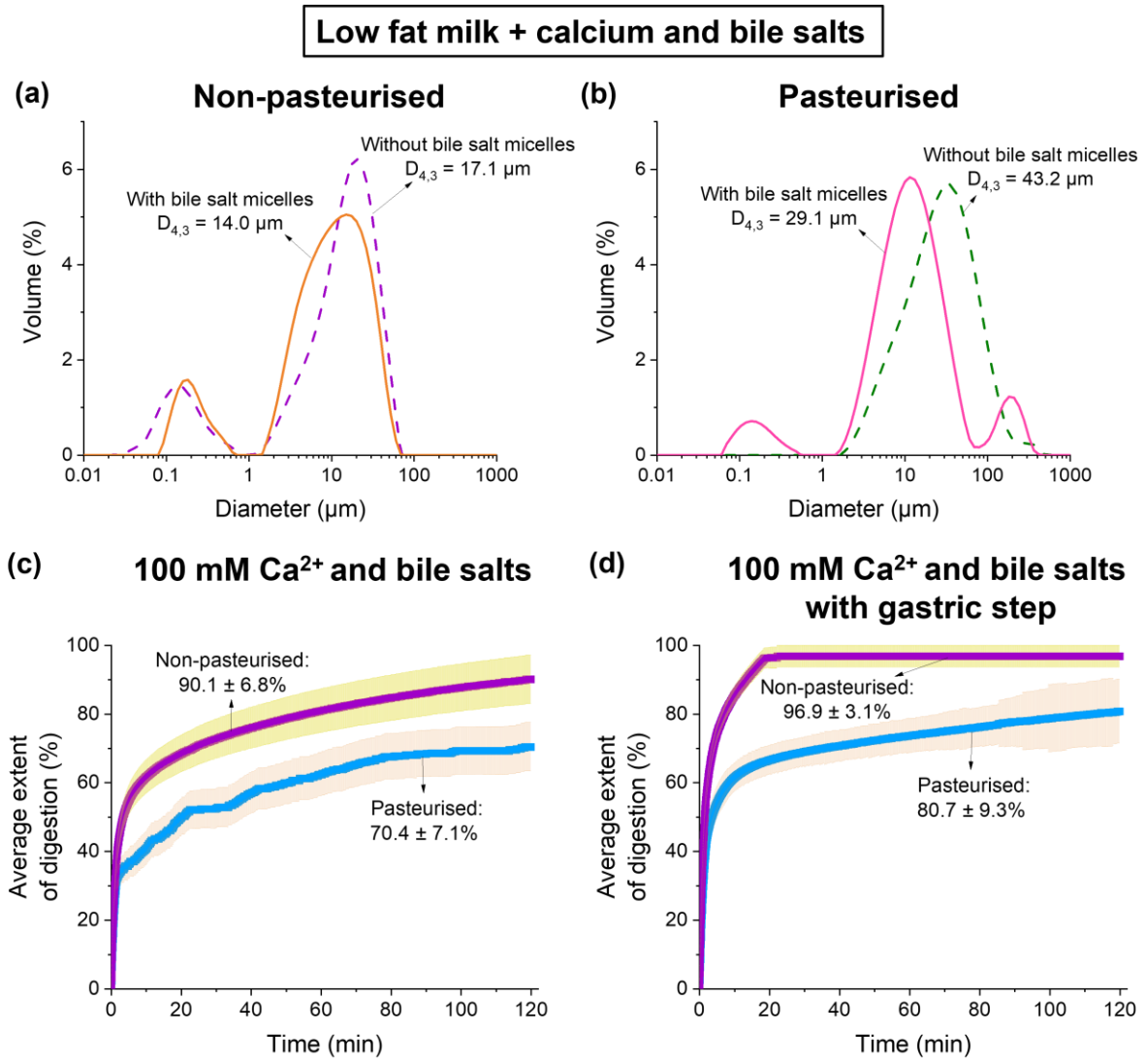

Figure 3.4. (a) Particle size distributions of digested non-pasteurised human milk (1.5% fat) without bile salt micelles (dashed purple line) and with bile salt micelles (orange line). (b) Particle size distribution of digested pasteurised donor human milk (1.4% fat) without bile salt micelles (dashed green line) and with bile salt micelles (pink line). Extent of digestion of low fat non-pasteurised human milk (purple with yellow error bars; 1.5% fat) and low fat pasteurised donor human milk (blue with

orange error bars; 1.4% fat) at pH 6.5 when 100 mM and bile salt micelles were added into mixtures (c) without gastric step and (d) with gastric step.

3.4.1.4 Effect of particle size on the digestibility of human milk

Aside from altering the concentration of calcium added to the digestion buffers, lowering the fat content or adding bile salt micelles to the samples, another way of accelerating the digestion process is through reducing the particle size of the lipid droplets in these milk systems. Following sonication, the particle size distributions of the mature non-pasteurised human milk and pasteurised DHM lipid droplets decreased to an average of $D_{4,3}$ = 6.0 μm and 13.6 μm, respectively (**Fig. 3.5a**). Taking low fat human milk samples with 5 mM calcium as the digestion conditions (**Fig. 3.3c**), the effect of reduction in particle size not only resulted in faster kinetics of digestion for both human milk samples but the sonicated non-pasteurised milk samples was observed to be completely digested (94.3 ± 5.7%) and the extent of digestion of pasteurised milk increased to 79.4 ± 8.7% (**Fig. 3.5b and c**). Similar trends were observed in high-fat milk, confirming the effects of particle size on lipid digestion (**Fig. A2** in the 'General Appendix' section).

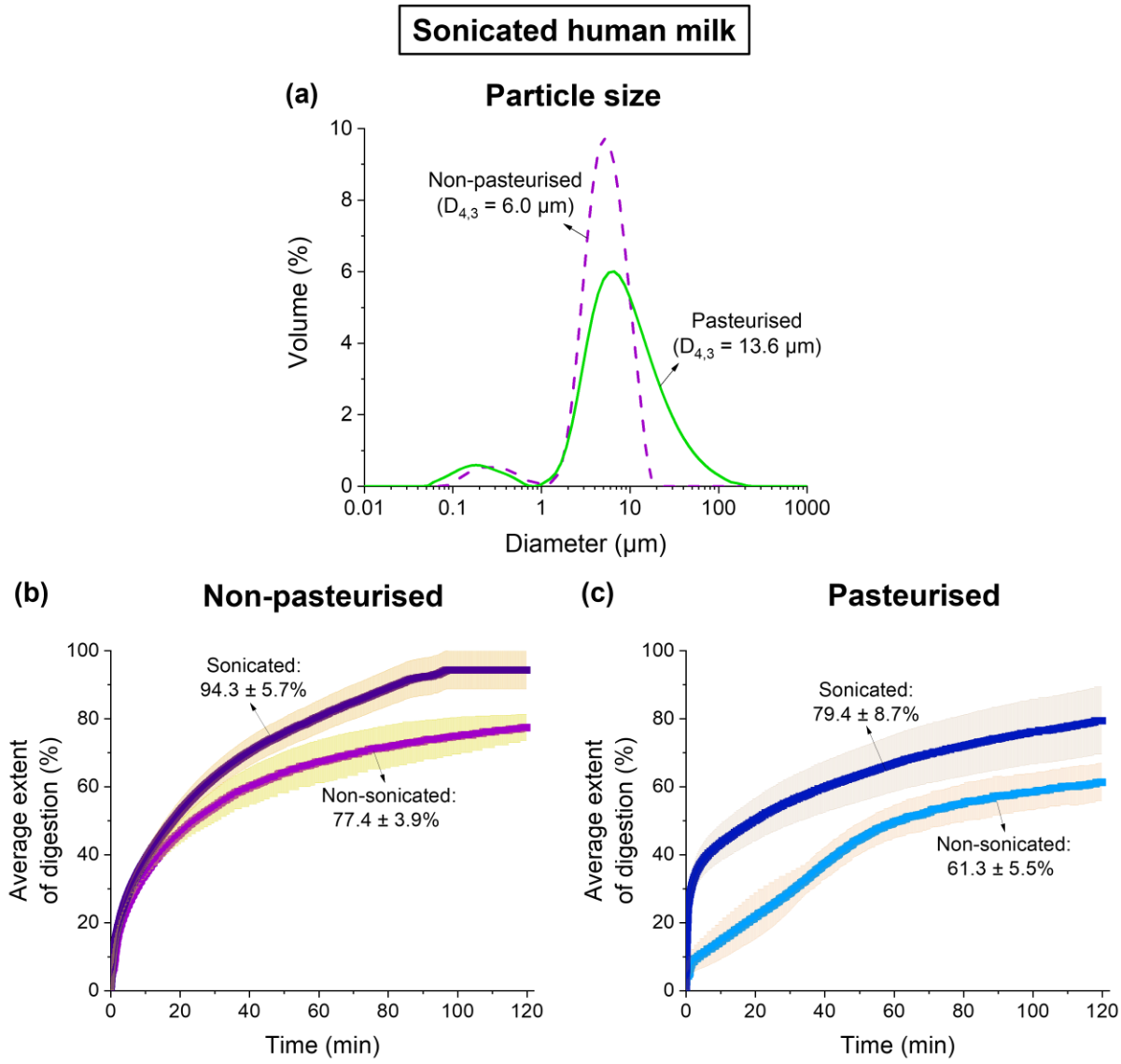

Figure 3.5. (a) Particle size distributions of sonicated non-pasteurised (purple dashed line) and pasteurised donor human milk (green solid line). (b) Extent of digestion of low fat (1.5% fat) non-sonicated (light purple with yellow error bars) and low fat (1.1% fat) sonicated non-pasteurised human milk (dark purple with orange error bars). (c) Extent of digestion of low fat (1.4% fat) non-sonicated (light blue with orange error bars) and low fat (0.9% fat) sonicated pasteurised donor human milk (dark blue with brown error bars).

3.4.2 Effect of increasing extents of digestion on the self-assembly of human milk lipids

It has been shown previously that a series of lipid LC structures appear during the digestion of human milk as a result of the self-assembly of amphiphilic DAGs, MAGs and FFAs [120, 135]. These lipid LC phases were determined based on the positional distribution of their respective diffraction peaks using the equations provided in Chapter 2 section '2.2.5 Determination of colloidal structures using small angle X-ray scattering (SAXS)'. The SAXS profiles were plotted as a function of extent of digestion (**Fig. 3.6 and 3.7**).

Following the addition of pancreatic lipase to mature non-pasteurised human milk with 5 mM calcium, diffraction peaks corresponding to a lamellar structure with a lattice parameter of 46-47 Å were observed and remained persistent throughout digestion (**Fig. 3.6a**). This phase is associated with the formation of calcium soaps through the binding of calcium ions that are naturally found in milk and the digestion buffer used in these *in vitro* experiments (**Fig. 3.6c**) [136]. To mimic the upper intestinal environment, the pH of the digestion buffer was set to 6.5, which resulted in the partial deprotonation of FFAs generated by lipolysis that are reported to have pKa values of 4-9 [193]. It should be noted that under these conditions incomplete digestion occurred, so the generation of self-assembling lipids was potentially limited only to FAs involved in soap formation.

As the concentration of calcium was increased from 5 to 100 mM in the digestion buffers to increase the extent of digestion, not only was a lamellar phase present during digestion but higher order lipid LC phases such as a cubic micellar (I_2) phase with *Fd*3*m* spacegroup (q = 0.065, 0.106, 0.124 $Å^{-1}$) and a H_2 phase (q = 0.134, 0.232 and 0.268 $Å^{-1}$) were observed (**Fig. 3.6a**). Moreover, a diffraction peak (q = 0.198 $Å^{-1}$) that is typically associated with a disordered inverse micellar L_2 phase was also observed when 100 mM calcium was included in the digestion buffer (**Fig. 3.6a**).

In contrast, the digestion of pasteurised DHM at 5 mM calcium resulted in the formation of a cubic micellar I_2 phase (*Fd*3*m* spacegroup) with peaks at q = 0.0712, 0.116, 0.136, 0.142, 0.164 $Å^{-1}$ in addition to a persistent lamellar phase (**Fig. 3.6b**), with the extent of digestion being 42.1 ± 8.1%. However, when the concentration of calcium was increased to 100 mM, no additional phases were observed for pasteurised DHM (**Fig. 3.6b**) unlike mature non-pasteurised human milk (**Fig. 3.6a**). Instead, a peak at approximately q = 0.189 $Å^{-1}$ that is indicative of a disordered micellar L_2 phase was again observed during the digestion of pasteurised DHM at the same concentration of calcium (**Fig. 3.6b**).

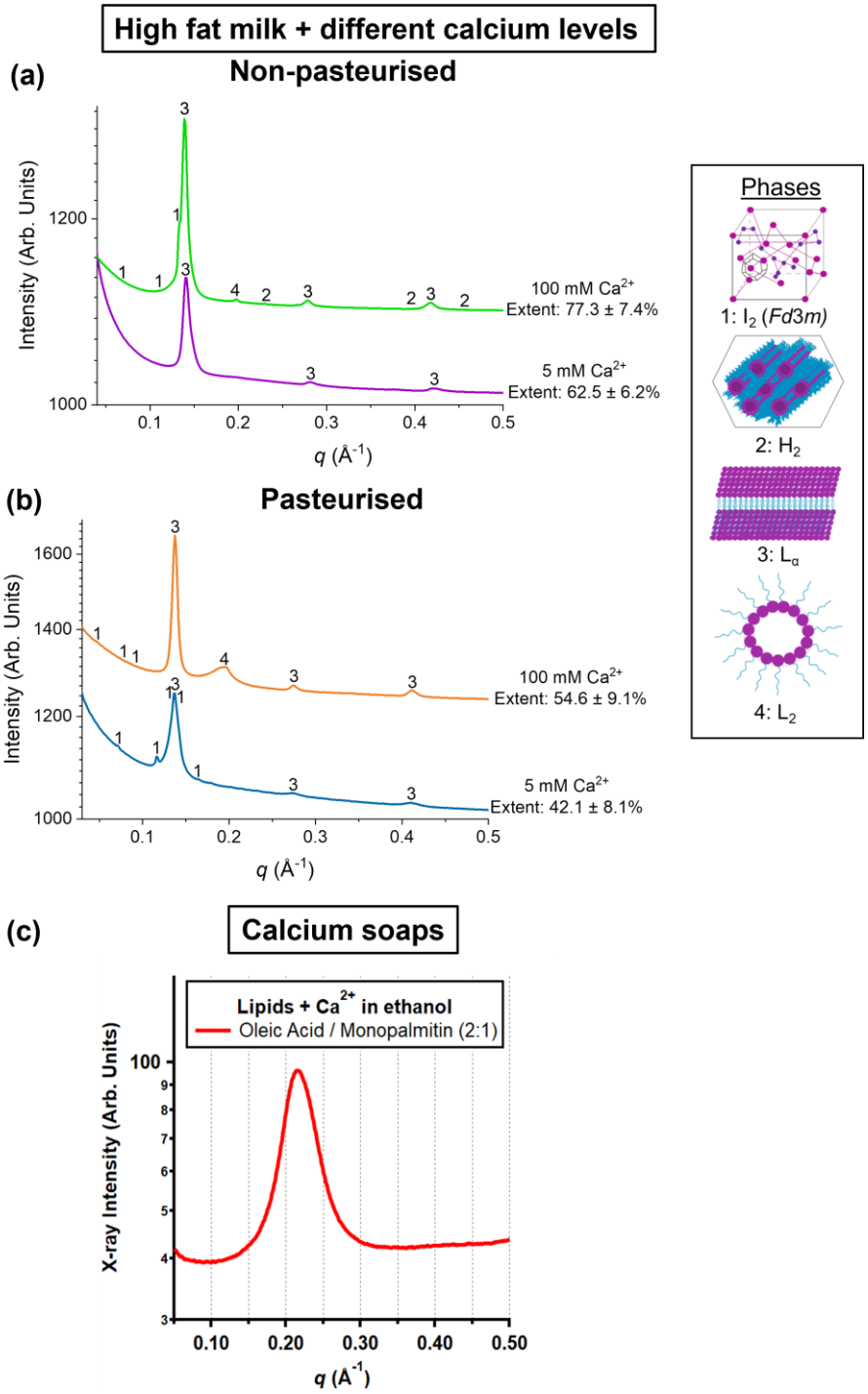

Figure 3.6. SAXS profiles for the digestion of non-sonicated (a) high fat (5.9% fat) non-pasteurised human milk with 5 mM calcium (purple line) and 100 mM calcium (green line) and non-sonicated (b) high fat (5.5% fat) pasteurised donor human milk with 5 mM calcium (blue line) and 100 mM calcium (orange line) after the addition of lipase at pH 6.5, 37 °C. "1" represents the cubic micellar I_2 phase (*Fd*3*m* spacegroup), with peak *q* ratios of √3: √8: √11, "2" is annotated as the hexagonal H_2 phase with peak *q* ratios of 1:√3: √4: , "3" and "4" represent the lamellar L_α phase with peak *q* ratios of 1: 2: 3 and disordered inverse micellar L_2 phase, respectively. (c) X-ray scattering profile of calcium oleate with monopalmitin present. The precipitates were formed by dissolving the lipids in the legend in ethanol saturated with calcium chloride dihydrate before one molar equivalent (with respect to oleic acid) of ethanolic sodium hydroxide was added. The scattering profiles are that of the dispersion in ethanol. (SAXS profiles are offset on the Intensity axis for clarity)

The self-assembly of lipids during the digestion of mature non-pasteurised human milk and pasteurised DHM were the same when the samples were diluted to generate 'low fat milk' (**Fig. 3.7a and b**). However, when bile salt micelles were introduced to the systems, the non-lamellar phases were not observed during digestion (**Fig. 3.7a and b**). Instead, a weak broad peak indicative of a disordered inverse micellar L_2 phase with the peak centred around q = 0.187-0.205 Å was observed for both types of human milk.

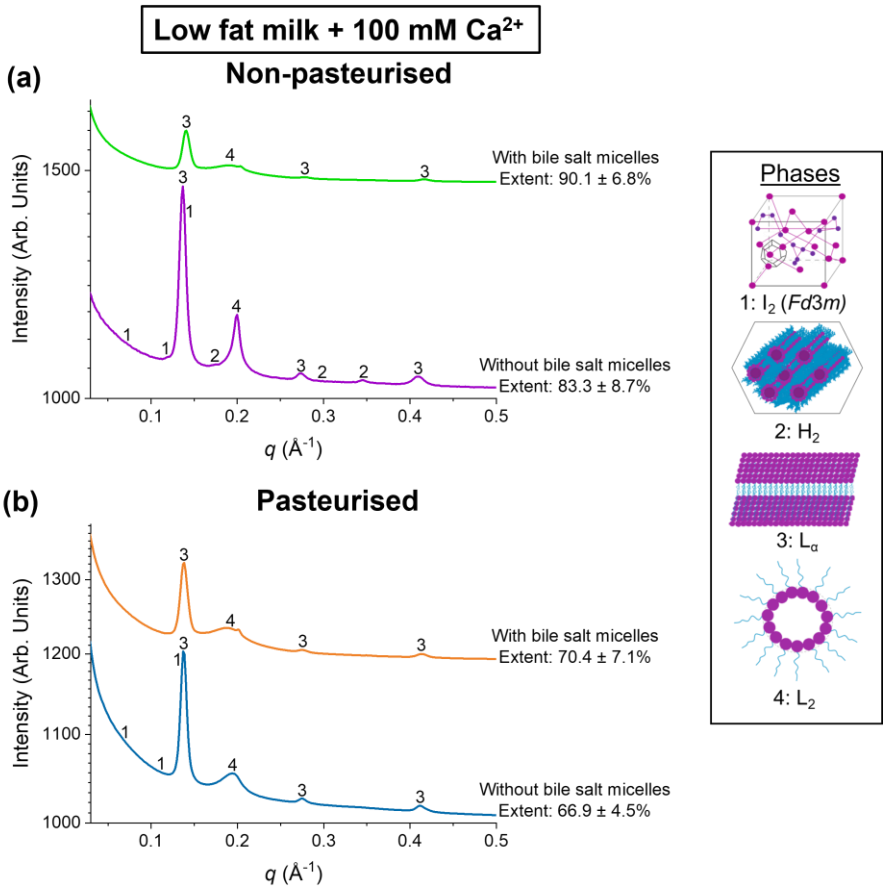

Figure 3.7. (a) SAXS profiles for the digestion of non-sonicated low fat (1.5% fat) non-pasteurised human milk with 100 mM calcium in the absence of bile salt micelles (purple line) and with bile salt micelles (green line). (b) SAXS profiles for the digestion of non-sonicated low fat (1.4% fat) pasteurised donor human milk with 100 mM calcium in the absence of bile salt micelles (blue line) and with bile salt micelles (orange line) after the addition of lipase at pH 6.5, 37 °C. "1" represents the cubic micellar I_2 phase (*Fd*3*m* spacegroup), with peak q ratios of √3: √8: √11, "2" is annotated as the hexagonal H_2 phase with peak q ratios of 1:√3: √4: , "3" and "4" represent the lamellar L_α phase with peak q ratios of 1: 2: 3 and disordered inverse micellar L_2 phase, respectively. (SAXS profiles are offset on the Intensity axis for clarity)

3.4.3 Comparison of the digestibility and structural behaviour of lipids between human milk and colostrum

The above sections illustrate that the digestion process of human milk can be accelerated through factors such as introducing a gastric step, altering the calcium and fat content, adding bile salt micelles and reducing the particle size of lipid droplets. These factors were hypothesised to exert similar

effects on the digestibility of human colostrum as well. However, due to the limited supply of human colostrum, the number of variables that could be explored was limited so the colostrum samples were diluted 4-fold initially in digestion buffer containing 5 mM calcium. The colostrum samples were thereby diluted from fat content of 3.3% (high fat colostrum) to 0.8% (low fat colostrum) (section 3.3.5.1 **Table 3.3**). In addition, only non-sonicated colostrum samples with an average particle size distribution of $D_{4,3}$ = 1.8 μm (**Table 3.5**) were used in the following digestion experiments. Although sonicated non-pasteurised milk displayed the greatest extent of digestion (94.3 ± 5.7%), the final extent of digestion of colostrum was still within error of the former (**Fig. 3.8a**).

Despite the smaller particle size distribution of the colostrum lipid droplets than both human milks (**Table 3.5**), pasteurised DHM showed the fastest initial rate of digestion while non-pasteurised milk digested the fastest towards the later stages of digestion. Regardless of the differences in kinetics of digestion, the final average extent of digestion of colostrum was similar to that of non-pasteurised milk.

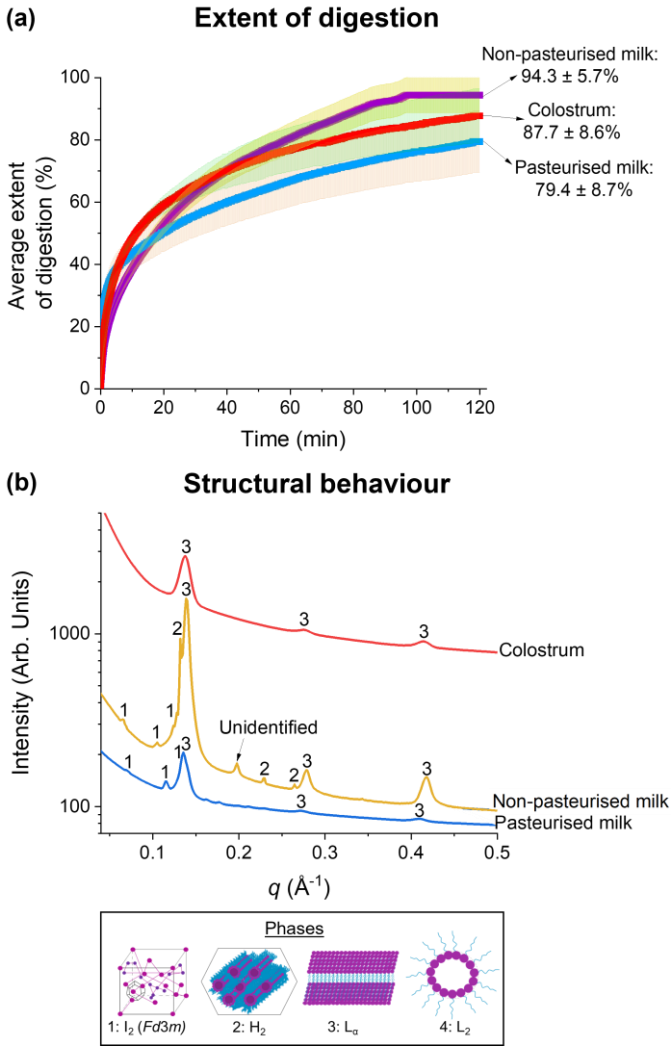

Figure 3.8. (a) Extent of digestion of non-sonicated low fat human colostrum (red with green error bars; 0.8% fat), sonicated low fat non-pasteurised human milk (purple with yellow error bars; 1.1% fat) and sonicated low fat pasteurised donor human

milk (blue with orange error bars; 0.9% fat) at pH 6.5 when 5 mM calcium was added into mixtures with gastric step. (b) Corresponding SAXS profile for the digestion of colostrum (red), non-pasteurised milk (yellow) and pasteurised donor human milk (blue) after the addition of lipase at pH 6.5, 37 °C. "1" represents the cubic micellar I_2 phase (*Fd*3*m* spacegroup), with peak *q* ratios of √3: √8: √11, "2" is annotated as the hexagonal H_2 phase with peak *q* ratios of 1:√3: √4: , "3" and "4" represent the lamellar L_α phase with peak *q* ratios of 1: 2: 3 and disordered inverse micellar L_2 phase, respectively (SAXS profiles are offset on the Intensity axis for clarity).

The structural behaviour of colostrum was different to the other milks during and at the end of digestion. Despite human colostrum digesting to a similar extent as that of mature non-pasteurised human milk and pasteurised DHM under similar conditions (low fat colostrum/milk with 5 mM calcium) (**Fig. 3.8a**), only a lamellar phase was formed and persisted throughout the digestion of colostrum (**Fig 3.8b**). The absence of additional non-lamellar phases such as the cubic micellar and H_2 structures could instead be due to variations in the composition of FFAs released during the digestion of colostrum compared to the other milk systems (sections 3.4.5 and 3.4.6). A summary of the extents of lipid digestion and the corresponding types of lipid LC structures formed during the digestion of mature non-pasteurised human milk, pasteurised DHM, and human colostrum are presented in **Table 3.5** below.

Table 3.5. Summary table of the different digestion conditions of mature non-pasteurised human milk, pasteurised donor human milk (DHM), and human colostrum and the corresponding particle size, maximum extent of digestion and the liquid crystal structures formed. Note that fewer digestive conditions were able to be trialled for human colostrum due to its limited supply.

Digestion conditions						
Fat content	**Added calcium (Ca^{2+}) concentration (mM)**	**Bile salt micelles**	**Sonicated**	**$D_{4,3}$ (µm)**	**Maximum extent of digestion (%)**	**Phases and lattice parameter (or characteristic distance for L_2) (Å)**
Mature non-pasteurised human milk						
High	-	-	No	53.2	45.4 ± 7.6	L_α: 45
High	5	-	No	26.9	62.5 ± 6.2	L_α: 46
Low	5	-	No	24.4	77.4 ± 3.9	L_α: 44
Low	5	-	Yes	6.0	94.3 ± 5.7	L_α: 46;*Fd*3*m*: 165; H_2: 54
High	100	-	No	24.0	77.3 ± 7.4	L_α: 47; *Fd*3*m*: 167; H_2: 56; L_2: 37
Low	100	-	No	17.2	83.3 ± 8.7	L_α: 46; *Fd*3*m*: 164; H_2: 55; L_2: 40
Low	100	Yes	No	14.0	90.1 ± 6.8	L_α: 45; L_2: 38
Pasteurised DHM						
High	-	-	No	118.9	27.5 ± 4.6	L_α: 46
High	5	-	No	72.5	42.1 ± 8.1	L_α: 46; *Fd*3*m*: 164
Low	5	-	No	65.9	61.3 ± 5.5	L_α: 45; *Fd*3*m*: 162
Low	5	-	Yes	13.6	79.4 ± 8.7	L_α: 44; *Fd*3*m*: 163
High	100	-	No	60.3	54.6 ± 9.1	L_α: 47; *Fd*3*m*: 166; L_2: 38
Low	100	-	No	43.2	66.9 ± 4.5	L_α: 46; *Fd*3*m*: 167; L_2: 40
Low	100	Yes	No	29.1	70.4 ± 7.1	L_α: 47; L_2: 39
Human colostrum						
High	-	-	No	32.1	75.0 ± 6.1	L_α: 44
Low	5	-	No	1.8	87.7 ± 8.6	L_α: 46

3.4.4 Total lipid content and fatty acid (FA) composition of human colostrum and milk

Human colostrum and milk lipids were extracted using a gravimetric analysis and subsequently quantified with GC-FID. As shown in **Table 3.6**, it can be observed that while the average total lipid content increased from 3.3% *w/v* to 4.3% *w/v* as lactation progressed from non-sonicated colostrum to mature non-pasteurised human milk, there was no statistical difference in the lipid content between non-pasteurised milk and pasteurised DHM. Although these trends are consistent with some previously reported studies, other studies indicated either a greater lipid content in colostrum than milk or a significant loss of fat following the pasteurisation of human milk [4, 59, 71, 73, 84, 85, 88, 89, 118, 194-196]. These variations could be due to factors such as the diet, age and parity of mothers [11].

Table 3.6. Total lipid content of human colostrum, mature non-pasteurised human milk and pasteurised donor human milk (DHM) from current study and previously reported studies: human colostrum [4, 59, 84, 85, 88, 194], non-pasteurised and pasteurised human milk [71, 73, 89, 118, 194-196].

	Lipid content (g/ 100 mL)					
	Human colostrum		**Mature non-pasteurised human milk**		**Pasteurised DHM**	
	Non-sonicated	Sonicated	Non-sonicated	Sonicated	Non-sonicated	Sonicated
Current study	3.3 ± 0.5	-	5.9 ± 1.6	4.3 ± 1.0	5.5 ± 1.9	3.7 ± 1.1
Previous studies	2.0 – 4.4		2.5 – 5.4		1.4 – 4.7	

Regardless of the stage of lactation or effects of pasteurisation, colostrum, mature non-pasteurised human milk and pasteurised DHM were abundant in carbon number 52 (C52) TAG (**Fig. 3.9a and b, Table A1**; 'General Appendix' section). This was consistent with previous studies [11, 121, 197]. Within this C52 TAG, it can be inferred that the predominant FA composition is 18:1/16:0/18:1 (O/P/O; oleic/palmitic/oleic). The high abundance of oleic acid (C18:1) is further validated as the FA compositions of colostrum and human milk were also determined in this study (**Fig. 3.9c**). All three samples were rich in long-chain oleic acid (C18:1) followed by palmitic acid (C16:0) (**Fig. 3.9c**).

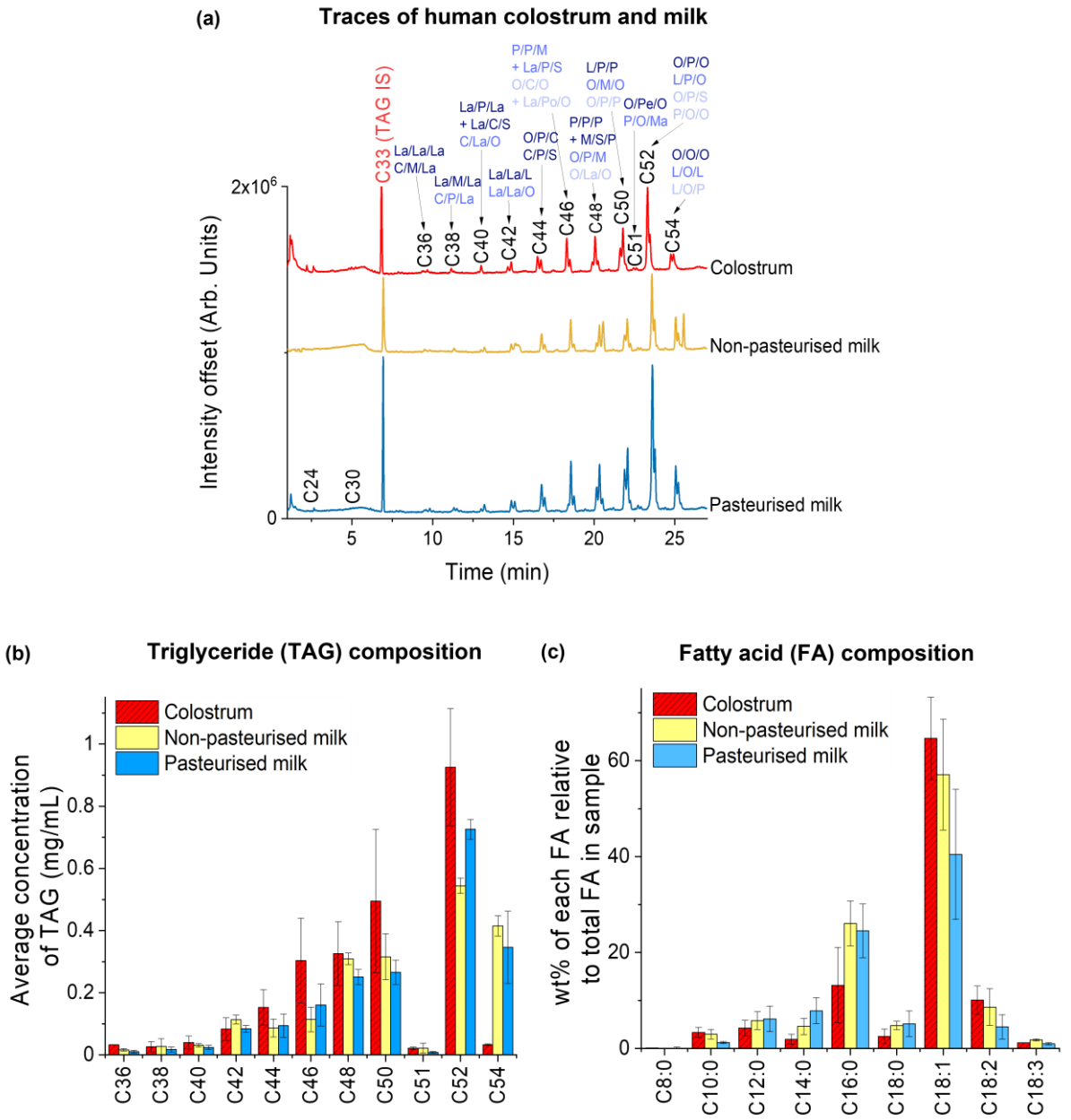

Figure 3.9. Triglyceride (TAG) composition of human colostrum (red), mature non-pasteurised human milk (yellow) and pasteurised donor human milk (blue) used in this study. (a) Gas chromatography coupled to a flame ionisation detector (GC-FID) traces of human colostrum and human milk lipids, dissolved in chloroform. Abbreviations for the FAs are: C – capric (C10:0), La – lauric (C12:0), M – myristic (C14:0), Pe – pentadecanoic (C15:0), P – palmitic (C16:0), Po – palmitoleic (C16:1), Ma – margaric (C17:0), S – stearic (C18:0), O – oleic (C18:1), L – linoleic (C18:2). Triundecanoin [C33 (IS)] was included as an internal standard. (b) The relative amounts of TAGs in human colostrum (red), mature non-pasteurised human milk (yellow) and pasteurised donor human milk (blue). (c) Fatty acid (FA) composition relative to the total FA content in human colostrum (red), mature non-pasteurised human milk (yellow) and pasteurised DHM (red). Results are mean ± SD (n = 3 each).

3.4.5 Composition of free fatty acids (FFAs) released during the digestion of colostrum and human milk

Similar to determining the FA composition of undigested human colostrum and milk, GC-FID was also used to characterise the composition of FFAs produced after 120 min of digestion of these

colostrum and milk lipids. To compare the relative percentages of each FFA released from colostrum and milk, low fat non-sonicated colostrum and sonicated milk samples with added 5 mM calcium were chosen as these digestion conditions resulted in the greatest extent of digestion for these samples. The aim of this aspect was to determine whether the FFA composition did have an influence on the self-assembly of lipids during digestion.

Within the same digestion time frame, sonicated non-pasteurised milk and pasteurised DHM were 94.3 ± 5.7% and 79.4 ± 8.7% digested, respectively while colostrum was 83.3 ± 8.7% digested (**Fig. 3.8a, Table 3.5**). Analogous to the extent of digestion, non-pasteurised milk generated the greatest total amount of 25.9 mg/mL of FFAs whereas colostrum only released 16.9 mg/mL of FFAs under similar *in vitro* intestinal conditions (**Table A2** in the 'General Appendix' section). While there were differences in the percentages of each FFAs released from colostrum, mature non-pasteurised human milk and pasteurised DHM, free oleic acid (C18:1) made up the largest fraction of FFA released from all three systems. However, non-pasteurised milk and pasteurised DHM liberated a higher percentage of oleic acid from the *sn*-1 and *sn*-3 positions than colostrum (**Fig. 3.10**). This is followed by palmitic acid (C16:0), which also accounted for a large proportion of FFAs released being the second largest fraction after oleic acid. Consequently, both non-pasteurised milk and pasteurised DHM released a lower amount of palmitic acid at the *sn*-1 and *sn*-3 positions than colostrum (**Fig. 3.10**). Additionally, the absolute amount of long-chain unsaturated FFAs released from non-pasteurised milk was the greatest followed by pasteurised DHM and colostrum (table insert in **Fig. 3.10**). The high abundance in long-chain unsaturated FFAs resulted in a greater ratio between long-chain saturated to unsaturated FFAs from the human milk systems as compared to colostrum.

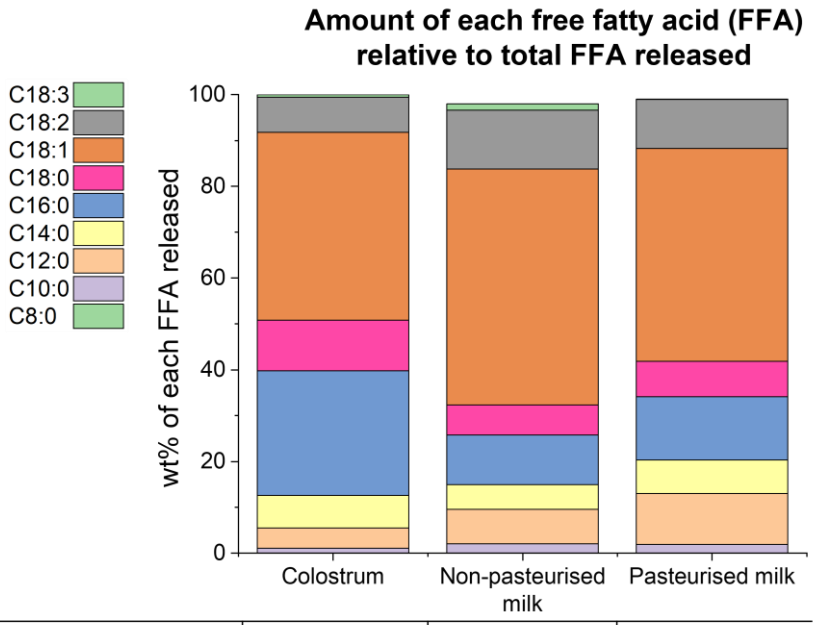

Long-chain saturated (C14:0 + C16:0 + C18:0) (mg/mL)	7.7	5.7	4.1
Long-chain unsaturated (C18:1 + C18:2) (mg/mL)	8.2	17.2	11.0

Figure 3.10. Amount of each free fatty acid (FFA) (*wt%*) released relative to the total FFA from non-sonicated low fat human colostrum (0.8% fat), sonicated low fat low fat (1.4% fat) non-pasteurised milk and sonicated low fat (0.9% fat) pasteurised donor human milk. Note that the total percentage of FFAs do not add up to 100% as only the top 9 species of FFAs are shown, which account for >90% of the lipids detected in human colostrum and milk.

3.4.6 Relationship between free fatty acid (FFA) composition and self-assembly during digestion

Principal component analysis (PCA) was used to probe the relationship between the amount of each FFA released during digestion from colostrum, mature non-pasteurised human milk and pasteurised DHM (**Fig. 3.11**). **Table A2** ('General Appendix' section) summarises the average concentration and weight percent of each FFA released after 120 min of digestion of these samples. The percentages of FFAs released after 120 min of digestion for these systems were used to graph a scores plot (PC1 *vs* PC2) (**Fig. 3.11a**). Based on this plot alone, it can be seen that there is a clear separation between colostrum and human milk, with the final lipid LC structures formed at the end of digestion labelled around the clusters for each sample type. Interestingly, mature non-pasteurised human milk and pasteurised DHM displaying PC1 values < 0 formed I_2, H_2 or both phases whereas colostrum showing PC1 values > 0 formed only a lamellar phase. The corresponding loadings plot for PC1 in **Fig. 3.11b**, which differentiates colostrum from human milk, shows that myristic (C14:0), palmitic (C16:0) and stearic (C18:0) FFAs are in greater abundance in colostrum than mature non-pasteurised human milk and pasteurised DHM, which is also evident from **Table A2** ('General Appendix' section). Since

the PC1 loadings plot accounts for 91% of the variance, other differences in the FFA content of the two milks (accounted for by PC2) were minor (**Fig. 3.11c**).

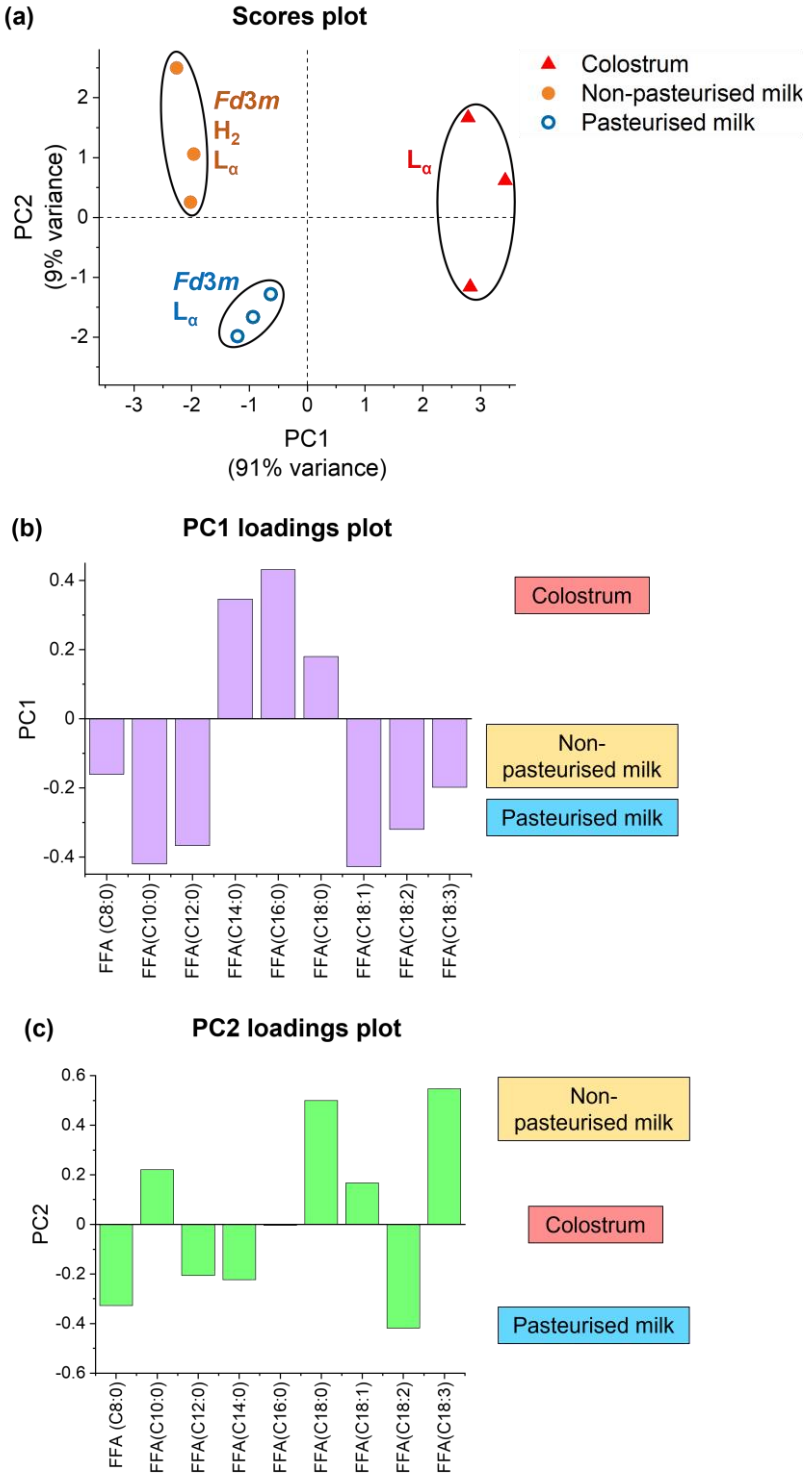

Figure 3.11. (a) Principal component analysis (PCA) scores plot separating colostrum from non-pasteurised milk and pasteurised donor human milk based on the respective percentages of free fatty acids (FFAs) released during digestion after 120 min. (b) PC1 and (c) PC2 loadings plot compares the percentages of FFAs based on the scores plot. Experiments were conducted in triplicate (samples pooled from a single donor), leading to three individual data points in the scores plot.

3.5 Discussion

Human colostrum and milk lipids are considered to be one of the most complex dietary fats with beneficial nutritional properties for infants [198]. Despite variations in the lipid and FA compositions due to disparities in diet, age and parity, human colostrum and milk are considered as a colloidal nutrient delivery system whose function depends on the digestion of lipids in the infant's GIT. TAGs comprise approximately 98 *wt%* of the total lipid fraction, which provides 45-55% of the total energy intake in infants. Regardless of the factors that might influence the composition of lipids and FAs in human colostrum and milk, the digestion of lipids and subsequently absorption of FFAs is important in the development of the brain and central nervous system in infants [13, 143]. Moreover, these digested lipids are able to self-assemble into colloidal structures [14] and potentially act as chaperones to deliver lipophilic nutrients to the systemic circulation.

Since the fate of lipophilic nutrients in the GIT is essential for the development of organs in infants, evaluating the factors that are able to drive the digestion process toward completion is important. First, a gastric step was introduced prior to the intestinal step with an aim to increase the extent of digestion. In adults, intestinal digestion contributes the majority of the lipolysis of TAG to products; however, in the duodenal contents of infants, the bile pool is lower than adults and could be below the critical micelle concentration [199-202]. Furthermore, although gastric lipases in the stomach aid in the digestion process, only 80-90% of lipids would be digested and absorbed in infants as opposed to 95% of lipids being digested in adults. In the current study, mature non-pasteurised human milk and pasteurised DHM were only partially digested after including a gastric step (**Fig. 3.2a and b**). Considering the limited contribution of gastric digestion, it was noted that several *in vitro* digestion studies have demonstrated the use of calcium as a tool to drive the digestion process of long-chain TAGs [203-205]. As the concentration of calcium ions in a mixture is increased, more calcium is available to interact with the FFAs that are located on the oil-water interface of the lipid droplets, thereby exposing fresh TAGs to be digested by pancreatic lipase [188]. This was seen in the present study as both human milks displayed an increase in the extent of lipid digestion as the concentration of calcium in the digestion buffers was increased (**Fig. 3.3a and b**). In addition, as the human milk samples were diluted with the digestion buffer, the fat content was lowered, thereby increasing the ratio of calcium:fat. Thus, this further amplified the increase in extent of digestion of mature non-pasteurised human milk and pasteurised DHM (**Fig. 3.3c and d**).

Aside from increasing the concentration of calcium to enhance the extent of lipid digestion, adding bile salt micelles to the samples can stimulate the digestion of lipids toward completion (**Fig. 3.4c and d**). While lipases in the stomach and small intestine digest TAGs, bile salts aid in the emulsification of chime, thereby decreasing the particle size of the lipid droplets (**Fig. 3.4a and b**). In turn, this increases the overall surface area for lipolysis and thus catalyses the activity of lipases through the removal of digestion products from the oil-water interface in mixed micelles [206]. The

concentration of bile salts has been reported to vary according to age with adults having a bile salt concentration of 5–25 mM and infants having only 1–5 mM bile salts intraduodenally [142]. Based on several studies, the pooled data from 225 infants were calculated to be 4.7 ± 1.4 mM in the fasted state [207-209]. Therefore, this bile salt concentration was used in these digestion experiments. However, despite adding bile salts to high fat pasteurised milk (5.5% fat) with 5 mM calcium, the sample was only partially digested (48.5 ± 8.3%, **Fig. A3** in 'General Appendix' section). Instead, both types of human milk attained almost complete digestion when a high calcium to milk fat ratio and bile salts were added to the systems (**Fig. 3.4c and d**).

Alternatively, it was shown in this study that the extent of digestion of human milk and theoretically colostrum, could instead be driven to completion by sonicating these samples. Milk/colostrum lipid droplets are surrounded by milk fat globular membranes, comprising a trilayer of phospholipids intercalated with an array of glycoproteins and other compounds [210]. During sonication, the milk fat globular membranes are disrupted thereby reducing the particle size of the lipid droplet [211]. Consequently, the reduced particle size caused a larger overall surface area available for hydrolysis by the lipases thereby accelerating the digestion process. While the purpose of analysing the particle size of the lipid droplets was to determine the effect of reducing the particle size on the extent of digestion, non-pasteurised human milk and colostrum are not sonicated prior to feeding an infant, especially in households. Thus, the question remains – why are infants able to fully digest human colostrum/milk lipids without modifying the aforementioned factors (calcium level, fat content and particle size)?

It should hence be noted that *in vitro* digestion models are closed systems, characterised by an absence of a sink to remove the digestion products [162]. As a result, this increases the concentration of lipid digestion products compared with what may be expected *in vivo*, and in turn, leads to the accumulation of digestion products at the oil-water interface [212, 213], which restricts further digestion from occurring. In contrast, in the *in vivo* situation, unlike the *in vitro* model, the presence of a sink enables the removal of digestion products through absorption by the epithelial cells in the small intestine. The concentration of calcium used in these experiments was either 5 or 100 mM, but the typical concentration of calcium in newborns and premature infants in the fasted state ranges from 1.55 to 2.75 mM with premature babies often experiencing hypocalcemia and thereby having a calcium concentration of < 2.00 mM in their body fluids [214]. Moreover, the concentration of calcium in human colostrum and mature human milk was 4.0 and 7.2 mM using ICP-OES in this study (**Table 3.2**). Hence, although the physiological concentrations of calcium are lower than those used in these *in vitro* digestion experiments, infants are still able to digest and absorb human colostrum and milk lipids, presumably to a degree attributable to coincident absorption.

It has been shown previously that during the digestion of mammalian milks and infant formulae that the initial formation of calcium soaps typically precedes the formation of non-lamellar LC phases, the identity of which depends both on the lipid composition and the extent of digestion [120, 215]. With 5 mM added calcium, non-pasteurised human milk reached a greater extent of digestion than pasteurised DHM (**Fig. 3.3a**). This difference could be attributed to the lack of homogeneity of the pasteurised DHM samples, which had partially phase separated during the pasteurisation process and were re-dispersed prior to digestion. The phase separation led to a larger particle size distribution of lipid droplets from pasteurised DHM than non-pasteurised human milk (**Fig. 3.2c**).

There appeared to be a threshold in extent of digestion required in order to observe non-lamellar structures on digestion of the milks. As the concentration of calcium was increased to 100 mM, additional inverse micellar cubic I_2 (*Fd*3*m* spacegroup) and H_2 phases were formed for non-pasteurised milk, but no changes were observed for pasteurised DHM (**Fig. 3.6 and Table 3.5**). This was due to differences in the extents of digestion for both milks. The maximum extent of digestion of non-pasteurised milk was 77.3% when the 100 mM of calcium was added to the digestion buffer (**Fig. 3 .3b**). This led to the formation of non-lamellar structures (I_2 and H_2 phases) at around 60% of digestion of non-pasteurised milk (**Fig. 3.6a and Table 3.5**). In contrast, the extent of digestion of pasteurised DHM, which was 54.6%, was less than that of non-pasteurised human milk with the same added concentration of calcium (**Fig. 3.3b**). As a result, there were no changes in the types of lipid LC structures and only a cubic micellar I_2 phase and lamellar phase were observed after increasing the concentration of added calcium from 5 mM to 100 mM (**Fig. 3.6b and Table 3.5**). The extent of digestion therefore appears to play a major role in the formation of additional self-assembled structures during the digestion of human milk.

Addition of bile salts to the digestion systems influenced the structural behaviour of milk lipids. The difference in self-assembly of lipids indicates an interaction between the bile salts and internal particle structure of the digested lipids, with the oil phase becoming more hydrophilic [135]. Instead of non-lamellar phases that were observed when bile salts were not added, a weak broad peak characteristic of a disordered inverse micellar L_2 phase appeared for both human milks in the presence of bile salts. Although the addition of bile salts increased the extent of digestion for both types of samples (**Fig. 3.4c and d**), the facial amphiphilic moiety of bile salts enables the molecule to incorporate into lipid bilayers and mixed micelles during digestion. As this occurs, the critical packing parameter of the lipid LC structures is reduced, thereby favouring a phase transition to a more lamellar phase [14, 216]. This observation is based on the absence of non-lamellar (I_2 and H_2) phases, leaving only the formation of a lamellar phase and disordered L_2 phase, which is indicated by the broad diffraction peak (**Fig. 3.7**). In addition, because of the high concentration of calcium in the digesting system, this caused the mixture of monopalmitin/oleic acid (1:2 mol/mol) to precipitate in a manner analogous to the same mixture in

basic ethanol saturated with calcium chloride (**Fig. 3.6c**). Consequently, the aggregation of free oleic acid in the presence of monopalmitin could have also contributed to the formation of this L_2 phase.

Despite variations in the structural behaviour of lipids in non-pasteurised milk and pasteurised DHM due to differences in extents of digestion, this was not the case for human colostrum. Firstly, although colostrum had the smallest particle size distribution, the final extent of digestion of colostrum was within errors of that of non-pasteurised milk (**Fig 3.8a**). The similar extents of digestion between the two systems could mainly be due to the similar ratios of fat:calcium almost being 1:1.2 for colostrum and non-pasteurised milk. Nonetheless, although colostrum digested to a similar extent as that of non-pasteurised milk, only a lamellar phase was formed (**Fig. 3.8b**). Therefore, in this instance, the differences in the self-assembly of lipids during digestion could be attributed to variations in the composition of FFAs released as elaborated below.

The O/P/O triglyceride structure is vital to the nutrition and development of infants [197]. Prior to digestion, human colostrum, non-pasteurised human milk and pasteurised DHM displayed an abundance of the C52 TAG species (**Fig. 3.9a and b and Table A1**; 'General Appendix' section). Within this C52 TAG, it can be inferred that the predominant FA composition is O/P/O (C18:1/C16:0/C18:1) with oleic acid (C18:1) being the most abundant in colostrum and human milk, followed by palmitic acid (C16:0) accounting for the second highest percentage of FAs in these colostrum and milk samples (**Fig. 3.9c**) [121, 197, 217]. While oleic acid displays preference for the *sn*-1 and *sn*-3 positions, palmitic acid is located primarily at the *sn*-2 position. The composition of these FAs in their respective esterification sites minimises calcium loss and contributes to important benefits, such as improved energy intake, healthy gut bacteria, and increased bone mineral density in infants [126, 187]. Furthermore, the distribution of FAs would ultimately dictate the 2-MAG and FFA products formed during digestion [120]. In the case of abundant O/P/O TAGs, the two outer oleic acids are first removed by pancreatic lipase and BSSL, liberating two free oleic acids and leaving 2-monopalmitin [122]. Therefore, the highly selective distribution of FAs along the glycerol backbone of a TAG molecule of undigested milk systems would influence the types of lipid LC phases formed and may in turn affect the ability of these colloidal phases to deliver lipophilic nutrients to be absorbed into the systemic circulation of infants.

It has been previously shown that there is a direct correlation between lipid composition and the lipid LC structures that form during digestion [120]. This can also be seen in this study, whereby differences in structural behaviour of lipids during digestion were observed because of differences in the amount and composition of FFAs released from colostrum and mature human milk. Non-pasteurised milk released the greatest total amount of FFAs at the end of 120 min intestinal digestion, followed by pasteurised DHM and colostrum producing similar total amounts of FFAs (**Table A2** in 'General Appendix' section). While the total FA composition among these colostrum/milk systems before

digestion is similar (**Fig. 3.9c**), the greater release of long-chain FFAs [oleic acid (C18:1) and linoleic acid (C18:2)] from non-pasteurised human milk and pasteurised DHM than colostrum could have contributed to the differences in colloidal structures formed during digestion (**Fig. 3.8b and 3.11a**). Pham *et al.* have demonstrated that systems comprising medium-chain and long-chain FAs would result in the formation of non-lamellar structures such as the H_2 and I_2 phases [120].

While the appearance of an unidentified peak at q = 0.198 $Å^{-1}$ during the digestion of non-pasteurised milk (**Fig. 3.8b**) could have been attributed to the presence of bile salts that might have altered the lattice parameter of the lipid LC structures, the release of free oleic acid (C18:1) has been reported to disrupt the self-assembly of lipids with the colloidal structures skewing towards a disordered inverse micellar L_2 phase and inverse micellar cubic I_2 phase [218]. Hence, as oleic acid displays a preference for the *sn*-1 and *sn*-3 positions, the greater percentage of free oleic acid (C18:1) produced during the digestion of non-pasteurised milk and pasteurised DHM than colostrum (**Fig. 3.10, 3.11b**) could have caused the formation of the additional I_2 phase (**Fig. 3.8b, 3.11a**). In comparison, the higher abundance of free palmitic acid (C16:0) generated during the digestion of colostrum than both types of human milk (**Fig. 3.10, 3.11b**), might be the predominant factor in driving the structures towards the formation of calcium soaps, as indicated by the L_α phase (**Fig. 3.8b, 3.11a**) [218].

Previous studies have shown the ability of colloidal lipid structures to act as a reservoir for the dissolution of lipophilic drugs during digestion and deliver these drugs to the intestinal sites of absorption [131, 219, 220]. The H_2 and inverse micellar cubic I_2 (*Fd*3*m* spacegroup) phases have been of great interest in the area of drug delivery as these phases have been shown to enhance the uptake of poorly water-soluble drugs *in vivo* [131, 219, 220]. Similarly, depending on the hydrophobicity/hydrophilicity of bioactive molecules such as proteins and carbohydrates found in human colostrum and milk, they would potentially be encapsulated either in the aqueous domain or within the lipid bilayers of the lipid LC structures. It was thus important to understand the influence of lipid composition before digestion on the composition of FFAs released and structural behaviour of milk and colostrum lipids during digestion. These findings provide a roadmap towards the formulation of colostrum substitute mixtures that encompass a similar initial lipid composition and self-assembly of lipids during digestion as human colostrum. The similar structural behaviour of lipids between human colostrum and the colostrum substitute mixtures formed during digestion could potentially deliver bioactive nutrients. For example, although lamellar and inverse micellar cubic phases can both encapsulate bioactive compounds, the capacity for these phases to deliver hydrophobic and hydrophilic compounds differ from each other. In contrast to a lamellar phase, inverse micellar cubic phases are more effective at encapsulating hydrophilic nutrients (such as digested proteins—peptides and amino acids) within the aqueous pores, hydrophobic components within the lipid matrix and amphiphilic nutrients at the oil-water interfaces [221-225]. In turn, the capacity of hydrophilic nutrients escaping from closed aqueous micelles of inverse micellar cubic phase is less than if these nutrients were

encapsulated within a lamellar phase. The delivery of these bioactive factors present in the colostrum substitute mixtures to the gut of premature infants could hence promote a healthy gut microbiota and minimise the effects of NEC.

3.6 Conclusion

This study links the different stages of lactation and impact of pasteurisation with pre- and post-digestion lipid composition, particle size distribution and structural behaviour. While non-pasteurised milk and pasteurised DHM were able to self-assemble into non-lamellar lipid LC structures with coexisting lamellar phases associated with the formation of calcium soaps, colostrum only formed a lamellar phase, which remained persistent throughout digestion. Due to the higher percentage of long-chain free oleic acids liberated from human milk than colostrum, this led to a more negative curvature at the oil-water interface resulting in an inverse micellar cubic I_2 phase during digestion. In comparison, as colostrum produced a greater proportion of free palmitic acids than human milk, the negative curvature at the oil-water interface was reduced favouring the formation of a lamellar phase. Although pasteurised DHM and colostrum released similar total amount of FFAs at the end of digestion, the greater amount and bioactivity of proteins, enzymes and oligosaccharides in colostrum than pasteurised DHM and even non-pasteurised milk would override the latter as a preferred option of feeding for infants. These correlations between lipid composition, FFA composition released during digestion and lipid LC structure formation are therefore fundamental in the design of a colostrum substitute formulation for the delivery of nutrients to the gut of infants.

Chapter 4: Replicating the structural behaviour of lipids in human colostrum using a colostrum substitute

4.1 Introduction

The effect of the composition of free fatty acids (FFAs) released during the *in vitro* digestion of mature non-pasteurised milk, pasteurised donor human milk (DHM) and human colostrum on the structural behaviour of lipids was evaluated in the previous chapter. The lipid liquid crystalline (LC) structures that were formed during the digestion of these milk/colostrum systems were dependent on the chain-lengths and saturation of the FFAs generated. In summary, non-pasteurised milk and pasteurised DHM were able to self-assemble into non-lamellar LC structures simultaneously with lamellar phases that arose from the formation of calcium soaps during digestion. In contrast, human colostrum only formed a lamellar phase due to the difference in the abundance of medium- and long-chain FFAs as digestion products. Regardless, the greater amounts and bioactivity of nutritional factors such as proteins, vitamins and human milk oligosaccharides (HMOs) in colostrum than non-pasteurised milk and pasteurised DHM deem colostrum as the first choice of feeding to infants. The relationship between lipid composition, FFA composition released during digestion and lipid LC structure formation provide an insight into the design of colostrum substitute mixtures that closely resemble the behaviour of human colostrum.

Preterm birth is defined as birth before 37 weeks of gestation and is the leading cause of perinatal and neonatal death among children under the age of five with approximately 15 million infants born prematurely every year [1]. While 1 million die as result of complications, those who survive are vulnerable to mature onset of diseases such as a diminished immune system, poor body temperature regulation and impaired respiration [18, 19]. Consequently, these conditions could lead to a potential lack of efficacy and bioavailability of crucial bioactive proteins that are necessary for the development of organs [226]. In developing countries, premature death occurs due to a lack of feasible and hygienic interventions. While preterm death is less prevalent in developed than developing countries, premature infants still lack optimum nourishment. The absence of bioactive factors could potentially cause growth rates to accelerate too rapidly and compromise the development of organs, resulting in increased chances of mature onset of diseases [20].

Instead, a crucial component to ensure successful treatment for premature infants is the consumption of colostrum. However, as colostrum is produced in small quantities (5-20 mL) during postpartum, mothers of preterm infants and caregivers are limited to other alternatives such as pasteurised DHM or bovine milk-based fortifiers for human milk [21, 22, 50]. Unfortunately, vital nourishment might not be readily available from these alternatives to improve health outcomes [21-25]. In bovine-based formulas, the proteins are derived from bovine milk and have been shown to upregulate inflammatory processes that could compromise the integrity of the gut epithelial border [52]. Furthermore, while bovine milk is rich in medium-chain fatty acids (FAs), the small pool of bile salts in an infant's gut could potentially impede the hydrolysis of lipids consequently resulting in preterm

infants relying on alternate feeding procedures such as continuous nasogastric drip, nasojejunal feeding and intravenous alimentation to counter the loss in fluids [54].

Although pasteurised DHM is a preferred option to infant formula, the heating step during the pasteurisation process has been recognised as influencing the bioactivity and composition of nutritional factors [66]. For instance, the higher abundance and bioactivity of whey proteins in colostrum is able to provide a greater nutritional impact on the healthy postnatal development of an infant as compared to feeding infants with pasteurised DHM [96]. Additionally, while pasteurisation does not have any major influence on the activity of HMOs, the numerous freeze-thaw cycles and container changes could reduce the bioactivity and content of HMOs, which have a major role in reducing the onset of necrotising enterocolitis (NEC) [109]. Lastly, while the total lipid content is not affected due to pasteurisation, the adherence of lipids to the surface of containers, pipelines and feeding systems during pasteurisation might lead to a loss of lipid content [92]. The change in lipid content is an important aspect to consider as lipids in milk and colostrum are a major source of total energy intake in infants and provide important nutrients such as long-chain polyunsaturated fatty acid (LC-PUFAs: linoleic acid and α-linolenic acid) and transport lipid-soluble vitamins for improved gastrointestinal tract (GIT) function, growth and neurodevelopment [112]. It is thus imperative that the overall quality, total content and composition of lipids are monitored following pasteurisation. Moreover, although the FA composition remains unchanged after pasteurisation, variations in FA composition exist between human colostrum and pasteurised DHM. For example, colostrum consists of 52% and 41% of C18:1 being the predominant FA at *sn*-1 and *sn*-3, respectively, whereas mature milk contains a lower percentage of C18:1 at those positions with 49% at *sn*-1 and 35% at *sn*-3. Similarly, colostrum has a greater amount of C16:0 FA (58%) at *sn*-2 as compared to mature milk with 52% of C16:0 [87, 118]. The specificity of the placement of FAs along the glycerol backbone at the *sn*-1, *sn*-2 and *sn*-3 positions of milk TAGs by the mammary gland would influence the types of lipid LC phases formed and may in turn affect the ability of these colloidal phases to deliver lipophilic nutrients to be absorbed into the systemic circulation of infants.

4.1.1 Appropriate colostrum-based dosage forms for premature infants

Acknowledging that human colostrum is produced in minute quantities and that available alternatives present limitations, there is a need for an enhanced nutrient strategy through the formulation of a colostrum substitute mixture. This formulation contains the most abundant lipids, proteins and HMOs that are naturally occurring in human colostrum and essential for the growth of bacteria in the gut to reduce the onset of NEC. Currently, infants are given oral formulations including liquids and tablets. However, such formulations pose as an issue for neonates in terms of variability in doses and difficulty in swallowing [227-230]. This is further aggravated in preterm infants who are born with an immature gut, thus causing issues with swallowing and ADME (absorption, distribution, metabolism

and excretion). Hence, safe and effective dosage forms are required to ensure that these formulations are appropriate to the age, weight and physiological condition of the child.

A formulation that, in addition to better matching the nutritional and health outcomes of colostrum, also has improved storage stability over pasteurised DHM and can be potentially transported to low economy settings such as a dispersible tablet would have great application in reaching the least well served populations with regard to premature infant nutrition. The European Medicines Agency has highlighted the importance of accurate dosing to infants with dose volumes as low as 0.1 mL with a maximum of 5 mL being necessary [231]. To administer these dose volumes to infants, an oral syringe or dropper is often used [232]. In hospital settings, premature infants are fed through enteral tubes but in developing countries, access to health facilities might be difficult thereby restricting infants from receiving the required nourishment. Instead, oral delivery of dispersible tablets might alleviate these issues. The variability involved in breaking the tablet into smaller pieces and increasing the likelihood of affecting the dose would be averted as the desired dose can be controlled by the reconstituted volume for administration. Therefore, dispersible tablets prepared from a colostrum substitute formulation would be appropriate in developing countries where lack of health facilities and refrigeration would otherwise make storing liquid colostrum difficult.

This study thus aims to evaluate the formulation of a colostrum substitute mixture by comparing the lipid and FFA composition and subsequently, the types of lipid LC phases formed during the digestion of these mixtures to human colostrum (**Fig. 4.1**). The lipid and FFA composition of human colostrum and the colostrum substitute mixture were characterised using gas chromatography coupled to a flame ionisation detector (GC-FID). Based on these results, the influence of the FFAs liberated during digestion on the formation of colloidal structures was determined using small-angle X-ray scattering (SAXS). SAXS was also used to determine whether tableting of the colostrum substitute mixture would result in any changes of the structural behaviour of the colostrum substitute lipids.

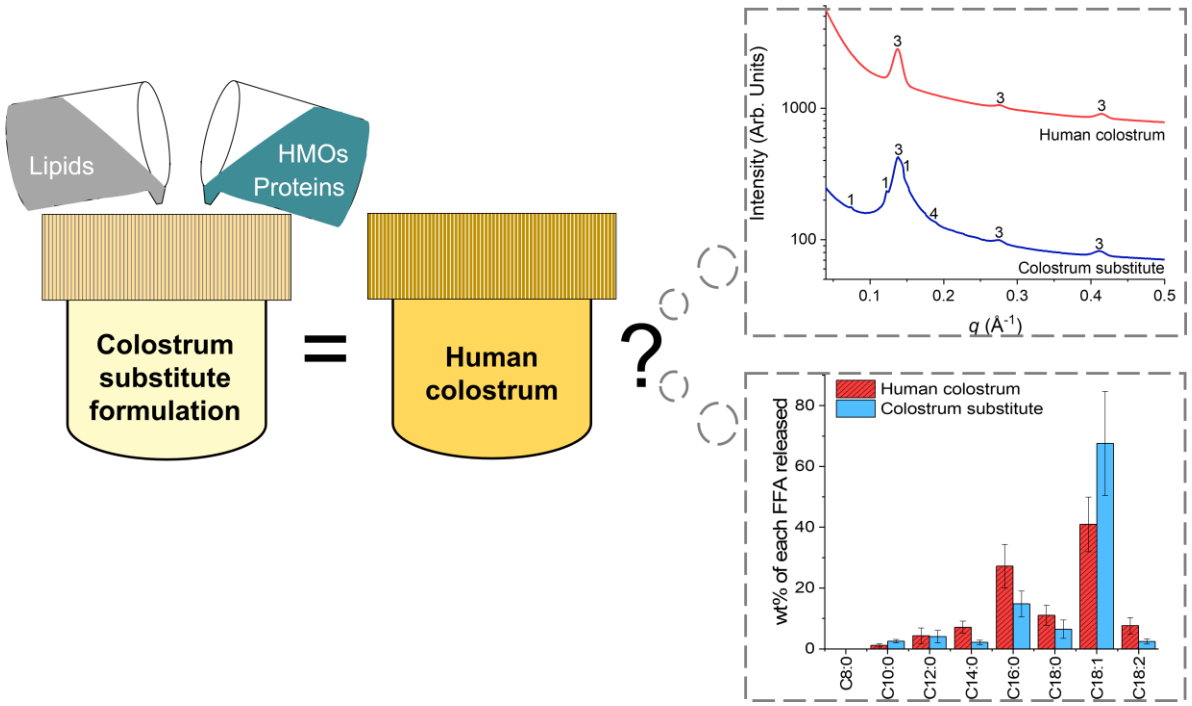

Figure 4.1. Schematic diagram illustrating the comparison of the colostrum substitute formulation against human colostrum in terms of the structural behaviour of lipids [monitored using an *in vitro* lipolysis model coupled to *in situ* small-angle X-ray scattering (SAXS)] and the composition of free fatty acids (FFA) [determined using gas chromatography coupled to a flame ionisation detector (GC-FID)] released during digestion.

4.2 Materials & methods

4.2.1 Standards and materials

Human colostrum samples were donated by the University of Western Australia with ethics approval from the Monash University Human Research Ethics Committee (Project ID 21047). The human colostrum samples were stored at -20 °C and prior to analysis, they were thawed and agitated using a vortex mixer for 5 min. The materials required for the formulation of the colostrum substitute mixtures were outlined in 'Chapter 2.1.1 Human milk, colostrum and colostrum substitute formulations'. Additional materials for the experiments in this study include the following:

Methyl undecenate (C11:1, > 99% purity), glyceryl tridecanoate (C13:0, > 99% purity), glyceryl triundecanoate (C11:0, > 99% purity), monopalmitin (C16:0, >99% purity) and oleic acid (C18:1, >99% purity) were obtained from Nu-Chek Prep. (Elysian, MN, USA). Fatty acid methyl esters (FAME) standard mixtures containing the following methyl esters were also purchased from Nu-Chek Prep. (Elysian, MN, USA): methyl butyrate (C4:0), methyl pentanoate (C5:0), methyl hexanoate (C6:0), methyl heptanoate (C7:0), methyl octanoate (C8:0), methyl nonanoate (C9:0), methyl decanoate (C10:0), methyl undecanoate (C11:0), methyl laurate (C12:0), methyl tridecanoate (C13:0), methyl myristate (C14:0), methyl pentadecanoate (C15:0), methyl palmitate (C16:0), methyl heptadecanoate (C17:0), methyl stearate (C18:0), methyl oleate (C18:1), methyl linoleate (C18:2), methyl α-linolenate

(C18:3). Calcium chloride dihydrate (> 99% purity) and sodium hydroxide pellets (> 97% purity) were purchased from Ajax Fine Chemicals (Seven Hills, NSW, Australia). Hydrochloric acid (36% aqueous solution) was obtained from LabServ (Longford, Ireland). Sodium chloride (> 99.7% purity) was purchased from Chem Supply (Gillman, SA, Australia). Sodium azide (> 99% purity), chloroform (ACS, ISO, reagent), and methanol (HPLC basic) were obtained from Merck (Darmstadt, Germany). Methanolic HCl (3 M), *n*-hexane (≥ 98% purity, gas chromatography), *tert*-butyl methyl ether (99.8% purity, anhydrous), acetic acid (99.8% purity, anhydrous), 4-bromophenylboronic acid (4-BPBA), sodium taurodeoxycholate hydrate (95% purity), trizma®-maleate (reagent grade) and pepsin from porcine gastric mucosa (lyophilised powder) were purchased from Sigma Aldrich (St Louis, MO, USA). Pancreatin extract (USP grade) was obtained from MP Biomedicals (Solon, OH, USA). Fungal lipase 8000 was purchased from Connell Bros Australasia Pty Ltd (Croydon South, VIC, Australia). The lipid standards were stored at -20 °C until further use and unless otherwise stated, all chemicals were used without further purification and water was acquired from a Merck Q-POD Ultrapure Water Remote Dispenser (Darmstadt, Germany).

4.2.2 Preparation of colostrum substitute formulations

The colostrum substitute mixtures were formulated by characterising the most abundant lipids found in human colostrum using GC-FID (Chapter 3.3.3) and the amount of each FAs added to the colostrum substitute using homo-triglycerides (**Table 4.1**) to prepare a total of 0.7 g lipid in 20 g emulsions (3.5 *wt %* total fat), which was explained in Chapter 2.2.1. The lipids were subsequently emulsified in tris buffer 'without water-soluble nutrients' or 'with water-soluble nutrients'. The former buffer contained 2.5% *w/v* casein proteins and 5.5% *w/v* lactose while the buffer termed 'with water-soluble nutrients' consisted of 7.9 % *w/v* reconstituted water-soluble nutrients, which were obtained from the supernatant of centrifuged pooled mature non-pasteurised human milk samples. Briefly, 35 mL of non-pasteurised human milk were centrifuged at 5000 *g* for 60 min at 4 °C. The supernatant was then aliquoted (5 mL) into 20 mL scintillation vials and freeze-dried for 48 h. Following this, the lyophilised supernatant was then reconstituted in tris buffer. After adding the buffers to the molten lipids, the colostrum substitute mixtures were then melted in an oven at 70-75 °C. The mixtures were then emulsified using tip ultrasonication while the mixtures were still hot before subsequent *in vitro* experiments.

Table 4.1. Amount of each fatty acid (FA) found in human colostrum using GC-FID and the amount of each FAs added to the colostrum substitute using homo-triglycerides. The composition of free fatty acids (FFA) released during digestion from human colostrum and the colostrum substitute formulation is also presented in the table below.

Fatty acid	FA composition before digestion (*sn*-1, *sn*-2 and *sn*-3 positions) (*wt%*)		FFA composition released during digestion (*sn*-1 and *sn*-3 positions) (*wt%*)	
	Human colostrum	**Colostrum substitute**	**Human colostrum**	**Colostrum substitute**
C10:0	3.4 ± 1.0	3.4 ± 0.8	1.14 ± 0.55	2.53 ± 0.73
C12:0	4.3 ± 1.6	4.3 ± 1.2	4.24 ± 2.59	4.02 ± 2.36
C14:0	1.9 ± 1.0	1.9 ± 0.9	7.11 ± 2.06	2.13 ± 0.85
C16:0	13.2 ± 7.9	13.2 ± 6.8	27.2 ± 7.2	14.8 ± 6.4
C18:0	2.5 ± 1.5	2.5 ± 0.9	11.1 ± 3.2	6.45 ± 3.63
C18:1 C18:2	74.7 ± 8.6	74.7 ± 7.8	47.8 ± 9.6	69.94 ± 14.85

4.2.2.1 Colostrum substitute tablet formulations

Freeze-dried colostrum: The colostrum substitute dispersions (5 mL) were added into 20 mL glass scintillation vials and freeze-dried for 48-72 h. The freeze-dried colostrum substitute mixtures (585 mg) were weighed into a 20 mL glass scintillation vial using an analytical balance.

Tablet compression: The freeze-dried colostrum substitute mixtures were tableted directly after vortex mixing. Magnesium stearate (0.5% *w/w* to tablet) was added to lubricate the tablet press (Gamlen Tableting Ltd, Nottingham, United Kingdom) before compressing the tablets with a compression force of 60 kg at 5 mm/min fitted with a 14 mm diameter flat-faced bevelled edge [220].

4.2.3 Determination of micronutrient composition using inductively coupled plasma - optical emission spectrometry (ICP-OES)

As the reconstituted water-soluble nutrients added to the colostrum substitute mixtures were obtained from the supernatant of non-pasteurised human milk, the micronutrient composition of human colostrum and non-pasteurised human milk were determined using inductively coupled plasma - optical emission spectrometry (ICP-OES). The ICP-OES experiments were carried out at the University of Melbourne in collaboration with the Melbourne TrACEES Platform and the ICP-OES operating parameters were elaborated in **Table 3.1** of Chapter 3.3.2.

4.2.4 Particle size measurement

Particle size distributions of the fat globules from the re-dispersed human colostrum and colostrum substitute mixtures were measured by laser light scattering using a Mastersizer 2000 (Malvern Panalytical, United Kingdom), equipped with a He-Ne red laser of wavelength 633 nm and an LED blue laser of wavelength 466 nm. Further details regarding the parameters for the particle size measurements were outlined in Chapter 3.3.4.

4.2.5 *In vitro* lipolysis

In vitro lipolysis was performed on human colostrum and the colostrum substitute mixtures using methods described previously [162, 165]. The human colostrum samples were stored at -20 °C and thawed immediately prior to digestion while the colostrum substitute mixtures were melted in an oven at 70-75 °C, emulsified using tip ultrasonication before being loaded into a thermostatted glass vessel (maintained at a constant temperature of 37 °C) connected to a pH stat auto titrator (Metrohm® AG) under constant magnetic stirring. The *in vitro* digestion conditions used for the human colostrum and colostrum substitute mixtures samples were explained in Chapter 3.3.5.

4.2.6 Small angle X-ray scattering (SAXS): flow through measurements

SAXS experiments were carried out on the SAXS/WAXS beamline at the Australian Synchrotron (ANSTO, Clayton, VIC, Australia) [163] to compare the structural behaviour of lipids from human colostrum and the colostrum substitute mixtures. Similar to determining the lipid LC structures during the digestion of human milk, the parameters adopted for these flow through measurements were elaborated in Chapters 2.2.6 and 3.3.6.

4.2.7 Triglyceride (TAG) and free fatty acid (FFA) composition analysis of human colostrum and colostrum substitute mixtures using gas chromatography coupled to a flame ionisation detector (GC-FID)

Total lipids were extracted from pooled human colostrum samples from a single donor (n = 3) following the method previously described by Folch *et al.*, [113]. Further details regarding the lipid extraction, GC-FID method and chromatographic conditions were described in 'Chapter 3.3.3 Analysis of triglyceride (TAG) composition using gas chromatography coupled to a flame ionisation detector (GC-FID)'. To separate the FFAs from the other components of human colostrum and the colostrum substitute mixtures, a solid phase extraction method was adopted as explained in 'Chapter 3.3.8 Free fatty acid (FFA) composition analysis using GC-FID'. The steps taken to derivatise the FFAs into free fatty acid methyl esters (FAME) and the chromatographic conditions for FAME analysis were also outlined in Chapter 3.3.8.

4.3 Results

The results and discussion in this chapter primarily revolves around the comparison between human colostrum and a colostrum substitute mixture with regards to the FFA composition released during digestion and the structural behaviour of lipids.

4.3.1 Effect of reconstituted water-soluble nutrients on the digestibility of colostrum substitute mixture lipids

As explained in section 4.2.2, two types of buffers were used to emulsify the lipids in the colostrum substitute mixtures. Since the water-soluble nutrients were extracted from mature non-

pasteurised human milk, the calcium content of mature milk was found to be 7.2 mM using ICP-OES. This amount of calcium was also added to the colostrum substitute mixtures, which were emulsified with the 'without water-soluble nutrients' buffer. The purpose of this was to determine whether only the presence of water-soluble nutrients such as proteins, HMOs and salts are able to influence the digestibility of lipids. During the digestion of the colostrum substitute mixtures 'without water-soluble nutrients' (lipids in digestion buffer containing casein and lactose only), the colostrum substitute lipids were digested to 91.2 ± 6.4% (**Fig. 4.2b**). In comparison, the extent of digestion of human colostrum was 87.7 ± 8.6% (**Fig. 4.2b**), which is within statistical error (p-value < 0.5). After adding reconstituted water-soluble nutrients to the colostrum substitutes, the extent of digestion increased to 95.7 ± 4.3% (**Fig. 4.2b**). **Fig. 4.2a** shows the particle size distribution of undigested lipids from the colostrum substitutes with and without the water-soluble nutrients. The similar particle size distribution between both mixtures resulted in no change in the initial rate of digestion (**Fig. 4.2b**). Moreover, the final extent of digestion of the colostrum substitute mixtures with and without the water-soluble nutrients were within errors of each other. Overall, the similar particle size distributions and extents of digestion between the colostrum substitute mixture and human colostrum show that the digestion behaviour of these two systems are almost identical (**Fig. 4.2b**).

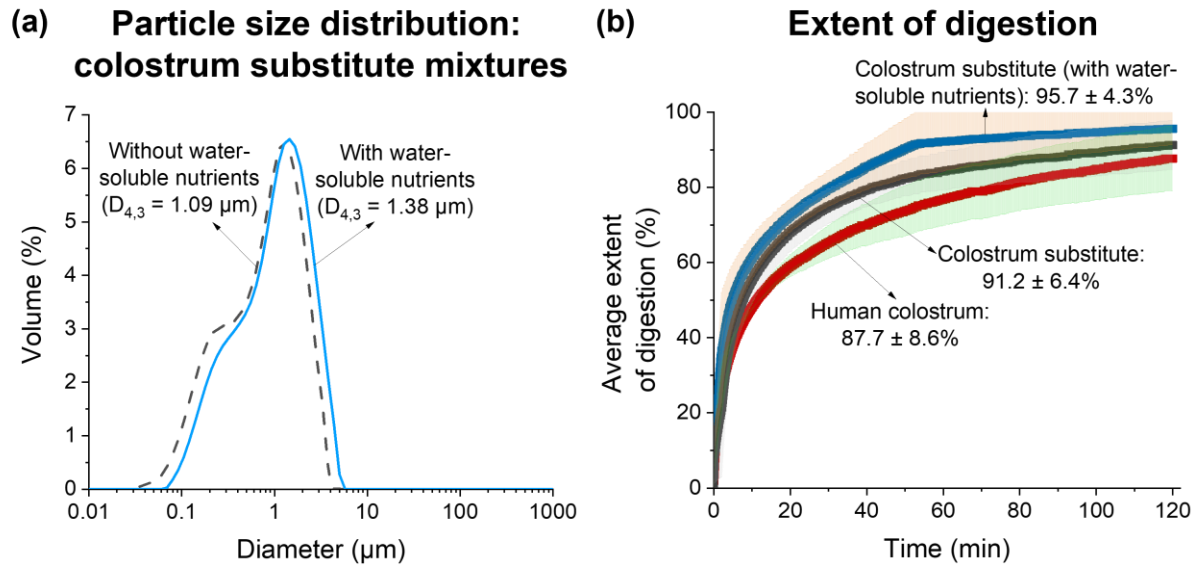

Figure 4.2. (a) Particle size distributions of colostrum substitutes mixtures without water-soluble nutrients (dashed grey lines) and with water-soluble nutrients (blue line) before the addition of pancreatic lipase. (b) Extent of lipid digestion of human colostrum (red with green error bars), colostrum substitutes (digestion buffer containing 7.2 mM $CaCl_2$, casein and lactose only) (dark grey with grey error bars) and colostrum substitutes containing reconstituted water-soluble nutrients (with a calcium content of 7.2 mM) (blue with orange error bars) by pancreatic lipase at pH 6.5. Pancreatic lipase was added into the digestion mixtures and pH was maintained constant at 6.5 for 120 min through the addition of 0.2 M NaOH before increasing the pH to 9.0 for back titration. Results are expressed as means (n = 3) ± SD.

4.3.2 Impact of water-soluble nutrients on the self-assembly of lipids from colostrum substitute mixtures during digestion

It has been shown previously that a series of lipid LC structures appear during the digestion of human milk as a result of the self-assembly of amphiphilic diglycerides (DAGs), monoglycerides (MAGs) and FFAs [120, 135]. These lipid LC phases were determined based on the positional distribution of their respective diffraction peaks and the SAXS profiles, acquired during the experiment over *time*, were converted, using titration data, to the much more informative format as a function of *extent of digestion* (**Fig. 4.3a and b**). Following the addition of pancreatic lipase to the colostrum substitutes with and without water-soluble nutrients, diffraction peaks corresponding to a lamellar structure with a lattice parameter of 46-47 Å were observed and remained persistent throughout digestion (**Fig. 4.3a and b**). A cubic micellar (I_2) phase with *Fd*3*m* spacegroup was also evident after the lipids from both systems were 40-60% digested (**Fig. 4.3a and b**). In addition, the lattice parameters of the lamellar (43-45 Å) and I_2 phases (152-155 Å) throughout the digestion of both mixtures (**Fig. 4.3c and d**) remained consistent throughout digestion.

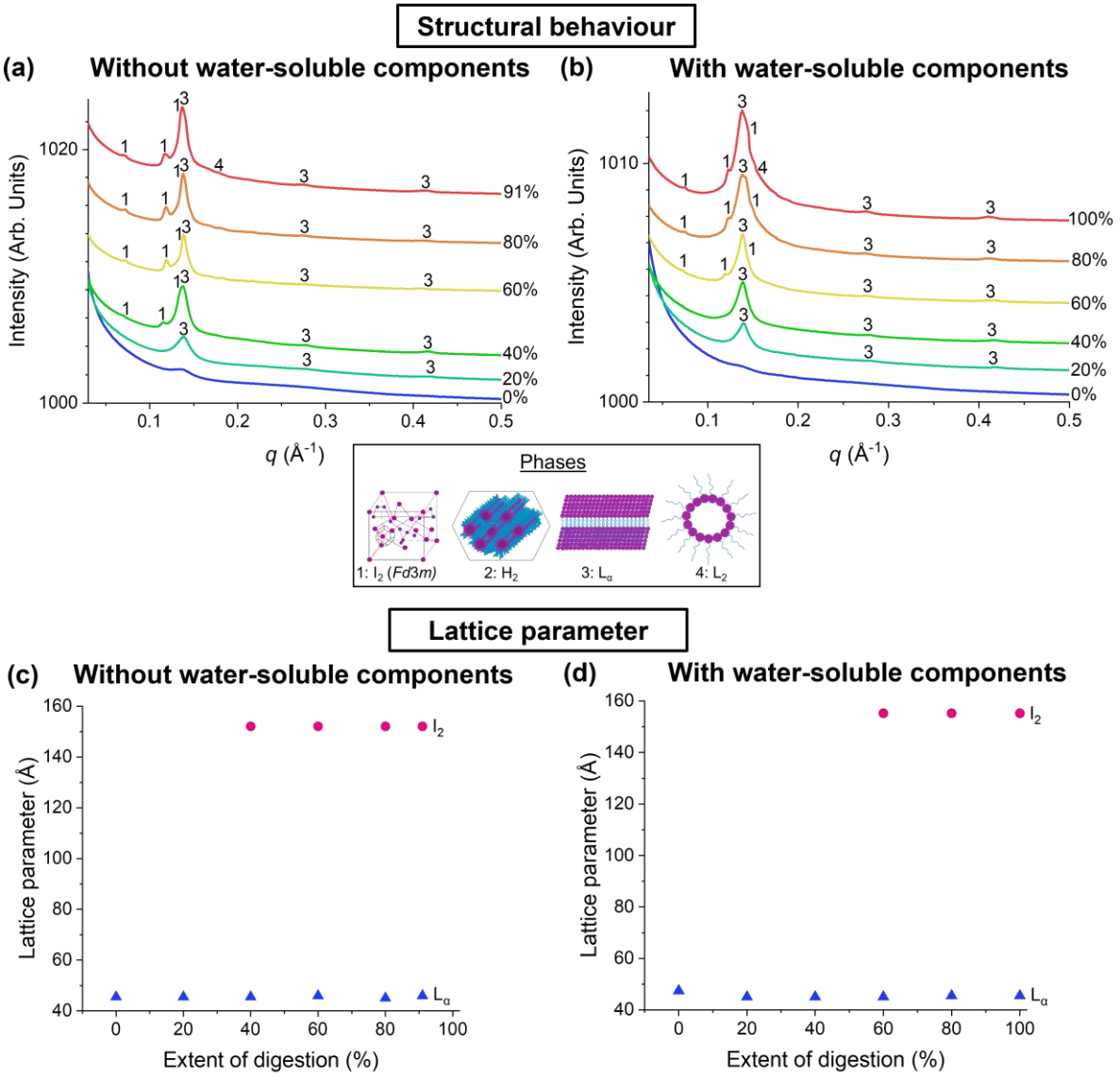

Figure 4.3. SAXS profiles of (a) colostrum substitute mixture without water-soluble components and (b) with water-soluble after the addition of lipase at pH 6.5, 37 °C. "1" represents the cubic micellar I_2 phase (*Fd*3*m* spacegroup), with peak *q* ratios of √3: √8: √11, "2" is annotated as the hexagonal H_2 phase with peak *q* ratios of 1: √3: √4, "3" and "4" represent the lamellar L_α phase with peak *q* ratios of 1: 2: 3 and disordered inverse micellar L_2 phase, respectively. Trends in lattice parameters as a function of extent of digestion of the phases formed from the self-assembly of colostrum substitute lipids (c) without and (d) with water-soluble components.

4.3.3 Differences in the structural behaviour of lipids and free fatty acid (FFA) composition between human colostrum and colostrum substitute mixtures

In contrast to the self-assembly of colostrum substitute lipids, human colostrum only exhibited the formation of a lamellar phase prior to the addition of pancreatic lipase. Furthermore, no other phases were observed while the lamellar phase, which was associated to the formation of calcium soaps, remained persistent throughout digestion (**Fig. 4.4a**). In addition to the differences in structural behaviour of lipids between the colostrum substitute mixtures and human colostrum, variations in the relative percentages of FFAs released during the digestion of both systems were also observed. Within

the same digestion time frame, a greater amount of free oleic acid (67.5% of C18:1) was released from the colostrum substitute mixtures than human colostrum (40.9% of C18:1) (table insert in **Fig. 4.4b**). Also, the absolute amount of long-chain unsaturated FFAs released from the colostrum substitute mixtures was greater than that of human colostrum. The colostrum substitute mixtures released 5.0 ± 2.3 mg/mL of saturated (C14:0, C16:0, C18:0) and 14.9 ± 3.2 mg/mL of unsaturated (C18:1 and C18:2) long-chain FFAs while human colostrum liberated 7.7 ± 2.1 mg/mL of saturated and 8.2 ± 1.6 mg/mL of unsaturated long-chain FFAs (**Fig. 4.4b**).

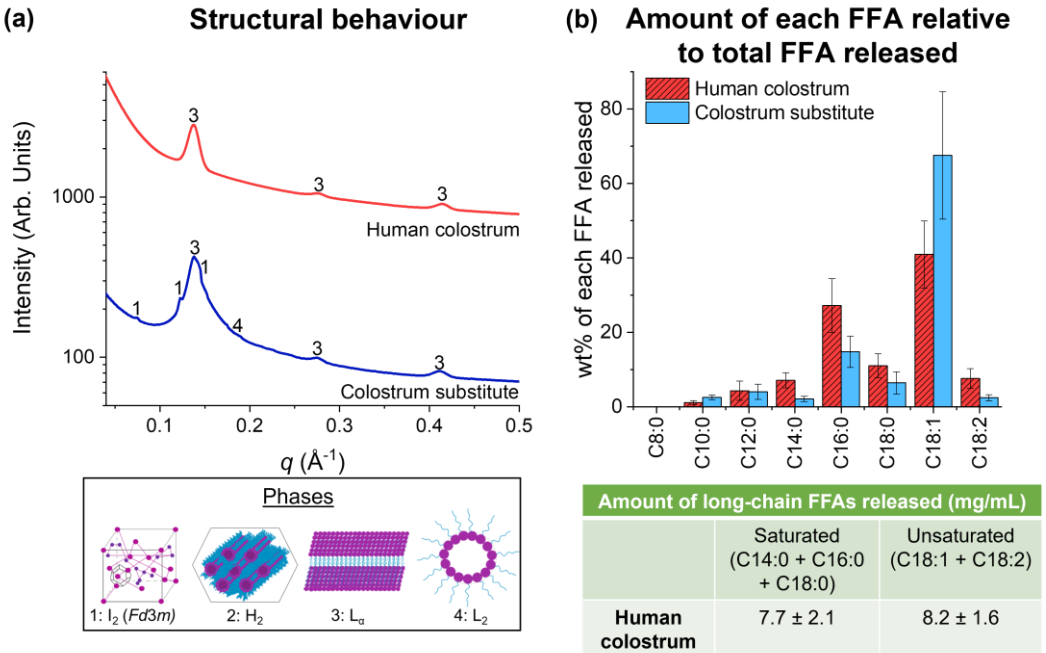

Amount of long-chain FFAs released (mg/mL)		
	Saturated (C14:0 + C16:0 + C18:0)	Unsaturated (C18:1 + C18:2)
Human colostrum	7.7 ± 2.1	8.2 ± 1.6
Colostrum substitute	5.0 ± 2.3	14.9 ± 3.2

Figure 4.4. (a) SAXS profiles of digested human colostrum (red) and colostrum substitute mixture with water-soluble nutrients (blue) at pH 6.5, 37 °C. "1" represents the cubic micellar I_2 phase (*Fd3m* spacegroup), with peak *q* ratios of √3: √8: √11, "2" is annotated as the hexagonal H_2 phase with peak *q* ratios of 1: √3: √4, "3" and "4" represent the lamellar L_α phase with peak *q* ratios of 1: 2: 3 and disordered inverse micellar L_2 phase, respectively. (b) Amount of each free fatty acid (FFA) (*wt%*) released relative to the total FFA from human colostrum and the colostrum substitute mixtures. The table insert shows the absolute amount of long-chain saturated and unsaturated FFAs liberated from human colostrum and the colostrum substitute mixtures. Results in (b) are expressed as means (n = 3) ± SD.

4.3.4 Effect of tableting on the self-assembly of colostrum substitute lipids

Following the freeze-drying and reconstitution of the colostrum substitute tablets, peaks at *q* = 0.155 and 0.194 $Å^{-1}$ were observed prior to the addition of pancreatic lipase (**Fig. 4.5b**) whereas these peaks were not seen for the colostrum substitute mixtures before tableting (**Fig. 4.5a**). The appearance of the peaks before the digestion of the colostrum substitute tablets could be indicative of the recrystallisation of long-chain TAGs during tableting followed by re-dispersion of the tablets. As digestion progressed for the colostrum substitute tablets, the aforementioned lamellar phase disappeared while another lamellar phase at *q* = 0.136, 0.272 and 0.409 $Å^{-1}$ started to grow (**Fig. 4.5b**). Similar to

the formation of a lamellar phase during the digestion of the colostrum substitute prepared by direct dispersion (**Fig. 4.5a**), this lamellar phase was due to the formation of calcium soaps. While the lamellar phase remained persistent throughout digestion, peaks corresponding to an inverse micellar cubic I_2 phase (*Fd*3*m* spacegroup) started to grow after 60% of the tableted colostrum substitute lipids were digested, consistent with that seen of the non-tableted colostrum substitute mixture (**Fig. 4.5b**).

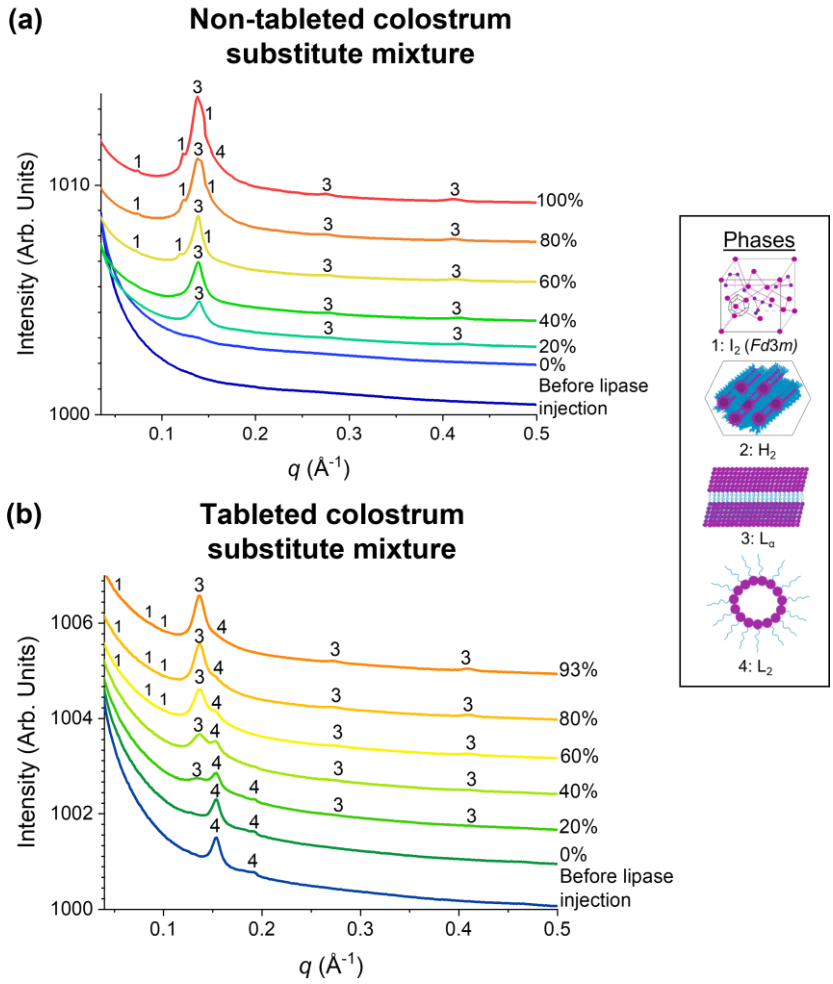

Figure 4.5. SAXS profiles of (a) non-tableted colostrum substitute mixture and (b) tableted colostrum substitute mixture following the addition of lipase at pH 6.5, 37 °C. "1" represents the cubic micellar I_2 phase (*Fd*3*m* spacegroup), with peak *q* ratios of √3: √8: √11, "2" is annotated as the hexagonal H_2 phase with peak *q* ratios of 1: √3: √4, "3" and "4" represent the lamellar L_α phase with peak *q* ratios of 1: 2: 3 and disordered inverse micellar L_2 phase, respectively.

4.4 Discussion

The first source of nourishment for the healthy development of term infants is through the consumption of human colostrum. Otherwise known as 'liquid gold', human colostrum contains the necessary bioactive components that are responsible for regulating the immune and respiratory systems as well as reduce the likelihood of generating diseases such as NEC [27]. Unfortunately, as human colostrum is produced in small quantities during postpartum, premature infants are either fed with pasteurised DHM or infant formulas. However, these alternatives lack the nutrients required to ensure

a healthy growth and development of infants [21-25]. Moreover, although variations exist in the lipid and FA compositions of human colostrum between mothers due to disparities in diet, age and parity [11], human colostrum is still considered as a colloidal nutrient delivery system whose function depends on the digestion of lipids in the infant's GIT [135]. Together with the high abundance and bioactivity of HMOs and proteins, these nutritional factors in human colostrum, which differ in terms of composition and content in pasteurised DHM and infant formulas, serve to provide immunological and protective functions in infants [49]. Therefore, since the fate of these nutrients is critical in providing optimum nourishment to infants, the aim of this study was to evaluate the lipid and FFA composition of homo-triglyceride emulsions with the addition of reconstituted water-soluble nutrients to formulate colostrum substitute mixtures. The purpose of formulating these colostrum substitute mixtures was to determine how closely these mixtures could replicate the digestibility and self-assembly of human colostrum lipids.

The reconstitution of water-soluble nutrients in the colostrum substitute mixtures did not significantly affect the digestibility of the colostrum substitute lipids, with both colostrum substitute mixtures displaying similar extents of digestion as human colostrum. In this study, two types of buffers were used for the colostrum substitute mixtures – termed as 'without water-soluble nutrients' (buffer contained casein and lactose) and 'with water-soluble nutrients' (reconstituted HMOs, proteins and salts from mature non-pasteurised human milk). Despite the addition of reconstituted water-soluble nutrients to the emulsified lipids, there was no change in the particle size distributions (**Fig. 4.2a**). This indicated that the presence of proteins in the buffer had a minimal effect on the stabilisation of the emulsion droplets, thereby resulting in no change in the initial rate of digestion (**Fig. 4.2b**). While the rate of digestion remained similar after the addition of reconstituted water-soluble nutrients, the final extent of digestion of the colostrum substitute lipids in the presence of water-soluble nutrients was greater than in the absence of these nutrients. Scow and Olivecrona have previously demonstrated that the addition of whey proteins such as albumin can enhance lipolysis. In excess of these proteins, they are able to bind to the MAGs and FFAs that surround the lipid droplets and thus accelerate the lipid digestion process (**Fig. 4.2b**) [233]. In contrast, when these proteins are absent, lipolysis decreases as the surface-active digestion products accumulate on the oil-water interface of the lipid droplets. Regardless, the average extent of digestion of the colostrum substitute mixtures was similar to human colostrum illustrating that the digestion behaviour of these two types of samples were almost identical (**Fig. 4.2b**).

Although the average extents of digestion of human colostrum and the colostrum substitute mixtures were within errors of each other, differences in the self-assembly of lipids were observed between the two systems. It has been shown previously that during the digestion of mammalian milks and infant formulae that the initial formation of calcium soaps typically precedes the formation of non-lamellar LC phases, the identity of which depends both on the lipid composition and the extent of digestion [120, 215, 218]. The appearance of a lamellar phase was also seen during the digestion of the

colostrum substitutes with and without the water-soluble nutrients. This lamellar phase was associated with calcium soaps, which were formed through the binding of calcium ions that were added to the digestion buffer used in these *in vitro* experiments [136]. Aside from the formation of a lamellar phase, a cubic micellar (I_2) phase was also evident when the lipids from both types of mixtures were 40-60% digested (**Fig. 4.3a and b**). This observation correlates with the digestion profiles in **Fig. 4.2b** whereby the addition of water-soluble nutrients did not significantly influence the average extent of digestion and hence, the types of lipid LC structures formed. The minimal impact of water-soluble nutrients on the digestibility of lipids was further validated by the consistent lattice parameters of the lamellar and I_2 phases throughout the digestion of both mixtures (**Fig. 4.3c and d**). While both lamellar and inverse cubic micellar I_2 phases can encapsulate bioactive molecules [221, 223], the capacity for these phases to deliver hydrophobic and hydrophilic compounds differ from each other [222, 223, 225]. Although a lamellar phase is able to encapsulate hydrophilic nutrients (such as digested proteins—peptides and amino acids) within the aqueous pores, an inverse micellar cubic phase such as an I_2 phase (*Fd*3*m* spacegroup), has a greater capacity to not only encapsulate hydrophilic nutrients but also hydrophobic components within the lipid matrix and amphiphilic nutrients at the oil-water interfaces [221, 222, 225].

In comparison to the self-assembly of colostrum substitute lipids, the digestion of human colostrum lipids displayed peaks corresponding to a lamellar phase prior to the addition of pancreatic lipase (**Fig. 4.4a**). Salentinig *et al.,* have demonstrated that before the addition of pancreatic lipase, human breast milk was able to initiate self-digestion by the breast milk's own bile salt-stimulated lipase to form a lamellar phase at q = 0.137, 0.273 and 0.408 $Å^{-1}$ [135]. Following the addition of pancreatic lipase, the earlier lamellar phase disappeared while another lamellar phase, which is due to the formation of calcium soaps, emerged. The formation of the additional lipid LC structures that were only seen during the digestion of the colostrum substitute lipids could be attributed to subtle differences in the composition of FFAs released from the two systems (**Fig. 4.4b and Table 4.1**). It has been established previously using FA quantification during digestion of mature human milk and a range of milk and milk substitutes that the generation of greater proportions of long chain unsaturated fatty acids favoured the formation of the inverse micellar cubic (I_2) phase [120]. Hence, the greater release of free oleic acid from the colostrum substitute mixtures than human colostrum (**Fig. 4.4b and Table 4.1**) is a strong predictor for the formation of the I_2 phase during the digestion of the colostrum substitute mixtures [120, 215]. The greater ratio between long-chain saturated to long-chain unsaturated FFAs released from the colostrum substitute (1:5) compared to human colostrum (almost 1:1) further suggests that it was likely to see different structural behaviours between the colostrum substitute mixtures and human colostrum. The greater release of long-chain unsaturated FFAs caused the digested colostrum substitute lipids to skew towards the formation of an inverse micellar cubic (I_2) phase while the release of more long-chain saturated FFAs from human colostrum, which precipitated as calcium soaps resulted in the appearance of a lamellar phase with low interfacial curvature [120]. The relative differences in the FFA

composition between the colostrum substitute and human colostrum thus caused variations in the self-assembly of lipids. Furthermore, although the initial total lipid content and FA composition between the colostrum substitute mixtures and human colostrum are the same (**Table 4.1**), these findings also demonstrate that the MAGs in the former likely contained more unsaturated FAs than human colostrum. This could have been due to the use of homo-triglycerides to prepare the colostrum substitute mixtures, which resulted in the re-arrangement of FAs positional distribution. Hence, a potential next generation of colostrum substitute mixtures would ideally contain a proportion of commercial O/P/O (oleic/palmitic/oleic) TAG to push the structural behaviour of lipids towards that of human colostrum. The greater abundance of oleic acid (a long-chain unsaturated FA) might skew the formation of colloidal structures to a more lamellar phase, which could thus encapsulate hydrophilic bioactive factors such as digested proteins.

Tableting of the colostrum substitute mixture - The preparation of a tablet form of the colostrum substitute with the same structural behaviour during digestion presents an opportunity for a broad use of the colostrum substitute formulation. Previously, it has been shown that no significant differences were obtained in the types of lipid LC structures formed during the digestion of commercial, raw, spray-dried, freeze-dried and frozen milk [136]. Specifically, the formation of the micellar cubic I_2 phase (*Fd*3*m* spacegroup), inverse hexagonal phase H_2, and bicontinuous cubic phase *Im*3*m*, with coexisting lamellar soaps were observed sequentially for these systems including freeze-dried milk [136]. Here, peaks indicative of the recrystallisation of long-chain TAGs during tableting followed by re-dispersion of the colostrum substitute tablets appeared before pancreatic lipase was added to the samples (**Fig. 4.5b**). Tilley and Lutton *et al.*, have reported that TAGs such as trimyristin and tristearin showed peaks corresponding to a lamellar phase at q values 0.148 $Å^{-1}$ and 0.179 $Å^{-1}$ thereby indicating that these TAGs possessed a crystalline structure [234-236]. Thus, this study indicates that the removal of water from the powder used to make the colostrum substitute tablets led to the recrystallisation of the TAGs in a crystalline lamellar phase.

The phase behaviour of the non-tableted and tableted colostrum substitute mixtures was the same during digestion and not altered by the drying, compression and rehydration processes. When the digestion of the non-tableted and tableted colostrum substitute mixtures exceeded 60% digestion, an additional inverse cubic micellar I_2 phase was observed for both systems (**Fig. 4.5**). The similar structural behaviour during the digestion of the non-tableted and tableted colostrum substitute mixtures shows that these lipid LC structures formed would potentially have the ability to deliver nutrients of varying extents of hydrophobicity or hydrophilicity.

These findings are especially important in the context of areas with low economy settings and even regional Australia where there is a lack of feasible and hygienic interventions. The formulation of these colostrum substitute mixtures in the form of dispersible tablets would translate to less requirement

for cold chain, reduced supply cost and increased shelf life as opposed to storing these mixtures in liquid form, which might also be an issue for households that do not possess a refrigerator.

While it was established here that the colostrum substitute can be digested, and that the water-soluble nutrients that are known to be critical in the efficacy of colostrum did not alter the digestion behaviour of the material, the potential efficacy of the colostrum substitute mixture is not at all understood. Towards this end, in the next chapter, the implications of the colostrum substitute mixture on reducing some of the biological markers of NEC are investigated through an *in vitro* NEC model (Chapter 5).

4.5 Conclusion

This study examined the design of a colostrum substitute mixture by comparing the digestibility, structural behaviour and FFA release of this formulation against human colostrum. Initially, the digestion performance of the colostrum substitute lipids was solely compared based on the absence and presence of water-soluble nutrients, which were reconstituted in the digestion buffer. It was found that the average final extents of digestion were essentially the same, indicating the minimal influence of these water-soluble components (proteins, HMOs and salts) on the digestion of lipids. The digestion profiles of these colostrum substitute mixtures were subsequently compared against that of human colostrum. Although the average extents of digestion of both systems were similar, the colostrum substitute mixtures exhibited additional non-lamellar phases, which were not seen for human colostrum (but were previously observed for mature human milk). These differences in the self-assembly of lipids during digestion was attributable to subtle differences in the ratio of long-chain saturated and unsaturated FFAs released during digestion, particularly the amount of free oleic and palmitic acids liberated. Lastly, it was established that tableting of the colostrum substitute mixtures, did not change the self-assembly of lipids during digestion. The formulation of these colostrum substitute mixtures in the form of a dispersible tablet could therefore potentially unlock such mixtures for use as nutrition for infants in a range of challenging settings.

Chapter 5: A synthetic colostrum substitute protects intestinal cells against inflammation in an *in vitro* NEC model

5.1 Introduction

Necrotising enterocolitis (NEC) remains the leading cause of gastrointestinal (GIT) surgical emergency in premature infants with the disease resulting in the damage and death of cells in the intestine that causes profound inflammation and intestinal injury [237, 238]. Although the survival rates of premature infants have been reported to exceed 80%, these infants would still be at risk with acute and chronic complications such as impaired neurodevelopment and bowel syndrome [42, 239, 240]. Furthermore, NEC has an incidence of approximately 5-10% among very low birth weight (< 1500 g) infants and a disproportionately higher rate among extremely low birth weight (≤ 1000 g at birth) with survival rates ranging from 41-55% [239, 241]. It is suggested that the early phases of NEC are strongly associated with the dysbiosis of preterm GIT leading to a combination of insufficient digestion and nutrient fermentation, inadequate immune responses stimulated by resident bacteria, decreased mucosal protection and weak bile pool for lipid absorption [43, 44]. One of the factors that contribute to intestinal barrier dysfunction is the disruption of tight junction proteins [242-244]. Among the several tight junction proteins identified, the cytoplasmic proteins zonula occludens (ZO-1) and the transmembrane proteins, claudin and occludin, form at the apical layer of the enterocyte membranes and act as a selectively permeable intercellular barrier [157, 242]. However, NEC-inducing factors can cause a change in the localisation and expression of these proteins thereby enabling pathogens and foreign antigens to cross the epithelial barrier [245]. With a compromised intestinal integrity, mucus levels remaining low and placental nutrient transport being impaired, preterm infants would be particularly vulnerable to NEC predisposition and thus be required to undergo surgical procedures [45-47]. Instead, to reduce the onset of NEC in preterm infants, the feeding of human colostrum would enable the bioactive factors present to provide protection against NEC by modulating the integrity of the intestinal barrier while exerting immunomodulatory, antioxidant and growth-promoting effects [48, 49].

Moreover, the consumption of human colostrum in the early days of life could minimise chronic side effects such as limited development of the GIT [23, 24, 26]. It has been reported that term infants who receive colostrum display a favourable composition of gut microbiota dominated by bifidobacteria as compared to preterm infants and/or term infants who are formula fed [25]. The difference in the composition of infant gut microbiome is a result of the presence of one of the bioactive factors in human colostrum/milk that is, human milk oligosaccharides (HMOs), which are absent in bovine-derived infant formulas [28]. While HMOs are not digestible by humans, these complex sugars provide a selective nutritional advantage to microbes specialised in metabolising HMOs [29]. One such subspecies is *Bifidiobacterium longum* subspecies (subsp.) infantis (*B. infantis*), which metabolises HMOs leading to the colonisation and remodelling of intestinal microbiome of colostrum/breast-fed infants [30, 31]. Despite more than 200 different HMOs identified, not all HMOs are responsible for the enrichment of this healthy gut microbiota. For instance, fructo- and galacto-oligosaccharides are unable to promote the growth of bifidobacteria whereas fucosyl- (2'-fucosyllactose; 2'-FL) and core (lacto-*N*-neotetraose;

LNnT) oligosaccharides are sufficient to cause persistence and enrich populations of *B. infantis* [166, 246, 247].

The composition of the intestinal microflora is central to immune development and intestinal epithelial function thereby protecting the mucosal surfaces of the gut from pathogens. Through the metabolism of HMOs, the bifidobacteria subspecies has been shown to exhibit beneficial effects including balancing and restoring intestinal microflora, protection against pathogens and maintenance and repair of intestinal barrier functions [176, 177, 248]. Furthermore, the high adhesion of *B. infantis* in particular, to the intestinal epithelial cells, has been shown to increase the expression of anti-inflammatory cytokines and thus, exerts an influence over the localisation of the tight junction proteins and paracellular permeability [158, 249]. However, as human colostrum is only secreted during postpartum, mothers are limited to other alternatives such as pasteurised donor human milk (DHM) or bovine milk-based fortifiers [21, 22]. While the carbohydrates added to fortifiers are mainly derived from bovine milk, which comprise a different composition to HMOs, the repeated freeze-thaw cycles and container changes to produce pasteurised DHM might reduce the bioactivity of these HMOs [109, 250, 251].

In Chapter 4, these potential issues and the lack of ability of these alternatives to provide vital nourishment to premature infants were raised in the discussion section. Hence, the need for an enhanced nutrient strategy through the formulation of a colostrum substitute mixture was introduced in the previous chapter. Firstly, the digestibility of the colostrum substitute lipids was shown in Chapter 4 with the reconstitution of water-soluble nutrients (proteins, HMOs and salts) exerting minimal impact on the extent of digestion or lipid self-assembly during digestion. Subsequently, the digestibility, structural behaviour and free fatty acid (FFA) composition of the colostrum substitute mixtures were compared against human colostrum. Both of these systems displayed similar extents of digestion but subtle differences in structural behaviour were observed due to variations in FFAs released during digestion. Therefore, while these analyses provide a further understanding towards the ability of these colostrum substitute mixtures to be a potential alternative feeding option to human colostrum/milk, it was still imperative that the effect of HMOs and subsequently the colostrum substitute mixture, on reducing some of the biological markers of NEC *in vitro* would be investigated.

This study thus focused on comparing extracted HMO fractions from mature non-pasteurised human breast milk with pure HMOs (2'-FL and LNnT) and lactose as a growth source for *B. infantis* by measuring the expression levels of a tight junction protein, occludin, and an anti-inflammatory cytokine, interleukin- (IL) 10. Following this, the effect of extracted HMO fractions when combined with the colostrum substitute mixture on altering the integrity and permeability of the intestinal monolayer was analysed. The purpose of this was to determine whether milk-like systems (preterm infant formula, mature non-pasteurised human breast milk and the colostrum substitute mixture) would

be able to exude similar effects as the listed carbohydrates and more importantly, whether the colostrum substitute mixture would have a greater effect in protecting the intestinal cells against inflammation as compared to preterm infant formula.

More specifically, Caco-2 and HT29-MTX intestinal epithelial cells were cultured until both cell lines were fully differentiated. Simultaneously, *B. infantis* was grown in the three types of aforementioned carbohydrate and milk-like systems. Following the differentiation of the cell lines, Caco-2 and HT29-MTX cells were treated with lipopolysaccharide (LPS) to induce NEC-like biochemical effects on the cells. This stimulus, which is commonly used in *in vitro* experiments, is a bacterial endotoxin and activates proinflammatory cytokines, immune receptors and adhesion molecules [155]. In particular, previous studies have reported that LPS-induced inflammation causes significant changes in the expression of tight junction proteins and hence, impair the intestinal barrier leading to gut barrier dysfunction in addition to increased intestinal permeability [252-254]. The intestinal cells were then incubated with the cultured *B. infantis* and the integrity of the tight junction proteins was determined using measurements of transepithelial electrical resistance (TEER), while the localisation of occludin was further visualised using immunofluorescent microscopy. Additionally, expression of occludin and IL-10 was determined using quantitative reverse-transcriptase real-time polymerase chain reaction (RT-qPCR) (**Fig. 5.1**).

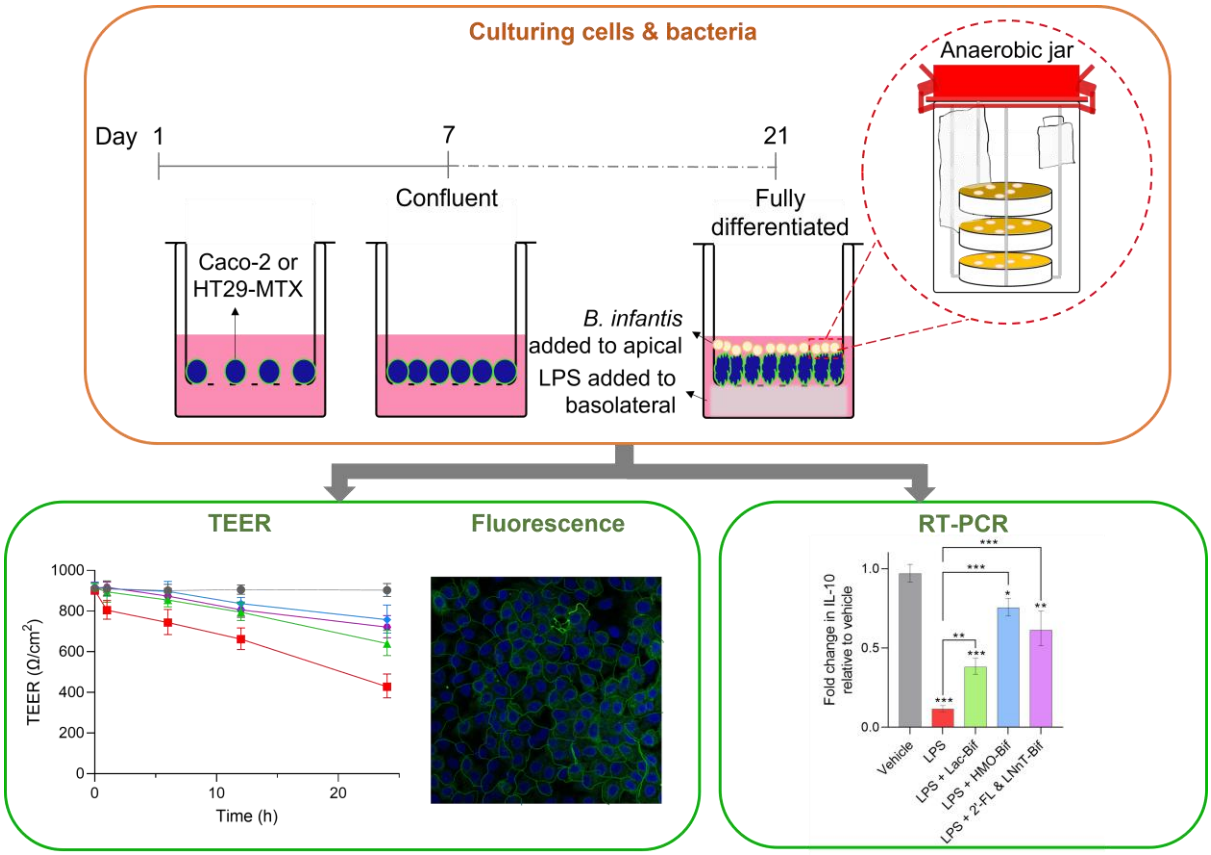

Figure 5.1. Schematic diagram illustrating the culturing of Caco-2 and HT29-MTX cells, which were grown 14 days postconfluence and the growth of *B. infantis* on either carbohydrates (lactose, extracted HMOs from human breast milk and

2'-FL and LNnT) or milk-like systems (preterm infant formula, mature non-pasteurised human breast milk and the colostrum substitute mixture) using an anaerobic jar (top panel). Results such as transepithelial electrical resistance (TEER) and immunofluorescence to determine the paracellular permeability (bottom left panel) and quantitative reverse-transcriptase real-time polymerase chain reaction (RT-qPCR) to measure the expression levels of occludin and IL-10 (bottom right panel) were obtained.

5.2 Materials & methods

5.2.1 Materials

Enterocyte-like human colon adenocarcinoma Caco-2 cells were obtained from ATCC (Manassas, Virginia, USA) HTB-37, passages 38-43 and HT29-MTX cells were purchased from Sigma Aldrich (St Louis, MO, USA) HTB-52, passages 54-59. Dulbecco's modified Eagle's medium/Nutrient Mixture F-12 (DMEM/F-12), RPMI-1640 medium, non-essential amino acids, trypsin-ethylenediamintetraacetic acid (EDTA), de Man-Rogosa-Sharpe (MRS) broth, PowerTrack™ SYBR Green Master Mix, paraformaldehyde primary and secondary anti-occludin and Hoechst were obtained from Thermo Fisher Scientific (VIC, Australia). Heat-inactivated fetal bovine serum (FBS), penicillin and streptomycin, Dulbecco's phosphate buffer saline (DPBS), LPS, L-cysteine hydrochloride, β-mercaptoethanol, Triton® X-100 and bovine serum albumin (BSA) and β-galactosidase (*Kluyveromyces fragilis*) were obtained from Sigma Aldrich (St Louis, MO, USA). Commercially available freeze-dried *B. infantis* (10^{10} CFU/g) powder was purchased from Creative Enzymes (Shirley, NY, USA) while pure 2'-FL and LNnT were obtained from Biosynth Carbosynth Ltd (Compton, UK). Galactooligosaccharide- (TOS) propionate agar (base) and lithium mupirocin (MUP) supplement were purchased from Merck (Darmstadt, Germany). Due to the limited supply of human colostrum, mature non-pasteurised human breast milk [with ethics approval from the Mercy Health Human Ethics Research Committee (Application 2017-035)] was used as a basis of comparison for the colostrum substitute formulation instead. Preterm infant formula was kindly donated by Mercy Health Breastmilk Bank (Heidelberg, VIC, Australia). The nutritional information of the human breast milk, preterm infant formula and colostrum substitute formulation is presented in **Table 5.1** below.

Table 5.1. Nutritional content of preterm infant formula, mature non-pasteurised human breast milk and colostrum substitute formulation (mass per 100 mL).

Nutrient (mass/100 mL)	Preterm infant formula	Mature non-pasteurised human breast milk	Colostrum substitute formulation [g]
Total fat	4.0 g	4.3 ± 1.0 g [a]	3.5 g
Protein (whey)	2.9 g	0.9 ± 0.2 g [b]	7.9 g
Carbohydrate	8.1 g	7.0 ± 1.4 g [c]	
- Lactose	3.7 g	6.4 ± 0.8 g [d]	

- Oligosaccharide	N/A	0.6 ± 0.2 g [e]	
Sodium	51 mg	111 mg [f]	111 mg
Calcium	116 mg	28.7 mg [f]	28.7 mg
Vitamin A	370 µg	N/A	N/A
Vitamin D	3.7 µg	N/A	N/A
Riboflavin	198 µg	N/A	N/A

[a] Total fat content of human breast milk was determined using a gas chromatography coupled to a flame ionisation detector (GC-FID) technique as described in 'Chapter 3.3.3.1 and 3.3.3.2'. [b] Total protein content of human milk was analysed using a Bradford assay (further elaborated in the 'General Appendix' section 'Appendix A4'). [c] Total carbohydrate content of human milk was determined using a colorimetric kit, which is modified based on the phenol-sulfuric acid method (as explained in 'General Appendix' section 'Appendix A5') [255]. [d] Lactose was quantified using an enzymatic kit (detailed in the following methods section 5.2.2). [e] HMOs were quantified using liquid chromatography-mass spectrometry (LCMS) (elaborated in section 5.2.3). [f] Sodium and calcium composition of human milk was determined using inductively coupled plasma-optical emission spectrometry (ICP-OES) as outlined in 'Chapter 3.3.2'. [g] Nutritional content of the colostrum substitute formulation was based on that of human colostrum. The lipids added to the colostrum substitute formulation were off the shelf while the water-soluble nutrients (proteins, carbohydrates and salts) were reconstituted from mature non-pasteurised human milk. These details were further elaborated in 'Chapter 4.2.2'.

5.2.2 Extraction of human milk oligosaccharides (HMOs)

Oligosaccharides were extracted from human milk as previously described by Gnoth *et al*., and Redmond and Packer [256, 257]. Briefly, mature non-pasteurised human milk samples were centrifuged at 5000 *g* for 30 min at 4 °C. The lipid layer was then removed and the supernatant was added to ethanol at a ratio of 1:2 *v/v* to remove the proteins. The solution was placed on a rotary plate and incubated overnight at 4 °C. Following this, the precipitate was removed by centrifugation at 5000 *g* for 30 min at 4 °C and the solvent was evaporated to dryness using a rotary evaporator (initially 175 mbar, 100 rpm, 45 °C and pressure was continuously decreased to 0 mbar to remove any traces of solvent remaining). To digest lactose, the dried extract was then reconstituted with 0.05 M of phosphate buffer pH 6.8 and 3,000 U β-galactosidase was added before incubating the solution for 1 h at 37 °C. Subsequently, the solution was extracted with 4 volumes of 2:1 *v/v* chloroform-methanol and monosaccharides and residual disaccharides in the aqueous layer were removed by solid phase extraction (SPE) using non-porous graphitised carbon cartridges (Supelco Inc; Pennsylvania, USA). The columns were first conditioned by washing with 3 volumes of acetonitrile (ACN) followed by 9 volumes of Merck Q-POD Ultrapure water. After washing the column, the reconstituted sample was loaded onto the column and washed with 10 volumes of water. HMOs were then eluted from the column with 10 volumes of 60:40 *v/v* water-ACN containing 0.01% trifluoroacetic acid. Subsequently, the HMO fractions were combined and dried using vacuum.

To validate that the amount of lactose and D-galactose remaining in the extracted HMOs was minimal, the residual content of these mono- and disaccharides was determined using an enzymatic

'Yellow line' kit (Roche Diagnostics; Darmstadt, Germany). The following protocol was based on the principle that lactose is first hydrolysed to D-glucose and D-galactose in the presence of β-galactosidase. D-galactose is then oxidised by nicotinamide-adenine dinucleotide (NAD) to D-galactonic acid in the presence of β-galactose dehydrogenase. The amount of NADH produced is stoichiometric to the amount of lactose and D-galactose found in these HMO extracts. To quantify the amount of lactose, the lyophilised HMO fractions were reconstituted with water. The samples (0.1 mL) together with 0.2 mL of 'solution 1' (citrate buffer pH 6.6, NAD and magnesium sulfate) and 0.05 mL of β-galactosidase suspension were aliquoted into a cuvette. Following this, the mixture was swirled and incubated for 20 min at 20-25 °C before adding 1.0 mL of potassium diphosphate buffer (pH 8.6) and 1.9 mL of water. After mixing, the absorbance (A_1) was read at 340 nm and 0.05 mL of galactose dehydrogenase suspension was added. After 15-30 min, the absorbance (A_2) was measured at 340 nm. The above steps were repeated for the quantification of D-galactose with the exception of adding β-galactosidase suspension to the mixture. The concentration of lactose and D-galactose remaining in the HMO extracts were calculated using Equation 1 below and was less than 2% of the total carbohydrate content – consistent with previous studies [256, 258].

$$c = \frac{V \times MW}{\varepsilon \times d \times v \times 1000} \times \Delta A \; (g/L) \qquad (1)$$

where V = final volume (mL), v = sample volume (mL), MW = molecular weight of lactose or D-galactose, d = light path (cm), ε = extinction coefficient of NADH at 340 nm; 6.3 and ΔA = net absorbance $[(A_2 - A_1)sample - (A_2 - A_1)blank]$.

5.2.3 Quantification of human milk oligosaccharides (HMOs) using liquid chromatography-mass spectrometry (LCMS)

Following the removal of lipids and proteins from the human milk samples and extraction of HMOs by SPE as explained in section 5.2.2 above, dried HMO extracts were reconstituted in water (50-60-fold dilution) and injected directly for liquid chromatography-mass spectrometry (LCMS) analysis. Milk oligosaccharide standards were obtained from Biosynth Carbosynth Ltd (Compton, UK) and stock solution for each HMO standard was prepared in water at a concentration of 1 mg/mL. A Shimadzu Nexera X2 UHPLC system coupled with a Shimadzu #8050 tandem triple quadrupole mass spectrometer, operated by Shimadzu LabSolutions software (Shimadzu, Sydney, NSW, Australia) was used for HMO profiling. A 100 × 2.1 mm, 3 μm, Hypercarb™ porous graphitic carbon column (Thermo Fisher Scientific, VIC, Australia) was used for HMO separation. The eluent system consisted of solvent A = 3% acetonitrile (ACN)/0.1% formic acid in water (*v/v*) and solvent B = 90% ACN/0.1% formic acid in water (*v/v*) with a flow rate of 0.3 mL/min. Separation of HMOs was performed using a 55 min binary gradient as previously developed by Hong *et al.,* [259], which consisted of 0-20 min, 0-16% solvent B; 20-30 min, 16-44% solvent B; 30-35 min, 44-100% solvent B; 35-40 min, 100% solvent B; 40-41 min, 100-0% solvent B, 41-45 min, 0% solvent B. The following parameters were optimised for

HMO analysis: capillary voltage 1.8 kV in positive mode, drying and sheath gas temperatures at 150 °C, drying gas and sheath gas flow rates at 11 L/min and 7 L/min, respectively. The injection volume was 2 µL and the LCMS parameters for each HMO can be found in **Table 5.2** below. Each HMO compound was identified based on its characteristic fragments and elution time using a HMO library from previous studies [260, 261]. The concentration of each HMO was then calculated based on the standard curves plotted for each HMO standard.

Table 5.2. Multiple reaction monitoring (MRM) transitions and concentrations of listed human milk oligosaccharides (HMOs). Note that only the six most abundant HMOs (2′-Fucosyllactose; 2′-FL, 3'-Fucosyllactose; 3'-FL, Lacto-N-Tetraose; LNT, Lacto-N-neotetraose; LNnT, 3′-Sialyllactose; 3'-SL and 6′-Sialyllactose; 6'-SL), which represent the three predominant classes of HMOs and contribute mainly to the enrichment of *B. infantis* [246, 247], were selected to estimate the total concentration of HMOs. [a] Numbers represent monosaccharide composition (for example 2010 represents 2Hex:0HexNAc:1Fuc:0Neu5Ac) Hex: hexose, HexNAc: N-acetylhexosamine; Fuc: fucose, Neu5Ac: N-acetylneuraminic acid.

HMO	Composition [a]	Precursor ion (*m/z*)	Product ion (*m/z*)	Collision energy (eV)	Concentration (g/100 mL)
2'-FL	2010	489.3	325.0	6	0.25 ± 0.06
3'-FL			163.4		0.20 ± 0.14
LNT	3100	708.4	365.7	15	0.10 ± 0.02
LNnT			203.6		$(0.23 \pm 0.18) \times 10^{-1}$
3'-SL	2001	634.3	453.8	12	$(0.13 \pm 0.08) \times 10^{-1}$
6'-SL			292.3		$(0.22 \pm 0.04) \times 10^{-1}$

5.2.4 Growth of *B. infantis*

As the growth sources for *B. infantis*, either carbohydrates or whole milk-like systems were used. For the 'carbohydrates-grown bifidobacteria' study, sterilised 2% *w/v* lactose, extracted HMOs or pure 2'-FL and LNnT were reconstituted in water while the 'milk-like systems-grown bifidobacteria' consisted of preterm infant formula, mature non-pasteurised human breast milk or the colostrum substitute mixture as the growth source. MRS broth supplemented with 1% *w/v* L-cysteine hydrochloride was autoclaved and after cooling the broth, the growth factors were added to the broth. *B. infantis* (10^{10} CFU/mL) was then added to each experimental group and diluted to a final concentration of 10^8 CFU/mL. Following this, the bifidobacteria was aliquoted into plates before adding autoclaved TOS-propionate agar with MUP supplement using the pour plate method. Directly after the agar was solidified, the plates were inverted and incubated in an Oxoid anaerobic jar (Merck; Darmstadt, Germany) at 37 °C for 72 h. An AnaeroGen sachet (Merck; Darmstadt, Germany) was clipped in the plate carrier within the jar to generate an anaerobic atmosphere (9-13% CO_2) and an Oxoid Anaerobic Indicator (Merck; Darmstadt, Germany) was also placed in the jar to provide a visual indication of anaerobiosis (colour changed from pink to white). After 72 h, cultured *B. infantis* were harvested from

the plates by pouring tris/EDTA buffer and gently stirring the surface with a cotton swab that was sterilised with saline solution. The suspended bacteria were aliquoted into Falcon tubes and centrifuged at 1000 *g* for 10 min at 4 °C. Lastly, the pelleted bacteria were resuspended in either DMEM/F-12 or RPMI-1640 media for Caco-2 or HT29-MTX cells, respectively for the subsequent cell culture experiments.

5.2.5 Culturing of cells and treatment with LPS and *B. infantis*

Caco-2 and HT29-MTX cells were kept cryogenically frozen in vapour phase in a cryo-storage solution consisting of 5% *v/v* dimethyl sulfoxide (DMSO) in heat-inactivated FBS prior to thawing. After the cells were thawed, the vials containing approximately 1 million cells/mL of the cryo-storage solution were aliquoted into 75 cm^2 (T75) flasks containing 14 mL of either DMEM/F-12 for Caco-2 cells or RPMI-1640 medium for HT29-MTX cells, both of which were supplemented with 10% heat-inactivated FBS (30 min at 56 °C), 1% non-essential amino acids, 50 IU/mL penicillin and 50 μg/mL streptomycin. For both cell lines, the media was aspirated off after 2 h and replaced with fresh pre-warmed media to remove any remaining traces of DMSO from the cryo-storage solution. Both cell lines were routinely cultured in T75 flasks at 37 °C in a 5% CO_2 constant humidity environment with media replaced every 2-3 days. At 80% confluence, the cells monolayers were rinsed twice with 10 mL of PBS after removing the spent media. The cells were then exposed to 4 mL of trypsin/EDTA solution and incubated at 37 °C for 5 min. Following this, 11 mL of either the DMEM/F-12 or RPMI media was added to the respective cell lines to halt the trypsinisation process. Cells were aliquoted into 50 mL Falcon tubes and 80 μL of the cell suspension was transferred into Eppendorf tubes containing 20 μL trypan blue staining solution and counted on a haemocytometer. The cell suspension in the Falcon tubes were centrifuged at 650 *g* for 5 min. The supernatant was removed and the pelleted cells were diluted in an appropriate volume of pre-warmed DMEM/F-12 or RPMI-1640 media. Subsequently, the cells were seeded on Transwell polycarbonate inserts (24 mm diameter, 0.4 μm pore size; Corning Inc, Ithaca, NY) at a density of 3×10^5 cells/cm^2 and grown for 14 days postconfluence to achieve fully differentiated monolayers. Following differentiation, 1 μg/mL of LPS was added to the apical chamber while 10^8 CFU/mL of carbohydrates-grown *B. infantis* or milk-like systems-grown *B. infantis* from each sub-experimental group in section 5.2.4, was added to the basolateral chamber. The treated cells were then incubated (37 °C, 5% CO_2, 95% room air) for 24 h before conducting TEER and RT-qPCR tests.

5.2.6 Integrity of monolayer and tight junctions using transepithelial electrical resistance (TEER) and immunofluorescence

The integrity of tight junctions formed between the treated Caco-2 and HT29-MTX cells seeded on Transwell polycarbonate inserts was measured through transepithelial electrical resistance (TEER) using a Millicell-ERS Voltmeter with chopstick electrodes (Millipore Corp; Merck, Darmstadt,

Germany). The resistance of a blank culture (containing only DMEM/F-12 or RPMI-1640 without cells) was first measured using the electrodes before transferring the incubated cell culture plates onto a heating plate, which was maintained at 37 °C. Following this, the integrity of the cell monolayers was measured by placing the shorter electrode into the apical side while the other electrode was inserted into the basolateral side.

In addition to TEER measurements, immunofluorescence was also conducted. Both intestinal epithelial cell lines were cultured in 8-well glass coverslips (Thermo Fisher Scientific; VIC, Australia), for 14 days postconfluence. Again, the cell monolayers were treated with 1 μg/mL LPS and 10^8 CFU/mL of carbohydrates-grown *B. infantis* or milk-like systems-grown *B. infantis* and incubated for 24 h (37 °C, 5% CO_2, 95% room air). The cells were washed with PBS three times before being fixed in 4% paraformaldehyde for 10 min at room temperature. Subsequently, all cells were permeabilised with 0.1% TritonX-100 in 1% BSA/PBS at room temperature for 30 min before blocking the cells with 10% BSA/PBS at room temperature for 1 h. The cells were washed with PBS three times and incubated with primary rabbit anti-occludin 1:50 overnight at 4 °C. After washing the cells three times with PBS, the cells were incubated with secondary rabbit anti-occludin 1:200 for 45 min at room temperature and nuclei were stained with Hoechst for 30 min at room temperature.

5.2.7 Quantification of occludin and IL-10 in treated cells using quantitative reverse-transcriptase real-time polymerase chain reaction (RT-qPCR)

Quantitative reverse-transcriptase real-time polymerase chain reaction (RT-qPCR) was employed to determine changes in the expression levels of occludin and IL-10 in LPS-induced Caco-2 and HT29-MTX cells incubated with carbohydrates-grown *B. infantis* or milk-like systems-grown *B. infantis*. Following incubation of the cells, RNA from both cell lines were isolated using the RNeasy Plus Mini Kit (Qiagen, Hilden, Germany) as per the manufacturer's protocol. Briefly, cells were washed twice with ice-cold PBS. Lysis buffer was then prepared by adding β-mercaptoethanol into Buffer RLT Plus from the kit. Cells were lysed with the buffer and lysates were loaded into a QiAshredder column before centrifuging the columns at 1000 *g* for 2 min. Homogenised lysates were transferred into a gDNA column to remove any genomic contamination. The flow through was then mixed with an equal volume of 70% ethanol and the mixture was loaded into RNeasy spin columns. The RNA samples were centrifuged again at 1000 *g* for 1 min. After adding 700 μL of Buffer RW1 to the RNeasy spin columns and centrifuging at 1000 *g* for 1 min, 500 μL of Buffer RPE was added to the columns and centrifuged again. Next, the RNA samples were washed with the Buffer RPE again but centrifuged for 2 min to remove any residual liquid from the columns. The RNeasy columns were then transferred into fresh collection tubes and 50 μL of RNase-free water was aliquoted into the columns before centrifuging at 1000 *g* for 1 min. Subsequently, RNA concentrations were measured using a NanoDrop® 1000 spectrophotometer (Thermo Fisher Scientific, VIC, Australia) at 260 nm with purity determined via the

260/280 ratio (value close to 2 indicates no or low protein contamination) and 260/230 ratio (value close to 2.5 represents no or low guanidine contamination from lysis buffer used).

To convert RNA to complementary DNA (cDNA), a SensiFast cDNA Synthesis Kit (Meridian Bioscience, Ohio, USA) was utilised according to the manufacturer's protocol. First, extracted RNA at a concentration of 0.05 µg/µL was transferred to a PCR tube containing 1 µL of Reverse Transcriptase and 4 µL TransAmp Buffer and made up to a total volume of 20 µL with RNase-free water. Tubes were then placed in a thermal cycler (Applied Biosystems, Massachusetts, USA) and set to the following program: 25 °C for 10 min (primer annealing), 42 °C for 15 min (reverse transcription), 85 °C for 5 min (inactivation). Converted cDNA samples (1 µL) were diluted to a final concentration of 5 ng/µL with nuclease-free water and mixed with 0.5 µL of Yellow Sample Buffer from the PowerTrack™ SYBR™ Green Master Mix (Applied Biosystems, Massachusetts, USA). The forward and reverse primers (1 µL each) (Integrated DNA Technologies Inc, Singapore) added to the mix are shown in **Table 5.3** below. Subsequently, 10 µL of SYBR Green fluorescence and 6.5 µL of nuclease-free water were added to the DNA mix with a final total volume of 20 µL. qPCR (Bio-Rad, California, USA) was then performed with the following conditions: 95°C for 2 min (enzyme activation), 40 cycles for 5 s at 95°C (denaturation), annealing temperature (refer to **Table 5.3** below) for 30 s and 60 °C for 30 s, followed by the standard denaturation curve.

Table 5.3. Primer sequences and annealing temperature implemented for RT-qPCR.

Primer name	Sequence	Annealing temperature
β-actin forward	5'-GGCGACGAGGCCCAGAGCAAGAGAGGCAT-3'	55°C
β-actin reverse	5'-CGATTTCCCGCTCGGCCGTGGTGGTGAAGC-3'	55°C
IL-10 forward	5'-ATGCCCCAAGCTGAGAACCAAGACCCA-3'	55°C
IL-10 reverse	5'-TCTCAAGGGGCTGGGTCAGCTATCCCA-3'	55°C
Occludin forward	5′-TCAGGGAATATCCACCTATCACTTCAG-3′	53°C
Occludin reverse	5′-CATCAGCAGCAGCCATGTACTCTTCAC-3′	53°C

The concentration of DNA from each sample was calculated based on Equation 2 below where Ct refers to the threshold cycle, ΔCt refers to the difference in Ct between the gene of interest (occludin or IL-10) and housekeeping gene, in this case, β-actin and $\Delta\Delta\mathrm{Ct} = \Delta\mathrm{Ct}\,(\text{treated cell groups}) - \Delta\mathrm{Ct}\,(\text{vehicle cell groups})$. All comparisons between vehicle and treatment groups were assessed by one-way analysis of variance (ANOVA) followed by a post hoc Dunnett's test to compare the mean of each treatment group to the mean of the vehicle or LPS only induced treated groups. Levels of significance are indicated for each experiment with a p-value < 0.05 being statistically significant.

$$2^{-\Delta\Delta Ct} \quad (2)$$

5.3 Results

The results and discussion in this chapter primarily revolves around the impact of carbohydrates-grown *B. infantis* and milk-like systems-grown *B. infantis* on reducing the permeability of cell monolayers and increasing the expression of occludin and anti-inflammatory IL-10 in LPS-induced intestinal epithelial cells.

5.3.1 Integrity of intestinal epithelial barrier

The integrity of fully differentiated Caco-2 and HT29-MTX cell monolayers following incubation with LPS and *B. infantis* was determined using TEER at multiple time points. As shown in **Fig. 5.2** below, the TEER results remained constant for the vehicle (untreated) groups of each cell line. However, Caco-2 cells reached higher TEER values at all time points as compared to HT29-MTX cells. For example, Caco-2 cells attained 903.0 ± 12.8 Ω/cm^2 whereas HT29-MTX cells reached a TEER value of 533.0 ± 11.5 Ω/cm^2 at t = 24 h. Upon treatment of both cell lines with only LPS, the TEER results consistently decreased at t = 1 h, 6 h and 12 h with the lowest TEER values of 428.7 ± 23.2 Ω/cm^2 for the Caco-2 cells and 222.3 ± 13.7 Ω/cm^2 for the HT29-MTX cells after 24 h. While the cells that were treated with LPS and carbohydrates-grown *B. infantis* displayed higher TEER results than those cells that were induced with only LPS at all time points, the final TEER measurement at t = 24 h was lower for the lactose-grown *B. infantis* than oligosaccharide- (HMO and 2'-FL and LNnT) grown bifidobacteria (**Fig. 5.2**).

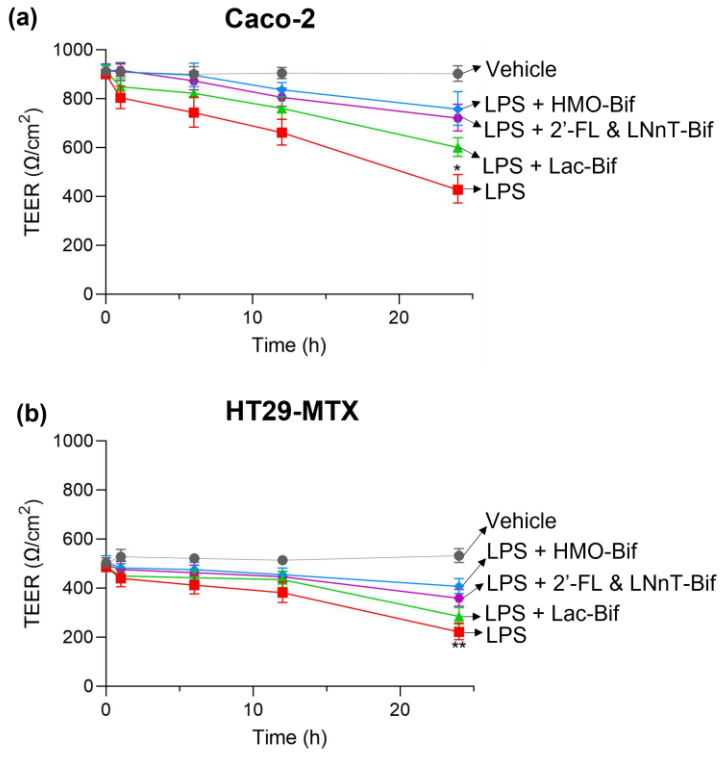

Figure 5.2. Changes in transepithelial electrical resistance (TEER) values (Ω/cm^2) of LPS only (red), LPS with lactose-grown *B. infantis* (LPS + Lac-Bif; green), LPS with 2'-FL and LNnT-grown *B. infantis* (LPS + 2'-FL & LNnT-Bif; purple) and LPS

with HMO-grown *B. infantis* (LPS + HMO-Bif; blue) treated (a) Caco-2 and (b) HT29-MTX cells are illustrated relative to vehicle (untreated) cells (grey) at t = 1 h, 6 h, 12 h and 24 h. Values were normalised to an empty Transwell, mean ± SD of 3 biological replicates. * $p < 0.05$, ** $p < 0.005$ when compared with vehicle.

5.3.2 Changes in localisation of a tight junction protein

The distribution of occludin, one of the major tight junction proteins, was analysed using an immunofluorescence method to determine the effect of carbohydrates-grown *B. infantis* on LPS-induced cells. Under baseline conditions (vehicle; no LPS nor bacteria), the structure of the cells was characterised by a bright fluorescence indicative of a high expression of occludin on the cell membrane (**Fig. 5.3a**) whereas cells that were treated with LPS only resulted in no fluorescence suggesting an absence of the tight junction protein (**Fig. 5.3b**). However, in the LPS-induced cells that were treated with carbohydrates-grown *B. infantis*, a more intense staining was observed both on the membrane and in the cytoplasm of the cells (**Fig. 5.3c-e**) as compared to the LPS only treated groups (**Fig. 5.3b**).

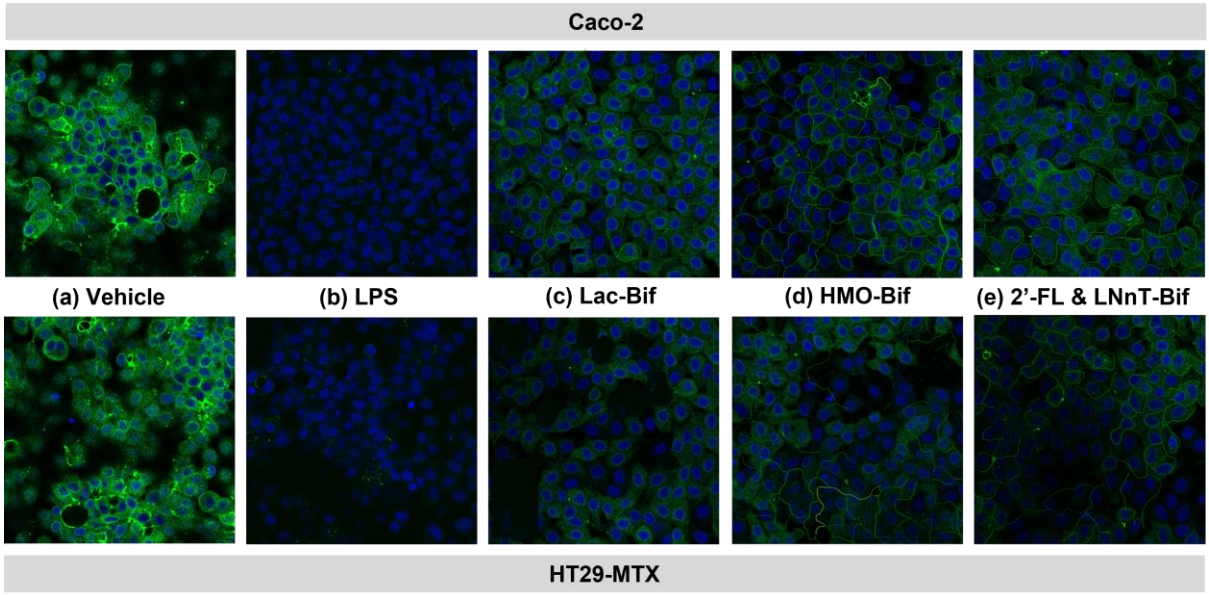

Figure 5.3. Immunofluorescence staining of occludin tight junction protein in Caco-2 (top panels) and HT29-MTX (bottom panels) for (a) vehicle, (b) LPS only, (c) LPS and lactose-*B. infantis* (Lac-Bif), (d) LPS and extracted HMO-*B. infantis* (HMO-Bif) and (e) LPS and 2'-FL & LNnT-*B. infantis* (2'-FL & LNnT-Bif) treated cells. Magnification: ×20.

5.3.3 Effect of carbohydrates-grown *B. infantis* on the expression levels of occludin and an anti-inflammatory cytokine

To assess whether carbohydrates-grown bifidobacteria influences the secretion of occludin and an anti-inflammatory cytokine, RT-qPCR was employed. **Fig. 5.4a and b** show that the expression of occludin in the LPS only treated cells for both Caco-2 and HT29-MTX cells was significantly downregulated (p-value < 0.0005) as compared to the vehicle groups. However, the LPS-induced groups that were stimulated with oligosaccharides- (HMO and 2'-FL and LNnT) grown bacteria illustrated a less significant difference in the expression levels of occludin with a p-value of less than

0.05 and 0.005 for the Caco-2 and HT29-MTX cells, respectively as compared to the vehicle (untreated) groups (**Fig. 5.4a and b**). Comparisons were also made between cells, which were treated with LPS only and those that were treated with both LPS and carbohydrates-grown bacteria. It can be observed that the variation in the abundance of occludin between the oligosaccharides- (HMO and 2'-FL and LNnT) grown bacteria induced cells and the LPS only treated cells were more significant than that of lactose-grown bacteria and the LPS group (**Fig. 5.4a and b**).

The expression of an anti-inflammatory cytokine, IL-10, was also assessed in addition to determining the levels of occludin. Similar to the pattern observed for occludin, the amount of IL-10 was significantly lower in the LPS only treated cells than in the vehicle groups for both cell lines (**Fig. 5.4c and d**). However, following the treatment of the LPS-induced Caco-2 and HT29-MTX cells with oligosaccharides-grown bacteria, particularly the extracted HMOs as opposed to the pure 2'-FL and LNnT, the increase in the expression levels of IL-10 was greater than that of lactose-grown bacteria when compared against the LPS only treated cells (**Fig. 5.4c and d**).

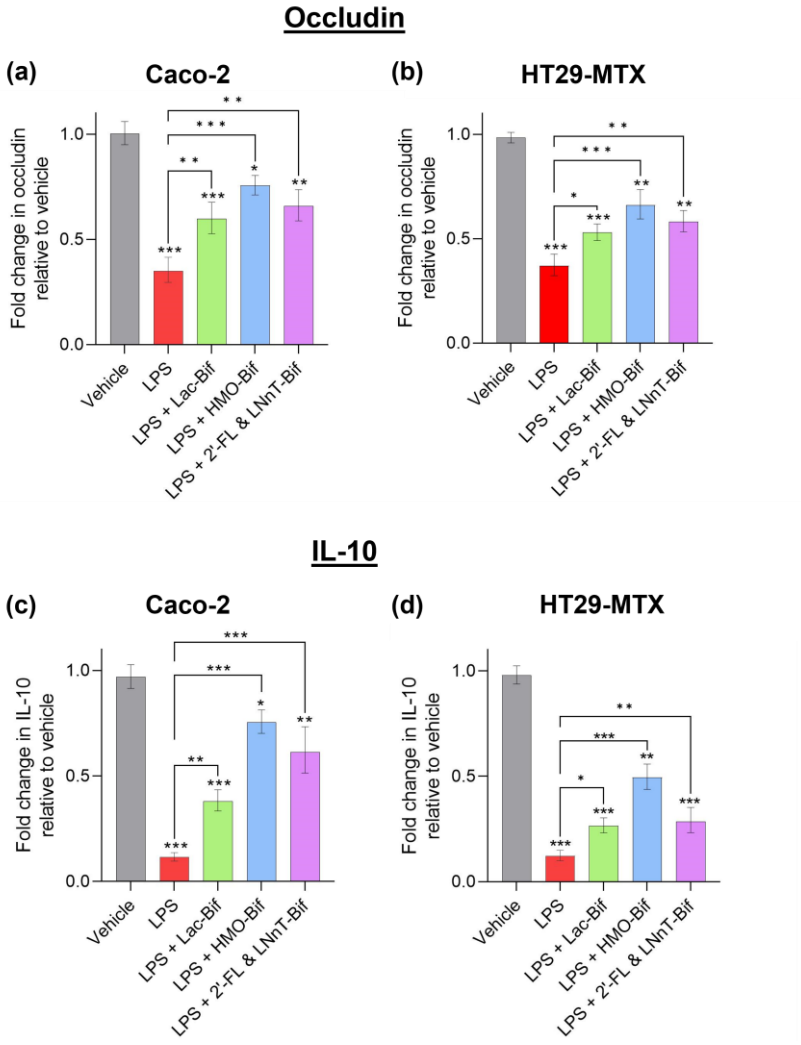

Figure 5.4. Expression of occludin in (a) Caco-2 and (b) HT29-MTX cells and interleukin- (IL) 10 in (c) Caco-2 and (d) HT29-MTX cells incubated with LPS only (red), LPS and lactose-*B. infantis* (LPS + Lac-Bif; green), LPS and extracted HMO-

B. infantis (LPS + HMO-Bif; blue) and LPS and 2'-FL & LNnT-*B. infantis* (LPS + 2'-FL & LNnT-Bif; purple). These data were measured using quantitative reverse-transcriptase real-time polymerase chain reaction (RT-qPCR), normalised to β-actin and illustrated as fold induction relative to vehicle group (grey). Results are mean ± SD, of 3 biological replicates, * $p < 0.05$, ** $p < 0.005$ and * $p < 0.0005$.

5.3.4 Comparisons of the integrity of intestinal epithelial monolayer and localisation of occludin between carbohydrates-grown *B. infantis* and milk-like systems-grown bifidobacteria

The next step in this study was to investigate whether *B. infantis* cultured on milk-like systems as a whole, would display similar resistance to the effects of LPS on the integrity of the intestinal epithelial monolayer and localisation of occludin as that of carbohydrates-grown bacteria. TEER measurements were conducted again to determine the permeability of the monolayer. While the TEER results for the vehicle groups of both cells remained constant until t = 24 h, the TEER measurements of the LPS only induced Caco-2 and HT29-MTX cells decreased significantly after 24 h reaching values of 431.7 ± 19.1 Ω/cm^2 and 220.3 ± 18.2 Ω/cm^2 for Caco-2 and HT29-MTX cells, respectively. Similar to the influence of the carbohydrates-grown bacteria on the integrity of tight junctions, the TEER measurements of the milk-like systems-grown bacteria were higher than the LPS only induced cells with *B. infantis* cultured on mature non-pasteurised human breast milk and colostrum substitute mixture exhibiting TEER results within errors of each other. In addition, the TEER values of these two milk-like systems-grown *B. infantis* were higher than that of infant formula-grown bacteria (**Fig. 5.5a and b**).

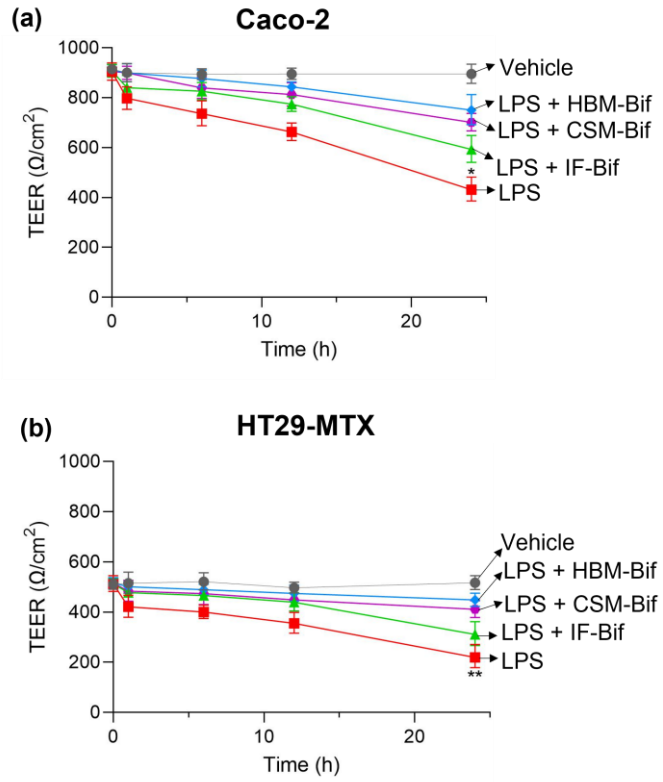

Figure 5.5. Changes in transepithelial electrical resistance (TEER) values (Ω/cm^2) of LPS only (red), LPS with infant formula-grown *B. infantis* (LPS + IF-Bif; green), LPS with colostrum substitute mixture-grown *B. infantis* (LPS + CSM-Bif; purple) and LPS with human breast milk-grown *B. infantis* (LPS + HBM-Bif; blue) treated (a) Caco-2 and (b) HT29-MTX cells are illustrated relative to vehicle (untreated) cells (grey) at t = 1 h, 6 h, 12 h and 24 h. Values were normalised to an empty Transwell, mean ± SD of 3 biological replicates. * $p < 0.05$, ** $p < 0.005$ when compared with vehicle.

Analogous to the effect of carbohydrates-grown bifidobacteria on the integrity of the intestinal monolayer, bifidobacteria cultured on human breast milk and colostrum substitute mixture displayed a more intense fluorescence as opposed to LPS only induced cells (treated without any bacteria) (**Fig. 5.6a**). These fluorescence images were further supported by analysing the fluorescence intensity between carbohydrates-grown *B. infantis* and milk-like systems-grown bacteria. As seen in **Fig. 5.6b**, the statistical difference between the carbohydrates-grown *B. infantis* and milk-like systems-grown *B. infantis* against the LPS only induced Caco-2 cells were similar. For instance, bifidobacteria cultured on HMOs and human breast milk displayed an increase in the relative fluorescence intensity, with a p-value less than 0.005 when compared against LPS only induced Caco-2 cells. This result was also determined for the HT29-MTX cells whereby *B. infantis* grown on infant formula, human breast milk, and colostrum substitute mixture showed similar differences as carbohydrates-grown bacteria when compared against LPS only treated cells (**Fig. 5.6c**). Moreover, it can be observed that bifidobacteria cultured on HMOs and human breast milk resulted in the highest expression of occludin (fluorescence intensity of 86.8-92.0% and 74.1-78.2% for Caco-2 and HT29-MTX cells, respectively). This is followed by colostrum substitute mixture-grown *B. infantis* and pure 2'-FL and LNnT-grown *B. infantis*

and lastly, lactose-grown *B. infantis* and infant formula-grown *B. infantis* with the lowest expression of occludin (**Fig. 5.6b and c**).

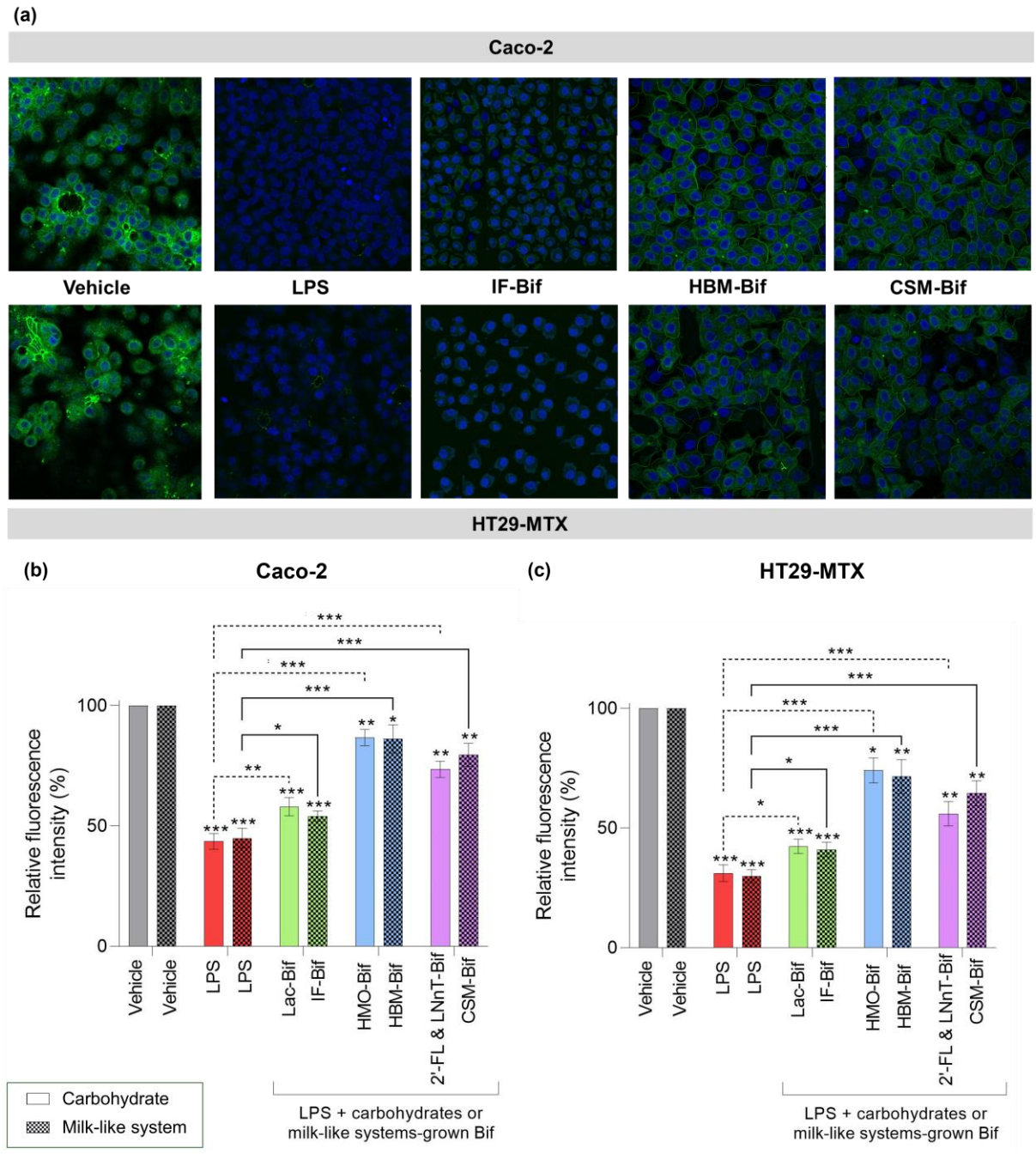

Figure 5.6. (a) Immunofluorescence staining of occludin tight junction protein in Caco-2 (top panels) and HT29-MTX (bottom panels) for vehicle, LPS only, LPS with infant formula-*B. infantis* (IF-Bif), LPS with human breast milk-*B. infantis* (HBM-Bif) and LPS with colostrum substitute mixture-*B. infantis* (CSM-Bif) treated cells. Magnification: ×20. Relative fluorescence intensity of treated (b) Caco-2 and (c) HT29-MTX cells where the filled bar graphs represent carbohydrates-grown *B. infantis* groups [vehicle; grey, LPS only; red, LPS with lactose-*B. infantis* (Lac-Bif); green, LPS with HMO-*B. infantis* (HMO-Bif); blue, LPS with 2'-FL and LNnT-*B. infantis* (2'-FL & LNnT-Bif); purple] and shaded bar graphs indicate milk-like systems-grown *B. infantis* [vehicle; grey shaded, LPS only; red shaded, LPS with lactose-*B. infantis* (Lac-Bif); green, LPS with HMO-*B. infantis* (HMO-Bif); blue shaded, LPS with colostrum substitute mixture-*B. infantis* (CSM-Bif); purple shaded]. Results are mean ± SD, of 3 biological replicates, * $p < 0.05$, ** $p < 0.005$ and * $p < 0.0005$.

5.3.5 Effect of milk-like systems-grown *B. infantis* on the expression levels of IL-10

Similar to the impact of carbohydrates-grown *B. infantis* on the expression levels of IL-10, the incubation of Caco-2 and HT29-MTX cells with milk-like systems-grown *B. infantis* increased the abundance of the anti-inflammatory cytokine in comparison to LPS only induced cells (**Fig. 5.7a and b**). In both cell lines, it can be observed that cells that were only treated with LPS and cells that were incubated with LPS and infant formula-grown bifidobacteria resulted in IL-10 levels that were significantly lower than the vehicle groups (p-value < 0.0005). However, when the cells were treated with either mature non-pasteurised human breast milk-grown *B. infantis* or colostrum substitute mixture-grown *B. infantis*, the statistical differences with the vehicle groups were less significant (either p-value < 0.005 or 0.05). These results not only show that milk-like systems-grown *B. infantis* are able to exude similar effects to carbohydrates-grown bacteria but more importantly, the similar expression levels of IL-10 and integrity of tight junctions (**Fig. 5.6**) between intestinal cells treated with colostrum substitute mixture-grown *B. infantis* and mature non-pasteurised human breast milk-grown *B. infantis* indicate how closely the formulation resembles human milk/colostrum.

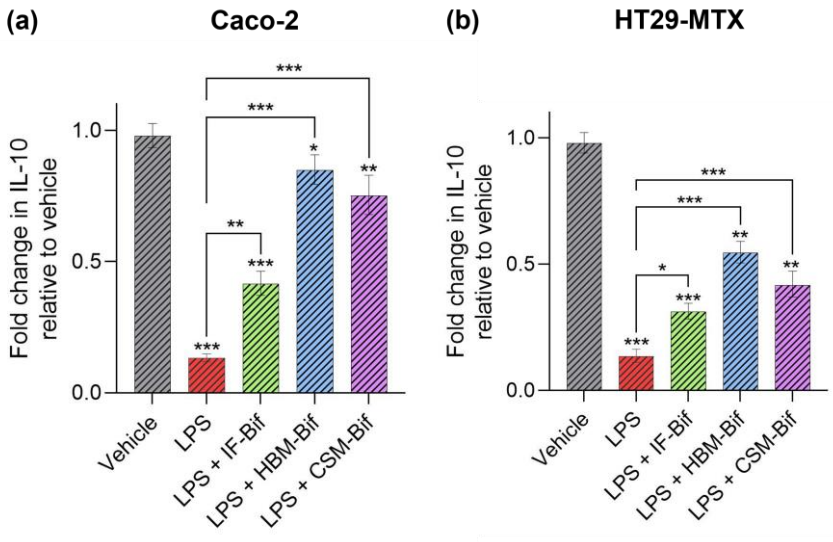

Figure 5.7. Expression of interleukin- (IL) 10 in (a) Caco-2 and (b) HT29-MTX cells incubated with LPS only (red shaded), LPS with infant formula-*B. infantis* (LPS + IF-Bif; green shaded), LPS with human breast milk-*B. infantis* (LPS + HBM-Bif; shaded blue), and LPS with colostrum substitute mixture-*B. infantis* (LPS + CSM-Bif; shaded purple). These data were measured using quantitative reverse-transcriptase real-time polymerase chain reaction (RT-qPCR), normalised to β-actin and illustrated as fold induction relative to vehicle group (grey). Results are mean ± SD, of 3 biological replicates, * $p < 0.05$, ** $p < 0.005$ and * $p < 0.0005$.

5.4 Discussion

The intestinal epithelium constitutes one of the body's largest mucosal surfaces and is the main physical barrier against pathogens while ensuring efficient absorption of essential nutrients. Although

most of the cells that line the epithelium are absorptive enterocytes, additional intestinal epithelial cells namely secretory, goblet and enteroendocrine cells, preserve the barrier and digestive functions of the intestinal epithelium. However, immaturity of the intestinal barrier and the GIT immune system might lead to abnormal patterns of intestinal microbial colonisation and inflammation [262]. Despite the pathogenesis of NEC remaining elusive, previous studies have suggested that NEC can be due to formula feeding, gut ischemia and intestinal colonisation [263, 264]. These perinatal insults lead to a cascade of hyperinflammatory responses, which includes increased intestinal permeability and translocation of bacteria and pathogens [265]. These effects are characteristic of NEC and is highly susceptible in preterm infants leading to mortality rates ranging from 10-30% and even reaching close to 100% for preterm infants experiencing severe NEC, which is characterised by pan-intestinal involvement [266].

Normally, infants naturally receive human colostrum from birth and subsequently human breast milk. Both are rich in bioactive factors such as proteins namely lactoferrin, lysozyme and sIgA that modulate local and systemic neonate immunity while fatty acids and peptides produce antimicrobial factors during digestion [267, 268]. However, unlike these bioactive factors that undergo the process of digestion into smaller absorbable units, HMOs remain intact and contribute towards innate immunity to pathogen colonisation through the saturation of the GIT with soluble glycans [269]. Additionally, HMOs serve as growth factors for bifidobacteria, which are proficient at utilising these soluble carbohydrate oligomers [270]. In this study, the bifidobacteria subspecies of interest was *B. infantis*, a Gram-positive bacteria, which is not only a mutualist coloniser of the human infant gut but has also been shown to modulate the risk of autoimmunity, atopic wheeze and potentially enteric inflammation during the early stages of life [36, 271, 272].

In contrast to term infants who are fed with human colostrum that is only secreted during postpartum, premature infants are fed with alternatives, namely pasteurised DHM and fortifiers. While probiotics have been added to these fortifiers in an attempt to promote a microbial community that attenuates or prevents dysbiosis, the limited negative trials and lack of regulation imposed on the safety and efficacy of these probiotics could cause harm to preterm infants [273, 274]. Moreover, these probiotics could have been derived from bovine milk, in which not only is the concentration of oligosaccharides lower than that of human colostrum/milk, but also vary in prevalence of specific oligosaccharide compositions [250, 251]. For example, instead of HMOs, which contain *N*-acetylglucosamine with D-glucose, D-galactose, L-fucose and *N*-acetylneuraminic acid residues, bovine (and other non-human mammalian) milk oligosaccharides include *N*-glycolylneuraminic acid residues that cannot be synthesised by humans [275]. The low prevalence and variation in the specific oligosaccharide compositions in these fortifiers and formulas could cause a lack of microbial diversity. This might be further attenuated by the low levels of commensal bacteria and increasing levels of pathogenic bacteria including *Enterobacter, Enterococcus, Escherichia,* and *Klebsiella* [276, 277].

Consequently, the integrity of the intestinal epithelial barrier could be compromised leading to characteristics associated with NEC such as bacterial translocation, activation of innate immune responses and inflammation [278-280]. It was thus important to firstly understand the role of HMOs as a growth source for *B. infantis*. This was established through the use of an *in vitro* (intestinal epithelial cells) NEC model. Subsequently, this model was tested with milk-like systems-grown *B. infantis* to examine whether an enhanced nutrient strategy, the colostrum substitute mixture, was able to exert a positive influence over the integrity of tight junction proteins and expression level of anti-inflammatory IL-10 cytokine.

Among the several human intestinal epithelial cell lines, Caco-2 and HT29-MTX are widely used to study the effects of NEC-associated factors and drug transport permeability [281]. While Caco-2 is derived from intestinal absorptive cells, HT29-MTX is a subset of goblet cells. The former spontaneously differentiates into enterocytes with a polarised monolayer and expresses brush border with intestinal enzymes and transporters on their apical surface [149, 282]. In addition, Caco-2 cells are characteristic of relatively tight junctions that limit the permeability of hydrophilic compounds. The integrity of the monolayers can be determined by measuring TEER, which is often used as a tool to study epithelial barrier function. **Fig. 5.2** shows that the TEER values of the Caco-2 monolayers were higher than the HT29-MTX cells for all the treatment groups at the various time points. Although confluent HT29-MTX cells develop functional tight junction complexes, this cell line is unable to express tight junctions to the same extent as that of Caco-2. Wikman *et al.,* demonstrated that the HT29 cell monolayers were more permeable with the TEER measurement being significantly lower than that of Caco-2 cells. The low integrity of tight junctions of the HT29 cells were further illustrated through the permeability of a hydrophilic marker molecule, mannitol, which was 50-fold higher in the HT29 monolayers than in the Caco-2 cells [283]. Despite the lower TEER measurements in the HT29-MTX cells than the Caco-2 cells in this present study, both cell lines illustrated a significant decrease in the expression of tight junctions following the treatment with LPS alone. The low TEER values validate the use of LPS in *in vitro* NEC experiments to disrupt the tight junction complexes thereby inducing a leakage in the cell monolayers [284]. Upon treatment of the LPS-induced Caco-2 and HT29-MTX cells with *B. infantis* grown on carbohydrates (lactose/HMO/2'-FL and LNnT), the TEER measurements increased for both cell lines. Due to the ability of *B. infantis* to consume carbohydrates, this allows the bifidobacteria to adhere to the intestinal cells and thus modulate the tight junctions. Chichlowski *et al.,* showed that HMO had an impact on the binding abilities of *B. infantis* with an induced expression of a cell membrane glycoprotein, SELPLG [182]. These results suggest the ability of carbohydrates-grown *B. infantis* in facilitating microbial colonisation and hence, result in a protective modulation of intestinal epithelial cells.

The effect of LPS and the subsequent influence of carbohydrates-grown *B. infantis* on the distribution of occludin was further justified through immunofluorescence studies. Typically, the tight

junction protein is localised on the apical end of the membrane of polarised Caco-2 and HT29 epithelial cells (**Fig. 5.3a**) and functions as a barrier against solutes [159, 242]. However, upon various stimuli and mediators, the localisation of occludin can be affected. In this study, the treatment of the intestinal epithelial cells with LPS alone destroyed the tight junction protein as seen by the absence of fluorescence staining (**Fig. 5.3b**). The disruption of occludin, together with other tight junction proteins such as ZO-1 and claudin, have been shown to cause barrier dysfunction leading to increased permeability and inflammatory responses [285]. In contrast to the LPS only induced cells, the Caco-2 and HT29-MTX cells that were incubated with carbohydrates- (lactose, extracted HMOs and 2'-FL and LNnT) grown *B. infantis* displayed a brighter fluorescence (**Fig. 5.3c-e**). While the lactose-grown bifidobacteria caused redistribution of occludin into the cytoplasm (**Fig. 5.3c**), cells that were treated with *B. infantis* cultured on extracted HMOs and 2'-FL and LNnT resulted in a less significant relocalisation of occludin, as seen by the distinct fluorescence surrounding the membrane (**Fig. 5.3d and e**). The difference in localisation of occludin between the cells incubated with lactose-grown *B. infantis* and those that were treated with oligosaccharide- (HMO and 2'-FL and LNnT) grown bifidobacteria illustrates that the barrier function in the former treatment group was still defective whereas the oligosaccharide-grown *B. infantis* was able to modulate the subcellular localisation of occludin. The restoration of the distribution of the tight junction protein results in the formation of a protective enterocyte barrier, which could thus prevent a cascade of inflammatory responses from occurring [286].

In addition to immunofluorescence studies, RT-qPCR was also utilised to further validate the expression levels of occludin. **Fig. 5.4a and b** show that the LPS only induced groups resulted in the downregulation of occludin. The decreased level of this tight junction protein constitutes one of the major factors that leads to the disruption of barrier function and increased permeability of the intestinal barrier [285]. While the lactose-grown *B. infantis* resulted in an increase in expression levels of occludin as compared to the LPS only treated cells, the abundance of this tight junction protein was still significantly lower (p-value < 0.0005) than the vehicle groups (**Fig. 5.4a and b**). It was only when the cells were treated with oligosaccharide- (HMO and 2'-FL and LNnT) grown bacteria that the p-value increased to 0.005-0.05 indicating a smaller variation compared to the vehicle groups (**Fig. 5.4a and b**). Furthermore, the expression levels of IL-10 anti-inflammatory marker in Caco-2 and HT29-MTX cells were significantly elevated upon the treatment with oligosaccharide-grown bifidobacteria as opposed to the LPS only treated groups (**Fig. 5.4c and d**). The balance of cytokines such as IL-10 is another crucial component in ensuring homeostasis and gut immunity against NEC. IL-10 is an example of an inhibitory cytokine, which has been shown to dampen inflammatory responses in *in vivo* models [287, 288]. For instance, Kühn *et al.*, illustrated that mice deficient in IL-10 developed intestinal inflammation as characterised by the presence of colitis [289]. In contrast, mice injected with IL-10 reduced local and systemic inflammation [290]. In this present study, it can hence be inferred that the

presence of HMOs acts as a source of nourishment for the bifidobacteria that in turn aids in the modulation of anti-inflammatory cytokines and intercellular tight junction proteins, thereby decreasing intestinal permeability, preventing pathogenesis and inflammatory responses [291].

Following the analysis of the effects of carbohydrates only grown *B. infantis* on the localisation of occludin and expression levels of IL-10, these measurements were conducted again but instead, to test whether milk-like systems- (preterm infant formula, mature human breast milk and colostrum substitute mixture) grown bacteria would have an influence on these anti-inflammatory markers. **Fig. 5.5 and 5.6** show that the LPS inflammatory stimulus increased paracellular permeability and reduced the localisation of occludin in both cell lines relative to the vehicle cell groups. However, milk-like systems-grown *B. infantis* were able to modulate the localisation of occludin tight junction protein, suggesting prevention of intestinal barrier disruption (**Fig. 5.6a**). The similar statistical difference between Caco-2 and HT29-MTX cells treated with *B. infantis* cultured on carbohydrates and milk-like systems against the LPS only induced cells further illustrates that the milk-like systems exerted a similar effect as pure carbohydrates in increasing the expression of occludin (**Fig. 5.3, 5.4a and b and 5.6**).

The expression of both occludin and IL-10 was impacted significantly in Caco-2 and HT29-MTX cells that were treated with *B. infantis* grown on human breast milk and the colostrum substitute formulation as opposed to infant formula-grown *B. infantis* (**Fig. 5.6 and 5.7**). It has been shown that infants who receive human milk or colostrum, harbour early gut microbiota dominated by bifidobacteria as compared to preterm infants and/or term infants who are formula fed [25, 292, 293]. The difference in the composition of infant gut microbiome and resulting inflammation responses such as NEC in preterm infants is due to the presence of oligosaccharides, which are absent in bovine-derived infant formulas [28]. In this study, the preterm infant formula used was mainly derived from bovine milk with a lactose content of 3.7% *w/v* and an absence of HMOs (**Table 5.1**). Although lactose is a source of energy for infants, bifidobacteria gene clusters that are linked to the fermentation of HMOs are only expressed during the growth on HMOs but not during the growth on lactose [31, 294]. Through the metabolism of HMOs by bifidobacteria, short-chain fatty acids are produced, which in turn contribute to the regulation of the integrity of the intestinal layer while increasing the expression levels of anti-inflammatory cytokines [295]. Hence, in contrast to lactose found in bovine derived infant formulas, HMOs in human milk and colostrum exert a probiotic effect that shapes gut microbiome in infants thereby reducing the possibility of inflammatory diseases, especially NEC, from occurring [296, 297].

Due to one of the characteristics of NEC being increased intestinal permeability, the ability of milk-like systems-grown *B. infantis* on restoring the monolayer was also determined. Cells that were incubated with colostrum substitute mixture-grown bacteria resulted in a greater localisation of occludin than infant formula-grown *B. infantis* in both cell lines (**Fig. 5.6a**). The effectiveness of the colostrum substitute mixture in modulating the integrity of the monolayer was further illustrated in **Fig. 5.6b and**

c whereby the statistical difference was significant (p-value < 0.0005) between the expression of occludin in the LPS only induced cells and the colostrum substitute mixture-grown *B. infantis* for both cell lines. In contrast to preterm infant formula, which contained lactose, the colostrum substitute mixture consisted of reconstituted HMOs from mature non-pasteurised human breast milk. While prebiotics such as fructo- and galacto-oligosaccharides are unable to promote the growth of bifidobacteria, Puccio *et al.,* reported that the abundance of specific HMOs such as fucosyl- (2'-FL) and core (LNnT) oligosaccharides together, supplement the growth of the bifidobacteria gene clusters and reduce the severity of the inflammatory disease in *in vivo* models [246, 298]. Aside from determining the effectiveness of the colostrum substitute mixture on the integrity of the monolayer, the effect of this mixture on the expression levels of IL-10 indicated that the abundance of this anti-inflammatory cytokine from the cells treated with colostrum substitute mixture-grown *B. infantis* and human breast milk-grown bacteria were within errors of each other (**Fig. 5.7**). These data indicate the importance of the symbiotic treatment between *B. infantis* and HMOs in human breast milk and colostrum substitute mixture, which provide persistent colonisation of HMO-catabolising subspecies and subsequently ensures active metabolism that may be connected to an array of host benefits including increase in expression of anti-inflammatory cytokines while preserving intestinal barrier function [32-34, 36]. Moreover, the closeness in expression levels of occludin and IL-10 between the cells incubated with colostrum substitute mixture-grown *B. infantis* and human breast milk-grown bifidobacteria shows that these two systems are comparable with each other, more so than infant formula is to human breast milk. Therefore, the implications of using colostrum substitute mixture as an alternative to infant formula could potentially be extended to reducing the onset of NEC in preterm infants.

5.5 Conclusion

In this study, the use of carbohydrates and subsequently milk-like systems, as a growth source for *B. infantis* in an *in vitro* NEC model was investigated by examining the permeability of the monolayer of intestinal epithelial cells and gene expression levels of a tight junction protein and anti-inflammatory cytokine. LPS was utilised as an inflammatory mediator, which caused disruption of the membrane of the intestinal epithelial cells, mimicking the onset of NEC in preterm infants. Following the treatment of LPS-induced cells with *B. infantis* cultured on pure and extracted HMOs and HMO-containing milk-like systems (human breast milk and colostrum substitute mixture), the biological markers of NEC were modulated. The increase in integrity of monolayers suggests that HMOs and HMO-containing milk-like systems act as a nutrient source for *B. infantis* as compared to lactose and infant formula. Not only do these findings highlight the necessary human milk bioactive factor required in shaping the infant microbiota but also demonstrate the close resemblance of the colostrum substitute mixture to mature non-pasteurised human milk in exerting a beneficial outcome. The formulation of the colostrum substitute mixture is a step closer to potentially using this mixture as an alternative feeding option in reducing the onset of NEC *in vivo.*

Chapter 6: Summary and future outlook

6.1 Summary

Human breast milk is regarded as the optimum source of infant nutrition during the first six months of life. However, human colostrum, a thick-yellowish liquid that is secreted prior to mature human milk is often overlooked for its importance. In comparison to human milk, colostrum is rich in bioactive factors such as lipids, proteins and human milk oligosaccharides (HMOs) that serve to stimulate the development of organs while preventing the onset of diseases from occurring in infants. Although the beneficial properties of these bioactive components have been researched extensively, the disposition of human colostrum and milk lipids during digestion was poorly understood. Recent works in the literature have demonstrated that during the digestion of infant formulae and mammalian milk, lipids self-assembled into several types of lipid liquid crystalline (LC) structures consisting of lamellar, bicontinuous cubic (*Im*3*m*), hexagonal (H_2) and inverse micellar cubic (I_2) phases [120, 215, 218]. It was thus hypothesised that these colloidal structures are important as acting as delivery vehicles for the transport of poorly water-soluble nutrients. This thesis focused on correlating the changes in lipid and free fatty acid (FFA) composition with structures formed during the digestion of human colostrum, mature human non-pasteurised milk and pasteurised donor human milk (DHM).

Furthermore, due to the small quantities of human colostrum being secreted only during postpartum, pasteurised DHM and infant formulas are fed to premature infants. However, due to differences in the content and composition of bioactive factors found in these alternatives, pasteurised DHM and formulas might not meet the nutritional demands of an infant. Therefore, another aim of this thesis was to evaluate the digestibility of a colostrum substitute formulation and compare the structural behaviour of lipids to that of human colostrum. Lastly, understanding the nutritional impact of the colostrum substitute mixture over preterm infant formula on protecting intestinal cells against inflammation was analysed using an *in vitro* NEC model.

The proposed hypotheses were that:

1. Different stages of lactation and pasteurisation of human milk will influence the FFA composition and structural behaviour of lipids during digestion.
2. Colostrum substitute mixtures designed to have a simplified TAG composition similar to human colostrum lipids will exhibit the same lipid self-assembly when emulsified and digested.
3. Addition of reconstituted HMOs to a colostrum substitute will provide equivalent performance with respect to biomarkers of NEC compared to human milk and better than infant formula.

The first experimental chapter (Chapter 3) compared milk from the different stages of lactation and the impact of pasteurisation on the FFA composition and the subsequent effect on the types of lipid LC phases formed during *in vitro* digestions. Earlier studies either highlighted the lipid composition of human colostrum and mature human milk prior to digestion or illustrated the types of lipid LC phases that formed during digestion [126, 189, 218]. However, the impact of lipid composition on the lipid LC

structures that formed and whether pasteurisation of human milk led to any changes in the self-assembly of lipids were unknown. In this chapter, it was demonstrated that different types of lipid LC structures were formed during the digestion of these colostrum and milk systems due to differences in the FFA composition. Despite colostrum digesting to a similar extent as that of mature non-pasteurised human milk and pasteurised DHM under similar conditions, only a lamellar phase was formed and remained persistent throughout the digestion of colostrum. In comparison, a cubic micellar I_2 phase (*Fd*3*m* spacegroup) and H_2 phase were evident during the digestion of both types of human milk. Instead, these variations in the self-assembly of lipids were attributed to differences in the FFAs composition released during digestion. Although the fatty acid (FA) composition [18:1/16:0/18:1 (O/P/O; oleic/palmitic/oleic)] prior to digestion was predominant regardless of the stage of lactation or effect of pasteurisation, mature non-pasteurised human milk and pasteurised DHM liberated a higher percentage of free oleic acid from the *sn*-1 and *sn*-3 positions than colostrum. This resulted in the formation of non-lamellar phases during the digestion of human milk. In contrast, the release of a higher proportion of free palmitic acid from colostrum than human milk favoured the formation of a more lamellar phase in the former. Hence, this first experimental chapter emphasised the relationship between lipid and FFA composition and the structural behaviour of lipids thereby providing a pathway for the design of a colostrum substitute formulation.

The next experimental chapter (Chapter 4) was founded on the issue of the importance of feeding premature infants with human colostrum over pasteurised DHM and formulas [21-25] and the need to evaluate the formulation of a colostrum substitute mixture, by comparing how closely the digestibility and structural behaviour of a colostrum substitute mixture was to that of human colostrum. The first aspect was to determine whether the presence of water-soluble nutrients that were extracted from mature non-pasteurised human milk and reconstituted in the digestion buffer used to prepare the colostrum substitute mixtures had an influence on the digestibility of lipids. It was found that regardless of the presence of the water-soluble nutrients in the colostrum substitute mixtures, the initial rates and final extents of digestion were within errors of each other. Moreover, the similar extents of digestion of the colostrum substitute mixtures and human colostrum illustrated that the digestion behaviours of these two systems were almost alike. Interestingly, despite the same initial total lipid content and similar extents of digestion of both systems, the digestion of human colostrum lipids only led to the formation of a lamellar phase whereas the digestion of the colostrum substitute mixtures resulted in the appearance of a cubic micellar (I_2) phase (*Fd*3*m* spacegroup) in addition to a lamellar phase. The variations in structural behaviour could have instead been attributed to the greater ratio of long-chain saturated to long-chain unsaturated FFAs that were released from the colostrum substitute mixtures than human colostrum. The higher percentage of long-chain unsaturated FFAs from the colostrum substitute mixture resulted in the self-assembly of lipids to adopt an inverse micellar cubic phase while the release of more long-chain saturated FFAs from human colostrum caused the formation of a lamellar phase. The issue

revolving around the lack of health facilities and refrigeration for storing liquid colostrum was also addressed in this chapter by preparing colostrum substitute tablets and determining whether tableting had any effect on the self-assembly of colostrum substitute lipids. Although peaks indicative of the recrystallisation of long-chain TAGs during tableting followed by re-dispersion of the colostrum substitute tablets were observed before digestion, the non-tableted and tableted colostrum substitute mixtures displayed lamellar and cubic micellar (I_2) phases when the two systems reached 60% digestion. The formulation of these colostrum substitute mixtures in the form of a dispersible tablet could potentially alleviate issues pertaining to storage in households. More importantly, the formulation of these colostrum substitute mixtures will aid in understanding the ability of these mixtures to reduce the effects of NEC and compare their performance against preterm infant formula.

The third experimental chapter (Chapter 5) was focused on the nutritional impact of the colostrum substitute formulation in reducing inflammatory responses due to NEC in intestinal epithelial cells. Through the implementation of an *in vitro* NEC model, lipopolysaccharide- (LPS) induced cells were incubated with *Bifidiobacterium longum* subspecies (subsp.) infantis (*B. infantis)* that was cultured on carbohydrates: extracted HMOs from mature human breast milk, selected pure HMOs (2'-fucosyllactose; 2'-FL and lacto-*N*-neotetraose; LNnT) and lactose. Subsequently, *B. infantis* was grown on milk-like systems: preterm infant formula, mature non-pasteurised human breast milk and the colostrum substitute mixture to determine whether these milk-like systems would be able to exude similar effects as carbohydrates-grown bifidobacteria in altering the integrity and permeability of the intestinal monolayer and more importantly, whether colostrum substitute mixture-grown *B. infantis* would have a greater effect in reducing intestinal inflammatory responses than infant formula-grown *B. infantis*. Here, it was found that bifidobacteria cultured on extracted HMOs (and pure 2'-FL and LNnT), human breast milk and the colostrum substitute mixture resulted in a significantly greater increase in the integrity of intestinal monolayers, localisation of tight junction occludin protein and expression of anti-inflammatory cytokine, interleukin- (IL) 10, compared to lactose-grown *B. infantis* and infant formula-grown *B. infantis.* These results indicate that the nutritional impact of human breast milk and the colostrum substitute mixture are comparable with each other. In addition, the lack of attenuation in the intestinal permeability and anti-inflammatory responses of LPS-incubated cells treated with the infant formula-grown bifidobacteria emphasises the minimal influence that infant formula has over shaping the gut microbiome. Hence, it was crucial to develop a more enhanced nutrient strategy; colostrum substitute mixture, that closely resembles human breast milk/colostrum and exerted a more beneficial outcome in reducing the effects of NEC than preterm infant formula.

6.2 Future directions

Several studies have either been directed at understanding the beneficial properties of bioactive components of human colostrum or the types of lipid LC structures formed during the digestion of human colostrum, but not the interplay between these. Not only has the importance of human colostrum

over current alternatives as the optimum enteral diet for infants been further elaborated in the previous chapters but the influence of the varying lipid and FFA compositions on the self-assembly of lipids from human colostrum, mature milk (non-pasteurised and pasteurised) and the colostrum substitute formulation have also been presented in these findings. However, as the colostrum substitute mixtures were formulated using homo-triglycerides, the potential next generation of colostrum substitute mixtures would contain a proportion of commercial O/P/O (oleic/palmitic/oleic) TAG to push the structural behaviour of lipids towards that of human colostrum. In addition to these studies, the effectiveness of the colostrum substitute formulation in protecting intestinal cells against inflammation using an *in vitro* NEC model has also been illustrated in the previous experimental chapter. Despite the findings obtained from this *in vitro* NEC study, the implications of the lipid LC structures formed during the digestion of colostrum substitute mixture lipids on their ability to potentially deliver the bioactive components such as proteins, salts and HMOs have not been demonstrated. In particular, there is a need to confirm whether the colostrum substitute formulation comprising these bioactive factors would be able to promote a healthy gut microbiota and in turn, reduce NEC *in vivo*.

6.2.1 Demonstrating the nutritional benefit of the colostrum substitute formulation *in vivo*

As the aim of the last experimental chapter (Chapter 5) was to highlight the importance of HMOs-grown *B. infantis* and subsequently the colostrum substitute mixture-grown *B. infantis* on modulating the effects of NEC *in vitro*, the next step would then be to implement this model in an *in vivo* setting. Briefly, mice pups would be co-housed in a human neonatal incubator and stressed with asphyxia and cold stress every 12 h to induce NEC over a period of 72 h [168]. These mice pups would then be separated into four groups and administered with *B. infantis* (10^8 CFU/mL) that was either cultured on mice own milk; breast-fed (Group 1 control), human colostrum (Group 2), colostrum substitute formulation (Group 3) or preterm infant formula (Group 4, negative control) every 3 h. Throughout the experimental procedure, luminal stools from all four groups of mice pups would be collected to quantify the gene expression of *B. infantis* and anti-inflammatory IL-10 cytokine in the gut using quantitative reverse-transcriptase real-time polymerase chain reaction (RT-qPCR). At the end of the experimental time point, the pups would be euthanised and the small intestine excised for lipid LC structure and pathological analysis. In the lipid LC structure experiment, SAXS analysis would be incorporated where the small intestine would be placed on a temperature-controlled (37 °C) mount and scattering profiles of the intestine would be measured at regular time intervals. The purpose of this is to determine whether the same types of colloidal structures *in vivo*, would be formed as those observed *in vitro* (Chapter 4). For the pathological changes in the intestinal architecture of the mice pups, colon sections from the treated mice would be embedded in paraffin and cut into sections before mounting on a slide and processed for hematoxylin and eosin (H&E) staining [299]. The tissues would then be scored

blindly from 3 sections from each pup on a scale of 1-4 based on mucosal architecture, muscle thickening and inflammatory cell infiltration [300, 301].

Moreover, although recent reports have suggested that minimal acquisition of bifidobacteria is observed in infants [302, 303], RT-qPCR as discussed above can also be conducted to determine the translocation of bacteria to intestinal cells. While this is to illustrate the effect of the colostrum substitute mixtures (and other milk-like systems) on the ability of *B. infantis* to adhere to intestinal cells, it is still important to consider that this is merely to indicate the process that could potentially happen in infants. Thus, a better alternative to mice pups would be piglets as this species is able to spontaneously develop full-scale clinical NEC that is contingent on the same biological conditions of human infants including prematurity, bacterial colonisation and feeding of formula [304]. Regardless of the animal species chosen, these *in vivo* experiments would illustrate the nutritional impact of the colostrum substitute formulation, in comparison to the other feeding samples, on the growth of healthy microbiota in the gut and the extent to which the effects of NEC could potentially be reduced *in vivo*.

Additionally, the feeding of colostrum substitute formulation-grown *B. infantis* on microbial diversity could be explored using 16S ribosomal RNA (rRNA). This technique has been widely used as an alternative to conventional culture methods for the analysis of intestinal flora community within a sample [305-307]. The 16S rRNA approach depends on the sequencing of the 16S rRNA gene as the genetic marker, which contains hypervariable regions thereby providing genus-level sensitivity for the detection of bacterial populations [308]. Thus, the bacterial DNA from the luminal stools could be further subjected to terminal restriction fragment length polymorphism analysis and library sequencing of the 16S rRNA gene to characterise whether colostrum substitute formulation-grown *B. infantis* would have an impact on the diversity and structure of gut microbiota *in vivo*.

6.2.2 Understanding the role of milk fat globules in the biological function of colostrum

One of the primary aims of this thesis was to understand the effect of composition of lipids prior to and during digestion on structural behaviour. Future studies could be conducted to interrogate other aspects of the dynamic and complex lipid structures that are fundamental to the functions of human colostrum. For instance, the size regulation of milk fat globules remains elusive. Milk fat globules originate from intracellular lipid droplets and consist of a trilayer of phospholipids intercalated with an array of glycoproteins and other compounds [210]. As the size of milk fat globules exert crucial implications for maternal and infant health in regard to human lactation, it is thus important to evaluate the size of these globules [309]. In Chapters 3 and 4, the particle size distribution of colostrum and milk fat globules were determined using laser light scattering. Other pathways to further analyse the intracellular lipid droplet size is by measuring the amount of TAGs stored in the cell [310]. Through metabolic signalling or regulating the localisation of proteins on the lipid droplets, the cellular TAG

content can be modulated [311]. For example, if a deficiency in one of the proteins is detected, this would result in smaller lipid droplets [312]. Alternatively, the regulation of globule size can be determined through the fusion of intracellular lipid droplets. In this process, substrate FA availability and net energy charge within the cell drive the flux of TAG into the particle [313]. These future studies will highlight metabolic pathways and intracellular compartments that are responsible for phospholipid composition, which in turn influence milk fat globules that provide beneficial outcomes for human lactation.

6.2.3 Improving the disintegration of the dispersible colostrum substitute tablets

For the purpose of this study, excipients were not included during the preparation of the colostrum substitute tablets as the focus was primarily to determine whether freeze-drying followed by tableting alone would induce any changes in the self-assembly of lipids (Chapter 4). However, future studies could include excipients such as poly(vinylpolypyrrolidone), crospovidone and sodium starch glycolate in the formulation of the dispersible colostrum tablets. The aim of adding these excipients is to reduce the disintegration time to less than 3 min in water at room temperature to produce a homogenous dispersion [314]. The development of colostrum substitute dispersible tablets would prevent issues relating to variability in doses and difficulty in swallowing for infants as the desired dose can be controlled by the reconstituted volume for administration [227-230]. In addition, access to health facilities might be difficult thereby restricting infants from receiving the required nourishment. Therefore, colostrum substitute dispersible tablets with an optimised disintegration time would not only alleviate issues for paediatrics but also aid those in developing countries where lack of health facilities and refrigeration would otherwise make storing liquid colostrum difficult.

6.2.4 Analysing the thermal properties of triglyceride mixtures in the colostrum substitute formulation

It was highlighted in Chapter 4 of this thesis that there were no significant differences in the self-assembly of lipids of non-tableted and tableted colostrum substitute mixtures. These studies on structural behaviour are a rationale to pursue further studies on the physical properties of the TAG mixtures. The melting and freezing behaviours of the TAG mixtures in the colostrum substitute formulation can be measured using differential scanning calorimetry. Pre-mixed lipid mixtures would be loaded at 30 °C and subjected to heating and cooling cycles between 80 °C and -30 °C. Lipids are fully molten upon heating and begin to crystallise upon cooling and thus differential scanning calorimetry would aid in determining the points at which the associated endo/exotherms deviated from the baseline [315, 316]. As a previous study has demonstrated that milk-mimicking lipids were molten at 59-64 °C and crystallise upon cooling at close to body temperatures (39-35 °C) [215], it is hypothesised that the TAGs in the colostrum substitute mixtures could be cooled significantly below

the fully melted temperature before they began to recrystallise. This future study would aid in considering the preparation and storage of these mixtures.

6.3 Conclusion

The majority of the proposed hypotheses were validated in this thesis, with the hypothesis that the colostrum substitute formulation being able to reduce the onset of NEC *in vivo* remaining unconfirmed. Despite differences in self-assembly of lipids between human colostrum and the colostrum substitute formulation, due to variations in FFA composition released during digestion, these findings provided a roadmap for the design of a more enhanced nutrient strategy than current preterm infant formulas. Moreover, this thesis has illustrated that the formulation of a colostrum substitute mixture is able to reduce the effects of NEC such as intestinal permeability and inflammation to a similar extent as human breast milk. Further research is still required to expand on the current understanding of the nutritional impact of the colostrum substitute formulation *in vivo*. These future studies are aimed at providing clarity regarding the ability of the lipid LC structures to deliver bioactive components responsible for colonising healthy gut microbiota such as *B. infantis* and reducing the effects of NEC. Therefore, the supplementation of colostrum substitute formulation in concert with the co-evolved *B. infantis* might emphasise the nutritional benefit of the formulation *in vivo* with the potential of reducing the reliance on pasteurised DHM and preterm infant formula as current feeding alternatives for premature infants in the future.

References

[1] World Health, O. Infant and Young Child Feeding. Geneva: World Health Organization; 2009.

[2] Isaacs, E.B., Fischl, B.R., Quinn, B.T., Chong, W.K., Gadian, D.G., Lucas, A. Impact of Breast Milk on Intelligence Quotient, Brain Size, and White Matter Development. Pediatr Res. 2010. 67(4):357-362.

[3] Vohr, B.R., Poindexter, B.B., Dusick, A.M., McKinley, L.T., Wright, L.L., Langer, J.C., *et al.* Beneficial Effects of Breast Milk in the Neonatal Intensive Care Unit on the Developmental Outcome of Extremely Low Birth Weight Infants at 18 Months of Age. Pediatrics. 2006. 118(1):e115-e123.

[4] Mitoulas, L.R., Kent, J.C., Cox, D.B., Owens, R.A., Sherriff, J.L., Hartmann, P.E. Variation in Fat, Lactose and Protein in Human Milk Over 24 h and Throughout the First Year of Lactation. Br J Nutr. 2002. 88(1):29-37.

[5] Ballard, O., Morrow, A.L. Human Milk Composition: Nutrients and Bioactive Factors. Pediatr Clin North Am. 2013. 60(1):49-74.

[6] Smilowitz, J.T., O'Sullivan, A., Barile, D., German, J.B., Lönnerdal, B., Slupsky, C.M. The Human Milk Metabolome Reveals Diverse Oligosaccharide Profiles. J Nutr. 2013. 143(11):1709-1718.

[7] Spevacek, A.R., Smilowitz, J.T., Chin, E.L., Underwood, M.A., German, J.B., Slupsky, C.M. Infant Maturity at Birth Reveals Minor Differences in the Maternal Milk Metabolome in the First Month of Lactation. J Nutr. 2015. 145(8):1698-1708.

[8] de Figueiredo, C.S.M., Palhares, D.B., Melnikov, P., da Cruz Montes Moura, A.J., dos Santos, S.C. Zinc and Copper Concentrations in Human Preterm Milk. Biol Trace Elem Res. 2010. 136(1):1-7.

[9] O'Brien, C.E., Krebs, N.F., Westcott, J.L., Fang, D. Relationships Among Plasma Zinc, Plasma Prolactin, Milk Transfer, and Milk Zinc in Lactating Women. J Hum Lact. 2007. 23(2):179-183.

[10] Uauy, R., Castillo, C. Lipid Requirements of Infants: Implications for Nutrient Composition of Fortified Complementary Foods. J Nutr. 2003. 133(9):2962S-2972S.

[11] Jensen, R.G. Handbook of Milk Composition. San Diego: Academic Press; 1995.

[12] Hernell, O., Bläckberg, L. Human Milk Bile Salt-Stimulated Lipase: Functional and Molecular Aspects. J Pediatr. 1994. 125(5 Pt 2):S56-S61.

[13] Bläckberg, L., Ängquist, K.-A., Hemell, O. Bile Salt-Stimulated Lipase in Human Milk: Evidence for its Synthesis in the Lactating Mammary Gland. FEBS Lett. 1987. 217(1):37-41.

[14] Salentinig, S., Sagalowicz, L., Leser, M.E., Tedeschi, C., Glatter, O. Transitions in the Internal Structure of Lipid Droplets During Fat Digestion. Soft Matter. 2011. 7(2):650-661.

[15] Lindquist, S., Hernell, O. Lipid Digestion and Absorption in Early Life: An Update. Curr Opin Clin Nutr Metab Care. 2010. 13(3):314-320.

[16] Riethorst, D., Mols, R., Duchateau, G., Tack, J., Brouwers, J., Augustijns, P. Characterization of Human Duodenal Fluids in Fasted and Fed State Conditions. J Pharm Sci. 2016. 105(2):673-681.

[17] Kamstrup, D., Berthelsen, R., Sassene, P.J., Selen, A., Müllertz, A. In Vitro Model Simulating Gastro-Intestinal Digestion in the Pediatric Population (Neonates and Young Infants). AAPS PharmSciTech. 2017. 18(2):317-329.

[18] Escobar, G.J., McCormick, M.C., Zupancic, J.A.F., Coleman-Phox, K., Armstrong, M.A., Greene, J.D., *et al.* Unstudied Infants: Outcomes of Moderately Premature Infants in the Neonatal Intensive Care Unit. Arch Dis Child Fetal Neonatal Ed. 2006. 91(4):F238-F244.

[19] Wang, X., Yan, X., Zhang, L., Cai, J., Zhou, Y., Liu, H., *et al.* Identification and Peptidomic Profiling of Exosomes in Preterm Human Milk: Insights Into Necrotizing Enterocolitis Prevention. Mol Nutr Food Res. 2019. 63(13):e1801247.

[20] Lee, A.C.C., Katz, J., Blencowe, H., Cousens, S., Kozuki, N., Vogel, J.P., *et al.* National and Regional Estimates of Term and Preterm Babies Born Small for Gestational Age in 138 Low-Income and Middle-Income Countries in 2010. Lancet Glob Health. 2013. 1(1):e26-e36.

[21] Bell, K.A., Wagner, C.L., Feldman, H.A., Shypailo, R.J., Belfort, M.B. Associations of Infant Feeding With Trajectories of Body Composition and Growth. Am J Clin Nutr. 2017. 106(2):491-498.
[22] Hylander, M.A., Strobino, D.M., Dhanireddy, R. Human Milk Feedings and Infection Among Very Low Birth Weight Infants. Pediatrics. 1998. 102(3):E38.
[23] Bardanzellu, F., Fanos, V., Reali, A. "Omics" in Human Colostrum and Mature Milk: Looking to Old Data With New Eyes. Nutrients. 2017. 9(8):843.
[24] Morales, Y., Schanler, R.J. Human Milk and Clinical Outcomes in VLBW Infants: How Compelling is the Evidence of Benefit? Semin Perinatol. 2007. 31(2):83-88.
[25] Penders, J., Thijs, C., Vink, C., Stelma, F.F., Snijders, B., Kummeling, I., *et al.* Factors Influencing the Composition of the Intestinal Microbiota in Early Infancy. Pediatrics. 2006. 118(2):511-521.
[26] Calvert, R., Beaulieu, J.F., Ménard, D. Epidermal Growth Factor (EGF) Accelerates the Maturation of Fetal Mouse Intestinal Mucosa In Utero. Experientia. 1982. 38(9):1096-1097.
[27] Ouwehand, A.C., Derrien, M., de Vos, W., Tiihonen, K., Rautonen, N. Prebiotics and Other Microbial Substrates for Gut Functionality. Curr Opin Biotechnol. 2005. 16(2):212-217.
[28] Kunz, C. Historical Aspects of Human Milk Oligosaccharides. Adv Nutr. 2012. 3(3):430S-439S.
[29] Sela, D.A., Mills, D.A. Nursing Our Microbiota: Molecular Linkages Between Bifidobacteria and Milk Oligosaccharides. Trends Microbiol. 2010. 18(7):298-307.
[30] Locascio, R.G., Desai, P., Sela, D.A., Weimer, B., Mills, D.A. Broad Conservation of Milk Utilization Genes in Bifidobacterium Longum Subsp. Infantis as Revealed by Comparative Genomic Hybridization. Appl Environ Microbiol. 2010. 76(22):7373-7381.
[31] Sela, D.A., Chapman, J., Adeuya, A., Kim, J.H., Chen, F., Whitehead, T.R., *et al.* The Genome Sequence of Bifidobacterium Longum Subsp. Infantis Reveals Adaptations for Milk Utilization Within the Infant Microbiome. Proc Natl Acad Sci USA. 2008. 105(48):18964-18969.
[32] Alex, P., Zachos, N.C., Nguyen, T., Gonzales, L., Chen, T.-E., Conklin, L.S., *et al.* Distinct Cytokine Patterns Identified From Multiplex Profiles of Murine DSS and TNBS-Induced Colitis. Inflamm Bowel Dis. 2009. 15(3):341-352.
[33] Srutkova, D., Schwarzer, M., Hudcovic, T., Zakostelska, Z., Drab, V., Spanova, A., *et al.* Bifidobacterium Longum CCM 7952 Promotes Epithelial Barrier Function and Prevents Acute DSS-Induced Colitis in Strictly Strain-Specific Manner. PLoS ONE. 2015. 10(7):e0134050.
[34] Krumbeck, J.A., Rasmussen, H.E., Hutkins, R.W., Clarke, J., Shawron, K., Keshavarzian, A., *et al.* Probiotic Bifidobacterium Strains and Galactooligosaccharides Improve Intestinal Barrier Function in Obese Adults but Show No Synergism When Used Together as Synbiotics. Microbiome. 2018. 6(1):121.
[35] Frese, S.A., Hutton, A.A., Contreras, L.N., Shaw, C.A., Palumbo, M.C., Casaburi, G., *et al.* Persistence of Supplemented Bifidobacterium Longum Subsp. Infantis EVC001 in Breastfed Infants. mSphere. 2017. 2(6):e00501-e00517.
[36] Henrick, B.M., Chew, S., Casaburi, G., Brown, H.K., Frese, S.A., Zhou, Y., *et al.* Colonization by B. infantis EVC001 Modulates Enteric Inflammation in Exclusively Breastfed Infants. Pediatr Res. 2019. 86(6):749-757.
[37] Moro, G., Arslanoglu, S., Stahl, B., Jelinek, J., Wahn, U., Boehm, G. A Mixture of Prebiotic Oligosaccharides Reduces the Incidence of Atopic Dermatitis During the First Six Months of Age. Arch Dis Child. 2006. 91(10):814-819.
[38] Arslanoglu, S., Moro, G.E., Schmitt, J., Tandoi, L., Rizzardi, S., Boehm, G. Early Dietary Intervention With a Mixture of Prebiotic Oligosaccharides Reduces the Incidence of Allergic Manifestations and Infections During the First Two Years of Life. J Nutr. 2008. 138(6):1091-1095.
[39] Stoddart, R.W., Widdowson, E.M. Changes in the Organs of Pigs in Response to Feeding for the First 24 h After Birth. Biol Neonate. 1976. 29(1-2):18-27.
[40] Yamashiro, Y., Sato, M., Shimizu, T., Oguchi, S., Maruyama, K., Kitamura, S. Possible Biological Growth Factors in Breast Milk and Postnatal Development of the Gastrointestinal Tract. Acta Paediatr Jpn. 1989. 31(4):417-423.

[41] Fitzgibbons, S.C., Ching, Y., Yu, D., Carpenter, J., Kenny, M., Weldon, C., *et al.* Mortality of Necrotizing Enterocolitis Expressed by Birth Weight Categories. J Pediatr Surg. 2009. 44(6):1072-1076.
[42] Hintz, S.R., Kendrick, D.E., Stoll, B.J., Vohr, B.R., Fanaroff, A.A., Donovan, E.F., *et al.* Neurodevelopmental and Growth Outcomes of Extremely Low Birth Weight Infants After Necrotizing Enterocolitis. Pediatrics. 2005. 115(3):696-703.
[43] Watkins, J.B., Szczepanik, P., Gould, J.B., Klein, P., Lester, R. Bile Salt Metabolism in the Human Premature Infant: Preliminary Observations of Pool Size and Synthesis Rate Following Prenatal Administration of Dexamethasone and Phenobarbital. Gastroenterology. 1975. 69(3):706-713.
[44] Signer, E., Murphy, G.M., Edkins, S., Anderson, C.M. Role of Bile Salts in Fat Malabsorption of Premature Infants. Arch Dis Child. 1974. 49(3):174-180.
[45] Battersby, C., Santhakumaran, S., Upton, M., Radbone, L., Birch, J., Modi, N. The Impact of a Regional Care Bundle on Maternal Breast Milk Use in Preterm Infants: Outcomes of the East of England Quality Improvement Programme. Arch Dis Child Fetal Neonatal Ed. 2014. 99(5):F395-F401.
[46] Hamilton, E., Massey, C., Ross, J., Taylor, S. Early Enteral Feeding in Very Low Birth Weight Infants. Early Hum Dev. 2014. 90(5):227-230.
[47] Meinzen-Derr, J., Poindexter, B., Wrage, L., Morrow, A.L., Stoll, B., Donovan, E.F. Role of Human Milk in Extremely Low Birth Weight Infants' Risk of Necrotizing Enterocolitis or Death. J Perinatol. 2009. 29(1):57-62.
[48] Lönnerdal, B. Bioactive Proteins in Human Milk: Mechanisms of Action. J Pediatr. 2010. 156(2 Suppl):S26-S30.
[49] Zhou, P., Li, Y., Ma, L.-Y., Lin, H.-C. The Role of Immunonutrients in the Prevention of Necrotizing Enterocolitis in Preterm Very Low Birth Weight Infants. Nutrients. 2015. 7(9):7256-7270.
[50] Kronborg, H., Harder, I., Hall, E.O.C. First Time Mothers' Experiences of Breastfeeding Their Newborn. Sex Reprod Healthc. 2015. 6(2):82-87.
[51] Davidson, M., Levine, S.Z., Bauer, C.H., Dann, M. Feeding Studies in Low-Birth-Weight Infants. I. Relationships of Dietary Protein, Fat, and Electrolyte to Rates of Weight Gain, Clinical Courses, and Serum Chemical Concentrations. J Pediatr. 1967. 70(5):695-713.
[52] Taylor, S.N., Basile, L.A., Ebeling, M., Wagner, C.L. Intestinal Permeability in Preterm Infants by Feeding Type: Mother's Milk versus Formula. Breastfeed Med. 2009. 4(1):11-15.
[53] Charman, W.N., Porter, C.J., Mithani, S., Dressman, J.B. Physiochemical and Physiological Mechanisms for the Effects of Food on Drug Absorption: The Role of Lipids and pH. J Pharm Sci. 1997. 86(3):269-282.
[54] Valman, H.B., Heath, C.D., Brown, R.J. Continuous Intragastric Milk Feeds in Infants of Low Birth Weight. Br Med J. 1972. 3(5826):547-550.
[55] Wight, N.E. Donor Human Milk for Preterm Infants. J Perinatol. 2001. 21(4):249-254.
[56] Anderson, D.M., Williams, F.H., Merkatz, R.B., Schulman, P.K., Kerr, D.S., Pittard, W.B., 3rd. Length of Gestation and Nutritional Composition of Human Milk. Am J Clin Nutr. 1983. 37(5):810-814.
[57] Beijers, R.J., Graaf, F.V., Schaafsma, A., Siemensma, A.D. Composition of Premature Breast-Milk During Lactation: Constant Digestible Protein Content (as in Full Term Milk). Early Hum Dev. 1992. 29(1-3):351-356.
[58] Faerk, J., Skafte, L., Petersen, S., Peitersen, B., Michaelsen, K.F. Macronutrients in Milk From Mothers Delivering Preterm. Adv Exp Med Biol. 2001. 501:409-413.
[59] Bauer, J., Gerss, J. Longitudinal Analysis of Macronutrients and Minerals in Human Milk Produced by Mothers of Preterm Infants. Clin Nutr. 2011. 30(2):215-220.
[60] Pang, W.W., Hartmann, P.E. Initiation of Human Lactation: Secretory Differentiation and Secretory Activation. J Mammary Gland Biol Neoplasia. 2007. 12(4):211-221.
[61] Hill, P.D., Aldag, J.C., Demirtas, H., Naeem, V., Parker, N.P., Zinaman, M.J., *et al.* Association of Serum Prolactin and Oxytocin With Milk Production in Mothers of Preterm and Term Infants. Biol Res Nurs. 2009. 10(4):340-349.

[62] Mikkola, K., Ritari, N., Tommiska, V., Salokorpi, T., Lehtonen, L., Tammela, O., *et al.* Neurodevelopmental Outcome at 5 Years of Age of a National Cohort of Extremely Low Birth Weight Infants Who Were Born in 1996-1997. Pediatrics. 2005. 116(6):1391-1400.
[63] Wojcik, K.Y., Rechtman, D.J., Lee, M.L., Montoya, A., Medo, E.T. Macronutrient Analysis of a Nationwide Sample of Donor Breast milk. J Am Diet Assoc. 2009. 109(1):137-140.
[64] Balmer, S.E., Williams, A.F. Guidelines for the Establishment and Operation of Human Milk Banks in the UK. Arch Dis Child. 1995. 73(5):481-482.
[65] Hartmann, B.T., Pang, W.W., Keil, A.D., Hartmann, P.E., Simmer, K. Best Practice Guidelines for the Operation of a Donor Human Milk Bank in an Australian NICU. Early Hum Dev. 2007. 83(10):667-673.
[66] Eidelman, A.I., Schanler, R.J., Johnston, M., Landers, S., Noble, L., Szucs, K., *et al.* Breastfeeding and the Use of Human Milk. Pediatrics. 2012. 129(3):e827-e841.
[67] Haschke, F., Haiden, N., Thakkar, S.K. Nutritive and Bioactive Proteins in Breastmilk. Ann Nutr Metab. 2016. 69 Suppl 2:17-26.
[68] Lönnerdal, B., Erdmann, P., Thakkar, S.K., Sauser, J., Destaillats, F. Longitudinal Evolution of True Protein, Amino Acids and Bioactive Proteins in Breast Milk: A Developmental Perspective. J Nutr Biochem. 2017. 41:1-11.
[69] Sanchez-Pozo, A., Lopez, J., Pita, M.L., Izquierdo, A., Guerrero, E., Sanchez-Medina, F., *et al.* Changes in the Protein Fractions of Human Milk During Lactation. Ann Nutr Metab. 1986. 30(1):15-20.
[70] Sever, O., Mandel, D., Mimouni, F.B., Marom, R., Cohen, S., Lubetzky, R. Macronutrients in Human Milk: Colostrum Lactose but Not Fat or Protein Predicts Mature Human Milk Content. Infant Child Adolesc Nutr. 2015. 7(3):162-165.
[71] Casadio, Y.S., Williams, T.M., Lai, C.T., Olsson, S.E., Hepworth, A.R., Hartmann, P.E. Evaluation of a Mid-Infrared Analyzer for the Determination of the Macronutrient Composition of Human Milk. J Hum Lact. 2010. 26(4):376-383.
[72] Paulaviciene, I.J., Liubsys, A., Molyte, A., Eidukaite, A., Usonis, V. Circadian Changes in the Composition of Human Milk Macronutrients Depending on Pregnancy Duration: A Cross-Sectional Study. Int Breastfeed J. 2020. 15(1):49.
[73] Quinn, E.A., Diki Bista, K., Childs, G. Milk at Altitude: Human Milk Macronutrient Composition in a High-Altitude Adapted Population of Tibetans. Am J Phys Anthropol. 2016. 159(2):233-243.
[74] Góes, H.C., Torres, A.G., Donangelo, C.M., Trugo, N.M. Nutrient Composition of Banked Human Milk in Brazil and Influence of Processing on Zinc Distribution in Milk Fractions. Nutrition. 2002. 18(7-8):590-594.
[75] Klotz, D., Joellenbeck, M., Winkler, K., Kunze, M., Huzly, D., Hentschel, R. High-Temperature Short-Time Pasteurisation of Human Breastmilk is Efficient in Retaining Protein and Reducing the Bacterial Count. Acta Paediatr. 2017. 106(5):763-767.
[76] Peila, C., Coscia, A., Bertino, E., Cavaletto, M., Spertino, S., Icardi, S., *et al.* Effects of Holder Pasteurization on the Protein Profile of Human Milk. Ital J Pediatr. 2016. 42:36.
[77] Piemontese, P., Mallardi, D., Liotto, N., Tabasso, C., Menis, C., Perrone, M., *et al.* Macronutrient Content of Pooled Donor Human Milk Before and After Holder Pasteurization. BMC Pediatr. 2019. 19(1):58.
[78] Adhisivam, B., Vishnu Bhat, B., Rao, K., Kingsley, S.M., Plakkal, N., Palanivel, C. Effect of Holder Pasteurization on Macronutrients and Immunoglobulin Profile of Pooled Donor Human Milk. J Matern Fetal Neonatal Med. 2019. 32(18):3016-3019.
[79] Viverge, D., Grimmonprez, L., Cassanas, G., Bardet, L., Solere, M. Variations in Oligosaccharides and Lactose in Human Milk During the First Week of Lactation. J Pediatr Gastroenterol Nutr. 1990. 11(3):361-364.
[80] Viverge, D., Grimmonprez, L., Cassanas, G., Bardet, L., Bonnet, H., Solère, M. Variations of Lactose and Oligosaccharides in Milk From Women of Blood Types Secretor A or H, Secretor Lewis, and Secretor H/Nonsecretor Lewis During the Course of Lactation. Ann Nutr Metab. 1985. 29(1):1-11.

[81] Coppa, G.V., Gabrielli, O., Pierani, P., Catassi, C., Carlucci, A., Giorgi, P.L. Changes in Carbohydrate Composition in Human Milk Over 4 Months of Lactation. Pediatrics. 1993. 91(3):637-641.
[82] Coppa, G.V., Pierani, P., Zampini, L., Carloni, I., Carlucci, A., Gabrielli, O. Oligosaccharides in Human Milk During Different Phases of Lactation. Acta Paediatr Suppl. 1999. 88(430):89-94.
[83] Bertino, E., Coppa, G.V., Giuliani, F., Coscia, A., Gabrielli, O., Sabatino, G., *et al.* Effects of Holder Pasteurization on Human Milk Oligosaccharides. Int J Immunopathol Pharmacol. 2008. 21(2):381-385.
[84] Zou, X.-Q., Guo, Z., Huang, J.-H., Jin, Q.-Z., Cheong, L.-Z., Wang, X.-G., *et al.* Human Milk Fat Globules From Different Stages of Lactation: A Lipid Composition Analysis and Microstructure Characterization. J Agric Food Chem. 2012. 60(29):7158-7167.
[85] Jensen, R.G. Lipids in Human Milk. Lipids. 1999. 34(12):1243-1271.
[86] Atwood, C.S., Hartmann, P.E. Collection of Fore and Hind Milk From the Sow and the Changes in Milk Composition During Suckling. J Dairy Res. 1992. 59(3):287-298.
[87] Zhao, P., Zhang, S., Liu, L., Pang, X., Yang, Y., Lu, J., *et al.* Differences in the Triacylglycerol and Fatty Acid Compositions of Human Colostrum and Mature Milk. J Agric Food Chem. 2018. 66(17):4571-4579.
[88] Antonakou, A., Skenderi, K.P., Chiou, A., Anastasiou, C.A., Bakoula, C., Matalas, A.-L. Breast Milk Fat Concentration and Fatty Acid Pattern During the First Six Months in Exclusively Breastfeeding Greek Women. Eur J Nutr. 2013. 52(3):963-973.
[89] Giuffrida, F., Austin, S., Cuany, D., Sanchez-Bridge, B., Longet, K., Bertschy, E., *et al.* Comparison of Macronutrient Content in Human Milk Measured by Mid-Infrared Human Milk Analyzer and Reference Methods. J Perinatol. 2019. 39(3):497-503.
[90] Hahn, W.-H., Kim, J., Song, S., Park, S., Kang, N.M. The Human Milk Oligosaccharides are Not Affected by Pasteurization and Freeze-Drying. J Matern Fetal Neonatal Med. 2019. 32(6):985-991.
[91] García-Lara, N.R., Vieco, D.E., De la Cruz-Bértolo, J., Lora-Pablos, D., Velasco, N.U., Pallás-Alonso, C.R. Effect of Holder Pasteurization and Frozen Storage on Macronutrients and Energy Content of Breast Milk. J Pediatr Gastroenterol Nutr. 2013. 57(3):377-382.
[92] Vieira, A.A., Soares, F.V.M., Pimenta, H.P., Abranches, A.D., Moreira, M.E.L. Analysis of the Influence of Pasteurization, Freezing/Thawing, and Offer Processes on Human Milk's Macronutrient Concentrations. Early Hum Dev. 2011. 87(8):577-580.
[93] Newburg, D.S., Walker, W.A. Protection of the Neonate by the Innate Immune System of Developing Gut and of Human Milk. Pediatr Res. 2007. 61(1):2-8.
[94] Böttcher, M.F., Jenmalm, M.C., Björkstén, B. Cytokine, Chemokine and Secretory IgA Levels in Human Milk in Relation to Atopic Disease and IgA Production in Infants. Pediatr Allergy Immunol. 2003. 14(1):35-41.
[95] Donovan, S.M. The Role of Lactoferrin in Gastrointestinal and Immune Development and Function: A Preclinical Perspective. J Pediatr. 2016. 173 Suppl:S16-S28.
[96] Xu, R.J. Development of the Newborn GI Tract and its Relation to Colostrum/Milk Intake: A Review. Reprod Fertil Dev. 1996. 8(1):35-48.
[97] Yen, C.-C., Lim, C.-Y., Chong, K.-Y., Tsai, T.-C., Shen, C.-J., Lim, M.-F., *et al.* Lactoferrin as a Natural Regimen for Selective Decontamination of the Digestive Tract: Recombinant Porcine Lactoferrin Expressed in the Milk of Transgenic Mice Protects Neonates From Pathogenic Challenge in the Gastrointestinal Tract. J Infect Dis. 2009. 199(4):590-598.
[98] Jiang, R., Lopez, V., Kelleher, S.L., Lönnerdal, B. Apo- and Holo-Lactoferrin are Both Internalized by Lactoferrin Receptor via Clathrin-Mediated Endocytosis but Differentially Affect ERK-Signaling and Cell Proliferation in Caco-2 Cells. J Cell Physiol. 2011. 226(11):3022-3031.
[99] Rogier, E.W., Frantz, A.L., Bruno, M.E.C., Wedlund, L., Cohen, D.A., Stromberg, A.J., *et al.* Secretory Antibodies in Breast Milk Promote Long-Term Intestinal Homeostasis by Regulating the Gut Microbiota and Host Gene Expression. Proc Natl Acad Sci USA. 2014. 111(8):3074-3079.

[100] Pellegrini, A., Thomas, U., Bramaz, N., Hunziker, P., von Fellenberg, R. Isolation and Identification of Three Bactericidal Domains in the Bovine α-Lactalbumin Molecule. Biochim Biophys Acta. 1999. 1426(3):439-448.
[101] Ellison, R.T., Giehl, T.J. Killing of Gram-Negative Bacteria by Lactoferrin and Lysozyme. J Clin Invest. 1991. 88(4):1080-1091.
[102] Lee-Huang, S., Huang, P.L., Sun, Y., Kung, H.F., Blithe, D.L., Chen, H.C. Lysozyme and RNases as Anti-HIV Components in Beta-Core Preparations of Human Chorionic Gonadotropin. Proc Natl Acad Sci USA. 1999. 96(6):2678-2681.
[103] Lima, H.K., Wagner-Gillespie, M., Perrin, M.T., Fogleman, A.D. Bacteria and Bioactivity in Holder Pasteurized and Shelf-Stable Human Milk Products. Curr Dev Nutr. 2017. 1(8):e001438.
[104] Silvestre, D., Ruiz, P., Martínez-Costa, C., Plaza, A., López, M.C. Effect of Pasteurization on the Bactericidal Capacity of Human Milk. J Hum Lact. 2008. 24(4):371-376.
[105] Cossey, V., Vanhole, C., Eerdekens, A., Rayyan, M., Fieuws, S., Schuermans, A. Pasteurization of Mother's Own Milk for Preterm Infants Does Not Reduce the Incidence of Late-Onset Sepsis. Neonatology. 2013. 103(3):170-176.
[106] Bode, L. Recent Advances on Structure, Metabolism, and Function of Human Milk Oligosaccharides. J Nutr. 2006. 136(8):2127-2130.
[107] Li, Y., Nguyen, D.N., de Waard, M., Christensen, L., Zhou, P., Jiang, P., *et al.* Pasteurization Procedures for Donor Human Milk Affect Body Growth, Intestinal Structure, and Resistance Against Bacterial Infections in Preterm Pigs. J Nutr. 2017. 147(6):1121-1130.
[108] Van Boekel, M.A.J.S. Effect of Heating on Maillard Reactions in Milk. Food Chem. 1998. 62(4):403-414.
[109] Hassinger, D., Clausen, D.M., Nitka, S., Herdt, A., Griffin, I. Analysis of Disialyllacto-N-Tetraose (DSLNT) Content in Milk From Mothers of Preterm Infants. J Hum Lact. 2020. 36(2):291-298.
[110] Lucas, A., Cole, T.J. Breast Milk and Neonatal Necrotising Enterocolitis. Lancet. 1990. 336(8730):1519-1523.
[111] Victora, C.G., Bahl, R., Barros, A.J., França, G.V., Horton, S., Krasevec, J., *et al.* Breastfeeding in the 21st Century: Epidemiology, Mechanisms, and Lifelong Effect. Lancet. 2016. 387(10017):475-490.
[112] Delplanque, B., Gibson, R., Koletzko, B., Lapillonne, A., Strandvik, B. Lipid Quality in Infant Nutrition: Current Knowledge and Future Opportunities. J Pediatr Gastroenterol Nutr. 2015. 61(1):8-17.
[113] Folch, J., Lees, M., Sloane Stanley, G.H. A Simple Method for the Isolation and Purification of Total Lipides From Animal Tissues. J Biol Chem. 1957. 226(1):497-509.
[114] Cerbulis, J., Custer, J.H. Casein Components Soluble in Chloroform-Methanol (2:1) and in Fifty Per Cent Aqueous Ethanol. J Dairy Sci. 1967. 50(9):1356-1359.
[115] Lucas, A., Gibbs, J.A., Lyster, R.L., Baum, J.D. Creamatocrit: Simple Clinical Technique for Estimating Fat Concentration and Energy Value of Human Milk. Br Med J. 1978. 1(6119):1018-1020.
[116] Gidrewicz, D.A., Fenton, T.R. A Systematic Review and Meta-Analysis of the Nutrient Content of Preterm and Term Breast Milk. BMC Pediatr. 2014. 14:216.
[117] Cavazos-Garduño, A., Serrano-Niño, J.C., Solís-Pacheco, J.R., Gutierrez-Padilla, J.A., González-Reynoso, O., García, H.S., *et al.* Effect of Pasteurization, Freeze-Drying and Spray Drying on the Fat Globule and Lipid Profile of Human Milk. J Food Nutr Res. 2016. 4(5):296-302.
[118] Fidler, N., Sauerwald, T.U., Demmelmair, H., Koletzko, B. Fat Content and Fatty Acid Composition of Fresh, Pasteurized, or Sterilized Human Milk. Adv Exp Med Biol. 2001. 501:485-495.
[119] Liu, Z., Wang, J., Cocks, B.G., Rochfort, S. Seasonal Variation of Triacylglycerol Profile of Bovine Milk. Metabolites. 2017. 7(2):24.
[120] Pham, A.C., Peng, K.-Y., Salim, M., Ramirez, G., Hawley, A., Clulow, A.J., *et al.* Correlating Digestion-Driven Self-Assembly in Milk and Infant Formulas With Changes in Lipid Composition. ACS Appl Bio Mater. 2020. 3(5):3087-3098.

[121] Martin, J.C., Bougnoux, P., Antoine, J.M., Lanson, M., Couet, C. Triacylglycerol Structure of Human Colostrum and Mature Milk. Lipids. 1993. 28(7):637-643.
[122] Patton, J.S., Carey, M.C. Watching Fat Digestion. Science. 1979. 204(4389):145-148.
[123] Nelson, S.E., Rogers, R.R., Frantz, J.A., Ziegler, E.E. Palm Olein in Infant Formula: Absorption of Fat and Minerals by Normal Infants. Am J Clin Nutr. 1996. 64(3):291-296.
[124] Carnielli, V.P., Luijendijk, I.H., van Goudoever, J.B., Sulkers, E.J., Boerlage, A.A., Degenhart, H.J., *et al.* Feeding Premature Newborn Infants Palmitic Acid in Amounts and Stereoisomeric Position Similar to That of Human Milk: Effects on Fat and Mineral Balance. Am J Clin Nutr. 1995. 61(5):1037-1042.
[125] Carnielli, V.P., Luijendijk, I.H., Van Goudoever, J.B., Sulkers, E.J., Boerlage, A.A., Degenhart, H.J., *et al.* Structural Position and Amount of Palmitic Acid in Infant Formulas: Effects on Fat, Fatty Acid, and Mineral Balance. J Pediatr Gastroenterol Nutr. 1996. 23(5):553-560.
[126] Filer, L.J., Jr., Mattson, F.H., Fomon, S.J. Triglyceride Configuration and Fat Absorption by the Human Infant. J Nutr. 1969. 99(3):293-298.
[127] Johnston, J.M., Rao, G.A. Intestinal Absorption of Fat. Protoplasma. 1967. 63(1):40-44.
[128] Carey, M.C., Small, D.M., Bliss, C.M. Lipid Digestion and Absorption. Annu Rev Physiol. 1983. 45:651-677.
[129] Norman, A., Strandvik, B., Ojamäe, Ö. Bile Acids and Pancreatic Enzymes During Absorption in the Newborn. Acta Paediatr Scand. 1972. 61(5):571-576.
[130] Macheras, P.E., Koupparis, M.A., Antimisiaris, S.G. Drug Binding and Solubility in Milk. Pharm Res. 1990. 7(5):537-541.
[131] Salim, M., Khan, J., Ramirez, G., Murshed, M., Clulow, A.J., Hawley, A., *et al.* Impact of Ferroquine on the Solubilization of Artefenomel (OZ439) During In Vitro Lipolysis in Milk and Implications for Oral Combination Therapy for Malaria. Mol Pharm. 2019. 16(4):1658-1668.
[132] Charkoftaki, G., Kytariolos, J., Macheras, P. Novel Milk-Based Oral Formulations: Proof of Concept. Int J Pharm. 2010. 390(2):150-159.
[133] Bernbäck, S., Bläckberg, L., Hernell, O. The Complete Digestion of Human Milk Triacylglycerol In Vitro Requires Gastric Lipase, Pancreatic Colipase-Dependent Lipase, and Bile Salt-Stimulated Lipase. J Clin Invest. 1990. 85(4):1221-1226.
[134] Kalantzi, L., Goumas, K., Kalioras, V., Abrahamsson, B., Dressman, J.B., Reppas, C. Characterization of the Human Upper Gastrointestinal Contents Under Conditions Simulating Bioavailability/Bioequivalence Studies. Pharm Res. 2006. 23(1):165-176.
[135] Salentinig, S., Phan, S., Hawley, A., Boyd, B.J. Self-Assembly Structure Formation During the Digestion of Human Breast Milk. Angew Chem Int Ed. 2015. 54(5):1600-1603.
[136] Clulow, A.J., Salim, M., Hawley, A., Boyd, B.J. A Closer Look at the Behaviour of Milk Lipids During Digestion. Chem Phys Lipids. 2018. 211:107-116.
[137] Identification of Lyotropic Liquid Crystalline Mesophases. Hyde, S.T., editor. West Sussex, England: John Wiley & Sons Ltd.; 2001.
[138] Cullis, P.R., Hope, M.J., Tilcock, C.P. Lipid Polymorphism and the Roles of Lipids in Membranes. Chem Phys Lipids. 1986. 40(2-4):127-144.
[139] Kaukonen, A.M., Boyd, B.J., Charman, W.N., Porter, C.J.H. Drug Solubilization Behavior During In Vitro Digestion of Suspension Formulations of Poorly Water-Soluble Drugs in Triglyceride Lipids. Pharm Res. 2004. 21(2):254-260.
[140] Feeney, O.M., Crum, M.F., McEvoy, C.L., Trevaskis, N.L., Williams, H.D., Pouton, C.W., *et al.* 50 Years of Oral Lipid-Based Formulations: Provenance, Progress and Future Perspectives. Adv Drug Deliv Rev. 2016. 101:167-194.
[141] van 't Hag, L., Gras, S.L., Conn, C.E., Drummond, C.J. Lyotropic Liquid Crystal Engineering Moving Beyond Binary Compositional Space - Ordered Nanostructured Amphiphile Self-Assembly Materials by Design. Chem Soc Rev. 2017. 46(10):2705-2731.
[142] Murphy, G.M., Signer, E. Bile Acid Metabolism in Infants and Children. Gut. 1974. 15(2):151-163.
[143] Hernell, O. Human Milk Lipases. III. Physiological Implications of the Bile Salt-Stimulated Lipase. Eur J Clin Invest. 1975. 5(3):267-272.

[144] Hernell, O., Bläckberg, L. Digestion of Human Milk Lipids: Physiologic Significance of sn-2 Monoacylglycerol Hydrolysis by Bile Salt-Stimulated Lipase. Pediatr Res. 1982. 16(10):882-885.
[145] Henderson, T.R., Fay, T.N., Hamosh, M. Effect of Pasteurization on Long Chain Polyunsaturated Fatty Acid Levels and Enzyme Activities of Human Milk. J Pediatr. 1998. 132(5):876-878.
[146] Fredrikzon, B., Hernell, O., Bläckberg, L., Olivecrona, T. Bile Salt-Stimulated Lipase in Human Milk: Evidence of Activity In Vivo and of a Role in the Digestion of Milk Retinol Esters. Pediatr Res. 1978. 12(11):1048-1052.
[147] de Oliveira, S.C., Bellanger, A., Ménard, O., Pladys, P., Le Gouar, Y., Dirson, E., *et al.* Impact of Human Milk Pasteurization on Gastric Digestion in Preterm Infants: A Randomized Controlled Trial. Am J Clin Nutr. 2017. 105(2):379-390.
[148] Goldblum, R.M., Dill, C.W., Albrecht, T.B., Alford, E.S., Garza, C., Goldman, A.S. Rapid High-Temperature Treatment of Human Milk. J Pediatr. 1984. 104(3):380-385.
[149] Artursson, P. Cell Cultures as Models for Drug Absorption Across the Intestinal Mucosa. Crit Rev Ther Drug Carrier Syst. 1991. 8(4):305-330.
[150] Behrens, I., Stenberg, P., Artursson, P., Kissel, T. Transport of Lipophilic Drug Molecules in a New Mucus-Secreting Cell Culture Model Based on HT29-MTX Cells. Pharm Res. 2001. 18(8):1138-1145.
[151] Hilgendorf, C., Spahn-Langguth, H., Regårdh, C.G., Lipka, E., Amidon, G.L., Langguth, P. Caco-2 versus Caco-2/HT29-MTX Co-Cultured Cell Lines: Permeabilities via Diffusion, Inside- and Outside-Directed Carrier-Mediated Transport. J Pharm Sci. 2000. 89(1):63-75.
[152] Hidalgo, I.J., Raub, T.J., Borchardt, R.T. Characterization of the Human Colon Carcinoma Cell Line (Caco-2) as a Model System for Intestinal Epithelial Permeability. Gastroenterology. 1989. 96(3):736-749.
[153] Elzinga, J., Benthe van der, L., Belzer, C., Steegenga, W.T. Characterization of Increased Mucus Production of HT29-MTX-E12 Cells Grown Under Semi-Wet Interface With Mechanical Stimulation. PLoS ONE. 2021. 16(12):e0261191.
[154] Cotter, P., López-Expósito, I., Verhoeckx, K. The Impact of Food Bioactives on Health : In Vitro and Ex Vivo Models. Cham: Springer Open; 2015.
[155] Aderem, A., Ulevitch, R.J. Toll-Like Receptors in the Induction of the Innate Immune Response. Nature. 2000. 406(6797):782-787.
[156] Logan, W.R. The Intestinal Flora of Infants and Young Children. J Pathol. 1913. 18(1):527-551.
[157] Turner, J.R. Molecular Basis of Epithelial Barrier Regulation: From Basic Mechanisms to Clinical Application. Am J Pathol. 2006. 169(6):1901-1909.
[158] Preising, J., Philippe, D., Gleinser, M., Wei, H., Blum, S., Eikmanns, B.J., *et al.* Selection of Bifidobacteria Based on Adhesion and Anti-Inflammatory Capacity In Vitro for Amelioration of Murine Colitis. Appl Environ Microbiol. 2010. 76(9):3048-3051.
[159] Ewaschuk, J.B., Diaz, H., Meddings, L., Diederichs, B., Dmytrash, A., Backer, J., *et al.* Secreted Bioactive Factors From Bifidobacterium Infantis Enhance Epithelial Cell Barrier Function. Am J Physiol Gastrointest Liver Physiol. 2008. 295(5):G1025-G1034.
[160] Buchgraber, M., Ulberth, F., Emons, H., Anklam, E. Triacylglycerol Profiling by Using Chromatographic Techniques. Eur J Lipid Sci Technol. 2004. 106(9):621-648.
[161] Ruiz-Samblás, C., González-Casado, A., Cuadros-Rodríguez, L. Triacylglycerols Determination by High-Temperature Gas Chromatography in the Analysis of Vegetable Oils and Foods: A Review of the Past 10 Years. Crit Rev Food Sci Nutr. 2015. 55(11):1618-1631.
[162] Williams, H.D., Sassene, P., Kleberg, K., Bakala-N'Goma, J.-C., Calderone, M., Jannin, V., *et al.* Toward the Establishment of Standardized In Vitro Tests for Lipid-Based Formulations, Part 1: Method Parameterization and Comparison of In Vitro Digestion Profiles Across a Range of Representative Formulations. J Pharm Sci. 2012. 101(9):3360-3380.
[163] Kirby, N.M., Mudie, S.T., Hawley, A.M., Cookson, D.J., Mertens, H.D.T., Cowieson, N., *et al.* A Low-Background-Intensity Focusing Small-Angle X-ray Scattering Undulator Beamline. J Appl Cryst. 2013. 46(6):1670-1680.

[164] Fong, C., Weerawardena, A., Sagnella, S.M., Mulet, X., Waddington, L., Krodkiewska, I., *et al.* Monodisperse Nonionic Phytanyl Ethylene Oxide Surfactants: High Throughput Lyotropic Liquid Crystalline Phase Determination and the Formation of Liposomes, Hexosomes and Cubosomes. Soft Matter. 2010. 6(19):4727-4741.
[165] Warren, D.B., Anby, M.U., Hawley, A., Boyd, B.J. Real Time Evolution of Liquid Crystalline Nanostructure During the Digestion of Formulation Lipids Using Synchrotron Small-Angle X-Ray Scattering. Langmuir. 2011. 27(15):9528-9534.
[166] Heiss, B.E., Ehrlich, A.M., Maldonado-Gomez, M.X., Taft, D.H., Larke, J.A., Goodson, M.L., *et al.* Bifidobacterium Catabolism of Human Milk Oligosaccharides Overrides Endogenous Competitive Exclusion Driving Colonization and Protection. Gut Microbes. 2021. 13(1):1986666.
[167] Sangild, P.T., Siggers, R.H., Schmidt, M., Elnif, J., Bjornvad, C.R., Thymann, T., *et al.* Diet- and Colonization-Dependent Intestinal Dysfunction Predisposes to Necrotizing Enterocolitis in Preterm Pigs. Gastroenterology. 2006. 130(6):1776-1792.
[168] Cho, S.X., Rudloff, I., Lao, J.C., Pang, M.A., Goldberg, R., Bui, C.B., *et al.* Characterization of the Pathoimmunology of Necrotizing Enterocolitis Reveals Novel Therapeutic Opportunities. Nat Commun. 2020. 11(1):5794.
[169] Jiminez, J.A., Uwiera, T.C., Douglas Inglis, G., Uwiera, R.R.E. Animal Models to Study Acute and Chronic Intestinal Inflammation in Mammals. Gut Pathog. 2015. 7:29.
[170] Zhang, D., Wen, J., Zhou, J., Cai, W., Qian, L. Milk Fat Globule Membrane Ameliorates Necrotizing Enterocolitis in Neonatal Rats and Suppresses Lipopolysaccharide-Induced Inflammatory Response in IEC-6 Enterocytes. JPEN J Parenter Enteral Nutr. 2019. 43(7):863-873.
[171] Khailova, L., Mount Patrick, S.K., Arganbright, K.M., Halpern, M.D., Kinouchi, T., Dvorak, B. Bifidobacterium Bifidum Reduces Apoptosis in the Intestinal Epithelium in Necrotizing Enterocolitis. Am J Physiol Gastrointest Liver Physiol. 2010. 299(5):G1118-G1127.
[172] Grothaus, J.S., Ares, G., Yuan, C., Wood, D.R., Hunter, C.J. Rho Kinase Inhibition Maintains Intestinal and Vascular Barrier Function by Upregulation of Occludin in Experimental Necrotizing Enterocolitis. Am J Physiol Gastrointest Liver Physiol. 2018. 315(4):G514-G528.
[173] Li, B., Zani, A., Martin, Z., Lee, C., Zani-Ruttenstock, E., Eaton, S., *et al.* Intestinal Epithelial Cell Injury is Rescued by Hydrogen Sulfide. J Pediatr Surg. 2016. 51(5):775-778.
[174] Shahedi, Z., Varedi, M., Bagheri, Z., Moatari, A., Sharafpour, H. Attenuation by l-Thyroxine of Oxidant-Induced Gut Epithelial Damage. Iran J Basic Med Sci. 2019. 22(9):1091-1096.
[175] Czerucka, D., Dahan, S., Mograbi, B., Rossi, B., Rampal, P. Saccharomyces Boulardii Preserves the Barrier Function and Modulates the Signal Transduction Pathway Induced in Enteropathogenic Escherichia Coli-Infected T84 cCells. Infect Immun. 2000. 68(10):5998-6004.
[176] Madsen, K., Cornish, A., Soper, P., McKaigney, C., Jijon, H., Yachimec, C., *et al.* Probiotic Bacteria Enhance Murine and Human Intestinal Epithelial Barrier Function. Gastroenterology. 2001. 121(3):580-591.
[177] Sartor, B.R. Targeting Enteric Bacteria in Treatment of Inflammatory Bowel Diseases: Why, How, and When. Curr Opin Gastroenterol. 2003. 19(4):358-365.
[178] Tanabe, S., Kinuta, Y., Saito, Y. Bifidobacterium Infantis Suppresses Proinflammatory Interleukin-17 Production in Murine Splenocytes and Dextran Sodium Sulfate-Induced Intestinal Inflammation. Int J Mol Med. 2008. 22(2):181-185.
[179] Sheil, B., MacSharry, J., O'Callaghan, L., O'Riordan, A., Waters, A., Morgan, J., *et al.* Role of Interleukin (IL-10) in Probiotic-Mediated Immune Modulation: An Assessment in Wild-Type and IL-10 Knock-Out Mice. Clin Exp Immunol. 2006. 144(2):273-280.
[180] Nam, D.K., Lee, S., Zhou, G., Cao, X., Wang, C., Clark, T., *et al.* Oligo(dT) Primer Generates a High Frequency of Truncated cDNAs Through Internal Poly(A) Priming During Reverse Transcription. Proc Natl Acad Sci USA. 2002. 99(9):6152-6156.
[181] Weickert, C.S., Sheedy, D., Rothmond, D.A., Dedova, I., Fung, S., Garrick, T., *et al.* Selection of Reference Gene Expression in a Schizophrenia Brain Cohort. Aust N Z J Psychiatry. 2010. 44(1):59-70.

[182] Chichlowski, M., De Lartigue, G., German, J.B., Raybould, H.E., Mills, D.A. Bifidobacteria Isolated From Infants and Cultured on Human Milk Oligosaccharides Affect Intestinal Epithelial Function. J Pediatr Gastroenterol Nutr. 2012. 55(3):321-327.
[183] Oftedal, O.T. The Evolution of Milk Secretion and its Ancient Origins. Animal. 2012. 6(3):355-368.
[184] Andersson, Y., Sävman, K., Bläckberg, L., Hernell, O. Pasteurization of Mother's Own Milk Reduces Fat Absorption and Growth in Preterm Infants. Acta Paediatr. 2007. 96(10):1445-1449.
[185] Lambert, D.M., Vandevoorde, S., Jonsson, K.O., Fowler, C.J. The Palmitoylethanolamide Family: A new Class of Anti-Inflammatory Agents? Curr Med Chem. 2002. 9(6):663-674.
[186] Bradshaw, H.B., Rimmerman, N., Hu, S.S., Burstein, S., Walker, J.M. Novel Endogenous N-acyl Glycines Identification and Characterization. Vitam Horm. 2009. 81:191-205.
[187] Robles, A., Jiménez, M.J., Esteban, L., González, P.A., Martín, L., Rodríguez, A., *et al.* Enzymatic Production of Human Milk Fat Substitutes Containing Palmitic and Docosahexaenoic Acids at sn-2 Position and Oleic Acid at sn-1,3 Positions. Food Sci Technol. 2011. 44(10):1986-1992.
[188] Alvarez, F.J., Stella, V.J. The Role of Calcium Ions and Bile Salts on the Pancreatic Lipase-Catalyzed Hydrolysis of Triglyceride Emulsions Stabilized With Lecithin. Pharm Res. 1989. 6(6):449-457.
[189] Christie, W.W., Clapperton, J.L. Structures of the Triglycerides of Cows' Milk, Fortified Milks (Including. Infant Formulae), and Human Milk. Int J Dairy Technol. 1982. 35(1):22-24.
[190] Agren, J.J., Julkunen, A., Penttilä, I. Rapid Separation of Serum Lipids for Fatty Acid Analysis by a Single Aminopropyl Column. J Lipid Res. 1992. 33(12):1871-1876.
[191] Demšar, J., Curk, T., Erjavec, A., Gorup, Č., Hočevar, T., Milutinovič, M., *et al.* Orange: Data Mining Toolbox in Python. J Mach Learn Res. 2013. 14(1):2349–2353.
[192] Cruz-Hernandez, C., Goeuriot, S., Giuffrida, F., Thakkar, S.K., Destaillats, F. Direct Quantification of Fatty Acids in Human Milk by Gas Chromatography. J Chromatogr A. 2013. 1284:174-179.
[193] Heider, M., Hause, G., Mäder, K. Does the Commonly Used pH-stat Method With Back Titration Really Quantify the Enzymatic Digestibility of Lipid Drug Delivery Systems? A Case Study on Solid Lipid Nanoparticles (SLN). Eur J Pharm Biopharm. 2016. 109:194-205.
[194] Hopperton, K.E., Pitino, M.A., Chouinard-Watkins, R., Shama, S., Sammut, N., Bando, N., *et al.* Determinants of Fatty Acid Content and Composition of Human Milk Fed to Infants Born Weighing <1250 g. Am J Clin Nutr. 2021. 114(4):1523-1534.
[195] Du, J., Gay, M.C.L., Lai, C.T., Trengove, R.D., Hartmann, P.E., Geddes, D.T. Comparison of Gravimetric, Creamatocrit and Esterified Fatty Acid Methods for Determination of Total Fat Content in Human Milk. Food Chem. 2017. 217:505-510.
[196] Ten-Doménech, I., Beltrán-Iturat, E., Herrero-Martínez, J.M., Sancho-Llopis, J.V., Simó-Alfonso, E.F. Triacylglycerol Analysis in Human Milk and Other Mammalian Species: Small-Scale Sample Preparation, Characterization, and Statistical Classification Using HPLC-ELSD Profiles. J Agric Food Chem. 2015. 63(24):5761-5770.
[197] Innis, S.M. Dietary Triacylglycerol Structure and its Role in Infant Nutrition. Adv Nutr. 2011. 2(3):275-283.
[198] Destaillats, F., De Wispelaere, M., Joffre, F., Golay, P.-A., Hug, B., Giuffrida, F., *et al.* Authenticity of Milk Fat by Fast Analysis of Triacylglycerols Application to the Detection of Partially Hydrogenated Vegetable Oils. J Chromatogr A. 2006. 1131(1-2):227-234.
[199] Brueton, M.J., Berger, H.M., Brown, G.A., Ablitt, L., Iyngkaran, N., Wharton, B.A. Duodenal Bile Acid Conjugation Patterns and Dietary Sulphur Amino Acids in the Newborn. Gut. 1978. 19(2):95-98.
[200] Hamosh, M., Scanlon, J.W., Ganot, D., Likel, M., Scanlon, K.B., Hamosh, P. Fat Digestion in the Newborn. Characterization of Lipase in Gastric Aspirates of Premature and Term Infants. J Clin Invest. 1981. 67(3):838-846.
[201] Borgström, B., Erlanson, C. Pancreatic Lipase and Co-Lipase. Interactions and Effects of Bile Salts and Other Detergents. Eur J Biochem. 1973. 37(1):60-68.

[202] Hofmann, A.F. The Function of Bile Salts in Fat Absorption. The Solvent Properties of Dilute Micellar Solutions of Conjugated Bile Salts. Biochem J. 1963. 89(1):57-68.
[203] Christensen, J.Ø., Schultz, K., Mollgaard, B., Kristensen, H.G., Mullertz, A. Solubilisation of Poorly Water-Soluble Drugs During In Vitro Lipolysis of Medium- and Long-Chain Triacylglycerols. Eur J Pharm Sci. 2004. 23(3):287-296.
[204] Hwang, S., Lee, S., Ahn, I.-S., Jung, J.-K. Highly Efficient Production of Monoglycerides by the Continuous Removal of Fatty Acids From Lipase-Catalyzed Oil Hydrolysis. Biocatal Biotransformation. 2009. 27(5-6):290-295.
[205] Zangenberg, N.H., Müllertz, A., Kristensen, H.G., Hovgaard, L. A Dynamic In Vitro Lipolysis Model: I. Controlling the Rate of Lipolysis by Continuous Addition of Calcium. Eur J Pharm Sci. 2001. 14(2):115-122.
[206] Porter, C.J.H., Trevaskis, N.L., Charman, W.N. Lipids and Lipid-Based Formulations: Optimizing the Oral Delivery of Lipophilic Drugs. Nat Rev Drug Discov. 2007. 6(3):231-248.
[207] Encrantz, J.C., Sjövall, J. On the Bile Acids in Duodenal Contents of Infants and Children. Bile Acids and Steroids 72. Clin Chim Acta. 1959. 4:793-799.
[208] Boehm, G., Braun, W., Moro, G., Minoli, I. Bile Acid Concentrations in Serum and Duodenal Aspirates of Healthy Preterm Infants: Effects of Gestational and Postnatal Age. Biol Neonate. 1997. 71(4):207-214.
[209] Glasgow, J.F., Dinsmore, H., Molla, A., Macfarlane, T. A Comprehensive Study of Duodenal Bile Salts in Newborn Infants and Their Relationship to Fat Absorption. Ir J Med Sci. 1980. 149(9):346-356.
[210] Heid, H.W., Keenan, T.W. Intracellular Origin and Secretion of Milk Fat Globules. Eur J Cell Biol. 2005. 84(2-3):245-258.
[211] Liu, L., Pan, Y., Zhang, X., Zhang, Y., Li, X. Effect of Particle Size and Interface Composition on the Lipid Digestion of Droplets Covered With Membrane Phospholipids. J Agric Food Chem. 2021. 69(1):159-169.
[212] Scow, R.O., Desnuelle, P., Verger, R. Lipolysis and Lipid Movement in a Membrane Model. Action of Lipoprotein Lipase. J Biol Chem. 1979. 254(14):6456-6463.
[213] Brockerhoff, H. Substrate Specificity of Pancreatic Lipase. Influence of the Structure of Fatty Acids on the Reactivity of Esters. Biochim Biophys Acta. 1970. 212(1):92-101.
[214] Gittleman, I.F., Pincus, J.B., Saito, M., Schmerzler, E. Hypocalcemia Occurring on the First Day of Life in Mature and Premature Infants. Pediatrics. 1956. 18(5):721-729.
[215] Clulow, A.J., Salim, M., Hawley, A., Boyd, B.J. Milk Mimicry – Triglyceride Mixtures That Mimic Lipid Structuring During the Digestion of Bovine and Human Milk. Food Hydrocoll. 2021. 110:106126.
[216] de Buy Wenniger, L.M., Pusl, T., Beuers, U. Bile Salts. In: Lennarz, W.J., Lane, M.D., editors. Encyclopedia of Biological Chemistry (Second Edition). Waltham: Academic Press; 2013. p. 167-171.
[217] López-López, A., López-Sabater, M.C., Campoy-Folgoso, C., Rivero-Urgell, M., Castellote-Bargalló, A.I. Fatty Acid and sn-2 Fatty Acid Composition in Human Milk From Granada (Spain) and in Infant Formulas. Eur J Clin Nutr. 2002. 56(12):1242-1254.
[218] Clulow, A.J., Binte Abu Bakar, S.Y., Salim, M., Nowell, C.J., Hawley, A., Boyd, B.J. Emulsions Containing Optimum Cow Milk Fat and Canola Oil Mixtures Replicate the Lipid Self-Assembly of Human Breast Milk During Digestion. J Colloid Interface Sci. 2021. 588:680-691.
[219] Boyd, B.J., Salim, M., Clulow, A.J., Ramirez, G., Pham, A.C., Hawley, A. The Impact of Digestion is Essential to the Understanding of Milk as a Drug Delivery System for Poorly Water Soluble Drugs. J Control Release. 2018. 292:13-17.
[220] Binte Abu Bakar, S.Y., Salim, M., Clulow, A.J., Hawley, A., Boyd, B.J. Revisiting Dispersible Milk-Drug Tablets as a Solid Lipid Formulation in the Context of Digestion. Int J Pharm. 2019. 554:179-189.
[221] Angelova, A., Ollivon, M., Campitelli, A., Bourgaux, C. Lipid Cubic Phases as Stable Nanochannel Network Structures for Protein Biochip Development: X-ray Diffraction Study. Langmuir. 2003. 19(17):6928-6935.

[222] Zabara, A., Amar-Yuli, I., Mezzenga, R. Tuning In-Meso-Crystallized Lysozyme Polymorphism by Lyotropic Liquid Crystal Symmetry. Langmuir. 2011. 27(10):6418-6425.
[223] Templer, R.H. Thermodynamic and Theoretical Aspects of Cubic Mesophases in Nature and Biological Amphiphiles. Curr Opin Colloid Interface Sci. 1998. 3(3):255-263.
[224] Huang, Y., Gui, S. Factors Affecting the Structure of Lyotropic Liquid Crystals and the Correlation Between Structure and Drug Diffusion. RSC Adv. 2018. 8(13):6978-6987.
[225] Meikle, T.G., Drummond, C.J., Separovic, F., Conn, C.E. Chapter Three - Membrane-Mimetic Inverse Bicontinuous Cubic Phase Systems for Encapsulation of Peptides and Proteins. In: Iglič, A., Garcia-Sáez, A., Rappolt, M., editors. Adv Biomembr Lipid Self-Assem. 25: Academic Press; 2017. p. 63-94.
[226] O'Brien, F., Clapham, D., Krysiak, K., Batchelor, H., Field, P., Caivano, G., *et al.* Making Medicines Baby Size: The Challenges in Bridging the Formulation Gap in Neonatal Medicine. Int J Mol Sci. 2019. 20(11):2688.
[227] Nunn, T., Williams, J. Formulation of Medicines for Children. Br J Clin Pharmacol. 2005. 59(6):674-676.
[228] Linakis, M.W., Roberts, J.K., Lala, A.C., Spigarelli, M.G., Medlicott, N.J., Reith, D.M., *et al.* Challenges Associated With Route of Administration in Neonatal Drug Delivery. Clin Pharmacokinet. 2016. 55(2):185-196.
[229] Rouse, C., Mistry, P., Rayner, O., Nickless, J., Wan, M., Southern, K.W., *et al.* A Mixed Methods Study of the Administration of Flucloxacillin Oral Liquid Identifying Strategies to Overcome Administration Issues of Medicines With Poor Palatability. Int J Pharm Pract. 2017. 25(5):326-334.
[230] Davies, E.H., Tuleu, C. Medicines for Children: A Matter of Taste. J Pediatr. 2008. 153(5):599-604.
[231] Formulations of Choice for the Paediatric Population. Canary Wharf, London, UK; 2006.
[232] Brown, D., Ford, J.L., Nunn, A.J., Rowe, P.H. An Assessment of Dose-Uniformity of Samples Delivered From Paediatric Oral Droppers. J Clin Pharm Ther. 2004. 29(6):521-529.
[233] Scow, R.O., Olivecrona, T. Effect of Albumin on Products Formed From Chylomicron Triacylglycerol by Lipoprotein Lipase In Vitro. Biochim Biophys Acta. 1977. 487(3):472-486.
[234] Tilley, A.J., Dong, Y.-D., Chong, J.Y.T., Hanley, T., Kirby, N., Drummond, C.J., *et al.* Transfer of Lipid Between Triglyceride Dispersions and Lyotropic Liquid Crystal Nanostructured Particles Using Time-Resolved SAXS. Soft Matter. 2012. 8(20):5696-5708.
[235] Lutton, E.S. The Polymorphism of Tristearin and Some of its Homologs. J Am Chem Soc. 1945. 67(4):524-527.
[236] Lutton, E.S. Binary Systems From Palmitic-Stearic Triglycerides. J Am Chem Soc. 1967. 44(5):303-304.
[237] Zani, A., Pierro, A. Necrotizing Enterocolitis: Controversies and Challenges. F1000Res. 2015. 4:1373.
[238] Stoll, B.J., Hansen, N.I., Bell, E.F., Walsh, M.C., Carlo, W.A., Shankaran, S., *et al.* Trends in Care Practices, Morbidity, and Mortality of Extremely Preterm Neonates, 1993-2012. JAMA. 2015. 314(10):1039-1051.
[239] Rowe, M.I., Reblock, K.K., Kurkchubasche, A.G., Healey, P.J. Necrotizing Enterocolitis in the Extremely Low Birth Weight Infant. J Pediatr Surg. 1994. 29(8):987-991.
[240] Jackman, S., Brereton, R.J., Wright, V.M. Results of Surgical Treatment of Neonatal Necrotizing Enterocolitis. Br J Surg. 1990. 77(2):146-148.
[241] Dimmitt, R.A., Meier, A.H., Skarsgard, E.D., Halamek, L.P., Smith, B.M., Moss, R.L. Salvage Laparotomy for Failure of Peritoneal Drainage in Necrotizing Enterocolitis in Infants With Extremely Low Birth Weight. J Pediatr Surg. 2000. 35(6):856-859.
[242] Fanning, A.S., Mitic, L.L., Anderson, J.M. Transmembrane Proteins in the Tight Junction Barrier. J Am Soc Nephrol. 1999. 10(6):1337-1345.
[243] Anand, R.J., Leaphart, C.L., Mollen, K.P., Hackam, D.J. The Role of the Intestinal Barrier in the Pathogenesis of Necrotizing Enterocolitis. Shock. 2007. 27(2):124-133.
[244] Sharma, R., Tepas, J.J. Microecology, Intestinal Epithelial Barrier and Necrotizing Enterocolitis. Pediatr Surg Int. 2010. 26(1):11-21.

[245] Arrieta, M.C., Bistritz, L., Meddings, J.B. Alterations in Intestinal Permeability. Gut. 2006. 55(10):1512-1520.
[246] Puccio, G., Alliet, P., Cajozzo, C., Janssens, E., Corsello, G., Sprenger, N., *et al.* Effects of Infant Formula With Human Milk Oligosaccharides on Growth and Morbidity: A Randomized Multicenter Trial. J Pediatr Gastroenterol Nutr. 2017. 64(4):624-631.
[247] Good, M., Sodhi, C.P., Yamaguchi, Y., Jia, H., Lu, P., Fulton, W.B., *et al.* The Human Milk Oligosaccharide 2′-Fucosyllactose Attenuates the Severity of Experimental Necrotising Enterocolitis by Enhancing Mesenteric Perfusion in the Neonatal Intestine. Br J Nutr. 2016. 116(7):1175-1187.
[248] Czerucka, D., Dahan, S., Mograbi, B., Rossi, B., Rampal, P. Saccharomyces Boulardii Preserves the Barrier Function and Modulates the Signal Transduction Pathway Induced in Enteropathogenic Escherichia Coli-Infected T84 Cells. Infect Immun. 2000. 68(10):5998-6004.
[249] Bruewer, M., Luegering, A., Kucharzik, T., Parkos, C.A., Madara, J.L., Hopkins, A.M., *et al.* Proinflammatory Cytokines Disrupt Epithelial Barrier Function by Apoptosis-Independent Mechanisms. J Immunol. 2003. 171(11):6164-6172.
[250] Tao, N., DePeters, E.J., Freeman, S., German, J.B., Grimm, R., Lebrilla, C.B. Bovine Milk Glycome. J Dairy Sci. 2008. 91(10):3768-3778.
[251] Urashima, T., Saito, T., Nakamura, T., Messer, M. Oligosaccharides of Milk and Colostrum in Non-Human Mammals. Glycoconj J. 2001. 18(5):357-371.
[252] Yoshioka, N., Taniguchi, Y., Yoshida, A., Nakata, K., Nishizawa, T., Inagawa, H., *et al.* Intestinal Macrophages Involved in the Homeostasis of the Intestine Have the Potential for Responding to LPS. Anticancer Res. 2009. 29(11):4861-4865.
[253] Noerr, B. Part 1. Current Controversies in the Understanding of Necrotizing Enterocolitis. Adv Neonatal Care. 2003. 3(3):107-120.
[254] Duffy, L.C., Zielezny, M.A., Carrion, V., Griffiths, E., Dryja, D., Hilty, M., *et al.* Concordance of Bacterial Cultures With Endotoxin and Interleukin-6 in Necrotizing Enterocolitis. Dig Dis Sci. 1997. 42(2):359-365.
[255] DuBois, M., Gilles, K.A., Hamilton, J.K., Rebers, P.A., Smith, F. Colorimetric Method for Determination of Sugars and Related Substances. Anal Chem. 1956. 28(3):350-356.
[256] Redmond, J.W., Packer, N.H. The Use of Solid-Phase Extraction With Graphitised Carbon for the Fractionation and Purification of Sugars. Carbohydrate Res. 1999. 319(1):74-79.
[257] Gnoth, M.J., Rudloff, S., Kunz, C., Kinne, R.K.H. Investigations of the In Vitro Transport of Human Milk Oligosaccharides by a Caco-2 Monolayer Using a Novel High Performance Liquid Chromatography-Mass Spectrometry Technique. J Biol Chem. 2001. 276(37):34363-34370.
[258] Ward, R. Isolation of Milk Oligosaccharides Using Solid-Phase Extraction. Open Glycosci. 2009. 2:9-15.
[259] Hong, Q., Ruhaak, L.R., Totten, S.M., Smilowitz, J.T., German, J.B., Lebrilla, C.B. Label-Free Absolute Quantitation of Oligosaccharides Using Multiple Reaction Monitoring. Anal Chem. 2014. 86(5):2640-2647.
[260] Wu, S., Grimm, R., German, J.B., Lebrilla, C.B. Annotation and Structural Analysis of Sialylated Human Milk Oligosaccharides. J Proteome Res. 2011. 10(2):856-868.
[261] Wu, S., Tao, N., German, J.B., Grimm, R., Lebrilla, C.B. Development of an Annotated Library of Neutral Human Milk Oligosaccharides. J Proteome Res. 2010. 9(8):4138-4151.
[262] Neu, J., Walker, W.A. Necrotizing Enterocolitis. N Engl J Med. 2011. 364(3):255-264.
[263] Ford, H.R. Mechanism of Nitric Oxide-Mediated Intestinal Barrier Failure: Insight Into the Pathogenesis of Necrotizing Enterocolitis. J Pediatr Surg. 2006. 41(2):294-299.
[264] Jilling, T., Simon, D., Lu, J., Meng, F.J., Li, D., Schy, R., *et al.* The Roles of Bacteria and TLR4 in Rat and Murine Models of Necrotizing Enterocolitis. J Immunol. 2006. 177(5):3273-3282.
[265] Guo, S., Nighot, M., Al-Sadi, R., Alhmoud, T., Nighot, P., Ma, T.Y. Lipopolysaccharide Regulation of Intestinal Tight Junction Permeability is Mediated by TLR4 Signal Transduction Pathway Activation of FAK and MyD88. J Immunol. 2015. 195(10):4999-5010.
[266] Blakely, M.L., Lally, K.P., McDonald, S., Brown, R.L., Barnhart, D.C., Ricketts, R.R., *et al.* Postoperative Outcomes of Extremely Low Birth-Weight Infants With Necrotizing

Enterocolitis or Isolated Intestinal Perforation: A Prospective Cohort Study by the NICHD Neonatal Research Network. Ann Surg. 2005. 241(6):984-994.
[267] Phadke, S.M., Deslouches, B., Hileman, S.E., Montelaro, R.C., Wiesenfeld, H.C., Mietzner, T.A. Antimicrobial Peptides in Mucosal Secretions: The Importance of Local Secretions in Mitigating Infection. J Nutr. 2005. 135(5):1289-1293.
[268] Thormar, H., Hilmarsson, H. The Role of Microbicidal Lipids in Host Defense Against Pathogens and Their Potential as Therapeutic Agents. Chem Phys Lipids. 2007. 150(1):1-11.
[269] Gnoth, M.J., Kunz, C., Kinne-Saffran, E., Rudloff, S. Human Milk Oligosaccharides are Minimally Digested In Vitro. J Nutr. 2000. 130(12):3014-3020.
[270] Engfer, M.B., Stahl, B., Finke, B., Sawatzki, G., Daniel, H. Human Milk Oligosaccharides are Resistant to Enzymatic Hydrolysis in the Upper Gastrointestinal Tract. Am J Clin Nutr. 2000. 71(6):1589-1596.
[271] Vatanen, T., Kostic, A.D., d'Hennezel, E., Siljander, H., Franzosa, E.A., Yassour, M., *et al.* Variation in Microbiome LPS Immunogenicity Contributes to Autoimmunity in Humans. Cell. 2016. 165(4):842-853.
[272] Arrieta, M.-C., Arévalo, A., Stiemsma, L., Dimitriu, P., Chico, M.E., Loor, S., *et al.* Associations Between Infant Fungal and Bacterial Dysbiosis and Childhood Atopic Wheeze in a Nonindustrialized Setting. J Allergy Clin Immunol. 2018. 142(2):424-434.
[273] AlFaleh, K., Anabrees, J. Probiotics for Prevention of Necrotizing Enterocolitis in Preterm Infants. Cochrane Database Syst Rev. 2014. (4):CD005496.
[274] Sharif, S., Meader, N., Oddie, S.J., Rojas-Reyes, M.X., McGuire, W. Probiotics to Prevent Necrotising Enterocolitis in Very Preterm or Very Low Birth Weight Infants. Cochrane Database Syst Rev. 2020. 10(10):CD005496.
[275] Chou, H.-H., Takematsu, H., Diaz, S., Iber, J., Nickerson, E., Wright, K.L., *et al.* A Mutation in Human CMP-Sialic Acid Hydroxylase Occurred After the Homo-Pan Divergence. Proc Natl Acad Sci USA. 1998. 95(20):11751-11756.
[276] Schwiertz, A., Gruhl, B., Löbnitz, M., Michel, P., Radke, M., Blaut, M. Development of the Intestinal Bacterial Composition in Hospitalized Preterm Infants in Comparison With Breast-Fed, Full-Term Infants. Pediatr Res. 2003. 54(3):393-399.
[277] Arboleya, S., Ang, L., Margolles, A., Yiyuan, L., Dongya, Z., Liang, X., *et al.* Deep 16S rRNA Metagenomics and Quantitative PCR Analyses of the Premature Infant Fecal Microbiota. Anaerobe. 2012. 18(3):378-380.
[278] Hällström, M., Eerola, E., Vuento, R., Janas, M., Tammela, O. Effects of Mode of Delivery and Necrotising Enterocolitis on the Intestinal Microflora in Preterm Infants. Eur J Clin Microbiol Infect Dis. 2004. 23(6):463-470.
[279] Duar, R.M., Henrick, B.M., Casaburi, G., Frese, S.A. Integrating the Ecosystem Services Framework to Define Dysbiosis of the Breastfed Infant Gut: The Role of B. infantis and Human Milk Oligosaccharides. Front Nutr. 2020. 7:33.
[280] Pammi, M., De Plaen, I.G., Maheshwari, A. Recent Advances in Necrotizing Enterocolitis Research Strategies for Implementation in Clinical Practice. Clin Perinatol. 2020. 47(2):383-397.
[281] Cencič, A., Langerholc, T. Functional Cell Models of the Gut and Their Applications in Food Microbiology — A Review. Int J Food Microbiol. 2010. 141 Suppl 1:S4-S14.
[282] Hilgendorf, C., Spahn-Langguth, H., Regårdh, C.G., Lipka, E., Amidon, G.L., Langguth, P. Caco-2 versus Caco-2/HT29-MTX Co-Cultured Cell Lines: Permeabilities via Diffusion, Inside- and Outside-Directed Carrier-Mediated Transport. J Pharm Sci. 2000. 89(1):63-75.
[283] Wikman, A., Karlsson, J., Carlstedt, I., Artursson, P. A Drug Absorption Model Based on the Mucus Layer Producing Human Intestinal Goblet Cell Line HT29-H. Pharm Res. 1993. 10(6):843-852.
[284] Fan, H., Chen, Z., Lin, R., Liu, Y., Wu, X., Puthiyakunnon, S., *et al.* Bacteroides Fragilis Strain ZY-312 Defense Against Cronobacter Sakazakii-Induced Necrotizing Enterocolitis In Vitro and in a Neonatal Rat Model. mSystems. 2019. 4(4):e00305-e00319.
[285] Shiou, S.-R., Yu, Y., Chen, S., Ciancio, M.J., Petrof, E.O., Sun, J., *et al.* Erythropoietin Protects Intestinal Epithelial Barrier Function and Lowers the Incidence of Experimental Neonatal Necrotizing Enterocolitis. J Biol Chem. 2011. 286(14):12123-12132.

[286] Chichlowski, M., Hale, L.P. Bacterial-Mucosal Interactions in Inflammatory Bowel Disease: An Alliance Gone Bad. Am J Physiol Gastrointest Liver Physiol. 2008. 295(6):G1139-G1149.
[287] Yaseen, H., Butenko, S., Polishuk-Zotkin, I., Schif-Zuck, S., Pérez-Sáez, J.M., Rabinovich, G.A., *et al.* Galectin-1 Facilitates Macrophage Reprogramming and Resolution of Inflammation Through IFN-β. Front Pharmacol. 2020. 11:901.
[288] Emami, C.N., Chokshi, N., Wang, J., Hunter, C., Guner, Y., Goth, K., *et al.* Role of Interleukin-10 in the Pathogenesis of Necrotizing Enterocolitis. Am J Surg. 2012. 203(4):428-435.
[289] Kühn, R., Löhler, J., Rennick, D., Rajewsky, K., Müller, W. Interleukin-10-Deficient Mice Develop Chronic Enterocolitis. Cell. 1993. 75(2):263-274.
[290] Lane, J.S., Todd, K.E., Lewis, M.P., Gloor, B., Ashley, S.W., Reber, H.A., *et al.* Interleukin-10 Reduces the Systemic Inflammatory Response in a Murine Model of Intestinal Ischemia/Reperfusion. Surgery. 1997. 122(2):288-294.
[291] Ling, X., Linglong, P., Weixia, D., Hong, W. Protective Effects of Bifidobacterium on Intestinal Barrier Function in LPS-Induced Enterocyte Barrier Injury of Caco-2 Monolayers and in a Rat NEC Model. PLoS ONE. 2016. 11(8):e0161635.
[292] Arboleya, S., Binetti, A., Salazar, N., Fernández, N., Solís, G., Hernández-Barranco, A., *et al.* Establishment and Development of Intestinal Microbiota in Preterm Neonates. FEMS Microbiol Ecol. 2012. 79(3):763-772.
[293] De Leoz, M.L., Gaerlan, S.C., Strum, J.S., Dimapasoc, L.M., Mirmiran, M., Tancredi, D.J., *et al.* Lacto-N-Tetraose, Fucosylation, and Secretor Status are Highly Variable in Human Milk Oligosaccharides From Women Delivering Preterm. J Proteome Res. 2012. 11(9):4662-4672.
[294] Sela, D.A., Li, Y., Lerno, L., Wu, S., Marcobal, A.M., German, J.B., *et al.* An Infant-Associated Bacterial Commensal Utilizes Breast Milk Sialyloligosaccharides. J Biol Chem. 2011. 286(14):11909-11918.
[295] Wickramasinghe, S., Pacheco, A.R., Lemay, D.G., Mills, D.A. Bifidobacteria Grown on Human Milk Oligosaccharides Downregulate the Expression of Inflammation-Related Genes in Caco-2 Cells. BMC Microbiol. 2015. 15:172.
[296] Yang, Y., Guo, Y., Kan, Q., Zhou, X.G., Zhou, X.Y., Li, Y. A Meta-Analysis of Probiotics for Preventing Necrotizing Enterocolitis in Preterm Neonates. Braz J Med Biol Res. 2014. 47(9):804-810.
[297] Jacobs, S.E., Tobin, J.M., Opie, G.F., Donath, S., Tabrizi, S.N., Pirotta, M., *et al.* Probiotic Effects on Late-Onset Sepsis in Very Preterm Infants: A Randomized Controlled Trial. Pediatrics. 2013. 132(6):1055-1062.
[298] Good, M., Sodhi, C.P., Yamaguchi, Y., Jia, H., Lu, P., Fulton, W.B., *et al.* The Human Milk Oligosaccharide 2'-Fucosyllactose Attenuates the Severity of Experimental Necrotising Enterocolitis by Enhancing Mesenteric Perfusion in the Neonatal Intestine. Br J Nutr. 2016. 116(7):1175-1187.
[299] Halpern, M.D., Clark, J.A., Saunders, T.A., Doelle, S.M., Hosseini, D.M., Stagner, A.M., *et al.* Reduction of Experimental Necrotizing Enterocolitis With Anti-TNF-α. Am J Physiol Gastrointest Liver Physiol. 2006. 290(4):G757-G764.
[300] Appleyard, C.B., Wallace, J.L. Reactivation of Hapten-Induced Colitis and its Prevention by Anti-Inflammatory Drugs. Am J Physiol. 1995. 269(1 Pt 1):G119-G125.
[301] Erben, U., Loddenkemper, C., Doerfel, K., Spieckermann, S., Haller, D., Heimesaat, M.M., *et al.* A Guide to Histomorphological Evaluation of Intestinal Inflammation in Mouse Models. Int J Clin Exp Pathol. 2014. 7(8):4557-4576.
[302] Bernet, M.F., Brassart, D., Neeser, J.R., Servin, A.L. Adhesion of Human Bifidobacterial Strains to Cultured Human Intestinal Epithelial Cells and Inhibition of Enteropathogen-Cell Interactions. Appl Environ Microbiol. 1993. 59(12):4121-4128.
[303] Moroni, O., Kheadr, E., Boutin, Y., Lacroix, C., Fliss, I. Inactivation of Adhesion and Invasion of Food-Borne Listeria Monocytogenes by Bacteriocin-Producing Bifidobacterium Strains of Human Origin. Appl Environ Microbiol. 2006. 72(11):6894-6901.
[304] Sulistyo, A., Rahman, A., Biouss, G., Antounians, L., Zani, A. Animal Models of Necrotizing Enterocolitis: Review of the Literature and State of the Art. Innov Surg Sci. 2018. 3(2):87-92.
[305] Amann, R.I., Ludwig, W., Schleifer, K.H. Phylogenetic Identification and In Situ Detection of Individual Microbial Cells Without Cultivation. Microbiol Rev. 1995. 59(1):143-169.

[306] Olsen, G.J., Woese, C.R., Overbeek, R. The Winds of (Evolutionary) Change: Breathing New Life Into Microbiology. J Bacteriol. 1994. 176(1):1-6.
[307] Woese, C.R. Bacterial Evolution. Microbiol Rev. 1987. 51(2):221-271.
[308] Osman, M.-A., Neoh, H.-M., Ab Mutalib, N.-S., Chin, S.-F., Jamal, R. 16S rRNA Gene Sequencing for Deciphering the Colorectal Cancer Gut Microbiome: Current Protocols and Workflows. Front Microbiol. 2018. 9:767.
[309] Mizuno, K., Hatsuno, M., Aikawa, K., Takeichi, H., Himi, T., Kaneko, A., *et al.* Mastitis is Associated With IL-6 Levels and Milk Fat Globule Size in Breast Milk. J Hum Lact. 2012. 28(4):529-534.
[310] Smoczyński, M. Role of Phospholipid Flux During Milk Secretion in the Mammary Gland. J Mammary Gland Biol Neoplasia. 2017. 22(2):117-129.
[311] Rambold, A.S., Cohen, S., Lippincott-Schwartz, J. Fatty Acid Trafficking in Starved Cells: Regulation by Lipid Droplet Lipolysis, Autophagy, and Mitochondrial Fusion Dynamics. Dev Cell. 2015. 32(6):678-692.
[312] Russell, T.D., Schaack, J., Orlicky, D.J., Palmer, C., Chang, B.H., Chan, L., *et al.* Adipophilin Regulates Maturation of Cytoplasmic Lipid Droplets and Alveolae in Differentiating Mammary Glands. J Cell Sci. 2011. 124(Pt 19):3247-3253.
[313] Cohen, B.C., Raz, C., Shamay, A., Argov-Argaman, N. Lipid Droplet Fusion in Mammary Epithelial Cells is Regulated by Phosphatidylethanolamine Metabolism. J Mammary Gland Biol Neoplasia. 2017. 22(4):235-249.
[314] World Health, O. Revision of Monograph on Tablets. WHO Drug Information. Geneva: World Health Organization; 2011.
[315] Stewart, D.I., Chong, P.S., Stapley, A.G.F. Investigation of the Crystallization and Melting of the Tripalmitin/Triolein System via Hot Stage Microscopy, Differential Scanning Calorimetry, and Pulsed NMR. Cryst Growth Des. 2017. 17(6):3005-3016.
[316] Schubert, M.A., Schicke, B.C., Müller-Goymann, C.C. Thermal Analysis of the Crystallization and Melting Behavior of Lipid Matrices and Lipid Nanoparticles Containing High Amounts of Lecithin. Int J Pharm. 2005. 298(1):242-254.

General Appendix

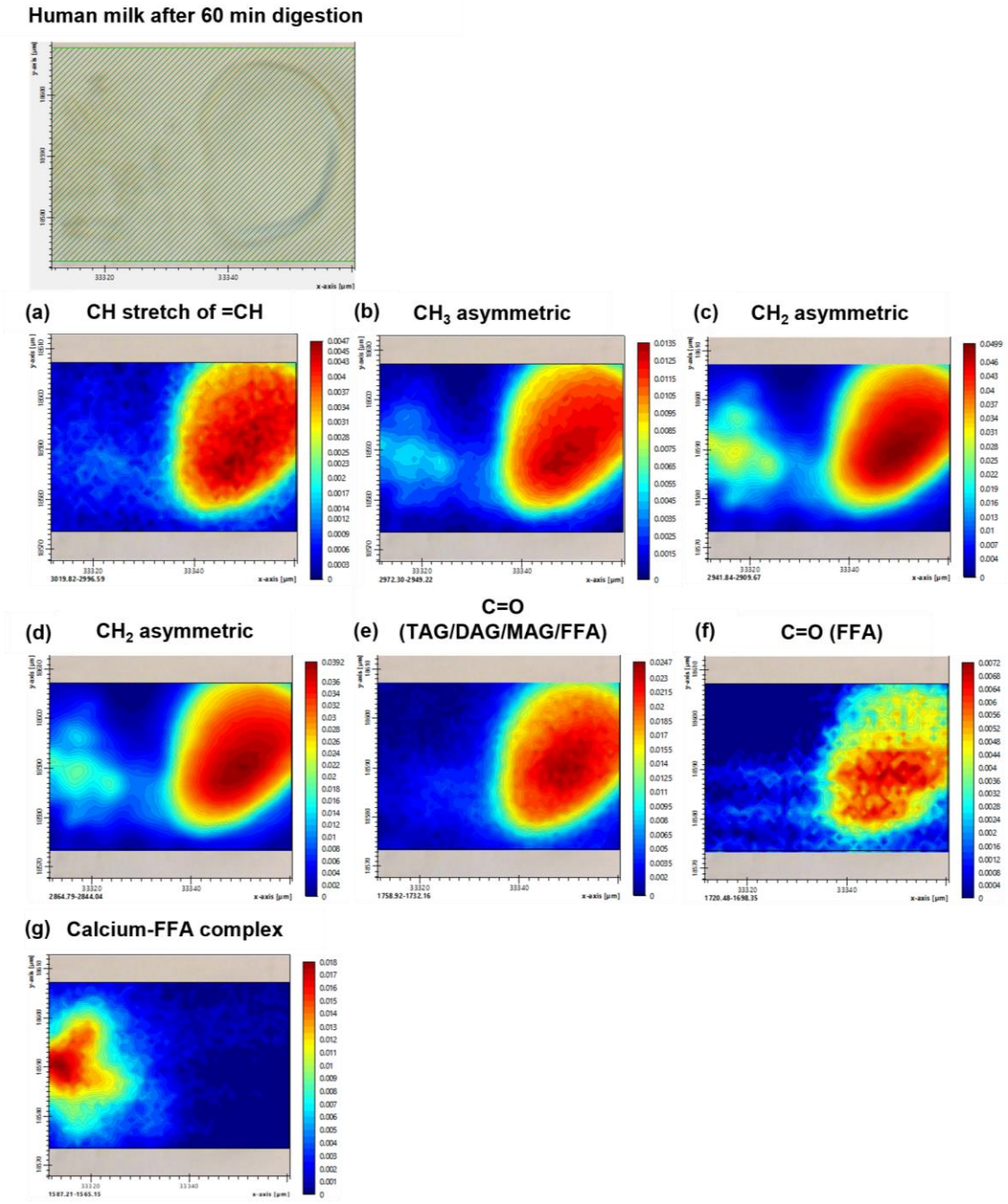

Appendix Figure A1. Synchrotron-source Infrared Microspectroscopy (IRM) of pasteurised human milk after 60 min of digestion, showing localisation of the digested milk components. Panels (a-d) illustrate the C-H stretching vibrations primarily from lipids; panel (e) shows the C=O stretch from triglyceride (TAG), diglyceride (DAG), monoglyceride (MAG) and free fatty acids (FFA); panel (f) displays from free fatty acids; and panel (g) from calcium-free fatty acids complexes. The formation of calcium soaps support findings from the X-ray scattering profile in Fig. 3.6c.

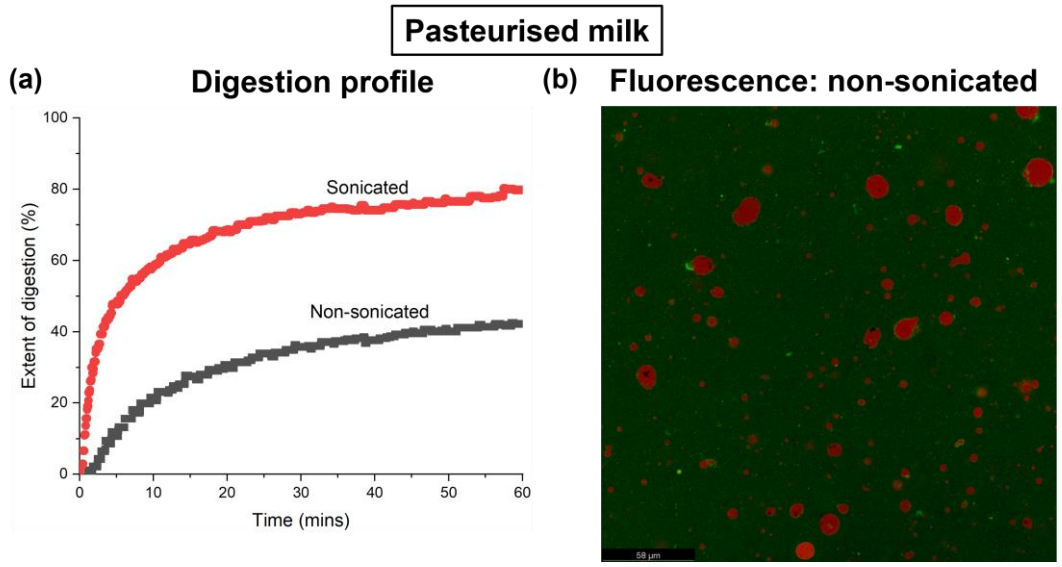

Appendix Figure A2. (a) Effect of particle size on the lipid digestion of sonicated (red) and non-sonicated (grey) pasteurised donor human milk (DHM). (b) Fluorescence microscopy image of pasteurised DHM with the lipids stained using Nile red and proteins stained with fast green FCF. Localisation of proteins at the surface of the fat globules was observed. Particle size of the lipid droplets are highly polydisperse, supporting that observed from the laser light scattering particle size measurements (Fig. 3.5).

Appendix Table A1. Average concentration and molar percentage of triglycerides (TAGs) determined from GC-FID analysis of human colostrum, mature non-pasteurised human milk and pasteurised donor human milk (DHM).

		Human colostrum			Mature non-pasteurised human milk			Pasteurised DHM		
Carbon number	**Molecular weight (g/mol)**	**Average concentration (mg/mL)**	**Molar percentage (%)**	**Contribution to overall molecular weight (g/mol)**	**Average concentration (mg/mL)**	**Molar percentage (%)**	**Contribution to overall molecular weight (g/mol)**	**Average concentration (mg/mL)**	**Molar percentage (%)**	**Contribution to overall molecular weight (g/mol)**
C36	639.02	0.0325 ± 0.0011	1.70 ± 0.17	10.88 ± 1.11	0.0163 ± 0.0038	1.06 ± 0.28	6.75 ± 1.79	0.0104 ± 0.0050	0.68 ± 0.36	4.36 ± 2.28
C38	667.07	0.0260 ± 0.0164	1.30 ± 0.99	8.70 ± 6.63	0.0268 ± 0.0253	1.67 ± 1.60	11.14 ± 10.72	0.0175 ± 0.0080	1.10 ± 0.53	7.32 ± 3.56
C40	695.12	0.0396 ± 0.0210	1.91 ± 1.18	13.26 ± 8.23	0.0308 ± 0.0053	1.84 ± 0.35	12.76 ± 2.43	0.0244 ± 0.0064	1.47 ± 0.41	10.20 ± 2.88
C42	723.18	0.0829 ± 0.0361	3.84 ± 1.84	27.77 ± 13.31	0.1135 ± 0.0143	6.51 ± 0.85	47.10 ± 6.15	0.0841 ± 0.0107	4.86 ± 0.65	35.16 ± 4.71
C44	751.23	0.15296 ± 0.0568	6.82 ± 2.71	51.26 ± 20.29	0.0863 ± 0.0288	4.77 ± 1.62	35.80 ± 12.17	0.0941 ± 0.0372	5.23 ± 2.10	39.32 ± 15.77
C46	779.29	0.3035 ± 0.1365	13.05 ± 6.04	101.72 ± 17.05	0.1141 ± 0.0397	6.07 ± 2.14	47.33 ± 16.71	0.1606 ± 0.0677	8.61 ± 3.66	67.11 ± 28.53
C48	807.34	0.3255 ± 0.1024	13.51 ± 4.42	109.10 ± 35.67	0.3093 ± 0.0187	15.89 ± 0.99	128.32 ± 8.00	0.2508 ± 0.0242	13.00 ± 1.28	104.81 ± 10.37

C50	835.39	0.4949 ± 0.2304	19.85 ± 9.41	165.87 ± 18.63	0.3159 ± 0.0740	15.69 ± 3.71	131.04 ± 30.96	0.2659 ± 0.0387	13.30 ± 1.97	111.10 ± 16.45
C51	848.81	0.0214 ± 0.0039	0.84 ± 0.32	7.17 ± 2.72	0.0215 ± 0.0163	1.05 ± 0.83	8.94 ± 7.03	0.0081 ± 0.0028	0.40 ± 0.17	3.38 ± 1.42
C52	863.45	0.9254 ± 0.1887	35.92 ± 7.49	310.15 ± 14.69	0.5440 ± 0.0246	26.14 ± 1.21	225.70 ± 10.47	0.7259 ± 0.0320	35.13 ± 1.58	303.31 ± 13.66
C54	891.5	0.0329 ± 0.00341	1.24 ± 0.29	11.012 ± 2.54	0.4150 ± 0.0326	19.31 ± 1.55	172.18 ± 13.83	0.3464 ± 0.1165	16.24 ± 5.49	144.76 ± 49.00
	Total	2.44 ± 0.80	100 ± 33	817 ± 141	1.99 ± 0.28	100 ± 15	827 ± 120	1.98 ± 0.35	100 ± 18	831 ± 148

Appendix Table A2. Average concentration and weight percentage of free fatty acids (FFAs) determined from GC-FID analysis of digested human colostrum, mature non-pasteurised human milk and pasteurised donor human milk (DHM) at t = 120 min.

	Human colostrum		**Mature non-pasteurised human milk**		**Pasteurised DHM**	
Free fatty acid	**Average concentration (mg/mL)**	**Weight percentage (*wt%*)**	**Average concentration (mg/mL)**	**Weight percentage (*wt%*)**	**Average concentration (mg/mL)**	**Weight percentage (*wt%*)**
C8:0	0.04 ± 0.01	0.09 ± 0.02	0.06 ± 0.03	0.08 ± 0.04	0.03 ± 0.02	0.07 ± 0.04
C10:0	0.19 ± 0.07	1.13 ± 0.15	0.55 ± 0.11	2.10 ± 0.34	0.28 ± 0.09	1.62 ± 0.23
C12:0	0.73 ± 0.12	4.33 ± 0.54	2.03 ± 0.31	7.82 ± 0.95	1.57 ± 0.22	9.25 ± 1.39
C14:0	1.20 ± 0.20	7.10 ± 0.99	1.43 ± 0.17	5.52 ± 0.68	1.03 ± 0.31	6.11 ± 0.74
C16:0	4.60 ± 0.62	27.11 ± 7.01	2.53 ± 0.30	9.74 ± 1.20	1.95 ± 0.20	11.52 ± 2.97
C18:0	1.87 ± 0.19	11.05 ± 2.00	1.76 ± 0.18	6.77 ± 0.73	1.10 ± 0.13	6.47 ± 1.06
C18:1	6.93 ± 0.87	40.74 ± 14.65	13.80 ± 3.32	53.21 ± 17.78	8.06 ± 1.04	47.58 ± 15.39
C18:2	1.29 ± 0.17	7.40 ± 0.85	3.45 ± 1.57	13.31 ± 3.03	2.93 ± 0.64	17.29 ± 4.82
C18:3	0.10 ± 0.14	0.51 ± 0.11	0.37 ± 0.14	1.43 ± 0.15	0.03 ± 0.01	0.07 ± 0.03
	16.92 ± 2.39	100 ± 26	25.92 ± 6.13	100 ± 25	16.94 ± 2.66	100 ± 26

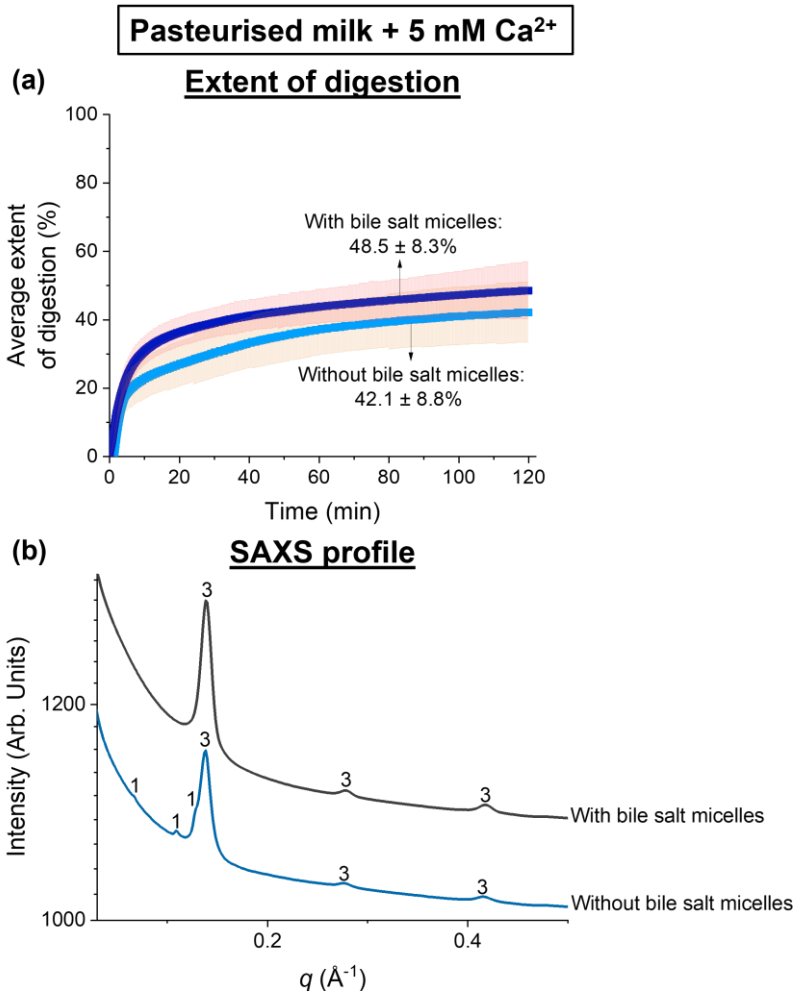

Appendix Figure A3. (a) Extent of digestion of high fat (5.5% fat) pasteurised donor human milk with 5 mM calcium in the absence (light blue with orange error bars) and presence (dark blue with red error bars) of bile salt micelles. (b) The corresponding SAXS profile where an I_2 phase (indicated by "1") and lamellar phase (indicated by "3") are seen when the sample was digested without bile salt micelles (blue line). In comparison, only a lamellar phase was formed in the presence of bile salt micelles (grey line).

Appendix A4. Determination of total protein content using Bradford assay

To quantify the total protein content of human milk, human serum albumin was used as the protein standard. Firstly, 2:1 chloroform/methanol was added to milk samples at a 1:20 *v/v* ratio of milk to solvent. The milk-solvent mixture was vortexed and centrifuged at 4500 *g* for 5 min. The solvent was then removed and the pellet was washed twice more with the chloroform/methanol solvent at a 1:10 *v/v* ratio with the sample and centrifuged in between. The solvent was removed again after the two additional washes and the pellet was dried in a vacuum oven for 1 h. Water (7 mL) was subsequently added to the pellet and the sample was diluted to concentrations ranging from 0.1-1.4 mg/mL. Each of the concentration of sample was aliquoted at 10 µL into a 96-well plate and 250 µL of Bradford reagent

was added to each well. The plate was mixed on a shaker for 30 s, incubated at room temperature for 10 min and absorbance was measured at 595 nm. The net absorbance was then plotted against the concentration of the sample.

Appendix A5. Quantification of total amount of carbohydrates in human milk

The quantification of total carbohydrate content in human milk was determined according to a colorimetric kit obtained from Abcam (Cambridge, UK). The kit consisted of 25 mL Assay Buffer, 3 mL Carbohydrate Developer (chemical composition unknown) and 0.2 mL of standard solution (D-glucose, 2 mg/mL). This technique is based on the principle that polysaccharides are hydrolysed to monomers in the presence of sulfuric acid and converted to furfural or hydroxyfurfural. These products are then reacted with the Developer to form a chromogen that is quantified by measuring the absorbance. Based on the glucose standard curve plotted, the total concentration of carbohydrates in the milk sample was calculated. To generate the standard curve, 0-10 µL of glucose standard was added into a 96-well plate. Following the removal of lipids and proteins from the milk samples, 2-30 µL of the supernatant was aliquoted into a 96-well plate and the volumes of samples and glucose standards were adjusted to 30 µL per well with water. Concentrated sulfuric acid (98%) was then aliquoted into each well at a volume of 150 µL. The samples were mixed on a shaker for 1 min and incubated at 85 °C for 15 min. After incubation, 30 µL of Developer was added to each well and the samples were mixed on the shaker again for 5 min. Subsequently, the plate was placed in a UV/Vis spectrophotometer and the absorbance was measured at 490 nm. The absorbance of milk samples was applied to the glucose standard curve to determine the total concentration of carbohydrates in the human milk samples.